

Multicomponent Copolymer Calculations.

I. Basic Equations

JEROME A. SEINER, *Pittsburgh Plate Glass Company,
Springdale, Pennsylvania*

Synopsis

A scheme is presented for simulating n -component vinyl polymerization on a digital computer. Price-Alfrey Q and e values are used to enhance usefulness of the equations into areas where reactivity ratios are not available.

The simulation of chemical processes with the aid of digital computers presents a unique method whereby complex multicomponent reactions and their kinetics may be studied. This paper is concerned with the simulation of n -component vinyl polymerization.

Mathematical description may have its foundations firmly set on theoretical principle, or may be based upon empirical relationships between variables. In the field of vinyl polymerization, no really acceptable theoretical scheme has been proposed to date. However, the well known Alfrey-Price Q and e scheme¹ represents an attempt to combine the recognized effects of resonance stabilization and polarity on the relative reactivities of various monomers with various free radicals in at least a semi-quantitative fashion. The usefulness of this empirical scheme has been well known for many years.^{2,3} Starting with the base equation

$$m_1 = d(M_1)/d\left(\sum_{i=1}^n M_i\right) \quad (1)$$

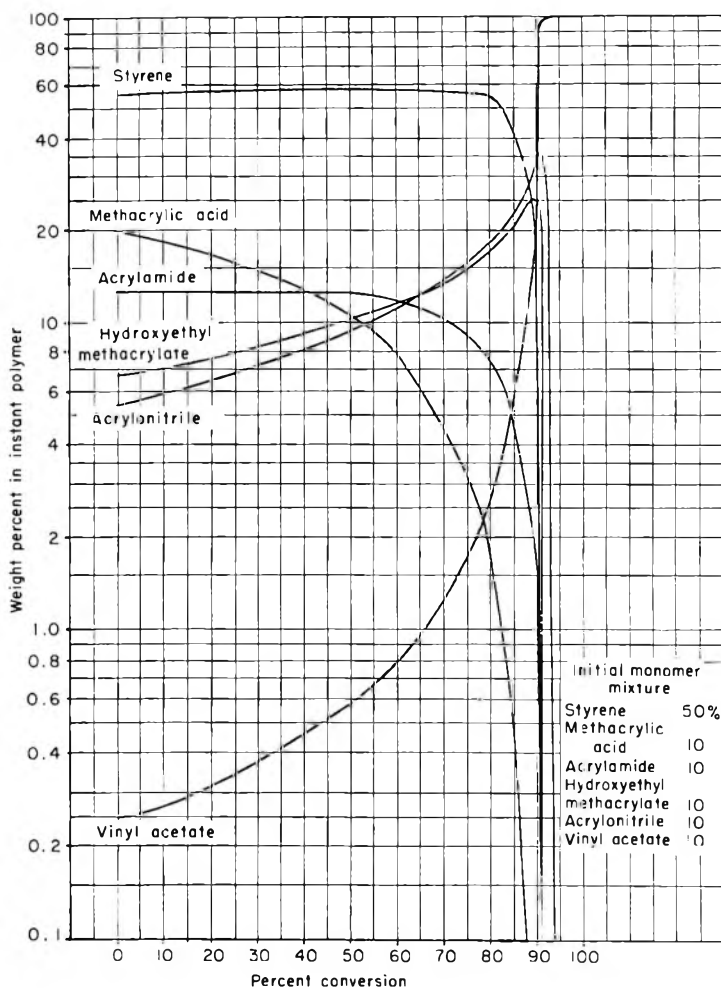
which states that instant polymer mole fraction equals the rate of consumption of M_1 with respect to the rate of consumption of all n monomers present, this expression can be easily transposed to the more useful form:

$$m_1 = 1/\sum_{i=1}^n [d(M_i)/dM_1] \quad (2)$$

here m_i and M_i are the mole fractions i in polymer and monomer, respectively.

Using the general n -monomer substitution of Walling and Briggs⁴ for $d(M_n)/d(M_1)$ as discussed by Fordyce, Chapin, and Ham,⁵ in its reciprocal form,



Fig. 1. Copolymer composition vs. α , system 1.

$$\frac{d(M_n)}{d(M_1)} = \frac{(M_n)^2 Q_n^2 \exp\{-e_n^2\} + (M_1)(M_n)Q_1Q_n \exp\{-e_1e_2\} \dots (M_n)(M_{n-1})Q_nQ_{n-1} \exp\{-e_n e_{n-1}\}}{(M_1)^2 Q_1^2 \exp\{-e_1^2\} + (M_1)(M_2)Q_1Q_2 \exp\{-e_1e_2\} \dots (M_1)(M_n)Q_1Q_n \exp\{-e_1e_n\}}$$

(3)

where Q_i and e_i are the general reactivity constant and general polarity constant, respectively, of i , it is noted that the denominators of all $d(M_n)/d(M_1)$ terms are the same.

From this, eq. (2) can now be put in the form:

$$m_1 = M_1 Q_1 \left(\sum_{i=1}^n M_i Q_i \exp \{-e_i e_i\} \right) / \sum_{j=1}^n M_j Q_j \sum_{i=1}^n (M_i Q_i \exp \{-e_i e_j\}) \quad (4)$$

or by using more commonly accepted summation notation

$$m_1 = M_1 Q_1 \left(\sum_{i=1}^n M_i Q_i \exp \{-e_i e_i\} \right) / \sum_{j=1}^n (M_i Q_i M_j Q_j \exp \{-e_i e_j\}) \quad (5)$$

Equation (5) can be represented by the ordered summation (6):

$$\begin{aligned} m_1 = & \frac{M_1 Q_1 (M_1 Q_1 \exp \{-e_1^2\} + M_2 Q_2 \exp \{-e_1 e_2\} \dots M_n Q_n \exp \{-e_1 e_n\})}{M_1 Q_1 (M_1 Q_1 \exp \{-e_1^2\} + M_2 Q_2 \exp \{-e_1 e_2\} \dots M_n Q_n \exp \{-e_1 e_n\})} \\ & + \frac{M_2 Q_2 (M_1 Q_1 \exp \{-e_2 e_1\} + M_2 Q_2 \exp \{-e_2^2\} \dots}{M_n Q_n \exp \{-e_2 e_n\}) \dots} \\ & + \frac{M_n Q_n (M_1 Q_1 \exp \{-e_n e_1\} + M_2 Q_2 \exp \{-e_n e_2\} \dots M_n Q_n \exp \{-e_n^2\})}{M_n Q_n \exp \{-e_n^2\}} \quad (6) \end{aligned}$$

Solving the summations (5) or (6) involves the computation of n numerator and n^2 denominator terms. Thus for a six-component system, $n^2 + n$ equals 42 arrays which must be calculated to compute the initial instantaneous polymer mole fraction of monomer 1. Since the denominator term for all monomers will be the same, and

$$\sum_{i=1}^n m_i = 1$$

by definition, $(n - 1)(n + n^2)$ equals 210 array terms which must be calculated to compute the initial instantaneous polymer mole fractions of each of the six components. Making the assumption that 1% of the monomer originally present is converted to polymer of the predicted composition, permits calculation of an overall material balance.

$$C_1 = \sum_{i=0}^{\alpha} (m_1) / (\alpha + 1) \quad (7)$$

$$M_1 = (M_1^0 - C_1 \alpha) / (1 - \alpha) \quad (8)$$

where M_i^0 is the initial mole fraction of i in monomer, C_i is the mole fraction of i in accumulated polymer, and α is the conversion (cumulative moles polymer/total moles in final polymer). This material balance yields new values for M_i after 1% conversion. By repeating this sequence 100 times, a very graphical picture of the polymerization process is drawn. Again for a six-component system, this sequence involves $(n - 1)100 = 500$ material balance and $(n - 1)(n + n^2)100 = 21,000$ summation calculations, each of which involves exponential terms.

A computer program written in Fortran II for processing on a Remington Rand Univac III has successfully generated data for the six-component system, an example of which is shown in Figures 1 and 2. The Q and e

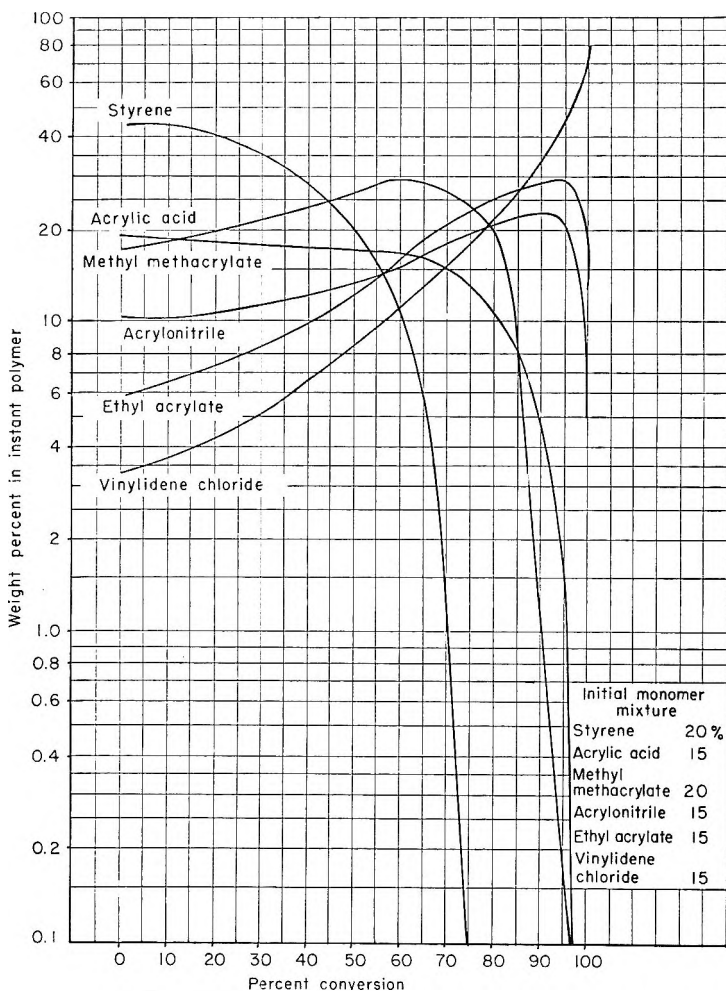


Fig. 2. Copolymer composition vs. α , system 2.

data used in these calculations are shown graphically in Figure 3. Various Q and e values came from a number of miscellaneous sources.^{1,5-8}

Analysis of Figure 1, which is a copolymer composition containing M_1 (styrene), 50%; M_2 (methacrylic acid), 10%; M_3 (acrylamide), 10%; M_4 (2-hydroxyethyl methacrylate) 10%; M_5 (acrylonitrile), 10%; M_6 (vinyl acetate), 10%, yields the following useful information.

(1) The first three monomers enter the polymer at greater than their monomer concentrations, while the final three enter at lower concentrations.

(2) Vinyl acetate, which is present at the 10% level, initially enters the polymer at the 0.25% level.

(3) The monomers M_4 and M_5 build up to peak concentrations in the polymer of 26% and 36%, respectively.

(4) The final 10% of conversion is essentially homopolymer of vinyl acetate.

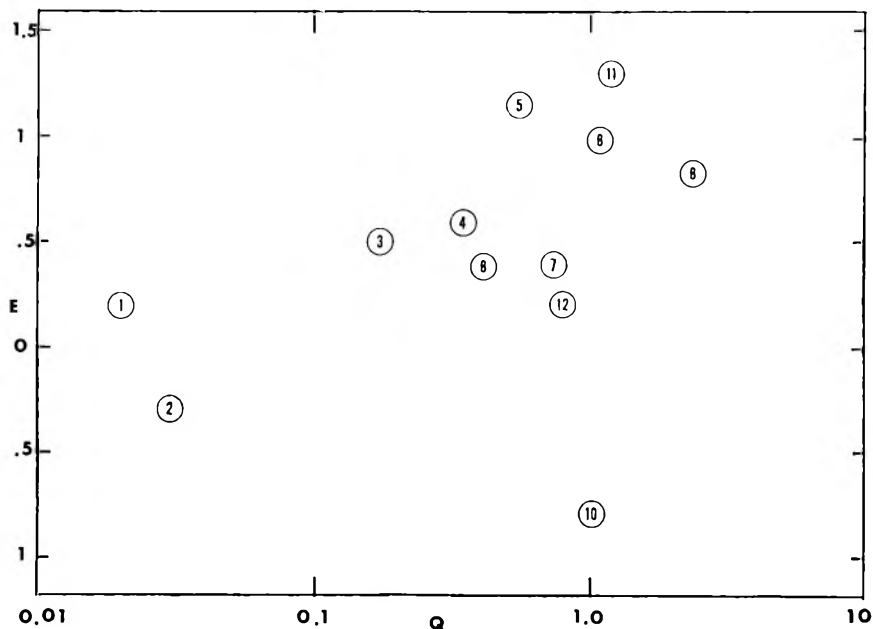


Fig. 3. Q and e values for various monomers: (1) vinyl chloride; (2) vinyl acetate; (3) vinylidene chloride; (4) ethyl acrylate; (5) acrylonitrile; (6) 2-ethylhexyl acrylate; (7) methyl methacrylate; (8) acrylic acid; (9) methacrylic acid; (10) styrene; (11) acrylamide; (12) 2-hydroxyethyl methacrylate.

(5) The first 90% of conversion produces polymer containing at least 25% functional monomers (M_2 , M_3 , M_4) out of an original 30%. This is a very useful distribution characteristic.

(6) Just prior to 90% conversion, the polymer forming consists of 26.2% M_4 , 31.6% M_5 , and 36.3% M_6 . This accounts for 94.1% exclusive of styrene which was originally present at the 50% level in the monomer.

Similar graphs for commercial multicomponent systems yield useful information and frequently pinpoint flaws for re-evaluation. Segments of composition which would contribute insolubility, structural weakness or other undesirable features can be modified through incremental addition of monomer or catalyst to adjust either monomer distribution along the chain or molecular weight distribution.⁹

References

1. Alfrey, T., J. J. Bohrer, and H. Mark, *Copolymerization*, Interscience, New York, 1952.
2. Bamford, C. H., and Jenkins, *Trans. Faraday Soc.*, **59**, 530 (1963).
3. Kawabata, Tsuruta, and Furukawa, *Makromol. Chem.*, **51**, 70 (1962).
4. Walling, C., and Briggs, *J. Am. Chem. Soc.*, **67**, 1774 (1945).
5. Fordyce, Chapin, and Ham, *J. Am. Chem. Soc.*, **70**, 2489 (1948).
6. Rohm & Haas Bulletin SP-251 (April 1963).
7. Charton and Capato, *J. Polymer Sci.*, **A2**, 1321 (1964).
8. Young, L. J., *J. Polymer Sci.*, **54**, 411 (1961).
9. Hoffman, Schreiber, and Rosen, *Ind. Eng. Chem.*, **54**, 411 (1964).

Résumé

On présente un schéma pour programmer, au moyen d'un compteur digitale, la polymérisation vinylique de n composants. Les valeurs de Price-Alfrey Q et e sont employées pour rendre les équations plus utiles dans les domaines où les rapports de réactivité ne sont pas accessibles.

Zusammenfassung

Ein Schema für die Simulierung einer Vinylpolymerisation mit n Komponenten auf einem Digitalcomputer wird angegeben. Q - und e -Werte nach Price-Alfrey werden verwendet, um den Gebrauch der Gleichungen in Gebieten, wo keine Reaktivitätsverhältnisse vorhanden sind, zu ermöglichen.

Received September 4, 1964

Revised October 30, 1964

(Prod. No. 4556A)

Stereospecific Polymerization of α -Olefins with Three-Component Catalyst Systems*

H. W. COOVER, JR., and F. B. JOYNER,
*Research Laboratories, Tennessee Eastman Company, Division
of Eastman Kodak Company, Kingsport, Tennessee*

Synopsis

It is well known that mixtures of alkylaluminum dihalides and transition metal halides, such as titanium(III) chloride, are ineffective as catalysts for the stereospecific polymerization of α -olefins. It has been discovered that the addition of a third compound, derived from one or more of the strongly complexing ligand elements such as nitrogen, oxygen, and phosphorus, to such mixtures leads to catalysts having the highest stereospecificities known. In the present work, studies were made of the effect of various third components on the activity and stereospecificity of these catalysts in the polymerization of propylene. The stereospecificity and activity of three-component catalysts of this type were dependent upon the ratio of the third component to the alkylaluminum dihalide. Optimum stereospecificity and activity were usually obtained at ratios in the range of 0.5-0.7. In general, catalytic activity increased with increasing basicity of the third component. Both stereospecificity and activity were influenced by the nature of the halogen atoms in the alkylaluminum dihalide, whereas the nature of the alkyl group affected only the activity, with the ethyl group providing the most active catalysts. The most stereospecific catalyst was made from a mixture of ethylaluminum diiodide, hexamethylphosphoric triamide, and violet titanium(III) chloride.

INTRODUCTION

Until the development of stereospecific catalysis during the last decade, stereoregular polymers were virtually unattainable by synthetic methods, and the stereoregular poly- α -olefins were completely unknown.^{1,2} The most important catalysts developed during this time for the stereoregulated polymerization of α -olefins comprise mixtures of metal alkyls and transition metal halides, although closely related catalyst systems had been known for several years.³⁻⁵

A recent publication from our laboratories described the polymerization of ethylene using a preactivated aluminum-titanium(IV) chloride catalyst in which part of the aluminum and part of the titanium(IV) chloride have been converted to aluminum chloride and titanium(III) chloride, respectively.⁶

During the study of the polymerization of ethylene with the preactivated aluminum-titanium(IV) chloride catalyst in our laboratories, it was found

* Presented at the 145th National Meeting of the American Chemical Society, New York, September 1963.

that neither this catalyst nor mixtures of alkylaluminum dihalides and transition metal halides, such as violet titanium(III) chloride, were catalysts for the stereospecific polymerization of propylene and other α -olefins.⁷ It was discovered, however, that the addition of a third component derived from one or more of the strongly complexing ligand elements of Groups VA and VIA, such as nitrogen, oxygen, and phosphorus, to mixtures of alkylaluminum dihalides and violet titanium(III) chloride led to catalysts having the highest stereospecificities known.

The principal objectives of this investigation were to study the effects of the various third components and other composition variables on the stereospecificity and activity of the three-component alkylaluminum dihalide-type catalysts in the polymerization of propylene.

This paper is a description of these three-component catalysts and a discussion of the influence of the nature of each component on the ability of the catalysts to promote the stereoregulated polymerization of propylene.

EXPERIMENTAL

Materials

Propylene (Sun Oil Company) was dried by passing it through a bed of Linde molecular sieve 4A.

ANAL.: propylene, 98.7%; propane, 1.2%; ethylene and carbon dioxide, <0.1%; oxygen, trace.

Benzene (Allied Chemical Corp., General Chemical Division, B and A reagent-grade) was dried over clean metallic sodium.

Heptane (Distillation Products Industries, Eastman grade) was dried over clean metallic sodium.

Titanium(III) chloride [Stauffer Chemical Co., hydrogen-reduced (HA), Lot No. HA71-747] was used as received.

Titanium(III) chloride, β -(brown) form, was prepared by low-temperature reduction of TiCl_4 with hydrogen in an electrical discharge.

ANAL. Calcd. for TiCl_3 : Ti, 31.05%; Cl, 68.94%. Found: Ti, 31.79%; Cl, 69.75%.

Titanium(III) fluoride was prepared by the reaction of titanium metal with hydrogen fluoride.⁸

ANAL. Calcd. for TiF_3 : Ti, 45.66%. Found. Ti, 46.10%.

Titanium(III) bromide (Stauffer Chemical Co.) was used as received.

ANAL. Calcd. for TiBr_3 : Ti, 16.65%; Br, 83.35%. Found: Ti, 16.48%; Br, 84.54%.

Titanium(III) iodide was prepared by the method of Rolsten and Sisler.⁹

Methylaluminum dichloride was prepared from $(\text{CH}_3)_3\text{Al}_2\text{Cl}_3$ (Texas Alkyls, Inc.) by reaction with aluminum chloride and was recrystallized from heptane.

ANAL. Calcd. for CH_3AlCl_2 : Al, 23.9%; Cl, 62.8%. Found: Al, 23.5%; Cl, 63.2%.

Ethylaluminum dichloride (Ethyl Corp.) was melt-recrystallized five times. The liquid fraction was decanted after each recrystallization.

ANAL. Calcd. for $\text{C}_2\text{H}_5\text{AlCl}_2$: Al, 21.25%; C_2H_5 , 22.89%. Found: Al, 21.14%; C_2H_5 , 21.81%.

Isobutylaluminum dichloride (Texas Alkyls, Inc.) was used without further purification.

ANAL. Calcd. for $\text{C}_4\text{H}_9\text{AlCl}_2$: Al, 17.4%; Cl, 45.7%. Found: Al, 17.7%; Cl, 47.4%.

Octylaluminum dichloride was prepared by reaction of trioctylaluminum with aluminum chloride and the product was recrystallized from hexane.

ANAL. Calcd. for $\text{C}_8\text{H}_{17}\text{AlCl}_2$: Cl, 33.6%. Found: Cl, 34.1%.

Ethylaluminum difluoride (Texas Alkyls, Inc.) was used as received.

Ethylaluminum dibromide (Texas Alkyls, Inc.) was melt-recrystallized three times. The liquid fraction was decanted after each recrystallization.

ANAL. Calcd. for $\text{C}_2\text{H}_5\text{AlBr}_2$: Al, 12.5%; Br, 74.0%. Found: Al, 12.9%; Br, 74.0%.

Ethylaluminum diiodide (Texas Alkyls, Inc.) was used without further purification.

ANAL. Calcd. for $\text{C}_2\text{H}_5\text{AlI}_2$: Al, 8.71%; I, 81.91%. Found: Al, 8.33%; I, 81.97%.

Diethylaluminum fluoride (Texas Alkyls, Inc.) was used without further purification.

ANAL. Calcd. for $\text{C}_4\text{H}_{10}\text{AlF}$: Al, 25.9%; F, 18.2%. Found: Al, 26.9%; F, 17.1%.

Diethylaluminum chloride (Texas Alkyls, Inc.) was used without further purification.

ANAL. Calcd. for $\text{C}_4\text{H}_{10}\text{AlCl}$: Al, 22.38%; Cl, 29.41%. Found: Al, 21.35%; Cl, 28.87%.

Diethylaluminum bromide (Texas Alkyls, Inc.) was distilled *in vacuo*; the middle fraction was collected and redistilled.

ANAL. Calcd. for $\text{C}_4\text{H}_{10}\text{AlBr}$: Br, 48.4%. Found: Br, 48.9%.

Diethylaluminum iodide (Texas Alkyls, Inc.) was used without further purification.

ANAL. Calcd. for $\text{C}_4\text{H}_{10}\text{AlI}$: Al, 12.7%; I, 59.9%. Found: Al, 12.8%; I, 58.6%.

Trimethylaluminum (Ethyl Corp.) was used without further purification.

ANAL. Calcd. for $\text{C}_3\text{H}_9\text{Al}$: Al, 37.4%. Found: Al, 37.0%; Cl, 0.04%.

Triethylaluminum (Texas Alkyls, Inc.) was redistilled before use; its purity was based on ethane evolution: 98.5%.

Hexamethylphosphoric triamide (HPT) (Tennessee Eastman Co.) was redistilled, and no impurities were detected by gas chromatography.

Tributylamine (Distillation Products Industries, Eastman grade) was fractionally distilled, and its purity by gas chromatography was 99.4%.

Tributylphosphine (Anderson Chemical Co.) was redistilled, and its purity by gas chromatography was 98.9%.

Butyl ether (Distillation Products Industries, Eastman grade) was fractionally distilled. No impurities were detected by gas chromatography.

Butyl sulfide (Distillation Products Industries, Eastman grade) was fractionally distilled, and its purity by gas chromatography was 99.1%.

1-Iodobutane (Distillation Products Industries, Eastman grade) was redistilled before using, and its purity by gas chromatography was 99.8%.

Apparatus

All polymerizations were carried out in a magnetically stirred glass reactor. The apparatus was designed to maintain a constant pressure of propylene in the reactor and to chart automatically and continuously the rate of absorption of propylene from a reservoir during the reaction. Heating was accomplished by circulating silicone oil, thermostatically controlled at the desired temperature. A detailed description of this apparatus is given elsewhere.¹⁰

Methods

Polymerization of Propylene. In a nitrogen-filled dry box, 50 ml. of pure, sodium-dried solvent consisting of 2 parts benzene and 3 parts heptane by volume was added to a dry, 250-ml. glass reaction bottle, creased to provide agitation baffles. The catalyst components were then introduced separately with the titanium(III) chloride always being the last component added. The alkylaluminum dihalide and the ligand component were added in the form of carefully prepared solutions in a $2/3$ benzene-heptane mixture. The titanium(III) chloride was weighed and introduced into the reaction mixture directly. The mixture was then adjusted to a total volume of 100 ml. by addition of dry benzene-heptane mixture. A Teflon-coated magnetic stirring bar was introduced, and the reaction bottle was fitted with an inlet valve, removed from the dry box, clamped into position in the oil bath (preheated to the desired temperature), and attached to the propylene supply line. The reaction bottle was purged with propylene, then the magnetic stirrer was activated, and propylene was added to the desired pressure. This pressure was maintained during the entire reaction period of about 1 hr. The crude polypropylene was refined by washing it with hot isobutyl alcohol to remove catalyst residues. The reaction rate was readily calculated from the straight-line portion of the curve showing the pressure drop occurring in the propylene reservoir versus time. All experiments were run in duplicate, and the rates re-

corded are averages. The difference between duplicate experiments was usually less than 5% and never greater than 20%.

Determination of Stereospecificity Index. A carefully weighed sample (2–5 g.) of the polypropylene was exhaustively extracted with 4-methyl-2-pentanone (methyl isobutyl ketone, MIBK) in a Soxhlet extractor (usually about 24 hr.). The residue was dried to constant weight. The stereospecificity index for the catalyst used was then calculated as the percentage of the polypropylene insoluble in refluxing MIBK.

Determination of Inherent Viscosity. The inherent viscosity of a given polymer was determined in a tetralin solution at 145°C. with the use of a Schulken-Sparks capillary viscometer.¹¹

Stereoregularity Distribution. A modified Desreux-Spiegels¹² fractionation technique was used. In this technique a thin layer of polymer was continuously extracted with tetralin at gradually increasing temperatures. The melting point of a given fraction was taken as the temperature at which the birefringence of the sample, observed with a polarized light microscope, disappeared when a heating rate of 1–2°C./min. was used. The melting points obtained in this manner were converted into percentage stereoregularity of the polymer molecules by using Flory's equation:¹³

$$-(R/\Delta H) \ln (S/100) = (1/T_m) - (1/T_m)^0,$$

where R = gas constant, ΔH = 2600 cal./mole, T_m = melting point of polymer, T_m^0 = 170°C. (443°K.), and S = percentage stereoregularity.

RESULTS AND DISCUSSION

Description of Stereospecific Three-Component Catalysts Based on Alkylaluminum Dihalide

Mixtures of alkylaluminum dihalides and transition metal halides, such as titanium(III) chloride, were ineffective as catalysts for the stereospecific polymerization of α -olefins.^{7,14} Ethylaluminum dichloride in combination with titanium(III) chloride was an excellent catalyst for converting propylene into liquid polymers of very low molecular weight, but gave little or no solid polymer. When a third component (TC) derived from one or more of the strongly complexing ligand elements of Groups VA and VIA was added, high yields of highly crystallizable polypropylene resulted (Table I). The crystalline nature and, especially, the narrow crystallinity distribution of the polymers indicated that the three-component catalyst systems, as a group, had the highest stereospecificities known.

The polymerization of propylene at moderate temperatures and pressures was readily effected by using a catalyst consisting of ethylaluminum dichloride, violet titanium(III) chloride, and HPT (Table I). Unlike many binary catalysts, no reduction reaction occurred between the components of this three-component catalyst system.¹⁵ Consequently, the transition element present in the system was substantially in one valence state, and the resulting active catalyst sites showed a high degree of uniformity which

TABLE I
Polymerization of Propylene with Various Organoaluminum-TiCl₃ Catalysts^a

| Organoaluminum component | Propylene pressure, psig | Polymerization rate, mmoles/l.-sec. | Polymer properties | |
|---|--------------------------|-------------------------------------|-------------------------|----------------------|
| | | | { η } ^b | Insoluble in MIBK, % |
| C ₂ H ₅ AlCl ₂ | 40 | — ^c | — | — |
| C ₂ H ₅ AlCl ₂ + 0.6 HPT | 10 | 0.229 | 2.35 | 97.2 |
| | 40 | 0.683 | 3.14 | 96.3 |
| C ₂ H ₅ AlCl ₂ + 0.6 HPT + 0.22 (C ₂ H ₅) ₂ Zn | 40 | 0.103 | 1.24 | 91.8 |
| (C ₂ H ₅) ₂ AlCl | 10 | 0.529 | 1.82 | 88.7 |
| (C ₂ H ₅) ₃ Al | 10 | 1.62 | 1.84 | 79.9 |
| (C ₂ H ₅) ₂ AlF | 10 | 0.563 | 1.26 | 43.8 |
| (C ₂ H ₅) ₂ AlF + 0.4 HPT | 40 | 0.115 | 5.58 | 92.8 |
| C ₂ H ₅ AlBr ₂ + 0.6 HPT | 40 | 0.529 | 3.14 | 98.3 |
| (C ₂ H ₅) ₂ AlBr | 10 | 0.362 | 1.99 | 94.4 |
| | 40 | 0.982 | 2.80 | 93.4 |
| C ₂ H ₅ AlI ₂ + 0.6 HPT | 40 | 0.575 | 2.50 | 99.2 |
| (C ₂ H ₅) ₂ AlI | 10 | 0.278 | 1.57 | 93.7 |
| | 40 | 0.725 | 2.50 | 95.7 |

^a At 70°C. with the use of equimolar quantities (3.33 mmole) of the alkylaluminum and titanium(III) chloride.

^b Determined on gross polymer.

^c No measurable rate. At 40 psig propylene pressure, amorphous polypropylene was produced at the average rate of 0.20 g./g. TiCl₃/hr.

was manifested in the high stereoregularity or structural uniformity of the resulting polymer. In many other systems, reduction reactions between the catalyst components lead to mixtures containing the transition element in two or more valence states. The resulting catalyst sites thus vary in ability to support sterically regulated polymerization. This variation in the stereospecificity of the individual catalyst sites gives rise to a spectrum of macromolecules differing widely in structural features and in crystallizability. A catalyst prepared from triethylaluminum and titanium(III) chloride, for example, was shown by Natta and co-workers¹⁶ to give polypropylene having a broad structural distribution.

Comparison With Two-Component Catalysts Based on Trialkylaluminum or Dialkylaluminum Halide

As shown in Table I, the three-component alkylaluminum dihalide catalysts were usually less active, but were significantly more stereospecific than comparable two-component catalysts containing either trialkylaluminum or dialkylaluminum halide. It can be seen that the more active catalyst types tended to be less stereospecific and gave propylene polymers of lower inherent viscosities.

The type of alkylaluminum used with violet titanium(III) chloride to polymerize propylene greatly influenced the stereoregularity of the polymer. In Figure 1, it can be seen that ethylaluminum dichloride in com-

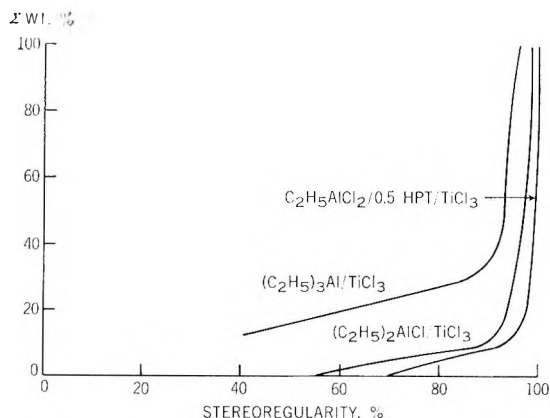


Fig. 1. Stereoregularity distribution of polypropylene obtained with various catalysts at 70°C. and 40 psig propylene pressure with the use of equimolar quantities (3.33 mmoles) of alkylaluminum and TiCl_3 .

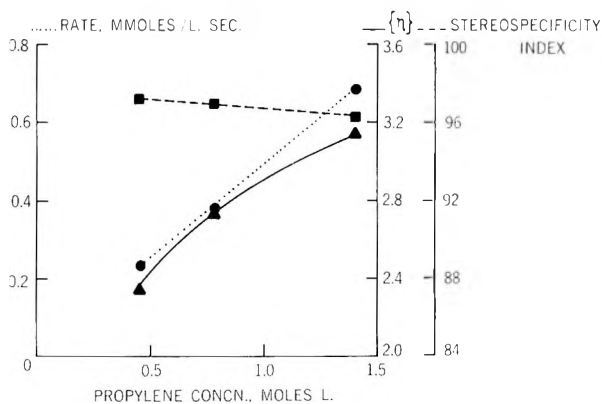


Fig. 2. Effect of monomer concentration on (●) polymerization rate, (▲) polymer inherent viscosity, and (■) stereospecificity index at 70°C. with the catalyst $\text{C}_2\text{H}_5\text{AlCl}_2-0.6 \text{ HPT}-\text{TiCl}_3$ with the use of equimolar quantities (3.33 mmole) of $\text{C}_2\text{H}_5\text{AlCl}_2$ and TiCl_3 .

bination with HPT (1/0.5) afforded a more narrow stereoregularity distribution than diethylaluminum chloride, which in turn gave a polymer having a much narrower distribution than that produced with triethylaluminum. Monomer concentration during the polymerization reaction appeared to have little or no influence on the stereoregularity distribution of the propylene polymers prepared with the three-component catalyst. Natta and Pasquon¹⁷ showed that the stereoregularity of the polypropylene produced at low propylene pressures with $(\text{C}_2\text{H}_5)_2\text{AlCl}-\text{TiCl}_3$ catalyst increased as the monomer concentration increased. In the present work, it was found that the stereospecificity index or stereoregularity of the polypropylene prepared with the $\text{C}_2\text{H}_5\text{AlCl}_2-0.6 \text{ HPT}-\text{TiCl}_3$ catalyst decreased with increasing monomer concentration, while the rate of polymerization and the inherent viscosity of the polymer increased (Fig. 2).

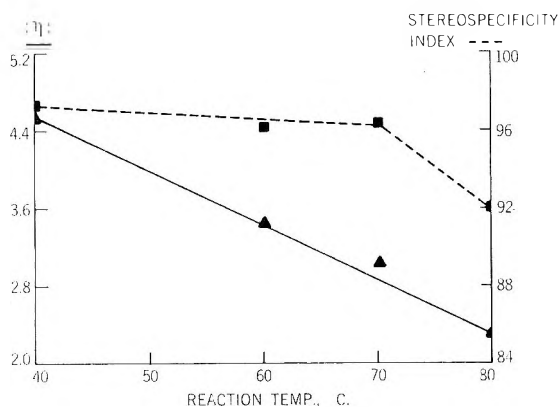


Fig. 3. Effect of reaction temperature on (▲) polymer inherent viscosity and (■) stereospecificity index at 40 psig propylene pressure with the catalyst $C_2H_5AlCl_2-0.6$ HPT- $TiCl_3$ with the use of equimolar quantities (3.33 mmole) of $C_2H_5AlCl_2$ and $TiCl_3$.

Figure 3 shows the effect of temperature on polymer inherent viscosity and on the stereospecificity index of the three-component catalyst. It can be seen that the stereospecificity index decreased sharply at 70–80°C., but was virtually constant over the range of 40–70°C. The inherent viscosity of the polypropylene decreased linearly with increasing temperature over the range studied.

Other investigators have shown that alkylzinc compounds can be added as chain-transfer agents to the $R_3Al-TiCl_3$ catalyst with little or no effect on the stereospecificity of the catalyst or on rates of polymerization.^{18,19} In the present study, however, it was found that in the polymerization of propylene addition of diethylzinc to the $C_2H_5AlCl_2-0.6$ HPT- $TiCl_3$ catalyst reduced the maximum reaction rate by as much as 80% and the inherent viscosity of the polymer by as much as 60% (Table I). It was concluded, therefore, that the alkylzinc compound in this system was a terminator.

Chemical Nature of the $C_2H_5AlCl_2-0.6$ HPT- $TiCl_3$ Catalyst System

It is generally accepted that olefin polymerization reactions based on titanium(III) chloride concentration follow first-order kinetics. It is further known that the stereospecificity and nature of the true catalyst depend on the cocatalyst which is reacted with the titanium(III) chloride.^{14,20} It is obvious, therefore, that the active sites of the catalyst are associated with the titanium(III) chloride and are produced by the interaction of the titanium(III) chloride with the cocatalysts (such as ethylaluminum dichloride and HPT). The bulk of the chemical system is not involved in the actual catalyst; hence, the formation of the active catalyst sites cannot be interpreted on the basis of the reactions of the individual components. Zambelli and co-workers²¹ have suggested, nevertheless, that the catalytic activity and stereospecificity of the three-component alkylaluminum dihalide-type catalyst result from a dismutation reaction in which the ethylaluminum dichloride, for example, is converted to a co-

ordinated aluminum trihalide complex and diethylaluminum chloride. These authors have concluded, therefore, that the three-component catalyst is identical with the catalyst obtained directly from violet titanium(III) chloride and diethylaluminum chloride. The data in Table I and Figure 1 which show significant differences between these catalyst systems cannot be interpreted on this basis, but rather indicate that the chemistry of active site formation is considerably more complex than suggested by Zambelli and co-workers.

McConnell and co-workers²² showed by infrared studies that preheated benzene solutions of ethylaluminum dichloride and HPT contain no detectable diethylaluminum chloride. These investigators showed also that the polymerization of propylene in benzene, using the three-component catalyst, gave results substantially identical to those reported in Table I.

Many polar compounds containing ligand atoms of relatively high coordinating affinities, such as dioxane and tetrahydrofuran, when used as third components in combination with ethylaluminum dichloride and violet titanium(III) chloride were substantially ineffective in providing active catalysts for polymerizing propylene. A similar observation was made by Razuvaev and co-workers²⁰ in studying the effect of polar additives on the stereospecific polymerization of propylene with $(C_2H_5)_3Al-TiCl_3$ catalyst. These investigators found that certain additives caused an increase in the activity of the catalyst, whereas other polar additives caused a decrease. In the present study, the stereospecificity index of the $(C_2H_5)_2AlF-TiCl_3$ catalyst at 70°C. was increased from 42–46% to 92–93% by the addition of 0.4 mole HPT/mole of diethylaluminum fluoride, although the activity of the catalyst was reduced by about 94% (Table I). The inherent viscosity of the polypropylene obtained was more than four times greater than that of polymer produced without the HPT. It is clearly evident, therefore, that the polar third component plays an important role in determining the nature of any catalyst system containing it.

Effect of Catalyst Variables on the Polymerization of Propylene

The nature and performance of the three-component alkylaluminum dihalide catalysts in the polymerization of propylene were critically dependent upon the chemical nature of each component and upon its mole proportion. The influence of catalyst composition on activity, stereospecificity, and polymer molecular weight is described below.

Catalyst Component Ratio. The effect of catalyst component proportion was studied for the system $C_2H_5AlCl_2-HPT-TiCl_3$. Polymerization reactions were carried out in which the concentration of each component of the catalyst was varied while the concentrations of the other two components were held constant. The results are shown in Tables II–IV and Figures 4–7.

Both stereospecificity and activity were dependent upon the mole ratio of HPT to ethylaluminum dichloride (Table II, Figs. 4 and 5). Optimum stereospecificity and activity were obtained at the HPT/ $C_2H_5AlCl_2$ ratio of 0.6–0.7. Reducing this ratio gave polypropylene having a much broader

TABLE II
Effect of Hexamethylphosphoric Triamide (HPT) Concentration on the
Polymerization of Propylene with the System $C_2H_5AlCl_2$ -HPT- $TiCl_3$ ^a

| HPT used, mmole | $HP\bar{T}/C_2H_5AlCl_2$ mole ratio | Polymerization rate, mmole/l.-sec. | Polymer properties | |
|--------------------|--|--|--------------------|-------------------------|
| | | | $\{\eta\}^b$ | Insoluble in MIBK, % |
| None | 0 | — ^c | — | — |
| 0.67 | 0.2 | 0.034 | 3.13 | 90.3 |
| 1.67 | 0.5 | 0.418 | 3.17 | 95.3 |
| 2.0 | 0.6 | 0.640 | 3.08 | 96.0 |
| 2.33 | 0.7 | 0.734 | 3.62 | 95.5 |
| 2.66 | 0.8 | 0.699 | 4.08 | 94.1 |
| 3.33 | 1.0 | — ^d | — | — |

^a At 70°C. and 40 psig propylene pressure with the use of equimolar quantities (3.33 mmole) ethylaluminum dichloride and titanium (III) chloride.

^b Determined on gross product.

^c No detectable rate. Polypropylene was produced at the average rate of 0.2 g./g. $TiCl_3$ /hr.

^d No polymerization.

TABLE III
Effect of $TiCl_3$ Concentration on the Polymerization of Propylene
with the System $C_2H_5AlCl_2$ -HPT- $TiCl_3$ ^a

| $TiCl_3$ used, mmole | $TiCl_3/-$ $C_2H_5AlCl_2$ mole ratio | Polymerization rate, mmole/l.-sec. | Polymer properties | |
|----------------------------|--|--|--------------------|-------------------------|
| | | | $\{\eta\}^b$ | Insoluble in MIBK, % |
| None | 0 | — ^c | — | — |
| 0.33 | 0.1 | 0.090 | 3.41 | 95.7 |
| 1.67 | 0.5 | 0.418 | 3.02 | 95.6 |
| 3.33 | 1.0 | 0.683 | 3.13 | 96.0 |
| 6.66 | 2.0 | 1.151 | 2.78 | 93.4 |

^a At 70°C. and 40 psig propylene pressure with the use of 3.33 mmole of ethylaluminum dichloride and 2.0 mmole of HPT (hexamethylphosphoric triamide).

^b Determined on gross product.

^c No polymerization.

crystallinity distribution. As shown in Figure 5, the activity of the catalyst increased with increasing HPT/ $C_2H_5AlCl_2$ mole ratio to a maximum value at the ratio of 0.7, then decreased rapidly as the mole ratio continued to increase. Similar observations were made by Boor,²³ who showed that certain polar compounds, when added to a so-called Ziegler-type catalyst, first caused a decrease and then an increase in the activity of the catalyst to a maximum value as the amount of polar additive was increased to the optimum concentration. The molecular weight as reflected by the inherent viscosity of the polymer produced was essentially independent of the HPT/ $C_2H_5AlCl_2$ mole ratio up to a value of about 0.6, but increased with increasing mole ratio above this value (Fig. 6).

At the optimum HPT/ $C_2H_5AlCl_2$ mole ratio of 0.6, catalyst stereo-

TABLE IV
Effect of $C_2H_5AlCl_2$ Concentration on the Polymerization of Propylene
with the System $C_2H_5AlCl_2$ -HPT- $TiCl_3$ ^a

| $C_2H_5AlCl_2$ used, mmole | HPT/ $C_2H_5AlCl_2$ mole ratio | $TiCl_3$ / $C_2H_5AlCl_2$ mole ratio | Polymeri- zation rate, mmole/l.-sec. | Polymer properties | |
|----------------------------------|---|---|---|-------------------------|-------------------------|
| | | | | $\{\eta\}$ ^b | Insoluble in MIBK, % |
| 1.67 | 1.2 | 2.0 | — ^c | — | — |
| 2.66 | 0.75 | 1.25 | 0.711 | 3.65 | 95.7 |
| 3.33 | 0.6 | 1.0 | 0.683 | 3.13 | 96.0 |
| 6.66 | 0.3 | 0.5 | 0.103 | 3.12 | 91.8 |
| 9.99 | 0.2 | 0.33 | 0.051 | 3.00 | — |

^a At 70°C. and 40 psig. propylene pressure with the use of 3.33 mmole of titanium(III) chloride and 2.0 mmole of HPT (hexamethylphosphoric triamide).

^b Determined on gross product.

^c No polymerization.

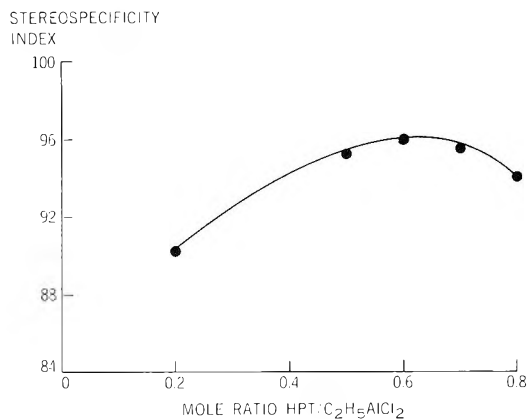


Fig. 4. Effect of varying HPT/ $C_2H_5AlCl_2$ mole ratio on the stereospecificity index of the three-component catalyst $C_2H_5AlCl_2$ -HPT- $TiCl_3$ in the polymerization of propylene at 40 psig and 70°C. with the use of equimolar quantities (3.33 mmole) of violet $TiCl_3$ and $C_2H_5AlCl_2$.

specificity and polymer inherent viscosity were independent of titanium(III) chloride concentration, but only if the $TiCl_3$ / $C_2H_5AlCl_2$ mole ratio did not appreciably exceed unity (Table III). Both stereospecificity and inherent viscosity were reduced, however, by increasing the titanium(III) chloride concentration. Catalyst activity increased with increasing titanium(III) chloride concentration (Fig. 7).

When molar concentrations of ethylaluminum dichloride equivalent to or less than that of HPT were used, catalytically inactive systems were obtained. Increasing the concentration of ethylaluminum dichloride to give HPT/ $C_2H_5AlCl_2$ mole ratios of slightly less than unity provided optimum catalytic activity and stereospecificity (Table IV). As was previously noted, both stereospecificity and activity decreased rapidly as the HPT/ $C_2H_5AlCl_2$ ratio was decreased below 0.6. Thus, the addition of ethyl-

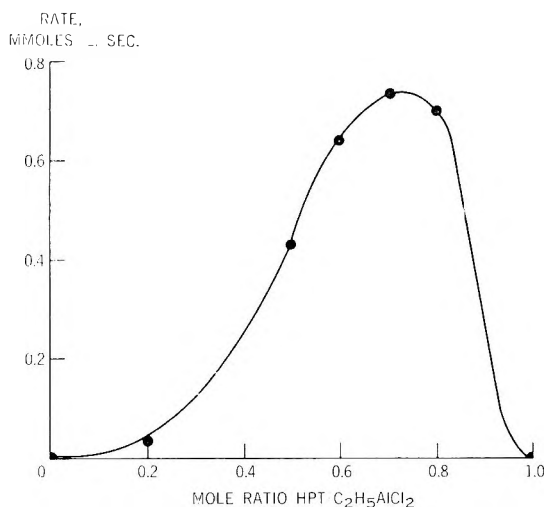


Fig. 5. Effect of varying HPT/C₂H₅AlCl₂ mole ratio on rate of propylene polymerization at 40 psig and 70°C. with the use of equimolar quantities (3.33 mmole) of violet TiCl₃ and C₂H₅AlCl₂.

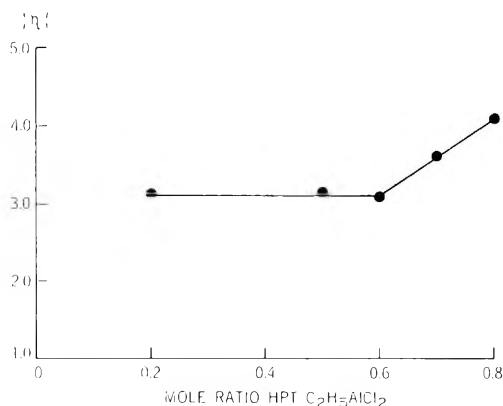


Fig. 6. Effect of varying HPT/C₂H₅AlCl₂ mole ratio on the inherent viscosity of the polypropylene produced at 40 psig propylene pressure and 70°C. with the use of equimolar quantities (3.33 mmole) of violet TiCl₃ and C₂H₅AlCl₂.

aluminum dichloride to the three-component system comprising C₂H₅AlCl₂-0.6 HPT-TiCl₃ decreased both the stereospecificity and activity of the catalyst (Table IV). Surprisingly, the inherent viscosity of the polymer was not affected appreciably even by a three-fold increase in the concentration of the ethylaluminum dichloride. This suggests that the ethylaluminum dichloride is relatively ineffective as a chain-transfer agent, but that in large excess it deactivates or prevents the formation of active sites.

Nature of the Third Component. A series of similar ligands were investigated as third components in combination with ethylaluminum dichloride and titanium(III) chloride in order to study their effects on the nature of

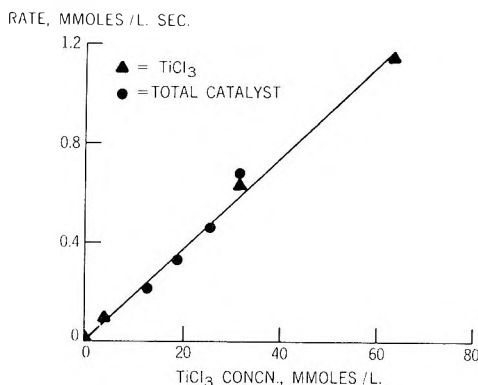


Fig. 7. Effect of TiCl_3 concentration on the rate of propylene polymerization at 40 psig, 70°C ., and HPT/ $\text{C}_2\text{H}_5\text{AlCl}_2$ mole ratio of 0.6.

the three-component catalysts. The results are shown in Table V for TC/ $\text{C}_2\text{H}_5\text{AlCl}_2$ mole ratios giving maximum reaction rates. It is evident that the ligands used in the various three-component catalysts can be separated into two groups based on the catalyst stereospecificities obtained. The highest stereospecificities (97.1–97.3%) were afforded by the group consisting of triphenylphosphine and butyl sulfide. The second group, providing slightly lower stereospecificities (95.5–95.6%), comprises HPT, tributylamine, and butyl ether. It should be noted that the various third components grouped in this manner are separated on the basis of the electronegativities of their ligand atoms. Catalyst stereospecificity thus appeared to increase as the electronegativity of the ligand atom in the third component decreased. In general, both aluminum and titanium com-

TABLE V
Effect of the Nature of the Third Component on the Polymerization of Propylene with $\text{C}_2\text{H}_5\text{AlCl}_2$ -TC- TiCl_3 ^a

| Substance | Third component (TC) | | Polymerization rate, mmole/l. sec. | Polymer properties | |
|---|---|---|------------------------------------|-------------------------|----------------------|
| | Electronegativity of ligand atom ^b | TC/ $\text{C}_2\text{H}_5\text{AlCl}_2$ mole ratio ^c | | { η } ^d | Insoluble in MIBK, % |
| (C_4H_9) ₂ O | 3.5 | 0.6 | 0.486 | 2.90 | 95.6 |
| (C_4H_9) ₃ N | 3.0 | 0.7 | 1.010 | 3.00 | 95.6 |
| HPT | 3.0 (N) | 0.7 | 0.734 | 3.62 | 95.5 |
| (C_4H_9) ₂ S | 2.5 | 0.7 | 0.154 | 3.15 | 97.1 |
| $\text{C}_4\text{H}_9\text{I}$ | 2.5 | 0.7 | — ^e | 2.42 | — |
| (C_6H_5) ₃ P | 2.1 | 0.7 | 0.729 | 3.10 | 97.3 |

^a At 70°C . and 40 psig propylene pressure with the use of equimolar quantities (3.33 mmole) of ethylaluminum dichloride and titanium(III) chloride.

^b Pauling electronegativity.

^c Mole ratio giving optimum rate.

^d Determined on gross product.

^e Too low to measure.

ห้องสมุด กรมวิทยาศาสตร์

TABLE VI
Effect of $(C_4H_9)_3N$ Concentration on the Polymerization of Propylene
with the System $C_2H_5AlCl_2-(C_4H_9)_3N-TiCl_3^a$

| $(C_4H_9)_3N$ used, mmole | $(C_4H_9)_3N/$ $C_2H_5AlCl_2$ mole ratio | Polymerization rate, mmole/l.-sec. | Polymer properties | |
|---------------------------------|--|--|--------------------|-------------------------|
| | | | $\{\eta\}^b$ | Insoluble in MIBK, % |
| 1.67 | 0.5 | 0.614 | 2.77 | 93.8 |
| 2.0 | 0.6 | 0.831 | 2.84 | 94.4 |
| 2.33 | 0.7 | 1.010 | 3.00 | 95.6 |
| 2.66 | 0.8 | 0.674 | 4.78 | 95.4 |
| 3.0 | 0.9 | — ^c | — | — |

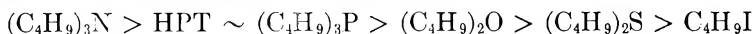
^a At 70°C. and 40 psig propylene pressure with the use of equimolar quantities (3.33 mmole) of ethylaluminum dichloride and titanium(III) chloride.

^b Determined on gross product.

^c No polymerization

pounds would be expected to form their most stable complexes with the nitrogen and phosphorus ligands. It is evident, therefore, that these small differences in stereospecificity cannot be interpreted on the basis of the complexing affinities of the ligands in question. These differences may indeed be insignificant.

The activity of a three-component catalyst increased with increasing basicity of the third component as follows:



The three-component catalyst containing tributylamine gave maximum activity and stereospecificity at a $(C_4H_9)_3N/C_2H_5AlCl_2$ mole ratio of 0.7, and maximum polymer molecular weight at a mole ratio of 0.8 (Table VI). Although the two catalysts had comparable stereospecificities, the maximum propylene polymerization rate at 70°C. obtained with the tributylamine system was about 40% greater than that observed for the optimum HPT system (Tables II and VI).

Catalysts containing either butyl ether or butyl sulfide as the third component showed maximum activity at the 0.6–0.7 mole ratio of third component to ethylaluminum dichloride. Catalyst systems containing butyl ether were about 66% as active as those containing HPT, whereas systems containing butyl sulfide were only about 21% as active. Catalysts containing the ether were considerably more sensitive to variations in the amount of third component used than those containing the sulfide.

Polymer inherent viscosity was, in general, independent of the nature of the third component, except that HPT afforded the highest inherent viscosity and 1-iodobutane afforded the lowest viscosity.

Nature of the Alkyl Group in Alkylaluminum Dichloride. The nature of the hydrocarbon radical in the alkylaluminum dichloride component of a three-component catalyst containing HPT and titanium(III) chloride had little effect on catalyst stereospecificity, but greatly affected catalyst activity. The data in Table VII show that there were no significant dif-

TABLE VII
Effect of the Nature of the Alkyl Group in RAlCl_2 on the
Polymerization of Propylene with the Systems RAlCl_2 -0.6 HPT- TiCl_3 ^a

| RAlCl_2 | Polymerization rate, mmole/l.-sec. | Polymer properties | |
|---|--|--------------------|-------------------------|
| | | $\{\eta\}^b$ | Insoluble in MIBK, % |
| CH_3AlCl_2 | 0.106 | 3.97 | 97.1 |
| $\text{C}_2\text{H}_5\text{AlCl}_2$ | 0.683 | 3.14 | 96.3 |
| $(\text{CH}_3)_2\text{CHCH}_2\text{AlCl}_2$ | 0.085 | 3.85 | 94.8 |
| $\text{C}_8\text{H}_{17}\text{AlCl}_2$ | 0.106 | 3.70 | 96.4 |

^a At 70°C. and 40 psig propylene pressure with the use of equimolar quantities (3.33 mmole) of alkylaluminum dichloride and titanium(III) chloride and 2.0 mmole of HPT (hexamethylphosphoric triamide).

^b Determined on gross product.

ferences in the stereospecificities of catalysts in which the alkyl group of the alkylaluminum dichloride component was unbranched. Branching in the alkyl group, as in isobutylaluminum dichloride, only slightly reduced stereospecificity.

Ethylaluminum dichloride provided by far the most active catalyst of any of the alkylaluminum dichlorides studied. As shown in Table VII, the methyl-, isobutyl-, and octylaluminum dichlorides gave catalysts which were essentially equivalent in activity, but which were only about 16% as active as that obtained from the ethyl homolog. Other investigators have shown that the nature of the alkyl group in trialkylaluminum catalysts has a pronounced effect on both catalyst stereospecificity and activity.²⁴ In these catalysts, maximum activity was observed when the alkyl group had four carbon atoms, although triethylaluminum gave the most stereospecific catalyst.

Nature of the Halogen in Ethylaluminum Dihalide. It has been reported that the stereospecificity of the $\text{R}_2\text{AlX-TiCl}_3$ catalyst system is strongly influenced by the nature of the halogen atom in the dialkylaluminum halide.¹⁴ In the present study, it was desired to determine if an analogous behavior could be found in the three-component alkylaluminum dihalide-type catalysts. Propylene polymerizations were carried out, therefore, with the use of the system $\text{C}_2\text{H}_5\text{AlX-0.6 HPT-TiCl}_3$ in which the halogen (X) was varied. Polymerizations were also carried out under the same conditions with a similar series of $(\text{C}_2\text{H}_5)_2\text{AlX-TiCl}_3$ catalyst systems in order to afford a direct comparison of the two types of catalysts. The data are summarized in Table I. Both types of catalysts showed increasing stereospecificity and decreasing activity as the electronegativity of the halogen atom in the alkylaluminum halide decreased. The data show, however, that the various three-component catalysts were more stereospecific than their $\text{R}_2\text{AlX-TiCl}_3$ counterparts. It is also evident from these data that the three-component catalyst $\text{C}_2\text{H}_5\text{AlI}_2$ -0.6 HPT- TiCl_3 which provided a propylene polymer that was 99.2% insoluble in MIBK, was the most stereospecific catalyst studied. This catalyst, however, was only about 84% as

active as the corresponding system containing ethylaluminum dichloride and gave propylene polymer having 20% lower inherent viscosity. It can be seen that the three-component catalysts were only 45–80% as active as the corresponding $(C_2H_5)_2AlX-TiCl_3$ catalysts under the conditions studied.

Nature of the Titanium(III) Halide. Natta and co-workers¹⁴ showed that the violet forms of titanium(III) chloride (α , γ , δ) are essentially equivalent as components of olefin polymerization catalysts and provide comparable stereospecificities. The brown, or β -form, of titanium(III) chloride, however, gave catalysts with lower stereospecificities.²³ Previous investigators, in studying catalysts prepared from triethylaluminum and various titanium(III) halides, found that catalyst stereospecificity decreased with decreasing electronegativity or increasing size of the halogen atoms in the titanium(III) halide.²⁵ In the present work, active three-component alkylaluminum dihalide catalysts were obtained only from violet titanium(III) chloride. As shown in Table VIII, a three-component system containing the brown, or β -form, of titanium(III) chloride was virtually inactive. Although this catalyst was far less stereospecific than the three-component catalyst containing violet titanium(III) chloride, it was much more stereospecific than the corresponding two-component

TABLE VIII
Effect of the Nature of the Titanium(III) Halide on Various
Catalyst Systems in the Polymerization of Propylene^a

| TiX ₃ | Organometallic component | Pro- pylene pressure, psig | Polymeri- zation rate mmole/l.- sec. | Polymer properties | |
|--------------------------------|--|-------------------------------------|---|-------------------------|-------------------------|
| | | | | { η } ^b | Insoluble in MIBK, % |
| TiF ₃ | C ₂ H ₅ AlCl ₂ + 0.6 HPT | 40 | — ^c | — | — |
| TiCl ₃ ^d | C ₂ H ₅ AlCl ₂ + 0.6 HPT | 40 | 0.683 | 3.14 | 96.3 |
| β -TiCl ₃ | C ₂ H ₅ AlCl ₂ + 0.6 HPT | 40 | — ^c | 3.72 | 74.6 |
| TiBr ₃ | C ₂ H ₅ AlCl ₂ + 0.6 HPT | 40 | — ^c | — | — |
| TiI ₃ | C ₂ H ₅ AlCl ₂ + 0.6 HPT | 40 | — ^c | — | — |
| TiF ₃ | (C ₂ H ₅) ₃ Al | 40 | — ^c | — | — |
| TiCl ₃ ^d | " | 10 | 1.62 | 1.84 | 79.9 |
| β -TiCl ₃ | " | 10 | 0.900 | 1.12 | 47.7 |
| TiBr ₃ | " | 40 | 0.048 | 1.46 | 52.5 |
| TiI ₃ | " | 40 | 0.075 | 0.87 | 46.1 |

^a At 70°C. with the use of equimolar quantities (3.33 mmole) of alkylaluminum and titanium(III) halide.

^b Determined on gross product.

^c No reaction under the conditions used.

^d Used Stauffer (HA) titanium(III) chloride.

^e No measurable rate. Polypropylene was formed at the average rate of about 1.02 g./g. TiCl₃/hr.

triethylaluminum catalyst which was studied for comparison. Three-component systems containing titanium(III) halides other than the chloride were inactive as olefin polymerization catalysts under the conditions studied.

CONCLUSION

It has been shown that the three-component catalysts consisting of alkylaluminum dihalides, violet titanium(III) chloride, and a third component derived from one or more of the strongly complexing ligand elements have the highest stereospecificities known. Propylene is easily polymerized in the presence of these catalysts to give highly stereoregular polypropylene. The use of these catalysts to polymerize other α -olefins will be described in a future publication.

The authors gratefully acknowledge the assistance of C. M. Shelton for carrying out the polymerization reactions, and M. A. McCall and Wayne Reynolds for the preparation of many of the catalyst intermediates.

References

1. Staudinger, H., *Die Hochmolekularen Organischen Verbindungen—Kautschuk and Cellulose*, Springer, Berlin, 1932, p. 165.
2. Huggins, M. L., *J. Am. Chem. Soc.*, **66**, 1991 (1944).
3. Kraus, C. A. (to Standard Oil Development Co.), U. S. Pat. 2,220,930 (1940).
4. Hall, F. C., and A. W. Nash, *J. Inst. Petrol.*, **23**, 679 (1937).
5. Fischer, M. (to Badische Anilin- und Soda-Fabrik A. G.), German Pat. 874,215 (1953).
6. Joyner, F. B., N. H. Shearer, Jr., and H. W. Coover, Jr., *J. Polymer Sci.*, **58**, 881 (1962).
7. Coover, H. W., Jr., and F. B. Joyner (to Eastman Kodak Co.), U. S. Pat. 2,969,345 (1961).
8. Brauer, G., *Handbuch der Preparativen Anorganischen Chemie*, Ferdinand Enke Verlag, Stuttgart, Germany, 1960, pp. 230–231.
9. Rolsten, R. F., and H. H. Sisler, *J. Am. Chem. Soc.*, **79**, 5891 (1957).
10. Coover, H. W., Jr., J. E. Guillet, R. L. Combs, and F. B. Joyner, *J. Polymer Sci.*, in press.
11. Schulken, R. M., Jr., and M. L. Sparks, *J. Polymer Sci.*, **26**, 227 (1957).
12. Desreux, V., and M. C. Spiegels, *Bull. Soc. Chim. Belges*, **59**, 476 (1950).
13. Flory, P. J., *Principles of Polymer Chemistry*, Cornell Univ. Press, Ithaca, N. Y., 1953, p. 569.
14. Natta, G., I. Pasquon, A. Zambelli, and G. Gatti, *J. Polymer Sci.*, **51**, 387 (1961).
15. Cash, G. O., Jr., unpublished data.
16. Natta, G., G. Mazzanti, G. Crespi, and G. Moraglio, *Chim. Ind. (Milan)*, **39**, 275 (1957).
17. Natta, G., and I. Pasquon, *Actes Congr. Intern. Catalyse 2^e, Paris*, **1**, 1373 (1961).
18. Natta, G., E. Giachetti, I. Pasquon, and G. Pajaro, *Chim. Ind. (Milan)*, **42**, 1091 (1960).
19. Ambroz, J., *Chem. Prumysl.*, **10**, 278 (1960).
20. Razuvaev, G. A., K. S. Minsker, G. T. Fedoseeva, and V. K. Bykhovskii, *Polymer Sci. (USSR) (Engl. Transl.)*, **2**, 299 (1961).
21. Zambelli, A., J. Dipietro, and G. Gatti, *J. Polymer Sci.*, **A1**, 403 (1963).
22. McConnell, R. L., M. A. McCall, F. B. Joyner, and H. W. Coover, Jr., G. O. Cash, Jr., *J. Polymer Sci.*, **A2**, 2135 (1964).

23. Boor, J., Jr., paper presented at the First Biennial Symposium of the American Chemical Society, Michigan State University, June 1962.

24. Natta, G., P. Pino, G. Mazzanti, and P. Longi, *Gazz. Chim. Ital.*, **88**, 219 (1958).

25. Cooper, W., *Progress in High Polymers*, Vol. I, J. C. Robb and F. W. Peaker, Eds., Academic Press, New York, 1961, pp. 281-333.

Résumé

Il est bien connu que des mélanges de dihalogénures d'alcoylaluminium et d'halogénures d'un métal de transition tel que le chlorure de titane(III) sont inefficaces comme catalyseurs pour la polymérisation stéréospécifique des α -oléfines. On a découvert que l'addition à de tels mélanges d'un troisième composé dérivé de l'un ou de plusieurs des éléments de coordination à pouvoir de complexation élevé tels que l'azote, l'oxygène et le phosphore, produit des catalyseurs possédant les stéréospécificités les plus élevées connues actuellement. Dans le présent travail on a étudié l'influence de plusieurs de ces composés additionnels sur l'activité et la stéréospécificité de ces catalyseurs dans la polymérisation du propylène. La stéréospécificité et l'activité des catalyseurs à trois composants de ce type dépendent du rapport du troisième composé vis-à-vis du dihalogénure d'alcoylaluminium. La stéréospécificité et l'activité optimum sont habituellement obtenues pour des rapports de l'ordre de 0.5 à 0.7. En général, l'activité catalytique augmente avec l'augmentation de basicité du troisième composant. La stéréospécificité ainsi que l'activité sont influencées par la nature des atomes d'halogène des dihalogénures d'alcoylaluminium, tandis que la nature du groupe alcoyle affecte seulement l'activité, le groupement éthyle fournissant les catalyseurs les plus actifs. Le catalyseur le plus stéréospécifique a été préparé au moyen d'un mélange de diiodure d'éthylaluminium, de triamide hexaméthylphosphorique et de chlorure de titane(III) violet.

Zusammenfassung

Bekanntermassen sind Mischungen von Alkylaluminiumdihalogeniden und Übergangsmetallhalogeniden, wie z.B. Titan(III) chlorid als Katalysatoren für die stereospezifische Polymerisation von α -Olefinen unwirksam. Es wurde gefunden, dass der Zusatz einer dritten, von einem oder mehreren der stark komplexierenden Ligandenelemente, wie Stickstoff, Sauerstoff, und Phosphor abgeleiteten Verbindung zu solchen Mischungen zu Katalysatoren mit der höchsten bekannten Stereospezifität führt. In der vorliegenden Arbeit wurde der Einfluss verschiedener dritter Komponenten auf die Aktivität und Stereospezifität dieser Katalysatoren bei der Propylenpolymerisation untersucht. Stereospezifität und Aktivität der Dreikomponentenkatalysatoren dieses Typs war vom Verhältnis der dritten Komponente zum Alkylaluminiumdihalogenid abhängig. Optimale Stereospezifität und Aktivität wurde gewöhnlich bei Verhältnissen im Bereich von 0,5 bis 0,7 erhalten. Im allgemeinen nahm die katalytische Aktivität mit steigender Basizität der dritten Komponente zu. Stereospezifität und Aktivität wurden durch die Natur der Halogenatome im Alkylaluminiumdihalogenid beeinflusst, während die Natur der Alkylgruppe nur Einfluss auf die Aktivität besass, wobei die Äthylgruppe die aktivsten Katalysatoren lieferte. Katalysatoren mit der höchsten Stereospezifität wurden aus einer Mischung von Äthylaluminiumdijodid, Hexamethylphosphorsäuretriamid und violetter Titan(III)-chlorid erzeugt.

Received September 28, 1964

Revised January 15, 1965

Prod. No. 4623A

Synthesis of Polyhydrazones and Polypyrazoles by a Polycyclization Reaction

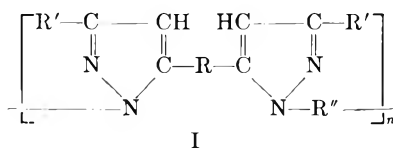
V. V. KORSHAK, E. S. KRONGAUZ, and A. M. BERLIN, *Institute of Elemento-Organic Compounds, Academy of Sciences, Moscow, U.S.S.R.**

Synopsis

By the interaction of linear or branched bis(β -diketones) and dihydrazides of dicarboxylic acids or dihydrazines unknown high molecular compounds with pyrazole rings in the chain have been prepared. Polypyrazoles of the second type (with a free NH-group in the pyrazole ring) were prepared by the interaction of bisdiazalkanes and diacetylenes. Some features of the polycyclization reaction as well as the structure and properties of polymers obtained are discussed.

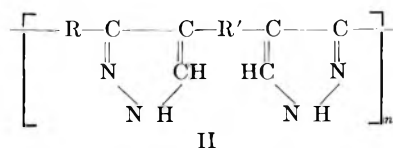
In our search for new types of polymers and novel methods of preparation of such polymers we synthesized some previously unknown high molecular compounds with pyrazole rings in the chain.¹⁻⁵

Polypyrazoles of the type of having the general formula I:



where R may be CH₂, CH₂-C₆H₄-CH₂, CH₂-C₆H₄-C₆H₄-CH₂, CH₂-C₆H₄-O-C₆H₄-CH₂, C₆H₄-O-C₆H₄, C₆H₄-CH₂-CH₂-C₆H₄, or (CH₂)₈; R' is CH₃ or C₆H₅; and R'' is CO(CH₂)₄CO, CO-C₆H₄-CO, (CH₂)₆, or C₆H₄, were obtained by the interaction of linear or branched bis-(β -diketones) and dihydrazides of dicarboxylic acids or dihydrazines.

Polypyrazoles of a second type with a free NH group, having the general formula II:



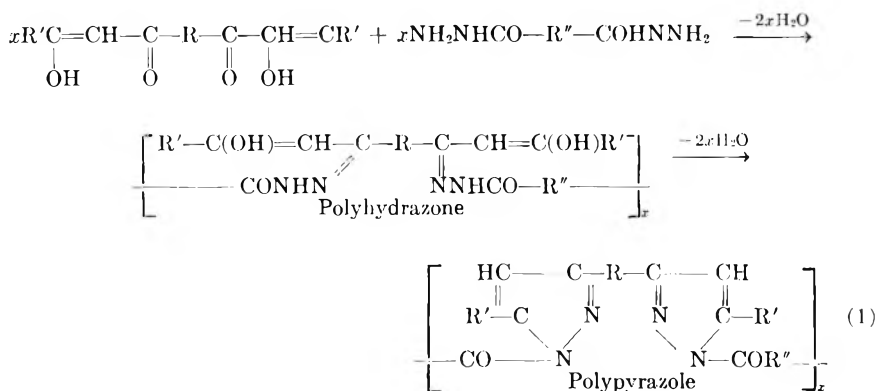
where R may be (CH₂)₄, or C₆H₄; and R' may be C₆H₄ or absent, were prepared through the interaction of bisdiazalkanes and diacetylenes.

* Translated by A. L. Pumpiansky Moscow.

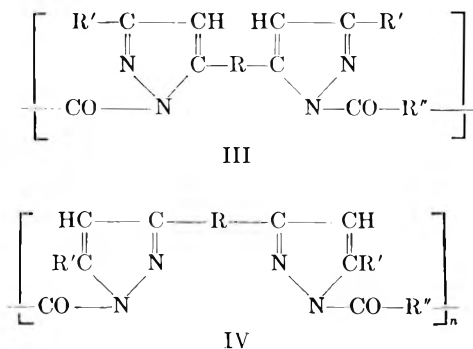
We refer to these reactions as polycyclization because the polymer is formed due to the closure of the pyrazole ring.

The polycyclization reaction of bis(β -diketones) of a linear structure ($R'COCH_2-CO-R-COCH_2COR'$) with dihydrazides proceeds by way of two steps. First, boiling an equimolecular mixture of bis(β -diketone) and dihydrazide in ethanol gives rise to the polyhydrazone, which is isolated as a precipitate. Subsequently, heating the polyhydrazones *in vacuo* at the temperature of melting under nitrogen results in the closure of the pyrazole rings and a quantitative yield of polypyrazoles.

The overall reaction can be schematically represented as shown in eq. (1):

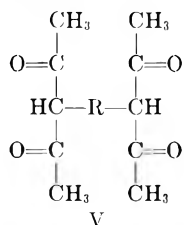


It is to be noted that we did not locate the exact position of the enol hydroxyl in the bis(β -diketones), depending on which the resulting polypyrazoles may have one of the two isomeric structures III or IV.



It is, however, reported in the literature that a benzoylacetone similar in structure to the linear bis(β -diketones) under investigation contains an 80% enolized acetyl carbonyl.⁶ This led us to choose structure IV as the more probable one. In branched bis(β -diketones), only one structure is, of course, possible, the molecule being symmetrical.

Investigation of the polycyclization reaction showed that bis(β -diketones) with a branched structure such as V



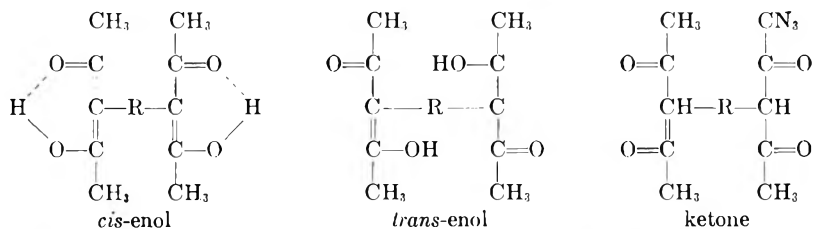
behave differently than do linear bis(β -diketones). Thus, tetracetylene gave only a polyhydrazone; it proved impossible to effect its closure to polypyrazole either on heating at a high temperature *in vacuo* or by using catalysts (ZnCl_2 , glacial CH_3COOH). Tetraacetylpropane also gave polyhydrazone that on continued heating invariably led to one and the same product with the same melting point and elementary analysis, corresponding to a mixture of polypyrazole and polyhydrazone in a 1:1 ratio.

ANAL. Calc.: C, 61.62%; H, 7.21%; N, 16.91%. Found: C, 61.62, 61.58%; H, 7.19, 7.22%; N, 16.82, 16.93%.

The reaction of 1,4-bis(2',2'-diacetoethyl)benzene, 4,4'-bis(2'',2''-diacetoethyl)diphenyl, and 4,4'-bis(2'',2''-diacetoethyl)diphenyloxide with adipic hydrazide proceeds much more vigorously than it does with other bis(β -diketones) under study to result under the same conditions directly in polypyrazole, without preliminary formation of polyhydrazones.

Such a difference in the behavior of these bis(β -diketones) seems to be accounted for by structural considerations. This suggestion is substantiated by the comparative infrared spectral investigation of bis(β -diketones) and acetyl acetones.

3-Alkyl-substituted acetylacetones have been shown by Kabachnik et al.⁷⁻¹⁰ and other workers¹¹ to exist in three tautomeric forms: ketone, *cis*-enol and *trans*-enol. Hence, our bis(β -diketones) may also exist such forms.



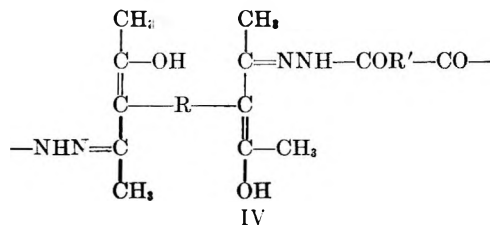
The infrared evidence showed all linear bis(β -diketones) under investigation to be 100% *cis*-enolic, as they revealed absorption bands over the range of 1600-1620 cm^{-1} that are characteristic of vibrations of a ring with intramolecular, bonding, assigned to vibrations of *cis*-enols. Tetraacetylene was also shown to be completely enolized, as seen from the absence of the absorption band peculiar to the stretching vibrations of a

ketone group ($1700\text{--}1730\text{ cm.}^{-1}$), but to be a *trans*-enol with an intensive maximum at 1580 cm.^{-1} . The infrared spectra of 3-alkyl acetylacetones with branched substituents in position 3 that would entail steric hindrance to *cis*-enolization revealed maxima at 1580 and 1680 cm.^{-1} , vibrations assigned to the *trans*-enol form. Tetraacetylpropane exhibited an almost similar absorption both in the range of *trans*-enols and in that of the vibration of ketone groups with maxima at 1580 and $1700\text{--}1730\text{ cm.}^{-1}$. 1,4-Bis-(2',2'-diacetoethyl)benzene, 4,4'-bis(2'',2''-diacetoethyl)diphenyl, and 4,4'-bis(2'',2''-diacetoethyl)diphenyl oxide revealed absorption bands only over the range of $1700\text{--}1730\text{ cm.}^{-1}$, being present only in the ketone form.

Considering, as we did, that the first step of the reaction under study, the formation of polyhydrazones, proceeds by way of an interaction between the carbonyl oxygen of the ketone and the amino group of the hydrazide, such an interaction should be facilitated in the case of *trans*-enol and rendered more difficult in the case of *cis*-enols. In the latter case, additional energy would be needed to break the hydrogen bond in the stable six-membered ring formed as a result of *cis*-enolization.

The production of polyhydrazones from bis(β -diketones) of linear structure, which were shown above to be *cis*-enols, does indeed take place less readily, the reaction proceeding at a slower rate and with sebacyl diaceto-phenone only in the presence of a catalyst, glacial acetic acid.

It is the *trans*-enol structure that seems to account for the fact that tetraacetylthane gives rise to polyhydrazone but fails to be converted to polypyrazole. Furthermore, steric hindrance resulting from *trans*-enolization of tetraacetylthane is enhanced by the formation of the polymeric chain of polyhydrazone (VI), for the molecule becomes less labile, and interaction and formation of a pyrazole ring is thereby even further hindered.



Ketones that react with hydrazides most readily are those in the ketone form leading directly to polypyrazoles. These ketones and dihydrazide of adipic acid were easily fused to give polypyrazoles, whereas with linear bis(β -diketones) the reaction in the melt failed to proceed.

On polycyclization, dihydrazine hydrochlorides (hexamethylene- or *p*-phenylene-dihydrazine) led to polypyrazoles containing no carbonyl group in the macromolecule.

Polypyrazoles with a free NH group were prepared by the interaction of equimolecular amounts of bisdiazocompounds and *p*-diethynylbenzene or diacetylene, according to the scheme shown in eq. (2).

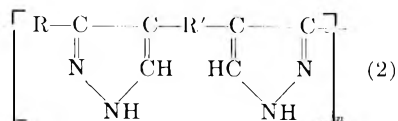
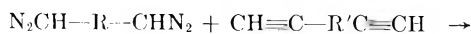
TABLE I
Properties of Polyhydrazones

| No. | Starting compounds | | Softening point, °C. | Reduced viscosity | Yield, % | Analysis | |
|-----|--------------------------------------|------------------|----------------------|-------------------|----------|--------------|---------------|
| | Bis-(β -diketone) | Hydrazide of | | | | N (found), % | N (calcd.), % |
| 1 | 4,4'-Bis(acetoacetyl)-diphenyl oxide | Adipic acid | 185-210 | 0.80 | 97.7 | 11.47 | 11.76 |
| 2 | 4,4'-Bis(acetoacetyl)-diphenylethane | Adipic acid | 156-180 | 1.0-0.08 | 100 | 11.98 | 11.48 |
| 3 | Sebacyl diacetophenone | Adipic acid | 65-75 | 0.08 | 90 | 9.9 | 10.29 |
| 4 | 4,4'-Bis(acetoacetyl)-diphenylethane | Isophthalic acid | 250-260 | 0.16 | 100 | 11.02 | 11.02 |
| 5 | Tetraacetylene | Adipic acid | 165-170 | 0.08 | 50 | 16.62 | 16.66 |
| 6 | Tetraacetylpropane | Adipic acid | 160-170 | 0.06 | 82 | 15.95 | 15.99 |

TABLE II
Properties of Polypyrazoles Prepared by Polycyclization of Bis(β -diketones) with Dihydrazides

| No. | Starting compounds | | Softening point, °C. | Reduced viscosity | Yield, % | Analysis | |
|----------------|--|------------------|----------------------|-------------------|----------|--------------|---------------|
| | Bis(β -diketone) | Hydrazide of | | | | N (found), % | N (calcd.), % |
| 1 | 4,4'-Bis(acetoacetyl)-diphenyl oxide | Adipic acid | 240-250 | 0.10 | Quant. | 12.43 | 12.73 |
| 2 | 4,4'-Bis(acetoacetyl)-diphenylethane | Adipic acid | 218-225 | 0.14 | Quant. | 12.38 | 12.42 |
| 3 | Sebacyl diacetophenone | Adipic acid | 100-120 | 0.08 | Quant. | 11.74 | 11.02 |
| 4 | 4,4'-Bis(acetoacetyl)-diphenylethane | Isophthalic acid | 260-280 | 0.07 | Quant. | 12.59 | 11.86 |
| 5 ^a | 1,4-Bis(2',2'-diacetoethyl)benzene | Adipic acid | 230-300 | 0.14 | Quant. | 14.20 | 13.86 |
| 6 ^a | 4,4'-Bis(2'',2''-diacetoethyl)diphenyl | Adipic acid | 248-260 | 0.14 | 96.8 | 11.95 | 11.65 |
| 7 ^a | 4,4'-Bis(2'',2''-diacetoethyl)diphenyl oxide | Adipic acid | 245-256 | 0.15 | Quant. | 11.52 | 11.28 |

^a Polymers were prepared by fusion of starting compounds. Viscosity was determined for 0.5% solutions in sulfuric acid.



The resulting polymers are yellow powders soluble in dimethylformamide and differ from the polymers considered above by higher melting points, apparently due to a different structure of their polymer chains.

Polypyrazoles from bis(β -diketones) may be regarded as heterochain polymers, because the nitrogen atom participates directly in the building up of the polymer chain, whereas the polymer chain of polypyrazoles from bisdiazalkanes consists solely of carbon atoms. The NH group is involved in the formation of hydrogen bonds, resulting in increased interaction of chains and enhanced thermal stability.

The properties of the polymers are listed in Tables I-V.

TABLE III
Properties of Polypyrazoles Prepared by Polycyclization
of Bis(β -diketones) with Dihydrazines

| No. | Starting compounds | | Polymer softening point, °C. | Reduced viscosity (0.5% solution in cresol) |
|----------------|---|--------------------------------|------------------------------|---|
| | Bis (β -diketone) | Dihydrazine (hydrochloride) | | |
| 1 ^a | 1,4-Bis(2',2'-diacetoethyl)-benzene | <i>p</i> -Phenylenedihydrazine | 262-265 | 0.15 |
| 2 ^a | 1,4-Bis(2',2'-diacetoethyl)-benzene | Hexamethylenedihydrazine | 150-162 | 0.18 |
| 2 ^b | 1,4-Bis(2',2'-diacetoethyl)-benzene | Hexamethylenedihydrazine | 156-174 | 0.25 |
| 3 | 4,4'-Bis(2'',2''-diacetoethyl)-diphenyl | Hexamethylenedihydrazine | 141-146 | 0.08 |
| 4 ^a | 4,4'-Bis(2'',2''-diacetoethyl)-diphenyl | <i>p</i> -Phenylenedihydrazine | 120-132 | 0.09 |
| 5 ^a | 4,4'-Bis(acetoacetyl)diphenyloxide | <i>p</i> -Phenylenedihydrazine | 122-140 | 0.09 |
| 6 ^a | 4,4'-Bis(acetoacetyl)diphenyl oxide | Hexamethylenedihydrazine | 118-124 | 0.12 |

^a Reaction was carried out in pyridine.

^b Reaction in the melt.

RESULTS AND DISCUSSION

The polyhydrazones are greenish powders, soluble in conventional organic solvents. They have no sharp melting point because heating leads to a partial formation of polypyrazoles melting at higher temperatures. The reduced viscosity of 0.5% solutions of polyhydrazones in cresol was as high as 0.4. During the formation of polypyrazoles from

TABLE IV
Properties of Polypyrazoles Prepared by Interaction of Bipyrzoles and Diisocyanates

| No. | Starting compounds | | Softening point, °C. | Reduced viscosity | Yield, % | Analysis | |
|-----|--|----------------------------|----------------------|-------------------|----------|--------------|---------------|
| | Bipyrzole | Diisocyanate | | | | N (found), % | N (calcd.), % |
| 1 | 1,4-Bis(3,5-dimethylpyrazolyl-4)-xylylene | Hexamethylene diisocyanate | 208-215 | 0.14 | 71.6 | 18.45 | 18.25 |
| 2 | 4,4'-Bis[5-(3-methylpyrazolyl-3(5))diphenyl]oxide | Hexamethylene diisocyanate | 220-235 | 0.16 | 82.75 | 17.28 | 17.45 |
| 3 | Di(3,5-dimethylpyrazolyl-4) | Hexamethylene diisocyanate | 230-246 | 0.26 | 86.84 | 22.69 | 22.68 |
| 4 | 1,4-Bis(3,5-dimethylpyrazolyl-4)-xylylene | Toluylene diisocyanate | 260-272 | 0.13 | 90 | 18.78 | 17.93 |
| 5 | 4,4'-Bis[5(3)-methylpyrazolyl-3(5)]-diphenyl oxide | Toluylene diisocyanate | 210-254 | 0.15 | 86.84 | 16.52 | 16.65 |
| 6 | Di(3,5-dimethylpyrazolyl-4) | Toluylene diisocyanate | 230-276 | 0.16 | 89.58 | — | — |

TABLE V
Properties of Polypyrazoles Prepared by Interaction of Bisdiazoalkanes and Diacetylenes

| No. | Starting compounds | | Softening point, °C. | Reduced viscosity | Yield, % | Analysis | | | |
|-----|--------------------|----------------------|----------------------|-------------------|----------|----------|------|--------|------|
| | Diazoalkane | Diacetylene | | | | Found | | Calcd. | |
| | | | | | C, % | H, % | C, % | H, % | |
| 1 | 1,6-Bisdiazohexane | 1,4-Diethynylbenzene | 440 (dec.) | 0.30 | Quant. | 72.48 | 6.47 | 72.69 | 6.69 |
| 2 | 1,6-Bisdiazohexane | Diacetylene | 350-375 | 0.31 | 50 | 64.05 | 6.88 | 63.80 | 6.42 |
| 3 | 1,4-Bisdiazoxyene | 1,4-Diethynylbenzene | >500 | 0.24 | 30 | 75.84 | 4.43 | 76.03 | 4.25 |

TABLE VI

| No. | Bipyrazoles | Melting point, °C. | Yield, % | Analysis | | | | | |
|-----|---|--------------------|----------|----------|------|-------|--------|------|-------|
| | | | | Found | | | Calcd. | | |
| | | | | C, % | H, % | N, % | C, % | H, % | N, % |
| 1 | 4,4'-Bis[5(3)-methylpyrazolyl-3(5)]-diphenylethane | 252-254 | 78 | 76.46 | 6.54 | 16.41 | 77.20 | 6.48 | 16.37 |
| 2 | 4,4'-Bis[5(3)-methylpyrazolyl-3(5)]-diphenyl oxide | 239-240 | 86 | 69.35 | 5.99 | 15.46 | 69.61 | 6.07 | 15.47 |
| 3 | 1,4-Bis(3,5-dimethylpyrazolyl-4)-xylene | 318-320 | 89 | 73.63 | 7.61 | 19.36 | 73.43 | 7.58 | 19.03 |
| 4 | 4,4'-Bis(3,5-dimethylpyrazolyl-4)-methyl(diphenyl oxide | 234-236 | 79 | 74.03 | 6.92 | 14.67 | 74.19 | 7.26 | 14.42 |
| 5 | 4,4'-Bis(3,5-dimethylpyrazolyl-4)-methyl(diphenyl | 292-294 | 88 | 77.92 | 7.18 | 15.00 | 77.80 | 7.07 | 15.12 |
| 6 | 1,8-Di[5(3)-phenylpyrazolyl-3(5)]-octane | 179 | 84 | 78.27 | 7.75 | 14.26 | 78.39 | 7.54 | 14.07 |
| 7 | Di-(3,5-dimethylpyrazolyl-4) ¹⁶ | 297-298 | 80 | | | | | | |
| 8 | 4,4'-Bis[5(3)-methylpyrazolyl-3(5)]-diphenyl disulfide | 251-252 | 80 | 63.11 | 4.91 | 14.16 | 63.46 | 4.79 | 14.80 |

methylene at $315\text{ m}\mu$, and while the model compounds showed maxima at 285 and $275\text{ m}\mu$, respectively. A similar picture was observed by Marvel et al. with polybenzimidazoles.¹²

Treatment of polyhydrazone from 4,4'-bis(acetoacetyl) diphenyl oxide with concentrated sulfuric acid resulted in the destruction of the polymer chain to give the bipyrazole, 4,4'-bis-[5(3)-methylpyrazolyl-3(5)]diphenyl oxide, which is identical with bipyrazole synthesized from the corresponding bis(β -diketone) and hydrazine hydrate. Treatment of the polyhydrazone with concentrated sulfuric acid gave bipyrazole hydrochloride as a sole product, just as with total hydrolysis.

Unlike polyhydrazones, polypyrazoles from bis(β -diketones) and acid hydrazides proved stable to water hydrolysis on boiling for 1 hr. and short exposure (0.5 hr.) to hot concentrated sulfuric acid. After the above treatment polypyrazoles exhibited the same melting and softening points as did the starting sample. Prolonged treatment with hot, concentrated sulfuric acid led to a complex mixture of sulfonated products that we did not study.

Alkaline hydrolysis of the same polyhydrazone and polypyrazole by boiling for 12 hr. with 25% solution of potassium hydroxide proceeds on similarly to acid hydrolysis and is also accompanied by complete destruction of the polymer chain to give as end products monohydrazone and bipyrazole, respectively. This is clearly seen from the infrared spectra of the starting material and the hydrolysis products.

The infrared spectrum of polypyrazole exhibits an intense band at 1725 cm.^{-1} that may be assigned to the carbonyl group vibration of the hydrazide residue bound to the pyrazole ring.¹³ In the infrared spectrum of the hydrolysis product of polypyrazole this band is absent, the spectrum being identical with that of authentic 4,4'-bis[5(3)-methylpyrazolyl-3(5)]diphenylethane. The infrared spectrum of the alkaline hydrolysis product of polyhydrazone has an absorption band at 1680 cm.^{-1} .

It will be seen from the data in the tables that our synthetic polymers have softening points in the range of $200\text{--}300^\circ\text{C}$. Polypyrazoles from branched bis(β -diketones) exhibit several peculiar properties, however. Although their softening points are in the same temperature range, within this range they are quite stable; unlike the linear ketones they do not undergo visible decomposition and are somewhat elastic; their melts can be drawn into filaments.

Elimination of the polymer chain of the carbonyl group affected the stability of polypyrazoles to the action of mineral acids and bases. Thus, after being boiled for 3 hr. with 25% potassium hydroxide solution their melting point and viscosity remained constant, in contrast to polypyrazoles from acid dihydrazides of dicarboxylic acid that were thereby split to bipyrazoles.

Introduction into the polymer chain of benzene rings in place of the methylene chains by using isophthalic acid dihydrazide rather than adipic acid did not raise the softening point of polymers.

for by increased interaction between the chains at the expense of hydrogen bond formation (Table V).

The infrared spectra of these polymers exhibit a broad smeared band over the 3100–3300 cm.^{-1} range which is assigned to the NH group and due to strong association characteristic of pyrazoles with a free NH group.

EXPERIMENTAL

Synthesis of Bis(β -diketones)

Linear Bis (β -diketones) $\text{R}'\text{—COCH}_2\text{CORCOCH}_2\text{COR}'$. 4,4 -Bis-(acetoacetyl)diphenylethane and 4,4'-bis(acetoacetyl)diphenyl oxide were prepared by direct acetylation of diphenylethane and diphenyl ether with acetic anhydride in the presence of boron fluoride according to a previously reported method.¹⁴

Sebacyl diacetophenone was prepared according to the method described in the literature.¹⁵

Branched Bis(β -diketones). Branched bis(β -diketones) were obtained in 60–70% yield by the interaction of the corresponding dibromomethyl derivatives and sodium acetylacetonate at 100°C. Synthesis of dibromomethyl derivatives of diphenyl and diphenyl oxide was carried out by our methods;³ tetraacetylene was prepared in 69% yield by the method of Mosby.¹⁶

Polycyclization (General Procedures)

Polycyclization in Solution. Equimolecular amounts of monomers were placed in a flat-bottomed flask with absolute ethanol and boiled under reflux. Polyhydrazone (and, in the case of branched ketones, polypyrazole) was formed as a precipitate and filtered off, and the filtrate evaporated *in vacuo* to give dissolved polyhydrazone. Polyhydrazone was then heated in a condensation flask flushed with pure nitrogen *in vacuo* at 200–300°C. to obtain polypyrazole.

Polycyclization in the Melt. Equimolecular amounts of carefully mixed monomers were placed in a condensation flask flushed with pure nitrogen and heated at a temperature of water evolution. The viscosity of the resulting polypyrazoles was measured on 0.5% polymer solutions in cresol at 20°C. For polymers insoluble in cresol the viscosity was measured on freshly prepared solutions in concentrated sulfuric acid.

Synthesis of Polypyrazoles with a Free NH Group

To a freshly prepared solution of diazo compounds in ether or alcohol were added equimolecular amounts of diethynyl derivative, either pure or in ether. The reaction mixture was allowed to stand at room temperature or in the refrigerator. The reaction usually started in 15–20 min. and required several days to go to completion. The polymers formed were isolated as precipitates. They are yellow powders, readily soluble in di-

methyl-formamide and cresol. The reduced viscosity of 0.5% solution in cresol is 0.2–0.3; the molecular weight is from 10,000–15,000. The polymer from 1,6-bisdiazohexane and 1,4-diethynylbenzene softens at 440°C. (with decomposition); that from 1,6-bisdiazohexane and diacetylene melts in the range of 350–375°C.; that from bisdiazoxylene and diethylbenzene does not melt up to 500°C.

Synthesis of Polypyrazoles by the Interaction of Bipyrazoles and Diisocyanates

Bipyrazoles such as 4,4'-bis[5(3)-methylpyrazolyl-3(5)] diphenyl oxide, 4,4'-bis(3,5-dimethylpyrazolyl-4)xylylene, and di(3,5-dimethylpyrazolyl-4) were obtained by the interaction of corresponding bis(β -diketones) and hydrazine hydrate.⁴

Polypyrazoles from hexamethylene diisocyanate were prepared by the interaction of equimolecular amounts of bipyrazole and diisocyanate in chlorobenzene at room temperature for several hours, the polymer being then isolated with heptane. Polymers were found to be soluble in dioxane, chlorobenzene, benzene, dimethylformamide, and cresol.

Synthesis starting from toluylene diisocyanate was carried out by heating equimolecular amounts of bipyrazole and diisocyanate in a condensation flask swept with dry nitrogen at 100°C. for 2 hr. and subsequently at 160°C. for 2 hr. The polymers obtained were dissolved in dimethylformamide and precipitated with ether. They were soluble in chlorobenzene, dioxane, and cresol.

References

1. Korshak, V. V., E. S. Krongauz, A. M. Berlin, and P. N. Gribkova, *Dokl. Akad. Nauk SSSR*, **149**, 602 (1963).
2. Korshak, V. V., E. S. Krongauz, and A. M. Berlin, *Dokl. Akad. Nauk USSR*, **152**, 1108 (1963).
3. Korshak, V. V., E. S. Krongauz, A. M. Berlin, *Vysokomolekul. Soedin.*, **6**, 1078 (1964).
4. Korshak, V. V., E. S. Krongauz, A. M. Berlin, and A. P. Travnikova, *Vysokomolekul. Soedin.*, **6**, 1087 (1964).
5. Korshak, V. V., E. S. Krongauz, A. M. Berlin, and T. Ya. Smirnova, *Vysokomolekul. Soedin.*, **6**, 1195 (1964).
6. Eistert, B., and E. Merkel, *Ber.*, **86**, 896 (1953).
7. Kabachnik, M. I., S. T. Yoffe, and K. V. Vatsuro, *Tetrahedron*, **1**, 317 (1957).
8. Kabachnik, M. I., E. M. Popov, S. T. Yoffe, and K. V. Vatsuro, *Tetrahedron*, **12**, 76 (1961).
9. Yoffe, S. T., E. M. Popov, E. V. Vatsuro, E. K. Tulikova, and M. I. Kabachnik, *Dokl. Akad. Nauk USSR*, **144**, 802 (1962).
10. Yoffe, S. T., E. M. Popov, K. V. Vatsuro, E. K. Tulikova, and M. I. Kabachnik, *Tetrahedron*, **18**, 923 (1962).
11. Campbell, K. D., and H. M. Gibon, *J. Am. Chem. Soc.*, **82**, 5426 (1960); *ibid.*, **84**, 1440 (1962).
12. Vogel, H., and C. S. Marvel, *J. Polymer Sci.*, **50**, 511, 541 (1961).
13. Ried, W., and F. J. Königstein, *Ann. Chem.*, **625**, 53 (1960).
14. Korshak, V. V., E. S. Krongauz, and V. E. Sheina, *Vysokomolekul. Soedin.*, **3**, 1203 (1961).

15. Korshak, V. V., E. S. Krongauz, and V. E. Sheina, *Vysokomolekul. Soedin.* **3**, 1456 (1961).
16. Mosby, W. Z., *J. Chem. Soc.*, **1957**, 3997.

Résumé

On a préparé des composés inconnus, de poids moléculaires élevés et possédant des cycles pyrazoles dans la chaîne, par interaction de bis- β -dicétones linéaires ou ramifiées avec des dihydrazides d'acides dicarboxyliques ou des dihydrazines. Des polypyrazoles du second type (avec un groupe NH libre dans le cycle pyrazole) ont été préparés par interaction entre des bisdiazocalcanes et des diacétylènes. On discute de quelques caractéristiques de la réaction de polycyclisation ainsi que de la structure et des propriétés des polymères obtenus.

Zusammenfassung

Durch die Reaktion linearer oder verzweigter Bis(β -diketone) mit Dihydraziden von Dicarbonsäuren oder Dihydrazinen wurden neue hochmolekulare Verbindungen mit Pyrazolringen in der Hauptkette dargestellt. Polypyrazole vom zweiten Typ (mit einer freien NH-Gruppe im Pyrazolring) wurden durch Reaktion von Bisdiazalkanen mit Diacetylenen dargestellt. Einige Charakteristika der Polyzyklisierungsreaktion sowie Struktur und Eigenschaften der erhaltenen Polymeren werden diskutiert.

Received June 9, 1964

Revised December 21, 1964

(Prod. No. 4595A)

Polymerization of Trioxane by Crystallization on Activated Seeds from Cyclohexane Solutions*

F. MORELLI, G. MASETTI, E. BUTTA, and M. BACCAREDDA,
*Centro Nazionale di Chimica delle Macromolecole del
Consiglio Nazionale delle Ricerche, Sezione VI presso l'Istituto
di Chimica Industriale ed Applicata dell' Università di
Pisa, Italy*

Synopsis

The preparation of polyoxymethylene of high molecular weight by polymerization of trioxane, starting from concentrated solutions in hydrocarbon solvents (cyclohexane) initiated by addition of a cationic catalyst (BF_3 etherate) and inducing the crystallization of trioxane by cooling the system from the initial to room temperature, is investigated. The success of the method depends largely on the time of permanence of the solution at the initial temperature after the induction period (activation time) the initial solution, which can be controlled by following the temperature variations of the system during this stage. The cooling of the activated solution may be performed either continuously, in which case it may be varied from 15 to 200°C./hr., or in two stages: quenching from the initial temperature to the precipitation point followed by controlled cooling at a lower rate from this point to room temperature. The latter method is preferable when initial temperatures higher than the melting point of the pure trioxane are chosen. Products having inherent viscosities ranging from 2.0 to 3.0 dl./g. (in 0.5% solutions in *p*-chlorophenol at 60°C.) are obtained.

In a previous paper,¹ a method was presented for obtaining high yields of polyoxymethylene of high molecular weight and high crystallinity in the form of small fibers oriented along the *c*-axis of the chain, through a particular crystallization-polymerization process, initiated by cationic catalysts. It consisted of preparing a nearly saturated solution of trioxane in a viscous hydrocarbon solvent (vaseline oil) at temperatures above the melting point of trioxane (61–62°C.) and, after adding a small quantity of a cationic initiator (BF_3 etherate), cooling the solution in a continuous manner at a controlled rate to room temperature in order to favor the gradual precipitation of trioxane in the form of small crystals. Under these conditions, polymerization of trioxane occurred during its precipitation from the solution with formation of polyoxymethylene of high molecular weight in the form of fibers.

To explain the mechanism of this crystallization-polymerization process, it was suggested that during the first stage of the reaction (between the

* Research partially sponsored by the Continental Oil Company, Ponca City, Oklahoma, U.S.A.

initial temperature and the temperature of incipient precipitation) formation of "active" crystalline seeds occurred. In the successive cooling stages (from the precipitation point to room temperature), the majority of trioxane precipitated from the solution, and the "active" crystalline seeds grew and polymerized.

In effect, at the end of the reaction, a mixture of two different types of polymeric products was obtained, in addition to some crystalline unpolymerized trioxane: a fiberlike polymer of high molecular weight (η_{inh} in 0.5% solutions of *p*-chlorophenol at 60°C. = 1.1–2 dl./g.) and high melting point and a powdery product, composed of polyoxymethylene of relatively low molecular weight, lower melting point, which showed no preferential orientation of crystals on x-ray examination.

It was suggested that during the cooling stage, two competitive reactions occurred in the system: polymerization of trioxane in solution, which led to the formation of the powdery product of low molecular weight, and polymerization through growth of active crystalline seeds, which led to the formation of the fiberlike products of higher molecular weight. The extent of the first of these reactions could be limited by using low quantities of catalyst, low initial temperatures, solvents of high viscosity and of relatively low solvent power, and by operating with suitable rates of cooling. A rough evaluation of the relative abundance of the polymer obtained by polymerization in solution over that obtained through crystallization could be made by microscopic examination of the mixture of the reaction products or by treating the product mixture with acetic anhydride at the boiling point, in which only the powdery product is soluble.

All the experiments described above were carried out in viscous hydrocarbons of low solvent power such as vaseline oil. In the present paper, results of similar experiments in which a nonviscous hydrocarbon of relatively high solvent power (cyclohexane) is used as solvent are reported. Cyclohexane has been suggested as solvent for the polymerization of trioxane in a polymerization process invented by Bruni,² in which the reaction was initiated in solution at a certain temperature (in presence of cationic catalysts) and successively continued, after the precipitation of the majority of trioxane from the solution, by quenching from the initial temperature to the polymerization temperature. This method leads to good results, especially with respect to molecular weight, but the reproducibility of the method seems to be low.

Experimental

The experimental apparatus consisted of a small cylindrical glass vessel, about 2.50 cm. in diameter, furnished with a small stirrer and closed by a glass stopcock with a socket for the introduction of the reagents and catalyst. The reaction vessel was kept in a water bath furnished with cooling and warming coils for temperature control.

In the earlier experiments trioxane (Schuchardt of a commercial type) was used, after purification by successive crystallization from petroleum

ether m.p. 61–62°C., n_D^{66} 1.3902. Trioxane so purified is indicated in the tables as trioxane A.

In the later experiments, purer trioxane has been employed. Its purification involved repeated crystallizations from petroleum ether, followed by total reflux for 12 hr. and final distillation in the presence of sodium. Trioxane so purified is indicated in the tables as trioxane B.

The solvent (cyclohexane) was first introduced into the reaction vessel, which was immersed in the water bath kept at the initial temperature. Trioxane, sufficient to obtain a concentrated solution, was then added. After vigorous agitation, to allow complete solubilization of trioxane, the catalyst (BF_3 etherate), dissolved in a small quantity of benzene, was added in small amounts. When all the catalyst had been added, agitation was stopped completely and the mixture cooled, at a controlled nearly constant rate, to room temperature. At the end of the reaction, the product consisted of a very hard, compact mass, which was first crushed and then washed successively with petroleum ether and acetone to remove solvent and unreacted trioxane.

Polyoxymethylene so prepared did not have the fiberlike appearance of the corresponding product prepared starting from solutions in vaseline oil. This is probably due to the fact that the growth of crystals is disturbed by the excessive concentration of crystalline seeds. However, fibers of polyoxymethylene could be obtained if more diluted solutions were used. The product melted at 184–186°C.

a. Preliminary Experiments. In the first experiments, the cooling was started just after the addition of the catalyst. It was observed that, at high rates of cooling (50–200°C./hr.), no polymerization occurred at all; on the other hand, at low rates of cooling (5–15°C./hr.), polymerization occurred with relatively high yields. In the latter case, the majority of trioxane polymerized in solution before the precipitation point was reached, forming products of relatively low molecular weight. At intermediate rates of cooling, in many cases polymerization failed to occur and, when it did occur, very different results were obtained from experiment to experiment, even if exactly the same conditions were used.

These experiments indicated that, with cyclohexane as solvent, the process was much more difficult to control than that in which viscous hydrocarbons of low solvent power were used. It was observed in successive experiments that with cyclohexane, better results could be obtained, if the initial solution was kept for a certain time at the initial temperature after addition of the catalyst, before cooling.

In Table I some results are reported, which refer to experiments carried out in the manner described above starting from concentrated solutions of trioxane A (about 50% by weight) in cyclohexane, with a fixed quantity of BF_3 etherate (1.7×10^{-4} mole/mole of trioxane) and kept at the initial temperature (67°C.) for a fixed time (10 min.) after addition of the catalyst before cooling. The rate of cooling from the initial temperature to room temperature was varied between 10 and 50°C./hr.

TABLE I
Polymerization of Trioxane A from Crystalline Seeds in Cyclohexane^a

| Expt. no. | Rate of cooling, °C./hr. | Yield, % | η_{inh} , dl./g. ^b |
|-----------|--------------------------|----------|------------------------------------|
| 1 | 10 | 81 | 2.49 |
| 2 | 10 | 72 | 2.42 |
| 3 | 30 | 78 | 2.74 |
| 4 | 30 | 60 | 2.68 |
| 5 | 30 | 77 | 2.57 |
| 6 | 50 | 76 | 2.53 |
| 7 | 50 | 77 | 2.99 |
| 8 | 50 | 74 | 2.86 |

^a Solution concentration = 50 wt.-%; quantity of catalyst = 1.7×10^{-4} mole/mole of trioxane; initial temperature = 67°C.; final temperature = 25°C.; time of permanence at 67°C. before cooling = 10 min.

^b η_{inh} at 0.5% in *p*-chlorophenol at 60°C.

From the examination of the data reported in columns 4 and 5 of Table I, it can be seen that, under these conditions, yields of 60–81% of a product with inherent viscosities of 2.5–3 dl./g. (determined in 0.5% solutions in *p*-chlorophenol at 60°C.) were obtained. Total yields did not seem to be much affected by the rate of cooling, in the range in which we operated. The lowest inherent viscosity was obtained when the lowest rate of cooling (10°C./hr.) was used.

Table II lists some results of experiments carried out isothermally, polymerizing trioxane A in solution at a temperature of 67°C. for different times (from 15 min. to 4 hr.), under the same conditions of concentration and quantity of catalyst as in preceding experiments. In the isothermal polymerization, yields increased from 19 to 51%, while the inherent viscosity of the polymer first increased and then decreased, passing through a maximum with increasing time of reaction. In any case, in the latter experiments, lower yields and lower inherent viscosities were obtained than in the experiments reported in Table I.

Other crystallization–polymerization experiments have been performed,

TABLE II
Isothermal Polymerization of Trioxane A in Solution of Cyclohexane at 67°C.^a

| Expt. no. | Reaction time, min. | Yield, % | η_{inh} , dl./g. ^b |
|-----------|---------------------|----------|------------------------------------|
| 1 | 15 | 19 | 0.85 |
| 2 | 60 | 31 | 1.10 |
| 3 | 120 | 46 | 1.60 |
| 4 | 180 | 49 | 1.40 |
| 5 | 240 | 51 | 1.02 |

^a Solution concentration = 50 wt.-%; quantity of catalyst = 1.7×10^{-4} mole/mole of trioxane.

^b η_{inh} at 0.5% in *p*-chloropheno. at 60°C.

starting from a lower initial temperature, below the melting point of trioxane (61–62°C.), using the same concentration and quantity of catalyst as in the above described experiments. The rate of cooling was varied from 30 to 90°C./hr. With the lower initial temperature, it was observed that much longer permanence times at the initial temperature after addition of the catalyst were necessary to induce the polymerization of trioxane by crystallization from the solution during the cooling stage. The permanence time chosen in these experiments was 60 min.; with shorter times, in the majority of experiments, polymerization failed to occur.

The results obtained in these experiments are reported in Table III, while the corresponding data relative to experiments carried out isothermally starting from the same initial conditions (concentration, quantity of catalyst, temperature) are reported in Table IV.

As can be seen from the examination of the data reported in Table III, starting from a temperature of 56°C., the yield ranged from 50 to 82% and inherent viscosities of the product varied from 2.0 to 3.15 dl./g. There does not seem to be any definite relation between either inherent viscosity or yields and the rate of cooling, at rates of cooling between 10 and 90°C./hr. Nevertheless, in these experiments, on the average, the highest yields and inherent viscosities were obtained with rates of cooling of 30°C./hr.

As already found in former experiments (Tables I and II), on comparing the data relative to the isothermal polymerization in solution at 56°C. (Table IV) with those relative to experiments carried out by cooling the solution at a certain time after the addition of the catalyst (Table III), higher yields and higher molecular weights were obtained in the latter case.

TABLE III
Polymerization of Trioxane A from Crystalline Seeds in Cyclohexane^a

| Expt. no. | Rate of cooling, °C./hr. | Yield, % | η_{inh} , dl./g. ^b |
|-----------|--------------------------|----------|------------------------------------|
| 1 | 10 | 82 | 2.10 |
| 2 | 30 | 79 | 3.15 |
| 3 | 30 | 80 | 2.84 |
| 4 | 30 | 75 | 2.98 |
| 5 | 50 | 75 | 2.67 |
| 6 | 50 | 65 | 2.76 |
| 7 | 50 | 50 | — |
| 8 | 50 | 67 | 2.96 |
| 9 | 70 | 76 | 2.49 |
| 10 | 70 | 76 | 2.52 |
| 11 | 70 | 66 | 2.06 |
| 12 | 90 | 71 | 2.87 |
| 13 | 90 | — | — |
| 14 | 90 | 50 | 2.74 |

^a Solution concentration = 50 wt.-%; quantity of catalyst = 1.7×10^{-4} mole/mole of trioxane; initial temperature = 56°C.; final temperature = 25°C.; time of permanence at 56°C. before cooling = 60 min.

^b η_{inh} at 0.5% in *p*-chlorophenol at 60°C.

TABLE IV
Isothermal Polymerization of Trioxane A in Solution of Cyclohexane at 56°C.^a

| Expt. no. | Reaction time, min. | Yield, % | η_{inh} , dl./g. ^b |
|-----------|---------------------|----------|------------------------------------|
| 1 | 60 | 19 | 0.97 |
| 2 | 120 | 30 | 1.20 |
| 3 | 180 | 37 | 1.42 |
| 4 | 240 | 43 | 1.61 |
| 5 | 300 | 47 | 1.35 |
| 6 | 480 | 53 | 1.21 |

^a Solution concentration = 50 wt.-%; quantity of catalyst = 1.7×10^{-4} mole/mole of trioxane.

^b η_{inh} at 0.5% in *p*-chlorophenol at 60°C.

As for the influence of reaction time on the isothermal polymerization in solution at 56°C., data reported in Table IV indicate that also in this set of experiments yields increased with increasing reaction time; such an increase of yields was, however, accompanied by a definite decrease of the average molecular weight of the polymer formed during far too long reaction times.

These results are in agreement with those found by Kern and Jacks³ for the isothermal polymerization of trioxane in concentrated solutions in cyclohexane at 60°C. in the presence of FeCl₃ initiator. The decrease of the average molecular weight with increasing time of reaction has been attributed to the degradation of the polymer chains, formed at the outset of the reaction, because of the long exposure to a relatively high temperature in presence of the initiator.

b. Experiments with Controlled Activation Times. In carrying out experiments of polymerization of trioxane from crystalline seeds, it was noticed that in the majority of cases the initial solution, after a certain induction period (during which yields were very low and only a progressive opalescence was observed in the mass), suddenly acquired a gellike consistency. At this stage, about 16–18% of the material is polymerized. The existence of an induction period in the polymerization of trioxane in solution has been attributed⁴ to the fact that the oligomers, in the first stages of the reaction, tend to decompose to free formaldehyde; only when the concentration of the latter has reached its equilibrium value, can the polymerization proceed further. The end of the induction period is marked by a sudden increase in the polymerization rate.

In our experiments if the cooling of the solution is started after the occurrence of gelation, the greatest part of trioxane, which has yet not reacted, can polymerize successively by crystallization during the cooling stage; on the contrary, if the cooling is started before the solution has reached its gel point, polymerization during cooling, fails to occur in the majority of cases or in any case, low yields are obtained.

In the preliminary experiments [paragraph (a)], we observed that the time required for gelation varied much from experiment to experiment, even

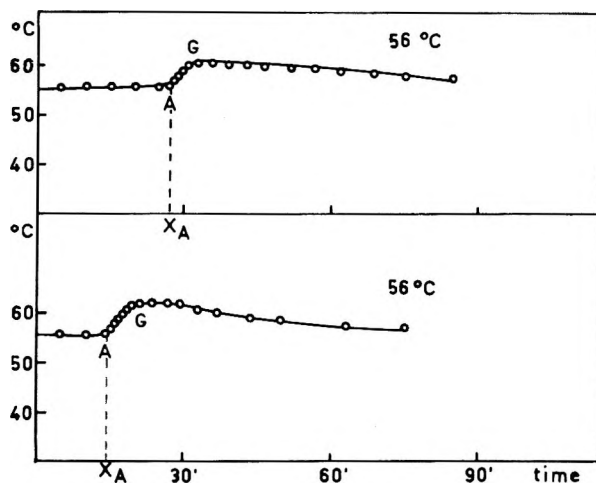


Fig. 1. Temperature-time curves of the reacting system (temperature of the thermostat = 56°C.); catalyst: (top) 1.7×10^{-4} mole/mole trioxane A; (bottom) 2.4×10^{-4} mole/mole trioxane.

if the same set of conditions was used (especially when the trioxane originated from different purification batches); so, in order to assure in any case the success to the polymerization by crystallization generally long times of permanence at the initial temperature, as compared with the induction period, were used; such times, as already indicated, were kept constant for each set of experiments.

It was therefore suggested that one of the main factors responsible for the poor reproducibility of results for the crystallization-polymerization process might be the excessive variability of the time of permanence of the reacting system at the initial temperature after the end of the induction period, the latter being largely influenced by the purity of the trioxane and the purity of the other reactants employed.

For a proper control of the first stage of the process, it is therefore necessary to dispose of a suitable method for detecting unambiguously the end of the induction period, in order to be able to fix the time of permanence of the system at the initial temperature with reference to the end of the induction period and not to the moment at which the catalyst is added.

Therefore, experiments were carried out to determine whether the end of the induction period, which is marked by a sudden increase of the polymerization rate, is accompanied by thermal effects, easily detectable in our experimental conditions. To this purpose, a thermocouple, connected with a galvanometer, was introduced into the reaction mixture.

In Figure 1, two typical temperature-time curves are shown relating to experiments carried out at an external temperature of 56°C. and with two different quantities of catalyst (1.7×10^{-4} and 2.4×10^{-4} mole/mole of trioxane), with the use of 50% (by weight) solutions of trioxane in cyclohexane. As can be seen from the behavior of the thermal curves, the temperature of the reaction system at first remains constant, after the addition

of the initiator, but suddenly, at a certain time, corresponding to the abscissa X_A of the point A , begins to rise to a value 4–5°C. higher than the initial temperature. Later it decreases slowly to the initial temperature. In the period of time during which the increase of temperature occurs (interval $X_G - X_A$), a rapid increase of the viscosity of the reaction medium is observed, which is followed by gelation of the mass; the gel point roughly corresponds to the time X_G at which the maximum temperature is reached (X_G). From the comparison of the thermal curves in Figure 1, it can be seen that, with an increasing quantity of catalyst, the height of the maximum temperature increases and both points A and G are shifted towards the origin of the time scale. The period X_A corresponding to the start of temperature increase can be reasonably assumed as "induction period."

Successively, experiments were carried out in which the time of permanence at the initial temperature, after the addition of the catalyst, was measured starting from the end of the induction period X_A , at which the first increase of temperature is verified in the system; such a time will be indicated from now on as "activation time."

Some results obtained in these experiments are reported in Table V. The data refer to experiments carried out with solutions of trioxane in cyclohexane (50% by weight), started at the temperature of 56°C. in the presence of a fixed quantity of BF_3 etherate (1.7×10^{-4} mole/mole of trioxane). The activation time was made to vary arbitrarily within certain limits in order to be shorter, the same as, or longer than the induction period X_A

TABLE V
Polymerization of Trioxane A from Crystalline Seeds in Cyclohexane for Different Effective Activation Times $X - X_A^a$

| Expt. no. | Total permanence time at the initial temperature \times min. | Total activation time, min. ^b | Activation time ($X - X_A$), min. | Rate of cooling, °C./hr. | Yield, % | η_{inh} , dl./g. ^c |
|-----------|--|--|-------------------------------------|--------------------------|----------|---|
| 1 | — ^b | 60 | — | 30 | 48 | 2.42 |
| 2 | 95 | 95 | 0 | 30 | 70 | 2.72 |
| 3 | 80 | 90 | 10 | 30 | 76 | 2.71 |
| 4 | 22 | 60 | 38 | 30 | 75 | 2.42 |
| 5 | 60 | 60 | 0 | 50 | 78 | 2.81 |
| 6 | 90 | 90 | 0 | 50 | 74 | 2.60 |
| 7 | 75 | 90 | 15 | 50 | 70 | 2.59 |
| 8 | 67 | 90 | 23 | 50 | 71 | 2.56 |
| 9 | 90 | 145 | 55 | 50 | 75 | 2.41 |
| 10 | 103 | 103 | 0 | 70 | 31 | — |
| 11 | 74 | 90 | 16 | 70 | 68 | 2.66 |
| 12 | 54 | 90 | 36 | 70 | 68 | 2.36 |

^a Solution concentration = 50 wt. %; quantity of catalyst = 1.7×10^{-4} mole/mole of trioxane; initial temperature = 56°C.; final temperature = 25°C.

^b Cooling is started before point A is reached.

^c η_{inh} at 0.5% in *p*-chlorophenol at 60°C.

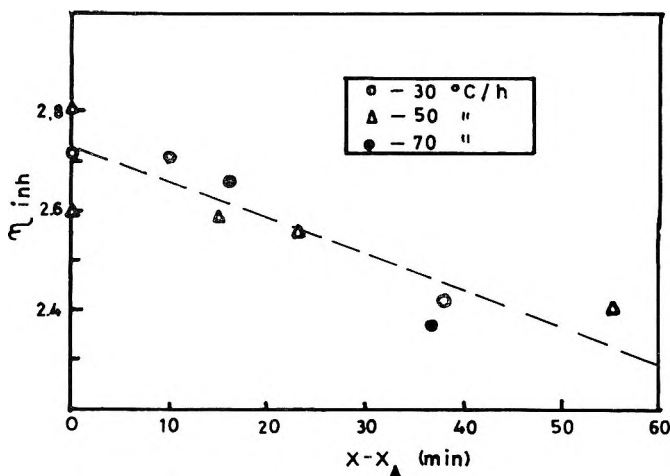


Fig. 2. Inherent viscosity (0.5% in *p*-chlorophenol at 60°C.) of polyoxymethylene formed as function of the activation time for different rates of cooling. Trioxane A/cyclohexane weight ratio = 50/50; initial temperature = 56°C.; final temperature = 25°C.; quantity of catalyst = 1.7×10^{-4} mole/mole of trioxane.

given by the relative thermal curve. The rates of cooling were varied between 30 and 70°C./hr.

The data reported in Table V, indicate that the induction period X_A varies much from experiment to experiment, during the activation stage in spite of the attempt to hold all variables constant. For each given rate of cooling, yields and inherent viscosities of the polymer obtained vary irregularly with the time X during which the solution was kept at the initial temperature, but are determined by $X - X_A$. In particular, for $X < X_A$, as already observed, practically no polymerization occurs during the cooling stage in most cases. However, polymerization may occur to a certain extent during the cooling stage if sufficiently low rates of cooling are employed (expt. 1 of Table V). On the contrary, for $X \geq X_A$, polymer is obtained in relatively a high yield. The inherent viscosities of the polymer reach their highest values when cooling is started at $X = X_A$ and tend to decrease steadily with increasing $X - X_A$ intervals (Fig. 2).

From the latter results, it can be deduced that, to obtaining the highest molecular weights, the cooling of the solution must be started as soon as the first increase of temperature is observed, that is to say immediately after the end of the induction period. Moreover, it is advisable to carry out the cooling at rates of the order of 30–50°C./hr.

To confirm these results, experiments were carried out in which the cooling of the solution was started at time X_A and in which cooling rates of 15, 30, 40, and 50°C./hr. were used. The results obtained in these experiments are reported in Table VI (experiments 1 to 12). Under these conditions the experimental results are actually quite reproducible, in spite of the fact that the position of X_A varies from experiment to experiment. The average induction period observed in these experiments is much shorter

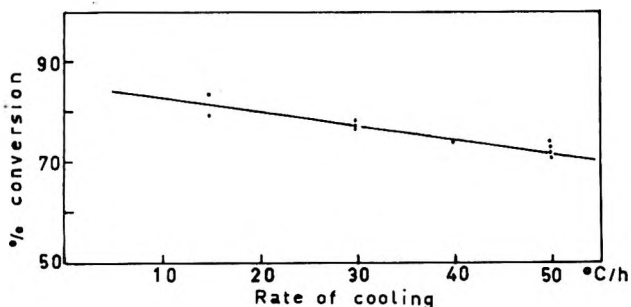


Fig. 3. Conversion as function of the rate of cooling in the polymerization of trioxane from crystalline seeds. Trioxane B/cyclohexane weight ratio = 50/50; initial temperature = 56°C.; final temperature = 25°C.; quantity of catalyst = 1.7×10^{-4} mole/mole of trioxane; cooling started at X_A time (end of the induction period).

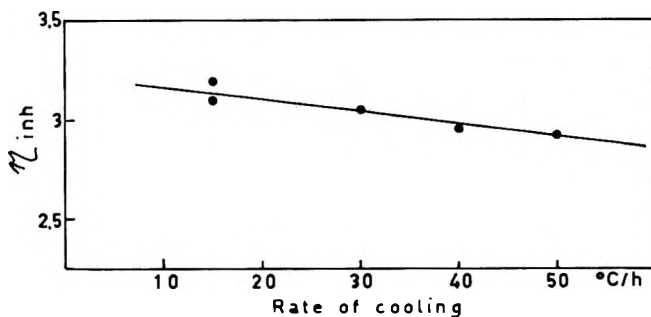


Fig. 4. Inherent viscosity (0.5% in *p*-chlorophenol at 60°C.) of the polymer formed in the polymerization of trioxane from crystalline seeds as function of the rate of cooling. Trioxane B/cyclohexane weight ratio = 50/50; initial temperature = 56°C.; final temperature = 25°C.; quantity of catalyst = 1.7×10^{-4} mole/mole of trioxane; cooling started at X_A time (end of the induction period).

than in preceding ones, in which the same quantity of catalyst, trioxane concentration, and temperature were used; this can be attributed to the higher degree of purity of the trioxane employed (trioxane B). The highest yields and molecular weights are obtained with relatively low rates of cooling (15–30°C./hr.) (Figs. 3 and 4).

In Table VI (experiments 13–20) some results are reported, which refer to experiments carried out under the same general conditions as in the experiments just described, but initiating the process at temperatures above the melting point of trioxane (namely, 70 and 75°C.). The cooling was started just after point X_A and the rate of cooling was varied from 30 to 200°C./hr. With increasing rate of cooling, total yields decrease and, at the same time, inherent viscosities of the products steadily increase; however, the latter remain at lower values than in preceding experiments in which lower initial temperatures were used.

These facts can be explained by assuming that if low rates of cooling are employed, the reacting system, after the end of the induction period, re-

mains too long at relatively high temperatures before the precipitation point is reached. The polymerization of trioxane in solution is then favored over the competitive reaction of polymerization from crystalline

TABLE VI
Polymerization of Trioxane B from Crystalline Seeds in Cyclohexane with Activation Times Equal to Induction Periods $X = X_A^a$

| Expt. no. | Initial temperature, °C. | Activation time $X = X_A$, min. | Rate of cooling, °C./hr. | Yield, % | η_{inh} , dl./g. ^b |
|-----------|--------------------------|----------------------------------|--------------------------|----------|------------------------------------|
| 1 | 56 | 27 | 15 | 79 | 3.08 |
| 2 | 56 | 18 | 15 | 84 | 3.21 |
| 3 | 56 | 25 | 30 | 78 | 3.04 |
| 4 | 56 | 30 | 30 | 77 | 3.04 |
| 5 | 56 | 25 | 30 | 77 | 3.04 |
| 6 | 56 | 15 | 40 | 74 | 2.95 |
| 7 | 56 | 62 | 50 | 74 | 2.90 |
| 8 | 56 | 20 | 50 | 73 | 2.84 |
| 9 | 56 | 35 | 50 | 71 | 2.92 |
| 10 | 56 | 25 | 50 | 73 | 2.92 |
| 11 | 56 | 30 | 50 | 72 | 2.93 |
| 12 | 56 | 50 | 50 | 77 | 2.82 |
| 13 | 70 | 8 | 30 | 77 | 2.00 |
| 14 | 70 | 15 | 50 | 72 | 2.15 |
| 15 | 70 | 10 | 70 | 68 | 2.20 |
| 16 | 70 | 7 | 90 | 55 | 2.45 |
| 17 | 70 | 12 | 200 | 40 | 2.60 |
| 18 | 75 | 10 | 30 | 78 | 1.89 |
| 19 | 75 | 5 | 70 | 71 | 2.00 |
| 20 | 75 | 6 | 200 | 44 | 2.70 |

^a Solution concentration (weight %) = 50%; quantity of catalyst = 1.7×10^{-4} mole/mole of trioxane; final temperature = 25°C.

^b η_{inh} at 0.5% in *p*-chlorophenol at 60°C.

TABLE VII
Polymerization of Trioxane B from Crystalline Seeds in Cyclohexane with Cooling in Two Stages^a

| Expt. no. | End of the induction period and start of cooling = X_A , min. | Rate of cooling in the second stage, °C./hr. | Yield, % | η_{inh} , dl./g. ^b |
|-----------|---|--|----------|------------------------------------|
| 1 | 10 | 15 | 84 | 3.15 |
| 2 | 9 | 30 | 78 | 3.02 |
| 3 | 11 | 50 | 74 | 2.94 |

^a Solution concentration = 50 wt.-%; quantity of catalyst = 1.7×10^{-4} mole/mole of trioxane; initial temperature = 70°C.; intermediate temperature 51–52°C.; final temperature = 25°C.

^b η_{inh} at 0.5% in *p*-chlorophenol at 60°C.

seeds. On the contrary, with high rates of cooling, the time at high temperature is shortened but, due to the excessive rate of cooling, a good deal of trioxane precipitates out of the solution in the unpolymerized state.

However, good yields together with high molecular weights can be obtained also in these cases, if the reacting system is cooled from the initial temperature to room temperature in two stages: (1) quenching from the initial temperature to an intermediate temperature between the melting point of trioxane and its precipitation point (51–52°C.), followed by (2) controlled cooling from the precipitation point to room temperature. The results obtained in some two-stage cooling experiments are reported in Table VII.

Discussion of Results

It is known that when trioxane is polymerized in solutions of hydrocarbons in presence of cationic catalysts, the molecular weight of the product is generally rather low. This has been attributed to chain-transfer reactions, particularly, to water molecules. The difficulty of removing water completely from trioxane, is the main reason why the polymerization of trioxane in solution has not been successful from the practical point of view. Moreover, in the solution polymerization of trioxane, yields are generally low; they may be increased by prolonging the reaction time, but this causes a further lowering of the molecular weight.

Much better results, as concerns both yields and molecular weight, can be obtained by using very concentrated solutions of trioxane and cooling them, after an initial activation time, from the initial temperature to room temperature at a suitable controlled rate. In this way, polymerization in solution is avoided to a large extent, and most of the trioxane polymerizes on precipitation from the solution (during the cooling stage) onto activated crystalline seeds.

In this procedure no particular care is required for the purification of the monomer (trioxane), since purification occurs during its crystallization from the solution. For instance, if commercial trioxane is used, the induction period increases very much, but yields are not much changed and the molecular weight of the product is lowered; the molecular weight, however, remains sufficiently high (inherent viscosity of the order of 2.0 dl./g.) to confer to the material good mechanical properties and thermal stability.

The time of activation of the solution is a very important factor which conditions the behavior of the reaction in the successive stages. In consequence, it must be controlled in a proper manner in order to obtain good and reproducible results. Maintaining the solution too long at the initial temperature favors polymerization of trioxane in solution; this leads to a decrease of the molecular weight; on the contrary, insufficient permanence at the initial temperature of the reacting system partly prevents the crystallization-polymerization process (because the concentration of active crystalline seeds becomes too low), during the precipitation of trioxane from the solution in the cooling stage. In order to obtain adequate activation of the

reaction system and avoid at the same time excessive polymerization of trioxane during this phase, it is necessary to start the cooling before the extent of the polymerization in solution (at the initial temperature) reach too high values.

The use of cyclohexane as solvent requires very stringent control of the initial stage, as compared with the use of hydrocarbons of high viscosity and low solvent power (vaseline oil); in fact, in the former case, the high concentrations of the solutions employed and the low viscosity of the medium, favor noticeably the rate of solution polymerization, which, occurs at a very high rate as soon as the induction period is passed.

Due to the excessive variability of the induction period, the extent of the initial phase of the process cannot be fixed on the basis of the period during which the solutions is kept at the initial temperature.

A much better control of the initial stage can be obtained by taking as a reference point the time at which the first increase of temperature is observed in the reacting system after addition of the catalyst (X_A), which can be assumed as the end of the induction period. Good results with respect to yields, molecular weight, and reproducibility of the experiments are obtained if the cooling is started just at the end of the induction period X_A . When vaseline oil is used as solvent, the initial temperature must be higher than the melting point of trioxane, because of the very low solubility of trioxane at temperatures below its melting point. With cyclohexane, a good solvent for trioxane, the activation temperature can be either higher or lower than the melting point of trioxane (61–62°C.). In the former case, it is advisable to cool the solution at rather high rates, to avoid keeping the solution too long at temperatures above the precipitation point of solid trioxane. This leads to rather high molecular weights but low yields. Good results can also be obtained if the cooling is carried out in two stages: (a) quenching of the solution from the initial temperature to the precipitation point, at the end of the induction period; (b) cooling of the reacting system at a controlled rate from the precipitation point to room temperature.

On the contrary, if the reaction is started at temperatures below the melting point of trioxane and sufficiently concentrated solutions are used, relatively low rates of cooling can be employed leading to the highest yield and molecular weights.

References

1. Baccaredda, M., E. Butta, P. Giusti, and F. Morelli, *J. Polymer Sci.*, **C4**, 953 (1964).
2. Bruni, G. J., U. S. Pat. 2,989,510 (June 20, 1961).
3. Jaacks, V., and W. Kern, *Makromol. Chem.*, **62**, 1 (1963).
4. Kern, W., and V. Jaacks, *J. Polymer Sci.*, **48**, 399 (1960).

Résumé

On a étudié la préparation du polyoxyméthylène de poids moléculaire élevé par polymérisation du trioxane à partir de solutions concentrées dans des solvants hydrocarbonés

(cyclohexane), activée par addition d'un catalyseur cationique (éthérate de BF_3) et en amorçant la cristallisation du trioxane en refroidissant le système activé depuis la température initiale jusqu'à la température de chambre. Le succès de la méthode dépend fortement du degré d'activation de la solution initiale, laquelle peut être contrôlée en suivant les variations de température du système pendant cette étape. Le refroidissement de la solution activée peut être effectué soit d'une façon continue, dans ce cas on peut faire varier la température depuis 15 jusqu'à 200°C/heure, ou bien en deux étapes: refroidissement brusque de la réaction depuis la température initiale jusqu'au point de précipitation suivi d'un refroidissement contrôlé à vitesse plus faible depuis ce point jusqu'à la température de chambre. Cette dernière méthode est préférable lorsqu'on choisit des températures initiales plus élevées que le point de fusion du trioxane pur. On a obtenu des produits possédant des viscosités inhérentes se situant entre 2.0 et 3.0 (en solutions à 0.5% dans le *p*-chlorophénol à 60°C).

Zusammenfassung

Die Darstellung von hochmolekularem Polyoxymethylen durch Polymerisation von Trioxan, ausgehend von konzentrierten Kohlenwasserstofflösungen (Cyklohexan) unter Aktivierung durch Zusatz eines kationischen Katalysators (BF_3 -Ätherat) und Anregung der Kristallisation des Trioxans durch Abkühlung des aktivierten Systems von der Anfangstemperatur auf Raumtemperatur wird untersucht. Der Erfolg der Methode hängt zum grossen Teil vom Aktivierungsgrad der Ausgangslösung ab, welcher durch Verfolgung der Temperaturänderung während dieser Phase kontrolliert werden kann. Die Abkühlung der aktivierten Lösung kann entweder kontinuierlich durchgeführt werden, in welchem Falle sie von 15 bis 200°C/h variiert werden kann, oder in zwei Schritten: Abschreckung von der Anfangstemperatur zum Fällungspunkt und darauffolgende kontrollierte Abkühlung bei niedrigerer Geschwindigkeit von diesem Punkt auf Raumtemperatur. Letztere Methode ist vorzuziehen, wenn Anfangstemperaturen höher als der Schmelzpunkt des reinen Trioxans gewählt werden. Produkte mit Viskositätszahlen im Bereich von 2,0 bis 3,0 dl/g (in 0,5 %iger *p*-Chlorphenollösung bei 60°C) werden erhalten.

Received October 20, 1964

Revised December 24, 1964

(Prod. No. 4613A)

Cationic Copolymerization of Isobutene. III. Solvent Effect in Cationic Copolymerization of Isobutene with Styrene in Mixed Solvents*

YUKIO IMANISHI, TOSHINOBU HIGASHIMURA, and SEIZO OKAMURA, *Department of Polymer Chemistry, Faculty of Engineering, Kyoto University, Kyoto, Japan*

Synopsis

Copolymerizations of isobutene (M_1) and styrene (M_2) were carried out at -78°C . with the use of titanium tetrachloride as the catalyst in *n*-hexane-methylene chloride mixed solvents of various compositions. A great variation of r_1, r_2 was observed. In *n*-hexane $r_1 < 1$ and $r_2 > 1$, in methylene chloride $r_1 > 1$ and $r_2 \simeq 1$, and in the mixed solvents both r_1 and r_2 were greater than unity. These experimental facts were interpreted on the basis of a large difference between the reactivities of isobutene cation and styrene cation. A values, on which the discussion of the decrease in the degree of copolymer polymerization can be based, were maximal in *n*-hexane and decreased with increasing ratio of methylene chloride in the mixed solvent. This is characteristic of the styrene-type monomer transfer reaction.

I. INTRODUCTION

Since Landler's investigation² of ionic copolymerization, it has generally been accepted that the monomer reactivity ratio, r_1 and r_2 , for ionic copolymerization for a set of monomers is independent of the polymerization condition, and that in most cases the product of $r_1 r_2$ is around unity. However, it has recently been recognized that the above holds only for copolymerization between styrene derivatives,^{3,4} that the monomer reactivity ratio is affected by the polymerization conditions, and that $r_1 r_2$ deviates from unity in copolymerizations where two monomers of different structures,^{5,6} and hence two ions of different reactivities, participate, or in copolymerization between two monomers with different steric requirements in the activated state.⁷

Overberger and Kamath⁵ reported a change of monomer reactivity ratio depending on the polymerization conditions in cationic copolymerization of isobutene and *p*-chlorostyrene. Variation of monomer reactivity ratio depending on polymerization conditions in cationic copolymerization of isobutene and styrene has been reported from this laboratory.⁸

* For the previous paper, see Imanishi et al.¹

This paper will describe experimental results for the cationic copolymerization of isobutene and styrene. Copolymerizations were carried out by titanium tetrachloride at -78°C . in *n*-hexane (low dielectric constant), methylene chloride (high dielectric constant) and mixtures of them, and a dependency of monomer reactivity ratio on dielectric constant of solvent was observed. A previous paper⁸ noted a considerable difference between the stabilities of the isobutene and styrene cations. The experimental facts in the present paper were therefore discussed in terms of difference between the stabilities of isobutene and styrene cations and of the effect of the dielectric constant of the solvent on the stability of the growing ion.

The previous paper¹ mentions a cross-transfer reaction between isobutene cation and styrene monomer, and here the effect of the solvent dielectric constant on the cross-transfer reaction will be discussed.

The paper will thus deal with the effect of solvent on the propagation and transfer reactions.

2. EXPERIMENTAL

Reagents

Isobutene (Phillips, purity 99.3 wt.-%) was distilled from a cylinder at room temperature, dehydrated through a long potassium hydroxide tube, and condensed into a buret precooled to -78°C . A given amount of isobutene was taken from the buret.

Styrene (Koppers) was washed repeatedly with alkali and water, then dried over anhydrous sodium sulfate, distilled in a vacuum, dried over metallic sodium, and again distilled (b.p. $55^{\circ}\text{C}/32\text{ mm.}$).

n-Hexane (guaranteed reagent) was washed with concentrated sulfuric acid, water, 10% aqueous sodium hydroxide solution, an aqueous alkaline solution of potassium permanganate, and finally water, dried over calcium chloride, and distilled from sodium metal (b.p. $65.5\text{--}66.1^{\circ}\text{C}$.).

Methylene chloride (guaranteed reagent) was washed with water, 10% aqueous potassium carbonate solution, and finally water, dried over phosphorus pentoxide, and twice distilled from phosphorus pentoxide just before use (b.p. $39.5\text{--}40^{\circ}\text{C}$.).

Titanium tetrachloride (extra pure) was distilled into a small glass ampule, which was broken in the polymerization solution to initiate the polymerization (b.p. $136^{\circ}\text{C}/760\text{ mm. Hg}$). Sometimes the titanium tetrachloride ampule was broken in the polymerization solvent to make a catalyst solution, which was added to the polymerization solution to initiate the polymerization.

Stannic chloride (extra pure) was distilled from phosphorus pentoxide into a small glass ampule, which was broken in the polymerization solution to initiate polymerization (b.p. $111.6\text{--}111.8^{\circ}\text{C}$.).

Procedure

Five kinds of solvent were used in the present investigation: 100% *n*-hexane, 75% *n*-hexane–25% methylene chloride, 50% *n*-hexane–50% methylene chloride, 25% *n*-hexane–75% methylene chloride, and 100% methylene chloride (all volume percentages). All copolymerizations were effected at -78°C . (Dry Ice–methanol) usually by titanium tetrachloride but sometimes by stannic chloride, adventitious water being regarded as the cocatalyst. The polymerization solution (total volume 50 ml.) comprised one of the above solvents (40 ml.), plus monomer mixture (10 ml.) containing varying ratios of isobutene and styrene.

Solvent and monomers were put in a 100 ml. flask equipped with a long calcium chloride tube and a catalyst inlet (a syringe). The polymerization solution was cooled to -78°C . and the polymerization started by addition of precooled catalyst solution through the inlet, or by breaking a catalyst ampule in the polymerization solution. Polymerization was stopped by adding a large amount of methyl alcohol. Conversion was usually kept below 10%. Polymer precipitated was repeatedly washed by methyl alcohol and dried in a vacuum at 40°C .

Determination of Copolymer Composition

Elementary analysis is not suitable for determining copolymer composition, since the elementary compositions of polystyrene (C:92.27%) and polyisobutene (C:85.63%) differ but little. In the present investigation, therefore, infrared spectroscopy was used for copolymer analysis. For this purpose, the calibration curve between optical density of the key band and copolymer composition has to be known, and it was assumed that the mole extinction coefficient of the key band in the copolymer is same as in a mixture of the corresponding homopolymers, though at present this has not been established experimentally. However, the optical densities ratio, D_{3061}/D_{2923} , for copolymer prepared at up to 100% conversion at an initial monomer composition of 0.7 mole fraction styrene and 0.3 mole fraction isobutene differs only by experimental error from that of a mixture of 0.7 mole fraction polystyrene and 0.3 mole fraction polyisobutene (D_{3061}/D_{2923} was 0.289 for the copolymer and 0.293 for the mixture.). This experimental finding suggests that the above assumption is reasonable.

Polyisobutene and polystyrene were prepared under the same conditions as in the copolymerization. A carbon disulfide solution of the mixture of polyisobutene and polystyrene (concentration 25 g./l. solvent) was made up for the infrared measurements. The absorption at 3061 cm.^{-1} , which appears only in polystyrene and is ascribed to C–H stretching of the phenyl group, and that at 2923 cm.^{-1} , which appears both in polystyrene and in polyisobutene and is ascribed to C–H stretching of the methylene group, were found to correlate well with moles of styrene, and moles of styrene plus isobutene of the mixed polymer, respectively. On plotting the optical densities ratio, D_{3061}/D_{2923} , against mole fraction of styrene in the mixed

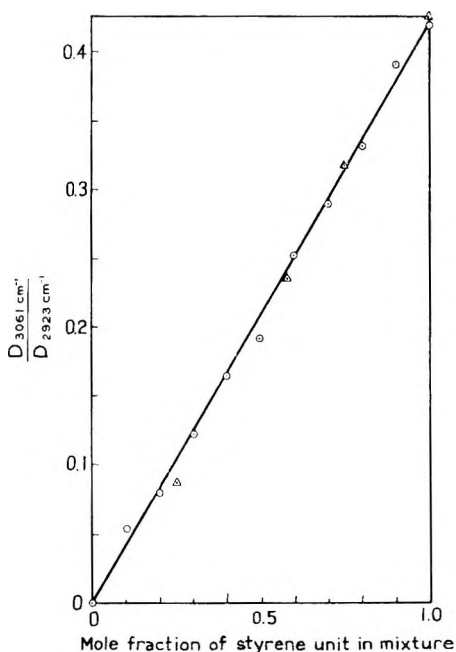


Fig. 1. Relationship between mole fraction of styrene unit in polymer mixture and D_{3061}/D_{2923} of infrared spectrum.

polymer, the linear relationship shown in Figure 1 was obtained. In the present investigation, copolymer composition was determined from the infrared spectra optical densities ratio of the copolymers on the basis of Figure 1. This method is based on the optical densities ratio (not on absolute optical density), affording the advantage that it is not necessary to prepare carbon disulfide solutions of accurately known concentration. The reproducibility obtainable by this method is shown in Table I.

TABLE I
Reproducibility of Determining F_1 by Infrared Spectroscopy

| F_1 in first run | F_1 in second run |
|--------------------|---------------------|
| 0.125 | 0.135 |
| 0.175 | 0.187 |
| 0.272 | 0.314 |
| 0.492 | 0.455 |
| 0.830 | 0.810 |
| 0.924 | 0.939 |

Determination of the Degree of Polymerization of Copolymer

The intrinsic viscosity-molecular weight relationship for isobutene-styrene copolymer of various compositions has never been reported. In

the present investigation, the molecular weight of the copolymer was calculated from the intrinsic viscosity of the copolymer in toluene solution at 30°C., by eqs. (1) and (2), assuming that the copolymer is identical with polyisobutene or polystyrene.

For polyisobutene in toluene at 30°C.:⁹

$$[\eta] = 2.0 \times 10^{-4} \bar{M}_n^{0.67} \quad (1)$$

For polystyrene in toluene at 30°C.:¹⁰

$$[\eta] = 1.22 \times 10^{-4} \bar{M}_n^{0.70} \quad (2)$$

Since the true molecular weight of the copolymer is considered to lie between the molecular weights given by eqs. (1) and (2), an algebraic mean of the two was taken as the copolymer molecular weight. The degree of polymerization was calculated from the copolymer molecular weight and composition.

Measurement of Solvent Dielectric Constant

Dielectric constants of *n*-hexane and methylene chloride were obtained from the literature.¹¹ The dielectric constants of solvent mixtures were measured in a stainless steel cell which was connected to a circuit comprising a frequency oscillator, a Wheatstone bridge and a multiplier at 1 Kcycle/sec.

3. RESULTS

Dielectric Constant of Mixed Solvents

Dielectric constants of mixed solvents as measured by the method described above are shown in Table II.

TABLE II
Dielectric Constant of Polymerization Solvents

| Solvent composition | | Dielectric constant at -78°C. |
|---|--|----------------------------------|
| <i>n</i> -C ₆ H ₁₄ , % | CH ₂ Cl ₂ , % | |
| 100 | 0 | 2.046 |
| 75 | 25 | 3.95 |
| 50 | 50 | 6.53 |
| 25 | 75 | 10.65 |
| 0 | 100 | 14.89 |

Cationic Copolymerization of Isobutene and Styrene in Mixed Solvents and Determination of r_1 and r_2

Cationic copolymerization of isobutene (M_1) and styrene (M_2) was carried out in five different solvents. The copolymer was analyzed by infrared spectroscopy and the monomer reactivity ratio determined by the cross-

section method. Typical experimental results obtained in *n*-hexane 25%—methylene chloride 75% are shown in Table III and Figures 2 and 3.

Monomer reactivity ratios in other solvents were obtained similarly. Copolymer composition curves are shown in Figure 4, and monomer reactivity ratios are listed in Table IV.

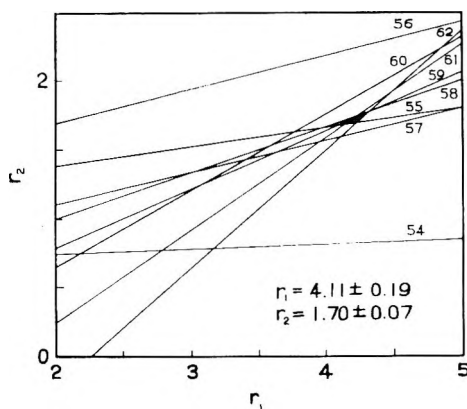


Fig. 2. Determination of monomer reactivity ratio by cross-section method. Solvent: *n*-hexane 25%—methylene chloride 75%.

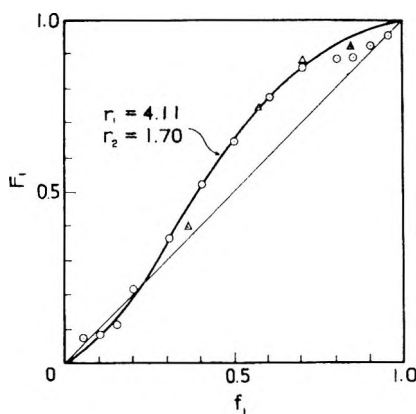


Fig. 3. Copolymer composition curve for *n*-hexane 25%—methylene chloride 75% system.

Some of the copolymers obtained in three kinds of mixed solvent were submitted to elementary analysis; the results were found to agree well with those of infrared spectroscopy.

The effect of the nature of the counterion on monomer reactivity ratio was also investigated. Copolymerizations with stannic chloride as the catalyst were carried out in *n*-hexane 25%—methylene chloride 75%. Copolymer analysis as above gave for the monomer reactivity ratio $r_1 = 3.75 \pm 0.45$ and $r_2 = 1.92 \pm 0.41$. Figure 5 shows the copolymer composition curve. Figure 5 also shows for comparison the copolymer composition

TABLE III
 Copolymerization in Solvent Composed of *n*-Hexane (25%)–Methylene Chloride (75%)

| Run no. | Isobutene, ml. | Styrene, ml. | f_1^a | TiCl ₄ , mg. | Polymerization time, sec. | Yield, g. | Conversion, % | R_{p1} , %/g./sec. | $D_{20/61}$ | | F_1^c |
|---------|----------------|--------------|---------|-------------------------|---------------------------|-----------|---------------|----------------------|-------------|---------|---------|
| | | | | | | | | | D_{2923} | F_2^b | |
| 53 | 0.0 | 10.0 | 0.000 | 30.1 | 120 | 3.4827 | 38.5 | 10.66 | 0.417 | 1.000 | 0.000 |
| 54 | 0.4 | 9.6 | 0.052 | " | 30 | 0.3312 | 3.7 | 4.10 | 0.387 | 0.929 | 0.071 |
| 55 | 0.8 | 9.2 | 0.103 | " | 37 | 0.6576 | 7.4 | 6.64 | 0.381 | 0.914 | 0.086 |
| 56 | 1.2 | 8.8 | 0.152 | " | 16 | 0.4159 | 4.7 | 9.76 | 0.369 | 0.885 | 0.115 |
| 57 | 1.6 | 8.4 | 0.201 | " | 16 | 0.5125 | 5.9 | 12.25 | 0.327 | 0.784 | 0.216 |
| 58 | 2.5 | 7.5 | 0.305 | " | 21 | 0.3243 | 3.9 | 6.17 | 0.265 | 0.635 | 0.365 |
| 59 | 3.4 | 6.6 | 0.404 | " | 16.5 | 0.3350 | 4.1 | 8.26 | 0.200 | 0.480 | 0.520 |
| 60 | 4.3 | 5.7 | 0.499 | " | 24 | 0.4241 | 5.4 | 7.48 | 0.149 | 0.357 | 0.643 |
| 61 | 5.4 | 4.6 | 0.607 | " | 60 | 0.1623 | 2.1 | 1.16 | 0.092 | 0.221 | 0.779 |
| 62 | 6.4 | 3.6 | 0.701 | " | 38.5 | 0.4267 | 5.8 | 5.00 | 0.057 | 0.137 | 0.863 |
| 63 | 7.5 | 2.5 | 0.798 | " | 120 | 0.1964 | 2.8 | 0.78 | 0.049 | 0.118 | 0.882 |
| 64 | 8.1 | 1.9 | 0.849 | " | 146 | 0.2073 | 3.0 | 0.68 | 0.048 | 0.117 | 0.883 |
| 65 | 8.7 | 1.3 | 0.898 | " | 46 | 0.1593 | 2.3 | 1.66 | 0.032 | 0.076 | 0.924 |
| 66 | 9.4 | 0.6 | 0.953 | " | 40 | 0.6665 | 10.1 | 8.39 | 0.020 | 0.048 | 0.952 |
| 67 | 10.0 | 0.0 | 1.000 | " | 71 | 0.3931 | 6.1 | 2.85 | 0.000 | 0.000 | 1.000 |

^a f_1 = mole fraction of isobutene in monomer feed.

^b F_2 = mole fraction of styrene units in copolymer.

^c F_1 = mole fraction of isobutene units in copolymer.

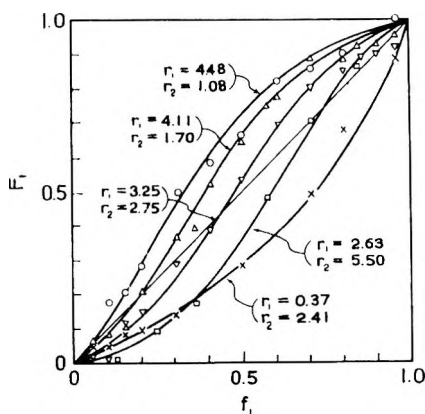


Fig. 4. Copolymer composition curves for isobutene(M_1)-styrene(M_2) copolymer obtained in various solvents: (O) methylene chloride 100%; (Δ) methylene chloride 75%-*n*-hexane 25%; (∇) methylene chloride 50%-*n*-hexane 50%; (\square) methylene chloride 25%-*n*-hexane 75%; (\times) *n*-hexane 100%.

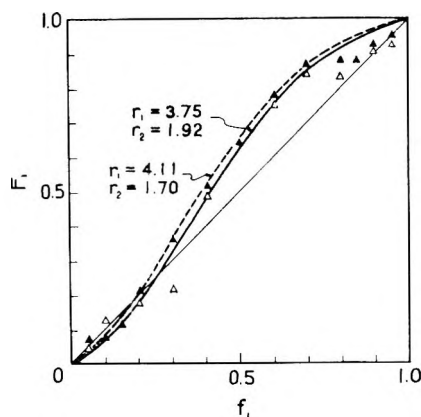


Fig. 5. Copolymer composition curves for isobutene(M_1)-styrene(M_2) copolymer produced in *n*-hexane 25%-methylene chloride 75% system: (\blacktriangle) TiCl_4 catalyst; (Δ) SnCl_4 catalyst.

TABLE IV
Monomer Reactivity Ratios and Solvent Composition

| Solvent composition | | r_1 | r_2 |
|---|--|-------------|-------------|
| <i>n</i> -C ₆ H ₁₄ , % | CH ₂ Cl ₂ , % | | |
| 100 | 0 | 0.37 ± 0.07 | 2.41 ± 0.12 |
| 75 | 25 | 2.63 ± 0.52 | 5.50 ± 0.55 |
| 50 | 50 | 3.25 ± 0.25 | 2.75 ± 0.25 |
| 25 | 75 | 4.11 ± 0.19 | 1.70 ± 0.07 |
| 0 | 100 | 4.48 ± 0.28 | 1.08 ± 0.07 |

curve for copolymerization catalyzed by titanium tetrachloride in the same solvent.

The following points emerged clearly from the experimental results.

(1) In copolymerization of isobutene and styrene the monomer reactivity ratios vary greatly with solvent and slightly with catalyst.

(2) Isobutene has generally been considered to be more reactive than styrene in cationic polymerization. This is true for polymerization in methylene chloride but not in *n*-hexane.

(3) In copolymerization in mixed solvents, a growing cation tends to add the same kind of monomer, leading to r_1 and r_2 larger than unity.

(4) The greater the solvent dielectric constant, the greater the reactivity of isobutene.

(5) Slightly more styrene is incorporated into the copolymer in copolymerization by stannic chloride than in copolymerization by titanium tetrachloride.

Degree of Polymerization of Copolymer Produced in Mixed Solvents and the Determination of the A Value

The previous paper¹ reported that in the cationic copolymerization of isobutene and styrene, the degree of polymerization of copolymer is considerably lower than that for the corresponding homopolymers under the same conditions because in the copolymerization system the isobutene cation, which is very reactive in the transfer reaction, and the styrene monomer, which is very reactive as a transfer reagent, coexist simultaneously, and the cross-transfer reaction from isobutene cation to styrene monomer takes place very readily. The A value, which comprises the cross-transfer constant ratios, was used as a measure of the drop in the degree of polymerization of the copolymer. The method of calculating the A value from the degree of polymerization of copolymer was explained in the previous paper.¹ The degree of polymerization of copolymer \bar{P} is given by eq. (3);

$$\bar{P} = \frac{r_1[M_1]^2 + 2[M_1][M_2] + r_2[M_2]^2}{(1/\bar{P}_1)r_1[M_1]^2 + A[M_1][M_2] + (1/\bar{P}_2)r_2[M_2]^2} \quad (3)$$

$$A \equiv k_{t_{12}}/k_{p_{12}} + k_{t_{21}}/k_{p_{21}}$$

where \bar{P}_1 and \bar{P}_2 are, respectively, the degrees of polymerization of homopolymer from monomers 1 and 2, and $[M_1]$ and $[M_2]$ are monomer concentrations (in mole/liter) of monomers 1 and 2, respectively; k_t and k_p are the rate constants of the monomer transfer and the propagation reactions, respectively. The subscript 12 means a reaction between cation 1 and monomer 2, and subscript 21 means the converse. With r_1 , r_2 and \bar{P}_1 , \bar{P}_2 given for a certain copolymerization system, and having determined the degree of copolymerization of copolymers obtained for various values of $[M_1]$ and $[M_2]$, A values can be calculated by using eq. (3).

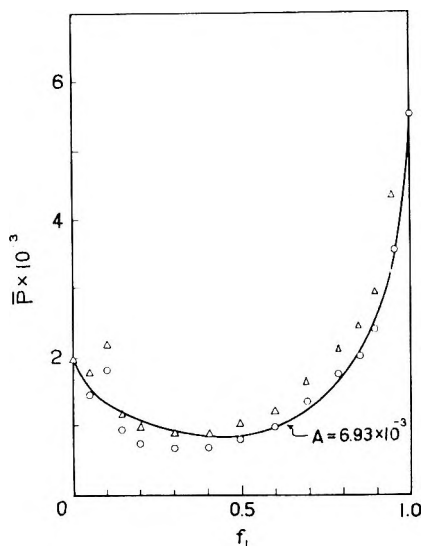


Fig. 6. Degree of polymerization of copolymer as a function of monomer feed: (O) \bar{P} from eq. (1); (Δ) \bar{P} from eq. (2). Solvent: *n*-hexane 50%–methylene chloride 50%.

In order to investigate the effect of solvent polarity on the monomer transfer reaction, *A* values in five kinds of solvent were calculated. Table V shows experimental results for *n*-hexane 50%–methylene chloride 50%.

Figure 6 shows the degree of polymerization of the copolymer and the calculated curve corresponding to the *A* value thus obtained.

TABLE V
Molecular Weight of Copolymer and *A* Value (*n*-Hexane
50%–Methylene Chloride 50%)

| Run no. | f_1 | F_1 | $[\eta]$ (30°C., toluene) | From eq. (1) | | From eq. (2) | | $A \times 10^{16}$ |
|---------|-------|-------|---------------------------------|--------------|-----------|--------------|-----------|--------------------|
| | | | | \bar{M}_n | \bar{P} | \bar{M}_n | \bar{P} | |
| 68 | 0.000 | 0.000 | 0.648 | — | — | 209,200 | 2009 | — |
| 69 | 0.052 | 0.021 | 0.585 | 148,700 | 1442 | 180,300 | 1748 | 78.11 |
| 70 | 0.103 | 0.012 | 0.673 | 183,000 | 1769 | 221,200 | 2138 | — |
| 71 | 0.152 | 0.119 | 0.420 | 90,800 | 917 | 112,800 | 1139 | 83.93 |
| 72 | 0.201 | 0.149 | 0.365 | 73,900 | 751 | 92,700 | 942 | — |
| 73 | 0.305 | 0.289 | 0.315 | 59,400 | 658 | 75,000 | 831 | 96.33 |
| 74 | 0.404 | 0.389 | 0.300 | 55,200 | 646 | 70,000 | 819 | 88.50 |
| 75 | 0.499 | 0.529 | 0.320 | 60,800 | 772 | 76,800 | 975 | 72.01 |
| 76 | 0.607 | 0.695 | 0.345 | 68,000 | 961 | 85,500 | 1208 | — |
| 77 | 0.701 | 0.799 | 0.408 | 87,000 | 1323 | 108,800 | 1655 | 52.73 |
| 78 | 0.798 | 0.852 | 0.476 | 109,000 | 1724 | 136,000 | 2151 | 53.38 |
| 79 | 0.849 | 0.892 | 0.522 | 125,000 | 2039 | 153,000 | 2496 | 55.85 |
| 80 | 0.898 | 0.899 | 0.583 | 148,000 | 2428 | 180,000 | 2953 | 61.14 |
| 81 | 0.953 | 0.918 | 0.754 | 216,500 | 3606 | 260,000 | 4330 | 51.25 |
| 82 | 1.000 | 1.000 | 0.953 | 308,500 | 5499 | — | — | — |

* Average value of $A = 69.33 \times 10^{-4}$.

TABLE VI
 A Values and Solvent Composition

| Solvent composition | | $A \times 10^3$ |
|------------------------------------|---------------------------------|-----------------|
| $n\text{-C}_6\text{H}_{14}$, % | CH_2Cl_2 , % | |
| 100 | 0 | 25.0 |
| 75 | 25 | 10.2 |
| 50 | 50 | 6.93 |
| 25 | 75 | 4.48 |
| 0 | 100 | 5.25 |

A values, determined in other solvents by the same procedure are shown in Table VI.

Similarly, in investigation of the monomer reactivity ratio, the effect of catalyst on A was studied. In the copolymerization by stannic chloride in the n -hexane 25%–methylene chloride 75% solvent mixture, A was found to be 4.53×10^{-3} .

The following points were made clear. (1) The more polar the solvent, the less readily the cross-transfer reaction occurs. (This is the same trend as in cationic polymerization of styrene.¹²) (2) The cross-transfer reaction is little affected by changing the catalyst, i.e., titanium tetrachloride or stannic chloride.

Effect of Solvent Composition on the Reactivity of Isobutene Cation and the Determination of B Values

As is seen in eq. (3), A is a combination of two kinds of transfer constant ratio. It is therefore difficult to use A to discuss the cross-transfer reaction, though it provides a good explanation for the lowering of the degree of polymerization of the copolymer. The previous paper¹ proposed calculating k_{t12}/k_{p11} , the ratio of the chain transfer constant of isobutene cation to styrene to the propagation constant for isobutene, to enable the cross-transfer reaction to be discussed quantitatively. k_{t12}/k_{p11} was determined from eq. (4) after calculating the degree of polymerization of polyisobutene obtained in a polymerization system consisting of solvent (45 ml.), isobutene (5 ml.), and a small amount of styrene. Introducing the relationship $[\text{M}_2] \ll [\text{M}_1]$ into eq. (3) gives eq. (4):

$$1/\bar{P} = (1/\bar{P}_1) + B([\text{M}_2]/[\text{M}_1]) \quad (4)$$

$$B \equiv (k_{t12}/k_{p11}) + (k_{t21}/k_{p21})(1/r_1) - (2/\bar{P}_1 r_1)$$

where \bar{P} and \bar{P}_1 are the degree of polymerization of polyisobutene obtained in polymerization with and without styrene, respectively. The slope of the straight line obtained on plotting \bar{P} against $[\text{M}_2]/[\text{M}_1]$ gives the B value. As k_{t21}/k_{p21} , \bar{P}_1 , and r_1 are known, k_{t12}/k_{p11} can be calculated from B . Determination of k_{t12}/k_{p11} for polymerization in n -hexane 75%–methylene

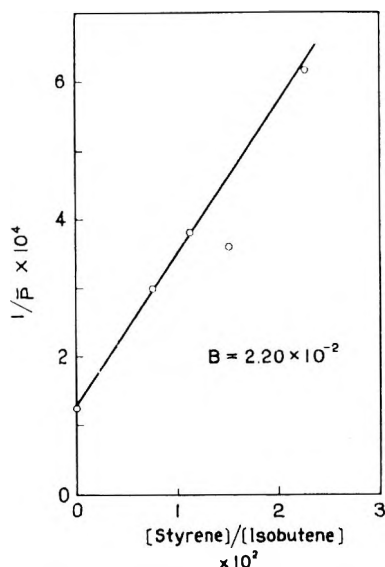


Fig. 7. Determination of B value. Solvent: n -hexane 75%–methylene chloride 25%.

chloride 25% will be adduced below by way of example. Figure 7 shows the determination of B .

In this system (k_{r21}/k_{p21}) $1/r_1$ and $2/(1\bar{P}r_1)$ were previously calculated to be 0.05×10^{-4} and 1.41×10^{-4} , respectively. Therefore, k_{r21}/k_{p11} was found to be 2.21×10^{-2} . B values and k_{r12}/k_{p11} were determined in other solvents, and the values obtained are shown in Table VII.

TABLE VII
 B Values, k_{r12}/k_{p11} , and Solvent Composition

| Solvent composition | | $B \times 10^3$ | $k_{r12}/k_{p11} \times 10^2$ |
|---|-------------------------------------|-----------------|-------------------------------|
| n -C ₆ H ₁₄ , % | CH ₂ Cl ₂ , % | | |
| 100 | 0 | 47.0 | 48.0 |
| 75 | 25 | 22.0 | 22.1 |
| 50 | 50 | 13.4 | 13.5 |
| 25 | 75 | 2.48 | 2.57 |
| 0 | 100 | 4.55 | 4.59 |

The following points emerged clearly from Table VII: (1) B and k_{r12}/k_{p11} are greatly affected by the nature of solvent; (2) k_{r12}/k_{p11} decreases with an increase of solvent polarity, which was what was found for the monomer transfer constant ratio in cationic polymerization of styrene.¹²

It is noted that the change in A value with change in solvent composition parallels that for k_{r12}/k_{p11} . Therefore, the lowering of the degree of polymerization of copolymer can be discussed in terms of the effect of solvent polarity on k_{r12}/k_{p11} .

TABLE VIII
Preparation of Copolymer for the Fractional Extraction

| Run no. | Iso-butene, ml. | Styrene, ml. | f_1 | Solvent composition | | TiCl ₄ , mg. | Yield, g. | Conversion, % | D_{3061} | | F_1 expected from Fig. 4 |
|---------|-----------------|--------------|-------|-------------------------------------|--------------------------------------|-------------------------|-----------|---------------|------------|-------|----------------------------|
| | | | | CH ₂ Cl ₂ , % | n-C ₆ H ₁₄ , % | | | | D_{2923} | F_1 | |
| F-1 | 4.9 | 15.1 | 0.300 | 100 | 0 | 93.7 | — | 100 | 0.289 | 0.310 | 0.300 |
| F-2 | 7.7 | 12.3 | 0.452 | 75 | 25 | 100.8 | 2.1884 | 13.6 | 0.174 | 0.584 | 0.590 |
| F-3 | 8.6 | 11.4 | 0.498 | 50 | 50 | 115.9 | 5.2617 | 33.1 | 0.222 | 0.470 | 0.550 |
| F-4 | 10.4 | 9.6 | 0.588 | 25 | 75 | 127.4 | 4.4383 | 28.9 | 0.212 | 0.494 | 0.493 |
| F-5 | 12.1 | 7.9 | 0.669 | 0 | 100 | 321.9 | 2.2007 | 14.7 | 0.194 | 0.537 | 0.446 |
| F-6 | 12.1 | 7.9 | 0.669 | 0 | 100 | 337.5 | 3.2000 | 21.4 | 0.194 | 0.537 | 0.446 |

TABLE IX
Fractional Extraction of Copolymer

| Run no. | Original sample, g. | Acetone-soluble | | Acetone-MEK-soluble | | MEK-soluble | | Cyclohexanone-soluble | | Residue, g. | Loss, g. | F_1 calculated $\sum \frac{F_1 \cdot \%}{100}$ | |
|---------|---------------------|-----------------|------|---------------------|--------|-------------|-------|-----------------------|------|-------------|----------|--|-------|
| | | g. | % | g. | % | g. | % | g. | % | | | | |
| F-1 | 10.0020 | 5.1495 | 51.5 | 0.297 | 4.0112 | 40.1 | 0.348 | 0 | 0 | 0 | 0.8419 | 8.4 | 0.319 |
| F-2 | 1.5318 | 0.3818 | 24.9 | 0.430 | 0.5761 | 37.6 | 0.497 | 0.2292 | 15.0 | 0.638 | 0.0208 | 1.3 | 0.760 |
| F-3 | 4.0902 | 1.9470 | 47.6 | 0.388 | 1.3042 | 31.9 | 0.537 | 0.3551 | 8.7 | 0.574 | trace | ~0 | 0.460 |
| F-4 | 3.8817 | 0.7877 | 20.3 | 0.527 | 1.4124 | 36.4 | 0.530 | 1.1593 | 30.0 | 0.563 | trace | ~0 | 0.541 |
| F-5 | 1.6507 | 0.9315 | 56.4 | 0.431 | 0.5582 | 33.8 | 0.429 | 0 | 0 | — | 0 | 0 | 0.430 |
| F-6 | 2.4577 | 1.3259 | 53.9 | 0.487 | 0.8037 | 32.7 | 0.536 | 0 | 0 | — | 0 | 0 | 0.505 |

Extraction of Copolymer

As shown in Table IV, the monomer reactivity ratios r_1 and r_2 obtained in the present investigation were mostly larger than unity. This suggests the possibility that a mixture of the two homopolymers was obtained instead of true copolymer. In order to elucidate this point, copolymers were subjected to solvent extraction.

The samples for the extraction were prepared by carrying out copolymerizations in five kinds of solvent. The feed monomer composition was controlled to give a copolymer having F_1 about 0.5. Table VIII shows details of this preparation. It is observed that these copolymers contain the isobutene unit, as expected from Figure 4. Since the conversion rose to 100% in polymerization 1, the expected F_1 of copolymer 1 is 0.3, which is same as the monomer composition of the feed.

Copolymer extraction was carried out by the method of Sparks et al.,¹³ i.e., the copolymer was extracted by acetone, an acetone-methyl ethyl ketone mixture, methyl ethyl ketone, and cyclohexanone in turn, and any final residue was recovered. The fraction of copolymer extracted by each solvent was submitted to infrared spectroscopy to determine its composition. It would be expected that the fractions extracted later would contain more isobutene units. The extraction results are shown in Table IX.

The copolymers obtained in methylene chloride, where r_1 is larger than unity and r_2 nearly unity, and in *n*-hexane, where r_1 is less than unity and r_2 larger than unity, were completely extracted by the acetone-methyl ethyl ketone mixture, and considered to be true copolymers having a random and sharply distributed composition. On the other hand, copolymers obtained in mixed solvents, where both r_1 and r_2 are larger than unity, were extracted even by cyclohexanone, and considered to be copolymers of widely distributed composition. This is due to the somewhat longer sequence of same kind of monomer arising because both r_1 and r_2 are larger than unity. However, as traces of cyclohexanone-soluble material and no residue were present in the copolymer, it appears that the sequence of the same kind of monomer is not so long. Hence the copolymer obtained here may be considered to be a true copolymer to which the Mayo equation is applicable.

A considerable amount of copolymer was lost during extraction. But weight-average F_1 (mole fraction of isobutene unit in copolymer) of the sample calculated from F_1 of each fraction is approximately equal to F_1 of the original sample; hence discussions of extraction results are considered to be valid.

4. DISCUSSION

Here the effects of the dielectric constant of the solvent and of catalyst on monomer reactivity ratio (the propagation reaction), A value, B value, and k_{r1}/k_{p11} (the transfer reaction) will be discussed. For this purpose, the experimental data are summarized in Table X and Figures 8 and 9.

Effect of Solvent on r_1 and r_2

Overberger and Kamath⁵ proposed selective solvation of the growing ion-pair by one of two comonomers in order to explain their experimental data on the copolymerizations of isobutene with *p*-chlorostyrene and of chloroprene with styrene. The results for methylene chloride and *n*-hexane in the present investigation can be satisfactorily explained on the basis of this theory. In order to explain the experimental results with mixed solvents, however, a new interpretation in addition to Overberger's theory is

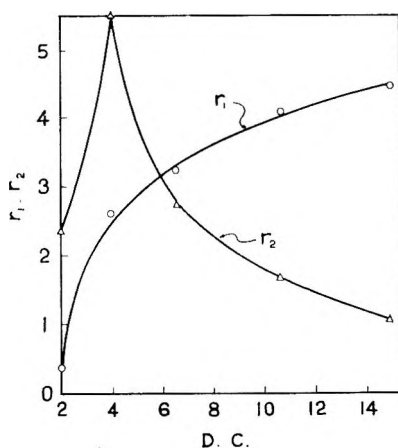


Fig. 8. Dependence of monomer reactivity ratio on dielectric constant of solvent.

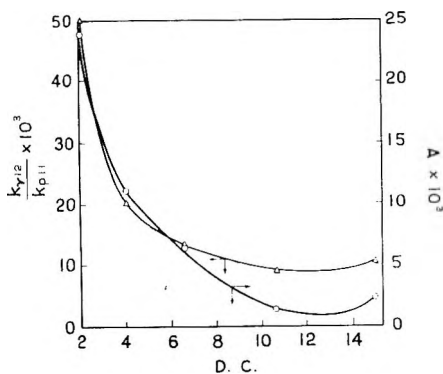


Fig. 9. Dependence of (O) A value and (Δ) k_{r12}/k_{p11} on dielectric constant of solvent.

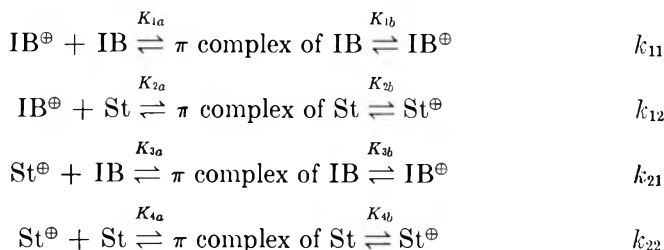
needed. All the experimental results may be considered explicable on the basis that the solvent effect arises out of differences in structures of the monomers giving rise to differences in the cation reactivities, the isobutene cation and styrene cation being affected differently by the solvent.

The following matters were considered in connection with explanation of the experimental results.

TABLE X
Summary of Experimental Data

| Solvent composition | | Dielectric constant at -78°C . | Catalyst | Reactivity ratios | | $A \times 10^3$ | $k_{12}/k_{p11} \times 10^3$ |
|---------------------------------|------------------------------|--|-----------------|-------------------|-----------------|-----------------|------------------------------|
| $n\text{-C}_6\text{H}_{14}$, % | CH_2Cl_2 , % | | | r_1 | r_2 | | |
| 100 | 0 | 2.046 | TiCl_4 | 0.37 ± 0.07 | 2.41 ± 0.12 | 25.0 | 48.0 |
| 75 | 25 | 3.95 | TiCl_4 | 2.63 ± 0.52 | 5.50 ± 0.55 | 10.2 | 22.1 |
| 50 | 50 | 6.53 | TiCl_4 | 3.25 ± 0.25 | 2.75 ± 0.25 | 6.92 | 13.5 |
| 25 | 75 | 10.65 | TiCl_4 | 4.11 ± 0.19 | 1.70 ± 0.07 | 4.48 | 2.57 |
| 25 | 75 | 10.65 | SnCl_4 | 3.75 ± 0.45 | 1.92 ± 0.41 | 4.53 | — |
| 0 | 100 | 14.89 | TiCl_4 | 4.48 ± 0.28 | 1.08 ± 0.07 | 5.25 | 4.59 |

(1) Four kinds of elementary reactions in copolymerization are divided into eight steps:¹⁴



Here IB^\oplus and St^\oplus represent, respectively, the growing isobutene and styrene cations, and IB and St denote, respectively, isobutene and styrene.

(2) The cation of isobutene is less stable and consequently more reactive than the cation of styrene which is resonance-stabilized by phenyl group. Therefore, $K_{1a} > K_{3a}$, $K_{2a} > K_{4a}$.

(3) Isobutene is more nucleophilic than styrene¹⁵ (greater rate of π -complex formation), but forms a carbonium ion with more difficulty.¹⁶ Therefore, $K_{1a} > K_{2a}$, $K_{3a} > K_{4a}$, $K_{2b} > K_{1b}$, and $K_{4b} > K_{3b}$.

(4) The ion pair can hardly be solvated in a nonpolar solvent such as *n*-hexane, so the stability of the resultant carbonium ion is an important determining factor of reaction facility. This means that the magnitude of K_b is important, whence k_{11} is smaller than k_{12} and k_{21} is smaller than k_{22} . This leads to r_1 smaller than unity and r_2 larger than unity, which is actually the case. Moreover, as Overberger and Kamath⁵ proposed, in a nonpolar solvent selective solvation of the ion pair by styrene is important. This effect tends to make r_1 (<1) still smaller and r_2 (>1) still larger than unity.

The instability of the isobutene cation is reflected in the rate of polymerization. The explosively fast polymerization of isobutene at -100°C . by boron trifluoride has been cited as an example of the rate of cationic polymerization being large even at low temperatures.¹⁷ However, this holds only for polymerization in polar solvents such as chlorinated hydrocarbons. We compared the initial rate of polymerization R_p of isobutene with that of styrene, expressing R_p as conversion per unit weight of catalyst per unit time. R_p in the polymerization at -78°C . by titanium tetrachloride at a monomer concentration of 10 vol-% was 27.65%/g./sec. for isobutene and 9.03%/g./sec. for styrene in methylene chloride, while in *n*-hexane the values for isobutene and styrene, respectively, were 1.70 and 1.26%/g./sec. Taking into account that in polymerization of isobutene in methylene chloride polyisobutene precipitates out and that occlusion of catalyst by polymer may occur, the difference in R_p in methylene chloride must be much larger. Moreover, allowing for the fact that in polymerization of styrene in *n*-hexane the resultant polystyrene is insoluble and that the same precipitation effect as in the polymerization of isobutene in methylene chloride may obtain, the R_p difference in *n*-hexane must be much smaller. It is also possi-

ble that R_p for styrene in hexane is larger than that for isobutene. The greater decrease in R_p for isobutene than for styrene accompanying a decrease in dielectric constant of the solvent suggests that stabilization by solvation is more important in the case of the unstable isobutene cation than with the stable styrene cation. This leads to the conclusion that an unstable isobutene cation is formed less easily in a nonpolar medium.

(5) In a polar solvent such as methylene chloride, both isobutene cation and styrene cation will be solvated almost completely, so that the difference in stabilities of the growing ion pairs is of minor importance in determining reaction rate, and consequently the magnitude of K_a is important. This results in $k_{11} > k_{12}$ and $k_{21} > k_{22}$, so in methylene chloride it is to be expected that r_1 will be larger and r_2 smaller than unity. However, in practice r_1 is larger than unity and r_2 is nearly equal to unity. This discrepancy can be explained satisfactorily on the basis that selective solvation⁵ of the growing ion pair by styrene obtains even in a polar medium to give higher concentration of styrene in the vicinity of the reaction site than in bulk. This makes r_2 nearly equal unity.

(6) In a solvent of intermediate polarity, the reaction between the olefinic double bond and a reactive cation such as isobutene cation is affected mainly by the equilibrium (a). On the other hand, the reaction of a stable cation such as styrene cation is affected mainly by equilibrium (b). Hence $k_{11} > k_{12}$ and $k_{22} > k_{21}$, leading to r_1 larger than unity and r_2 larger than unity.

On passing from a mixture consisting of 75% *n*-hexane to one with 25% *n*-hexane, stabilization of the growing ion pair increases and the significance of steps (a) gradually increases. This is why r_1 increases and r_2 decreases with increase of the polarity of mixed solvent with r_1 and r_2 remaining larger than unity.

To test the validity of the above ideas regarding growing ion pair reactivity in mixed solvents, the effect of stannic chloride on copolymerization was studied in methylene chloride 75%–*n*-hexane 25%. According to a previous paper,¹⁸ a growing ion pair including stannic chloride is less reactive than that including titanium tetrachloride. This means that in terms of the stability of the ion pair in solution, $\text{IB}^{\oplus}\text{SnCl}_4\text{X}^{\ominus}$ should be roughly equal to $\text{St}^{\oplus}\text{TiCl}_4\text{X}^{\ominus}$. Hence step (b) becomes to some extent important in the reaction of $\text{IB}^{\oplus}\text{TiCl}_4\text{X}^{\ominus}$, where step (a) dominates the reaction. This leads to $r_{1(\text{SnCl}_4)}$ smaller than $r_{1(\text{TiCl}_4)}$ with r_1 remaining larger than unity. On the other hand, the change from $\text{St}^{\oplus}\text{TiCl}_4\text{X}^{\ominus}$ to $\text{St}^{\oplus}\text{SnCl}_4\text{X}^{\ominus}$ means, on the same basis, that step (b) is much more important in the reaction of $\text{St}^{\oplus}\text{SiCl}_4\text{X}^{\ominus}$, where the step (b) dominates the reaction. This leads to the conclusion that $r_{2(\text{SnCl}_4)}$ is larger than $r_{2(\text{TiCl}_4)}$ with r_2 remaining larger than unity. This actually is the case for copolymerization of isobutene with styrene by stannic chloride. Overberger and Kamath⁵ reported that in the copolymerization of isobutene (M_1) and *p*-chlorostyrene (M_2) in nitrobenzene, $r_{1(\text{AIBr}_2)}$ was larger than $r_{1(\text{SnCl}_4)}$ and $r_{2(\text{AIBr}_2)}$ smaller than $r_{2(\text{SnCl}_4)}$. This is in good agreement with our experimental results and supports our views, if aluminum bromide forms a more reactive ion pair than stannic chloride.

Effect of Solvent on the A value and on k_{r12}/k_{p11}

As is seen from Figure 9, both A and k_{r12}/k_{p11} decrease with the increase of solvent dielectric constant. This is the same trend as was found for the monomer transfer reaction in cationic polymerization of styrene.¹² In cationic polymerization of isobutene¹⁹ and styrene,²⁰ k_p increases with increasing solvent dielectric constant, which is ascribed to greater dissociation of the growing ion pair. On the other hand, the monomer transfer reaction toward styrene monomer, which has been proved to be essentially a Friedel-Crafts alkylation, is not greatly accelerated by dissociation of the growing ion pair due to an increase in the dielectric constant of the solvent.²¹ Here the cross-transfer reaction is substantially the same as the styrene-type of monomer transfer reaction. Hence k_{r12}/k_{p11} behaved as expected.

In Figure 9 selective solvation by the solvent of greater polarity is seen to be absent in the present system. It is conceivable that the small change of k_{r12}/k_{p11} in the solvents containing over 50% of methylene chloride is conditioned by dissociation of the growing ion pair in such solvents gradually approaching its limiting value.

We have sometimes used mixed solvent to study the effect of solvent polarity on the monomer transfer reaction. In the present investigation it was found that selective solvation by one component of the mixed solvents is not important unless solvents of different structures are mixed. The mixing of solvents of analogous structure is considered to be a valid way of changing the polarity of the medium.

To sum up, the following can be stated. Isobutene (M_1) was copolymerized with styrene (M_2) by titanium tetrachloride in *n*-hexane-methylene chloride. The monomer reactivity ratio was found to be greatly affected by the mixing ratio of solvent. r_1 was larger than unity and r_2 was nearly unity in methylene chloride, while r_1 was smaller and r_2 was larger than unity in *n*-hexane. Both r_1 and r_2 were larger than unity in the mixed solvents. Furthermore, r_1 became larger with increasing dielectric constant of the solvent. These findings were interpreted in terms of the effect of solvent on stability of the growing ion pair.

The cross-transfer reaction from isobutene cation to styrene monomer was also affected by the ratio of solvents in the mixture, and this was explained in terms of the effect of solvent on the styrene-type monomer transfer reaction.

No evidence for selective solvation by one of the components of the mixed solvent was detected in the *n*-hexane-methylene chloride system.

The authors thank Miss Y. Yamada for her assistance in the experiments.

References

1. Imanishi, Y., Z. Momiyama, T. Higashimura, and S. Okamura, *Kobunshi Kagaku*, **20**, 369 (1963).
2. Landler, Y., *J. Polymer Sci.*, **8**, 63 (1952).
3. Overberger, C. G., L. H. Arond, and J. J. Taylor, *J. Am. Chem. Soc.*, **73**, 5541 (1951).
4. Overberger, C. G., R. J. Ehrig, and D. Tanner, *J. Am. Chem. Soc.*, **76**, 772 (1954).

5. Overberger, C. G., and V. G. Kamath, *J. Am. Chem. Soc.*, **85**, 446 (1963).
6. Dawans, F., and G. Smets, *Makromol. Chem.*, **59**, 163 (1963).
7. Okamura, S., T. Higashimura, A. Mizote, and I. Iwasa, paper presented to the Discussion Meeting of the Japan High Polymer Society, 1962.
8. Okamura, S., T. Higashimura, and K. Takeda, *Kobunshi Kagaku*, **18**, 389 (1961).
9. Fox, T. G., and P. J. Flory, *J. Phys. Colloid Chem.*, **53**, 197 (1949).
10. Abere, T., G. Goldfinger, H. Naidus, and H. Mark, *J. Phys. Chem.*, **49**, 211 (1945).
11. Morgan, S. O., and H. H. Lowry, *J. Phys. Chem.*, **34**, 2385 (1930).
12. Okamura, S., T. Higashimura, and Y. Sakurada, *Kogyo Kagaku Zasshi*, **61**, 1640 (1958).
13. Rehner, J., Jr., R. J. Zapp, and W. J. Sparks, *J. Polymer Sci.*, **11**, 21 (1953).
14. Taft, R. W., Jr., E. L. Purlee, P. Riesz, and C. A. DeFazio: *J. Am. Chem. Soc.*, **77**, 1584 (1955).
15. Yonezawa, T., T. Higashimura, K. Katagiri, K. Hayashi, S. Okamura, and K. Fukui, *J. Polymer Sci.*, **26**, 311 (1957).
16. Taft, R. W., Jr., *J. Am. Chem. Soc.*, **74**, 5372 (1952).
17. Pepper, D. C., *Quart. Revs.*, **8**, 88 (1954).
18. Imanishi, Y., S. Matsushita, T. Higashimura, and S. Okamura, *Makromol. Chem.*, **70**, 68 (1964).
19. Kennedy, J. P., I. Kirshenbaum, R. M. Thomas, and D. C. Murray, *J. Polymer Sci.*, **A1**, 331 (1963).
20. Kanoh, N., A. Gotoh, T. Higashimura, and S. Okamura, *Makromol. Chem.*, **63**, 115 (1963).
21. Brown, H. C., and M. Grayson, *J. Am. Chem. Soc.*, **75**, 6285 (1953).

Résumé

On a effectué des copolymérisations de l'isobutène (M_1) avec du styrène (M_2) à -78°C au moyen de tétrachlorure de titane comme catalyseur et dans des mélanges de différentes compositions en *n*-hexane-chlorure de méthylène comme solvants. On a observé une grande variation de r_1 , r_2 . Dans le *n*-hexane $r_1 < 1$ et $r_2 > 1$, dans le chlorure de méthylène $r_1 > 1$ et $r_2 \simeq 1$, et dans le mélange des solvants r_1 et r_2 sont plus grands que l'unité. Ces résultats expérimentaux sont interprétés sur la base d'une grande différence entre les réactivités du cation isobutène et du cation styrène. En examinant les valeurs de A , sur lesquelles on discute l'abaissement du degré de polymérisation du copolymère, on observe un maximum dans le *n*-hexane et une diminution lorsqu'on augmente le rapport de chlorure de méthylène dans le mélange de solvant, ce qui est caractéristique de la réaction de transfert sur monomère du type styrène.

Zusammenfassung

Kopolymerisation von Isobuten (M_1) und Styrol (M_2) wurde bei -78°C mit Titan-tetrachlorid als Katalysator in *n*-Hexan-Methylenchlorid-Mischungen als Lösungsmittel bei verschiedener Zusammensetzung ausgeführt und eine grosse Variation von r_1 und r_2 beobachtet. In *n*-Hexan ist $r_1 < 1$ und $r_2 > 1$, in Methylenchlorid $r_1 > 1$ und $r_2 \simeq 1$ und in Lösungsmittelgemischen sind r_1 und r_2 grösser als eins. Diese Versuchsergebnisse wurden unter dem Gesichtspunkt eines grossen Unterschiedes zwischen der Reaktivität des Isobuten- und des Styrolkations interpretiert. Bei den A -Werten, mit welchen die Erniedrigung des Polymerisationsgrades des Kopolymeren diskutiert werden kann, trat ein Maximum in *n*-Hexan auf und nahm mit steigendem Gehalt des Lösungsmittelgemisches an Methylenchlorid ab, was für die Übertragungsreaktion des Monomeren vom Styroltyp charakteristisch ist.

Received October 5, 1964

Revised December 15, 1964

(Prod. No. 4615A)

Alkaline Hydrolysis of Polyacrylamide

KUNIIHIKO NAGASE and KAHEI SAKAGUCHI, *Industrial Research Laboratories, Kao Soap Co., Ltd., Wakayama-shi, Japan*

Synopsis

Polyacrylamide has been reported to show an abnormal behavior on alkaline hydrolysis, that is, the reaction rate is quite high at the initial stage and decreases rapidly with increasing conversion. This phenomenon has been attributed to the polymer structure. We have found that the low molecular weight diamides show essentially the same behavior and concluded that this abnormality is due to the polyfunctionality and is not necessarily specific to polymers.

INTRODUCTION

In the alkaline hydrolysis of polyacrylamide, it has been reported by Smets et al.^{1,2} that the polymer shows higher initial rate than simple aliphatic amides, but the rate slows down quite rapidly as the reaction proceeds. Smets has suggested that this abnormality is mainly attributable to the polymeric structure of polyacrylamide.

In the present work we have investigated the rate of the alkaline hydrolysis of polyacrylamide in comparison with that of several of the low molecular weight amides.

The rates were expressed as the second-order rate constants and the comparison was made to determine whether the above stated abnormality is specific to the polymeric structure of a molecule.

EXPERIMENTAL

Polyacrylamide

Polyacrylamide was prepared by aqueous polymerization with the use of ammonium persulfate-isopropanol redox initiator. After polymerization, the polymer solution was poured into methanol, and the recovered polymer was redissolved in water and reprecipitated in methanol. Finally, the polymer was dried *in vacuo* at 50°C. and analyzed (Calculated for C₃H₅NO: N, 19.71%; found: N, 19.67%). The intrinsic viscosity [η] in water was 8.27 dl./g. at 30°C.

Amides

Acrylamide, propionamide, succinamide, and adipamide were obtained commercially. Results of analysis of these are shown in Table I.

TABLE I

| Amides | Melting point, °C. | N, % | |
|--------------|--------------------|--------|-------|
| | | Calcd. | Found |
| Acrylamide | 84-85 | 19.71 | 19.75 |
| Propionamide | 79.5 | 19.16 | 19.44 |
| Succinamide | | 24.13 | 23.18 |
| Adipamide | | 19.44 | 18.80 |

Rate of Hydrolysis

The hydrolysis reactions were carried out in a 100-ml. Erlenmeyer flask equipped with a reflux condenser in which amides and aqueous solution of sodium hydroxide were mixed. The flask was heated in a constant temperature bath. After a given time, the mixture was cooled and evacuated to strip off ammonia. The carboxyl group content was determined by the potentiometric titration with a Metrohm conductometer E 165.

The hydrolysis reaction of amides is usually second-order, first-order in amide and first-order in alkali. The rate constants k were calculated from the conventional second-order equation:

$$k = \frac{2.303}{t(a-b)} \log \frac{b(a-x)}{a(b-x)} \quad (1)$$

where a and b are the initial concentrations of amide and alkali, respectively, and t is time. x is the concentration of the carboxyl group at time t .

RESULTS AND DISCUSSION

Table II shows the results of the alkaline hydrolysis of polyacrylamide. The initial reaction is relatively rapid but the rate slows down progressively with the increase of conversion. This shows that the reaction order of the alkaline hydrolysis of polyacrylamide is higher than 2 and the reaction mechanism is more complicated than in the case of simple monoamides.

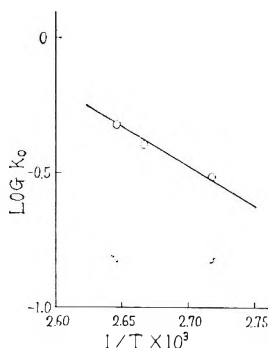


Fig. 1. Plot of $\log k_0$ vs. $1/T$ for the hydrolysis of polyacrylamide.

By an extrapolation the initial rate constant k_0 was determined. Table III shows the effect of temperature on the initial rate constant. From the slope of the $\log k_0$ versus $1/T$ plot, the activation energy was obtained. The obtained value of 13.5 kcal./mole is comparable to the result reported by Moens and Smets.² Figure 1 shows the Arrhenius plot for the hydrolysis of polyacrylamide.

TABLE II
Hydrolysis of Polyacrylamide at 94.9°C.*

| Time, min. | Degree of hydrolysis, % | x , mole/l. | $\frac{2.303}{a-b} \log \frac{b(a-x)}{a(b-x)}$ | k , l./mole- min. |
|---------------|-------------------------------|------------------|--|---------------------------|
| 0 | 0 | 0 | — | — |
| 15 | 9.24 | 0.00498 | 3.967 | 0.2645 |
| 30 | 13.05 | 0.00712 | 6.147 | 0.2049 |
| 60 | 17.81 | 0.00960 | 9.079 | 0.1513 |
| 90 | 19.51 | 0.01051 | 10.310 | 0.1146 |

$$k_0 = 0.305$$

* a = concentration of amide group = 0.05388 mole/l.; b = concentration of NaOH 0.02694 mole/l. x is the concentration of the carboxyl group at time t .

TABLE III

| Temperature, °C. | Initial rate constant k_0 , l./mole-min. |
|---------------------|--|
| 94.9 | 0.305 |
| 102.0 | 0.395 |
| 105.1 | 0.477 |

Under the same conditions, low molecular weight amides were hydrolyzed with alkali. Table IV shows the results of hydrolysis of propionamide and acrylamide.

These results show that in the case of low molecular weight monoamides, the initial rate is slower than that of polyacrylamide, but follows the second-order law accurately.

The slowdown of the rate of the hydrolysis of polyacrylamide has been explained by Moens and Smets² as follows: in the alkaline medium the increasing negative charge on the polymeric chain exerts an "electrostatic repulsion" effect towards the hydroxyl ion, and, as a consequence, causes a progressive decrease of the rate of reaction. Morawetz² has discussed the results obtained by Moens and Smets proposed an explanation that the initial higher rate may be due to catalysis by a specific neighboring group.

In order to verify the preceding explanations, it would be most interesting to hydrolyze polyfunctional aliphatic amides as fragmental model compounds of the polymer. Thus, diamides were hydrolyzed by alkali. Table V shows the results of hydrolysis of succinamide and adipamide. Glutar-

TABLE IV
 Hydrolysis of Low Molecular Weight Amides at 94.9°C.^a

| Amide | Time, min. | Degree of hydrolysis, % | x , mole/l. | $\frac{2.303}{a-b}$ | k , l./mole-min. |
|--------------|------------|-------------------------|---------------|------------------------------|--------------------|
| | | | | $\frac{\log b(a-x)}{a(b-x)}$ | |
| Propionamide | 0 | 0 | 0 | — | — |
| | 15 | 3.53 | 0.00190 | 1.376 | 0.0917 |
| | 30 | 7.39 | 0.00398 | 3.069 | 0.1023 |
| | 60 | 13.21 | 0.00712 | 6.121 | 0.1020 |
| | 90 | 17.56 | 0.00946 | 8.874 | 0.0986 |
| | | | | Avg. | 0.0987 |
| Acrylamide | 0 | 0 | 0 | — | — |
| | 15 | 3.01 | 0.00162 | 1.163 | 0.0775 |
| | 30 | 5.72 | 0.00308 | 2.342 | 0.0781 |
| | 60 | 10.65 | 0.00574 | 4.540 | 0.0757 |
| | 90 | 14.18 | 0.00764 | 6.711 | 0.0746 |
| | | | | Avg. | 0.0765 |

^a a = concentration of amide = 0.05388 mole/l.; b = concentration of NaOH = 0.02694 mole/l. x is the concentration of the carboxyl group at time t .

 TABLE V
 Hydrolysis of Diamides at 94.9°C.^a

| Amide | Time, min. | Degree of hydrolysis, % | x , mole/l. | $\frac{2.303}{a-b}$ | k , l./mole-min. |
|-------------|------------|-------------------------|---------------|------------------------------|--------------------|
| | | | | $\frac{\log b(a-x)}{a(b-x)}$ | |
| Succinamide | 0 | 0 | 0 | — | — |
| | 5 | 13.55 | 0.00730 | 6.343 | 1.269 |
| | 8 | 14.85 | 0.00800 | 7.113 | 0.889 |
| | 15 | 16.80 | 0.00905 | 8.369 | 0.558 |
| | 30 | 19.00 | 0.01024 | 9.900 | 0.330 |
| | 60 | 20.62 | 0.01111 | 11.165 | 0.186 |
| | 90 | 22.28 | 0.01200 | 12.516 | 0.139 |
| | | | | $k_0 = 2.20$ | |
| Adipamide | 0 | 0 | 0 | — | — |
| | 15 | 3.94 | 0.00212 | 1.251 | 0.1014 |
| | 30 | 5.57 | 0.00300 | 2.231 | 0.0744 |
| | 60 | 8.32 | 0.00448 | 3.514 | 0.0586 |
| | 90 | 11.47 | 0.00618 | 5.155 | 0.0573 |
| | | | | $k_0 = 0.130$ | |

^a a = concentration of amide group = 0.05388 mole/l.; b = concentration of NaOH = 0.02694 mole/l. x is the concentration of the carboxyl group at time t .

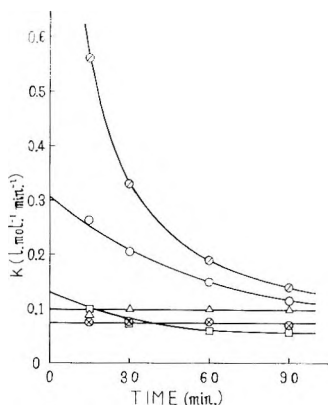


Fig. 2. Variation of k with time for: (O) polyacrylamide; (⊙) succinamide, (□) adipamide; (△) propionamide; (⊗) acrylamide.

amide would be the most suitable compound as a fragmental model of polyacrylamide, but, owing to the difficulties in its preparation and purification, we did not investigate this compound.

It is clear from Table V that the reactions of these low molecular weight diamides show the same abnormality as was noticed with polyacrylamide. The data were evaluated in terms of two successive constants. The first one is k_0 , and the second constant, k_2 , was calculated to be 0.0425 and 0.0454 for succinamide and adipamide, respectively. The k_2 of polyacrylamide was determined to be 0.0840 by the same technique. The order of the rate of various amides are as follows:

Succinamide Polyacrylamide Adipamide Propionamide

$$k_0 = 2.20 > k_0 = 0.305 > k_0 = 0.130 > k = 0.0987$$

Polyacrylamide Acrylamide Adipamide Succinamide

$$k_2 = 0.0840 > k = 0.0765 > k_2 = 0.0454 > k_2 = 0.0425$$

The variation of k 's with time are shown in Figure 2.

The value of k_0 is exceedingly high in succinamide and decreases in the order: succinamide, polyacrylamide, adipamide; but even the k_0 value of adipamide is still greater than k for the monoamides.

On the other hand, each polyfunctional amide shows the abnormality in the hydrolysis rate, whereas the monoamide does not.

The rate constant ratio k_2/k_0 , which gives a measure of this abnormality, is 0.0193 for succinamide, 0.275 for polyacrylamide, and 0.349 for adipamide.

These observations indicate that the abnormality is caused by intramolecular interactions between two or more adjacent amide groups. This interaction is greatest in succinamide, in which the two amide groups are placed on neighboring carbon atoms, and decreases as the distance of the adjacent amide groups increases. Even in adipamide, in which the two

amide groups are as much as four carbon atoms apart, there exists a definite amount of interaction.

It is, moreover, important that the k_0 and k_2/k_0 values of polyacrylamide fall between those of succinamide and adipamide, indicating that the distance between the neighboring amide groups plays the main role governing the abnormal behavior in the hydrolysis, and the effect of the polymeric structure suggested by Smets, if any, is of secondary importance.

At the initial stage of the reaction, the hydrolysis of polyfunctional amide, whether it be a polymer or a low molecular weight compound, is

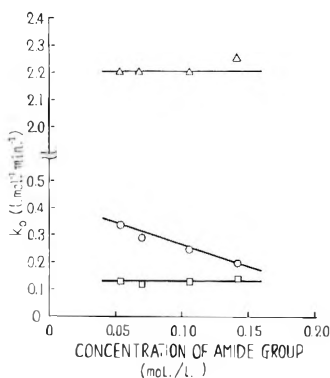
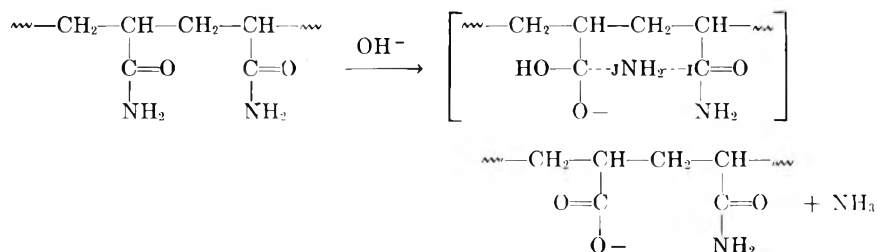


Fig. 3. Influence of the initial concentration of the amide group on the initial rate constant k_0 at 94.9°C. for a molar ratio (NaOH/amide group) = 0.5 for: (O) polyacrylamide; (Δ) succinamide; (□) adipamide.

accelerated by the catalytic effect of the neighboring amide group. However, the carboxyl ions produced by hydrolysis exert an electrostatic repulsion towards the hydroxyl ion which is going to attack the next amide group and cause the decrease of the rate of reaction. These effects are stronger the nearer the neighboring amide groups are located.

The catalytic effect of the neighboring amide group is well explained by the "concerted" polyfunctional mechanism.³ An amide group which is attacked by the hydroxyl ion pushes the NH_2 group away. Simultaneously, the NH_2 group is pulled by the neighboring amide group:



Consequently, the initial rate of the reaction of polyfunctional amides is faster than that of simple monoamides.

However, in the case of polyacrylamide a slight difference from the low molecular weight diamides was observed, in that the initial rate for the polymer decreases with the increase of initial concentration of the reactant, whereas that of diamides does not change. These results are shown in Figure 3.

In the aqueous solution of polyacrylamide the viscosity increases with the increase of concentration and with the degree of hydrolysis of the polymer. In a viscous solution, the diffusion of the reactants and the movement of the polymeric chain are retarded. This explanation seems to contradict Flory's classical finding that the viscosity does not affect the reaction rate between a polymer and a small molecule. A slight contradiction is known to occur, however, when the mobility of the reactant is low in the viscous solution and the diffusion becomes the rate-controlling step.⁴

The decrease in the rate of reaction with the increase of viscosity, that is, the increase of concentration would probably be due to this effect.

CONCLUSION

It was shown that the abnormal behavior in the alkaline hydrolysis of polyacrylamide is due to its polyfunctionality and not necessarily specific to polymers. The low molecular weight diamides show the same reaction behavior.

The initial acceleration of the rate of hydrolysis is explainable on the basis of the interaction between the neighboring amide groups, and the rapid decrease of the rate with the increase of conversion is due to the repulsion between the carboxyl ion and the hydroxyl ion.

References

1. Smets, G., *Makromol. Chem.*, **34**, 190 (1959).
2. Moens, J., and G. Smets, *J. Polymer Sci.*, **23**, 931 (1957); H. Morawetz, *ibid.*, 948 (1957).
3. Churchill, J. W., M. Lapkin, F. Martinez, and J. A. Zaslowsky, *J. Am. Chem. Soc.*, **80**, 1944 (1958).
4. Flory, P. J., *Principles of Polymer Chemistry*, Cornell Univ. Press, Ithaca, N. Y., 1953, p. 75.

Résumé

On a dit que le polyacrylamide présentait un comportement anormal lors de l'hydrolyse alcaline du fait de la vitesse de réaction très élevée au début de la réaction et de sa diminution rapide avec l'augmentation de la conversion. Ce phénomène a été attribué à sa structure polymérique. Nous avons trouvé que les diamides de faible poids moléculaire présentaient essentiellement le même comportement et nous concluons que cette anomalie est due à la polyfonctionnalité et n'est pas nécessairement spécifique aux polymères.

Zusammenfassung

Es wurde berichtet, dass Polyacrylamid bei der alkalischen Hydrolyse insofern ein abnormales Verhalten zeigt, als die Reaktionsgeschwindigkeit am Anfang recht gross ist

und mit wachsendem Umsatz rasch abnimmt. Diese Erscheinung wurde seiner Polymerstruktur zugeschrieben. Wir haben gefunden, dass die niedermolekularen Diamide im wesentlichen das gleiche Verhalten zeigen und kamen zu dem Schluss, dass diese Abnormalität durch die Polyfunktionalität verursacht und nicht notwendigerweise für Polymere spezifisch ist.

Received October 19, 1964

Revised January 15, 1965

(Prod. No. 4617A)

Thermochemistry of Polymerization. Part II. Thermochemical Aspects of Equilibrium Copolymerization

HIDEO SAWADA, *Central Research Laboratory, Dainippon Celluloid Company, Tsurugaoka, Oi, Irumagun, Saitama, Japan*

Synopsis

A new theory of equilibrium copolymerization is presented. The theory is based upon statistical thermodynamics and yields useful information about the sequence distribution along the chain. The effect of temperature on the sequence distribution of copolymerization is discussed.

Introduction

Alfrey and Tobolsky¹ first suggested a statistical mechanical method of treating equilibrium copolymerization. Tobolsky and Owen² developed a general theory of equilibrium copolymerization which gives a good agreement with experimental results.

In the first paper of this series³ we discussed the heat of copolymerization and introduced the randomness parameter ψ . In the present paper, using this parameter we present a new theoretical treatment of the dependence of sequence distribution on temperature for the case of equilibrium copolymerization. It is the purpose of this paper, therefore, to treat equilibrium copolymerization from the statistical thermodynamic point of view, which will yield more information about the sequence distribution than theories presented heretofore.^{1,2}

Theoretical

Consider copolymers made up of two types of monomer units, A and B. In order to simplify the problem, subsidiary reactions leading to branching are ignored in this paper. The interaction energies of AA, BB, AB, and BA pairs are denoted by H_{AA} , H_{BB} , H_{AB} , and H_{BA} , respectively, and the numbers of such pairs by N_{AA} , N_{BB} , N_{AB} , and N_{BA} , respectively. The total number of pairs in these copolymers is N_0 . The energy H_{AA} is approximately the heat of polymerization per mole of monomer A and similarly for H_{BB} , H_{AB} , and H_{BA} . We shall employ the convention of Lewis and Randall,⁴ according to which any gain in a quantity on the part of a system is considered to be positive and any loss negative. Since heat

is evolved during the copolymerization, the molar heat of copolymerization is given by

$$\Delta H = -[H_{AA}(N_{AA}/N_0) + H_{BB}(N_{BB}/N_0) + H_{AB}(N_{AB}/N_0) + H_{BA}(N_{BA}/N_0)] \quad (1)$$

Next we shall calculate the quantities N_{AA} , N_{BB} , N_{AB} , and N_{BA} . These quantities are sensitive to sequence distribution in copolymers. Recently, we proposed a convenient parameter³ for characterizing sequence distribution. The basic quantity used is the randomness parameter ψ . This parameter is defined as

$$\psi = P_{AB}/X_B = P_{AB}/(1 - X_A) \quad (2)$$

where X_A and X_B are the mole fractions of the monomer units A and B, respectively, and P_{AB} is the probability that a B monomer unit will occupy an adjoining site of an A monomer unit in the copolymer. The completely alternating copolymer corresponds to $\psi = 2$, and the random copolymer to $\psi = 1$, and the block copolymer to $\psi = 0$.

Thus, by the definition of ψ ,

$$P_{AB} = \psi X_B \quad (3)$$

$$P_{AA} = 1 - P_{AB} = 1 - \psi X_B \quad (4)$$

The number of A monomer units in the copolymers is $N_0 X_A$, and thus the total number of AB pairs is

$$N_{AB} = (N_0 X_A) P_{AB}$$

Similarly, the total number of BA pairs is

$$N_{BA} = (N_0 X_B) P_{BA}$$

Since the two alternation reactions always occur with equal frequency (steady-state assumption),

$$N_{AB} = N_{BA}$$

and thus

$$P_{BA} = P_{AB} X_A / X_B = \psi X_A \quad (5)$$

$$P_{BB} = 1 - P_{BA} = 1 - \psi X_A \quad (6)$$

Therefore, we get

$$N_{AB} = N_0 X_A X_B \psi \quad (7)$$

$$N_{BA} = N_0 X_A X_B \psi \quad (8)$$

$$N_{AA} = N_0 X_A (1 - \psi X_B) \quad (9)$$

$$N_{BB} = N_0 X_B (1 - \psi X_A) \quad (10)$$

The substitution of these values into eq. (1) leads to

$$\Delta H = -(H_{AA}X_A + H_{BB}X_B + X_AX_B\psi\Omega) \quad (11)$$

where

$$\Omega = (H_{AB} + H_{BA}) - (H_{AA} + H_{BB})$$

We now calculate the entropy change ΔS . Orr⁵ computed the number of ways of arranging the A sequences in the polymer chain. From this number the corresponding entropy per mole is given by

$$\begin{aligned} \Delta S_{\text{mix}} &= -R[P_{AA} \ln P_{AA} + (1 - P_{AA}) \ln (1 - P_{AA})] \\ &= -R\{(1 - \psi X_B) \ln (1 - \psi X_B) + \psi X_B \ln \psi X_B\} \quad (12) \end{aligned}$$

where P_{AA} is the probability that an A monomer unit in the chain would be followed by another A monomer unit and R is the gas constant per mole.

We see that the entropy has the proper limiting behavior: in the limit of $\psi = 1$, $\Delta S_{\text{mix}} = -R(X_A \ln X_A + X_B \ln X_B)$, which is the entropy for random copolymers. In the limit of $\psi = 0$, $\Delta S_{\text{mix}} = 0$ in agreement with what is expected for block copolymers. For alternating copolymers, $X_A = X_B = 0.5$, and $\psi = 2$; so $\Delta S_{\text{mix}} = 0$.

In the case of copolymerization involving monomers A and B there are four distinct propagation steps. S_{AA} , S_{BB} , S_{AB} , and S_{BA} are the corresponding entropy changes, per mole, for the reactions AA, BB, AB, and BA, respectively. The entropy change per mole of monomer polymerized is

$$\begin{aligned} \Delta S_{\text{poly}} &= -(S_{AA}X_AP_{AA} + S_{BB}X_BP_{BB} + S_{AB}X_AP_{AB} + S_{BA}X_BP_{BA}) \\ &= -(S_{AA}X_A + S_{BB}X_B + \chi\psi X_AX_B) \quad (13) \end{aligned}$$

where

$$\chi = S_{AB} + S_{BA} - (S_{AA} + S_{BB})$$

Thus, the total entropy change per mole involved in the copolymerization reaction can be written as

$$\begin{aligned} \Delta S &= -(S_{AA}X_A + S_{BB}X_B + \psi X_AX_B\chi) - \\ &\quad R[(1 - \psi X_B) \ln (1 - \psi X_B) + \psi X_B \ln \psi X_B] \quad (14) \end{aligned}$$

Consider the copolymerization reaction as occurring at some constant temperature, T . We may write for the change in free energy for this reaction

$$\Delta F = \Delta H - T\Delta S \quad (15)$$

For the sake of illustration, let us consider the copolymers which are 50% A and 50% B, and we may write eq. (15) as

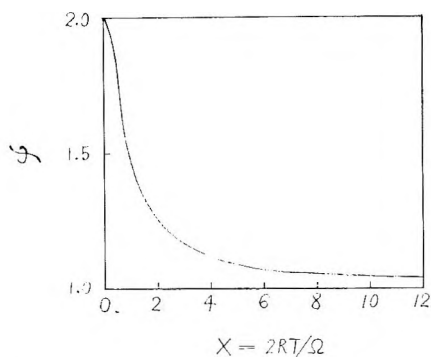


Fig. 1. Randomness parameter as a function of $2RT/\Omega$.

$$\Delta F = -1/2[H_{AA} + H_{BB} + (\psi\Omega/2)] + RT\{[1 - (\psi/2)] \ln [1 - (\psi/2)] + (\psi/2) \ln (\psi/2)\} + (T/2)[S_{AA} + S_{BB} + (\psi\chi/2)] \quad (16)$$

Interchange reactions occurring in copolymer chains will ultimately lead to copolymer equilibrium, that is, an equilibrium distribution of compositional sequence lengths along the chains.¹ This equilibrium sequence distribution is determined as a function of temperature by the requirement that the change in free energy ΔF be a minimum with respect to the randomness parameter ψ . Thus, the condition $\partial\Delta F/\partial\psi = 0$ gives

$$\psi = 2/[1 + \exp\{(-\Omega/2RT) + (\chi/2R)\}] \quad (17)$$

Equation (17) determines the equilibrium ψ as a function of T , provided Ω and χ are given.

In Figure 1 we have plotted ψ as a function of parameter $X = 2RT/\Omega$ for the case where $\chi = 0$ and $\Omega > 0$. Regardless of the sign of Ω terms, ψ will always be $2/(1 + \exp\{\chi/2R\})$ at sufficiently large values of T , since $\psi \rightarrow 2/(1 + \exp\{\chi/2R\})$ as $T \rightarrow \infty$. The values of entropy changes for most polymerizations are quite similar;⁶ thus χ will be very close to zero. If $\chi = 0$ the copolymer will be random at sufficiently elevated temperatures since $\psi \rightarrow 1$ as $T \rightarrow \infty$. When Ω, χ are zero, at any temperature ψ is unity, and hence the two types of units will be arranged at random along the polymer chains. When $\Omega < 0$, at low temperatures ψ is very close to zero, and hence the polymer structure deviates from the random, in the direction of clustering. When $\Omega > 0$, at low temperatures ψ is very close to two, and hence the polymer structure deviates from the random, in the direction of regular alternation.

The considerations presented above apply to the copolymerization of ring compounds, condensation copolymerizations, and vinyl copolymerizations. It is now well known that melt polymerization methods yield condensation copolymers with random distribution at high temperatures

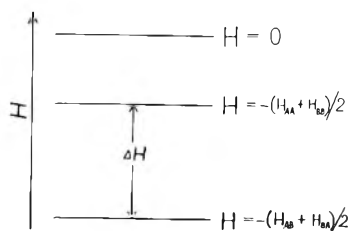


Fig. 2. Energy relation between unlike and like bonds.

and that the method of interfacial polycondensation yields condensation copolymers ranging in order from alternating to block arrangements at low temperatures.⁷

Let us consider the energetics of the attack of a radical on a double bond. The weaker the bond formed between the attacking radical and the carbon center of the double bond, the higher the activation energy.⁸ The more exothermic the reaction, the lower the activation energy. Therefore, the more exothermic the reaction between A and B, the stronger the bond formed between A and B.

If there is an attractive interaction between unlike monomer units (large electrostatic interaction of charges on the radical and monomer for example), the AB bond will be stronger than an AA bond or BB bond, and hence Ω will be positive in sign, yielding regular alternation. On the other hand, Joshi⁹ found experimentally that the monomer units alternate regularly along the chain only when $\Omega > 0$. Conversely, if there is a repulsive interaction between unlike monomer units Ω will be negative and repeating units occur in blocks.

An alternative approach to the problem is based on Boltzmann statistics,¹⁰ and almost similar conclusions are reached. Consider the copolymers with equal numbers of A and B monomer units, $X_A = X_B = 0.5$.

If the average enthalpy change on formation of like bonds $-(H_{AA} + H_{BB})/2$ is greater than that of unlike bonds $-(H_{AB} + H_{BA})/2$, we have then the simple energy level system indicated in Figure 2. If the change in entropy for the reaction is zero, in thermal equilibrium, the relative probability of occupancy of the high energy state to that of the low energy state is given by Boltzmann statistics.

$$P_{\text{high energy state}}/P_{\text{low energy state}} = \exp \{-\Delta H/RT\} \quad (18)$$

The probability of occupancy of the high energy state is

$$\begin{aligned} P_{\text{high energy state}} &= (N_{AA} + N_{BB})/N_0 \\ &= 1 - (\psi/2) \end{aligned} \quad (19)$$

Similarly the probability of the low energy state is

$$\begin{aligned} P_{\text{low energy state}} &= (N_{AB} + N_{BA})/N_0 \\ &= \psi/2 \end{aligned} \quad (20)$$

Substitution of eqs. (19) and (20) into eq. (18) yields

$$[1 - (\psi/2)]/(\psi/2) = \exp \{-\Omega/2RT\} \quad (21)$$

where

$$\Omega = 2\Delta H = H_{AB} + H_{BA} - (H_{AA} + H_{BB})$$

Therefore

$$\psi = 2/(1 + \exp \{-\Omega/2RT\}) \quad (22)$$

If χ is zero, eq. (17) is identical to eq. (22).

From eqs. (11) and (22) we obtain:

$$\begin{aligned} H &= - \left(H_{AA}X_A + H_{BB}X_B + \frac{2X_AX_B\Omega}{(1 + \exp \{-\Omega/2RT\})} \right) \\ &= -\frac{1}{2} \left(H_{AA} + H_{BB} + \frac{\Omega}{1 + \exp \{-\Omega/2RT\}} \right) \end{aligned} \quad (23)$$

for $X_A = X_B = 0.5$.

If Ω is positive, at low temperatures, H will approach $-(H_{AB} + H_{BA})/2$, yielding alternating copolymers. If Ω is negative, at low temperatures, H will approach $-(H_{AA} + H_{BB})/2$, yielding block copolymers. Regardless of the sign of Ω terms, at high temperatures, H will approach $-(H_{AB} + H_{BA} + H_{AA} + H_{BB})/4$, yielding random copolymers. If Ω is zero, the copolymer will be random at any temperature and hence H is given by

$$\begin{aligned} H &= -(H_{AA} + H_{BB})/2 = -(H_{AB} + H_{BA})/2 \\ &= -(H_{AB} + H_{BA} + H_{AA} + H_{BB})/4 \end{aligned}$$

Copolymerization reactions will exhibit ceiling temperatures.¹¹ At the ceiling temperature T_c , ΔF is zero, so that

$$\begin{aligned} H_{AA} + H_{BB} + \frac{\Omega}{1 + \exp \{-\Omega/2RT_c\}} \\ + 2RT_c \left[\frac{\ln (1 + \exp \{-\Omega/2RT_c\})}{1 + \exp \{-\Omega/2RT_c\}} + \frac{\ln (1 + \exp \{\Omega/2RT_c\})}{1 + \exp \{\Omega/2RT_c\}} \right] - \\ T_c(S_{AA} + S_{BB}) = 0 \end{aligned} \quad (24)$$

Equation (24) does not lend itself readily to the calculation of T_c . However, T_c is found by solving eq. (24) when H_{AA} , H_{BB} , S_{AA} , and S_{BB} are known and $\Omega = 0$. Thus, we obtain the ceiling temperature for the copolymer where $X_A = X_B = 0.5$ and $\chi = \Omega = 0$. The ceiling temperature for this case is

$$\begin{aligned} T_c &= (H_{AA} + H_{BB})/(S_{AA} + S_{BB} - 2R \ln 2) \\ &= [(H_{AA} + H_{BB} + H_{AB} + H_{BA})/2]/(S_{AA} + S_{BB} - 2R \ln 2) \end{aligned}$$

This is the ceiling temperature for random copolymers.

The author wishes to thank Dainippon Celluloid Company for permission to publish this work.

References

1. Alfrey, T., and A. V. Tobolsky, *J. Polymer Sci.*, **38**, 269 (1959); A. V. Tobolsky, *Properties and Structure of Polymers*, Wiley, New York, 1960, p. 280.
2. Tobolsky, A. V., and G. D. T. Owen, *J. Polymer Sci.*, **59**, 329 (1962).
3. Sawada, H., *J. Polymer Sci.*, **A2**, 3095 (1964).
4. Lewis, G. N., and M. Randall, *Thermodynamics and the Free Energy of Chemical Substances*, McGraw-Hill, New York, 1923, p. 97.
5. Orr, R. J., *Polymer*, **2**, 74 (1961).
6. Bevington, J. C., *Radical Polymerization*, Academic Press, New York, 1961, p. 63.
7. Lyman, D. J., and S. L. Jung, *J. Polymer Sci.*, **40**, 407 (1959).
8. Evans, M. G., in *Fibres from Synthetic Polymers*, R. Hill, Ed., Elsevier, New York, 1953, Chap. 3.
9. Joshi, R. M., *Makromol. Chem.*, **66**, 114 (1963).
10. Sawada, H., *J. Polymer Sci.*, **B1**, 659 (1963).
11. Dainton, F. S., and K. J. Ivin, *Trans. Faraday Soc.*, **46**, 346 (1950).

Résumé

On présente une nouvelle théorie de la copolymérisation. La théorie se base sur la thermodynamique statistique qui fournit des renseignements utiles sur la distribution des séquences le long de la chaîne. On discute de l'influence de la température sur la distribution des séquences lors de la copolymérisation.

Zusammenfassung

Eine neue Theorie der Gleichgewichtscopolymerisation wird vorgelegt. Die Theorie beruht auf statistisch-thermodynamischen Überlegungen, welche brauchbare Angaben über die Sequenzverteilung in der Kette liefern. Der Einfluss der Temperatur auf die Sequenzverteilung bei der Copolymerisation wird diskutiert.

Received November 20, 1964
(Prod. No. 4619A)

Copolymerization of α -Olefins with ω -Halo- α -Olefins by Use of Ziegler Catalysts*

R. BACSKAI, *California Research Corporation, Richmond, California*

Synopsis

The copolymerization of α -olefins with ω -halo- α -olefins by use of Ziegler catalysts has been investigated. It was found that ω -halo- α -olefins deactivate the catalyst, thus resulting in low copolymer yield and reduced molecular weight. The deactivation is caused by hydrogen halide formation which is greatly facilitated in the case of the allyl halides and 6-halo-1-hexenes. The different degrees of deactivation were interpreted by considering the ease of carbonium ion formation from the various ω -halo- α -olefins. The copolymer yields were considerably improved when a catalytic amount of a Lewis base was added to the polymerization system. It is proposed that the added Lewis base, by decreasing the Lewis acid character of the catalyst, suppresses the decomposition of the ω -halo- α -olefin leading to hydrogen halide formation. Depending on the Ziegler catalyst employed, the copolymers of α -olefins and ω -halo- α -olefins can be either crystalline or amorphous solids. The halogen, especially the bromine in the copolymers, is reactive in nucleophilic substitution reactions. Reaction with amines gave polymers which could be dyed by acid dyes.

INTRODUCTION

The homopolymerization and copolymerization of α -olefins with Ziegler catalysts is a versatile method for the synthesis of high molecular weight polymers. Depending on the monomers, catalyst, additives, and polymerization conditions, high-melting, crystalline solids of varying stereoregularity or amorphous rubbers can be readily obtained. While it is generally known¹ that polar monomers deactivate the Ziegler catalysts commonly used for the polymerization of olefinic hydrocarbons, there are examples reported in the literature where compounds containing atoms with unshared electron pairs do not interfere with the polymerization. In special cases even monomers containing nitrogen² or oxygen³ atoms have been polymerized by Ziegler catalysts.

It appears also that certain halogen compounds do not deactivate the Ziegler catalyst. For example, chlorobenzene and tetrachloroethylene⁴ are acceptable solvents in Ziegler polymerizations. The polymerization of vinyl aromatic compounds with halogen on the aromatic ring,⁵ vinyl chloride,^{6,7} perfluoroolefins,⁸ and monomers containing the trifluoromethyl group⁹ has been described. The carbon-halogen bond in these solvents and

* Presented at the Meeting of the American Chemical Society, Chicago, Illinois, September, 1964.

monomers is stabilized by resonance or by other structural factors to such an extent that the compounds are unreactive in many typical organic reactions (e.g., nucleophilic substitution or hydrogen halide elimination). Apparently, the carbon-halogen bond is unreactive under the conditions of the Ziegler polymerization as well. The polymers obtained from these monomers, with the exception of poly(vinyl chloride), also have an unreactive halogen functionality which limits their usefulness for further reactions.

Other halogen compounds which are reactive in a number of organic reactions apparently react with the Ziegler catalysts as well. For example, alkyl halides^{10,11} function as molecular weight regulators in Ziegler polymerizations. Similarly, allyl chloride¹² and 3-chlorocyclohexene¹³ undergo extensive dehydrohalogenation and form only low molecular weight polymers in the presence of Ziegler catalysts. Thus, at the outset of this work the possibility of using Ziegler catalysts for the polymerization of haloolefins with reactive halogen seemed doubtful.

We wish to report that ω -halo- α -olefins, except for allyl halides, can be copolymerized with α -olefins in good yields to high molecular weight products by using a slightly modified Ziegler catalyst. The copolymers obtained in these reactions contain relatively reactive halogen atoms. This should be of interest for further reactions such as grafting, crosslinking, displacement reactions, etc.

EXPERIMENTAL

Materials

The 5-chloro-1-pentene, 6-chloro-1-hexene, and 11-chloro-1-undecene were prepared from the corresponding ω -hydroxy-1-olefins. The 4-pentene-1-ol and 5-hexene-1-ol were obtained from Peninsular Chemical Research, Inc. The 10-undecene-1-ol was obtained from the Aldrich Chemical Co., Inc. The procedure followed was similar to that described by Perrine.¹⁴

The 8-chloro-1-octene, 7-chloro-1-octene, and 8-bromo-1-octene were prepared by conventional methods starting with 1,7-octadiene.

The 4-bromo-1-butene, 5-bromo-1-pentene, and 6-bromo-1-hexene were obtained from the Peninsular Chemical Research, Inc., and were purified on a preparative gas chromatograph.

The infrared and nuclear magnetic resonance spectra of the ω -halo- α -olefins and that of the 7-chloro-1-octene were consistent with their chemical structure. The compounds were redistilled before use; physicochemical constants and purity are summarized in Table I.

Allyl chloride and allyl bromide were obtained from the Matheson, Coleman, and Bell Company and redistilled before use.

The 1-chlorooctane and 2-chlorooctane were obtained from the Eastman Kodak Company and redistilled before use. The gas chromatographic purity of the compounds was 100% and 99.9%, respectively.

1-Bromobutane was obtained from the Matheson, Coleman, and Bell Company and redistilled before use. The gas chromatographic purity of the compound was 100%.

Propylene and ethylene were obtained from the Matheson Company (C.P. grade).

The 4-methyl-1-pentene was obtained from the California Chemical Company. It was redistilled, passed through a silica gel column, and stored over sodium wire under nitrogen. The gas chromatographic purity of the material was 98.8%.

Aluminum alkyls were obtained as 25% solutions in *n*-heptane from Texas Alkyls, Inc.

TABLE I
Some Physicochemical Constants and the Purity of Haloolefins

| Compound | Boiling point, °C./mm. | n_D^{25} | Gas chromatographic purity, % ^a |
|--------------------------------|------------------------|------------|--|
| 5-Chloro-1-pentene | 104/760 | 1.4284 | 99.8 |
| 6-Chloro-1-hexene | 72/95 | 1.4356 | 99.2 |
| 8-Chloro-1-octene ^b | 113.5/100 | 1.4430 | 98.5 |
| 11-Chloro-1-undecene | 75/0.7 | 1.4489 | 99.6 |
| 4-Bromo-1-butene | 53/165 | 1.4612 | 99.8 |
| 5-Bromo-1-pentene | 55/62 | 1.4622 | 99.0 |
| 6-Bromo-1-hexene | 67/37 | 1.4646 | 98.6 |
| 8-Bromo-1-octene ^c | 53.5/2.2 | 1.4662 | 94.6 |
| 7-Chloro-1-octene ^d | 79/35 | 1.4400 | 93.0 |

^a With 10-ft., 1/4-in., stainless steel column; 10% Apiezon L on silicon-treated Chromosorb W. The column separated the 1-chlorooctane and 2-chlorooctane isomers readily.

^b Contains 0.27% 7-chloro-1-octene.

^c Contains 4.4% 7-bromo-1-octene.

^d Contains 7% internal *trans*-olefins.

The $TiCl_3$ (grade $TiCl_3AA$, approximate composition $3TiCl_3 \cdot AlCl_3$) was obtained from the Anderson Chemical Company.

n-Heptane and *n*-hexane were obtained from the Phillips Petroleum Company (pure grade, 99 mole-% minimum). These solvents were purified by passing through a silica gel column and storing over sodium wire under nitrogen.

Pyridine and tetrahydrofuran were obtained from the J. T. Baker Chemical Company (Baker analyzed reagent grade).

Triethylamine and morpholine were obtained from the Eastman Kodak Company.

Calcocid Alizarin Blue SAPG (Acid Blue 45) was obtained from the American Cyanamid Company.

Igepal CO-710 (nonyl phenoxy polyoxyethylene ethanol) was obtained from General Aniline and Film Corporation.

Copolymer Preparation

The results of the copolymerizations are summarized in Tables II–X. Both yields are reported when duplicate experiments were carried out; the $[\eta]$ and halogen per cent in the respective columns always refers to the initial run.

The copolymer yields reported include only the methanol-insoluble solids and not the low molecular weight oils which were observed in some cases. Typical examples are given below.

Propylene/6-Chloro-1-hexene Copolymer. The polymerization apparatus, consisting of a 6-oz., thick-walled glass bottle (Fisher and Porter Company, Aerosol Compatibility Tube No. 110–106) equipped with a Teflon-coated magnetic stirring bar and stainless steel adapter for the introduction of reactants, was purged with nitrogen. It was immersed in a constant temperature oil bath maintained at $70^{\circ}\text{C} \pm 0.5^{\circ}\text{C}$. The stirrer was started; and in the following order 100 ml. *n*-heptane, 0.36 g. $\text{Al}(\text{C}_2\text{H}_5)_2\text{Cl}$, 0.20 g. TiCl_3AA , 0.079 g. pyridine, and 1.42 g. 6-chloro-1-hexene were charged into the bottle. Nitrogen was replaced with propylene, and the polymerization apparatus was pressurized to 50 psi with propylene for 1 hr. After releasing the pressure the catalyst was destroyed by adding 2 ml. of methanol. The reaction mixture was poured into 600 ml. of methanol, acidified with concentrated hydrochloric acid, and filtered. The fine polymer particles were repeatedly washed with methanol and dried in vacuum at 80°C .

Copolymer yield 8.04 g.; $[\eta] = 2.3$ dl./g., Cl = 2.09%, which corresponds to 6.98% 6-chloro-1-hexene in the copolymer.

A similar reaction conducted in the absence of pyridine yielded no methanol-insoluble solid polymer.

4-Methyl-1-Pentene/8-Bromo-1-octene Copolymer. Into the same polymerization apparatus as described above, 100 ml. of *n*-heptane, 0.36 g. $\text{Al}(\text{C}_2\text{H}_5)_2\text{Cl}$, 0.20 g. TiCl_3AA , 0.079 g. pyridine, 25.2 g. 4-methyl-1-pentene, and 2.30 g. 8-bromo-1-octene were charged successively. The reaction mixture was stirred continuously; the temperature was raised to 50°C . and maintained there for 2 hr. During the polymerization, the reaction mixture became very viscous. The catalyst was destroyed with 2 ml. methanol, and the copolymer was precipitated by pouring the reaction mixture into 600 ml. methanol. After acidification with concentrated hydrochloric acid, the solid product was filtered, washed with methanol, and dried at 80°C . in vacuum.

Copolymer yield 9.07 g.; $[\eta] = 4.1$ dl./g.; Br = 11.3%, which corresponds to 27.0% 8-bromo-1-octene in the copolymer.

A similar experiment carried out without pyridine gave only 2.54 g. of copolymer.

Ethylene/Propylene/8-Bromo-1-octene Terpolymer. A 500-ml., round-bottomed flask equipped with stirrer, thermometer, condenser, and gas inlet tube was purged with nitrogen. The nitrogen was replaced by passing a mixture of ethylene and propylene into the flask at rates of 129 and 426 ml./min., respectively. Stirring was started; and in the following order

300 ml. *n*-heptane, 1.48 g. $\text{Al}_2(\text{C}_2\text{H}_5)_3\text{Cl}_3$, 0.237 g. pyridine, 6.87 g. 8-bromo-1-octene, and 0.52 g. VOCl_3 were introduced into the flask at room temperature. The addition of the VOCl_3 instantly turned the reaction mixture purple, and an exothermic reaction was observed. The viscosity of the solution increased rapidly, and the temperature inside the flask rose to 39.5°C . Gas introduction was continued for 1 hr., after which the catalyst was destroyed with methanol, and the copolymer was precipitated from solution with methanol. The rubbery product was washed with methanol and concentrated hydrochloric acid. It was filtered and dried in vacuum.

Terpolymer yield 9.29 g.; $[\eta] = 1.0$ dl./g.; Br = 9.06%, which corresponds to 21.7% 8-bromo-1-octene in the copolymer.

When a similar reaction was carried out without pyridine only a trace of polymer was formed.

Reaction of a Propylene/8-Bromo-1-octene Copolymer with Pyridine.

A 2-g. portion of a propylene/8-bromo-1-octene copolymer powder ($[\eta] = 5.7$ dl./g.; Br = 1.59%), prepared with the $\text{Al}(\text{C}_2\text{H}_5)_2\text{Cl} + \text{TiCl}_3$ catalyst, was mixed with 20 ml. of pyridine. The slurry was stirred and heated in nitrogen at 100°C . for 2 hr. During the reaction the polymer particles swelled considerably. The reaction mixture was poured into methanol, and the polymer particles were filtered, washed several times with methanol, and dried in vacuum at 80°C .

Yield 1.89 g.; $[\eta] = 2.9$ dl./g.; N = 0.27%, Br = 1.44%. This corresponds to 1.53% pyridine incorporation in the polymer.

Dyeing of the Copolymer

A dye solution was prepared from 200 ml. distilled water, 0.16 g. Igepal CO-710 (a nonionic detergent), 0.5 ml. concentrated H_2SO_4 , and 0.1 g. Calcocid Alizarin Blue SAPG. A 0.5-g. portion of the above-described pyridine-treated copolymer was suspended in this solution, and it was stirred at 100°C . for 1 hr. The polymer powder became dark blue. It was filtered, resuspended in a 1% aqueous solution of Igepal CO-710, and stirred at 70°C . for 1 hr. After filtration and repeated washing with warm water, the polymer remained dark blue.

When the same dyeing conditions were applied to polypropylene or propylene/8-bromo-1-octene copolymer powder, no dyeing resulted.

Identification of Gaseous Decomposition Products of 5-Bromo-1-pentene

A 100-ml., round-bottomed flask equipped with a Teflon-coated, magnetic stirring bar, condenser, gas inlet tube, and serum cap was purged with nitrogen. The exit gas passing through the condenser was bubbled into distilled water. The flask was charged with 25 ml. *n*-hexane, 0.36 g. $\text{Al}(\text{C}_2\text{H}_5)_2\text{Cl}$, 0.20 g. TiCl_3AA , and 1.49 g. 5-bromo-1-pentene. The reaction mixture was heated to reflux and stirred at 71°C . for 1 hr. in a continuous nitrogen stream. Gaseous decomposition products evolved during the re-

action were absorbed in the water and were identified as HCl and HBr by standard analytical methods. The analytical results showed that the water solution contained 0.81 meq. of H^+ , 0.56 meq. of Br^- , and 0.25 meq. of Cl^- .

Polymer Characterization

Infrared spectra were obtained with a Perkin-Elmer grating infrared spectrophotometer (Model 337), with the use of compression-molded polymer films, approximately 0.5 mm. thick.

Intrinsic viscosities were determined in decalin at 135°C.

Melting points were measured by the penetrometer method.¹⁵

Polymer fractionation was carried out in Soxhlet extractors. Extractions were run with *n*-heptane for 8 hr.

X-ray diffraction patterns were obtained with a Phillips x-ray diffractometer (Cu x-ray tube).

Halogen analyses were carried out by the Schöniger method by using the flowing oxygen combustion technique.¹⁶ The error in the analysis is $\pm 5\%$ at the 1% halogen level.

Nitrogen analyses were carried out by the Dumas method. The error in the analysis is $\pm 10\%$ at the 0.2% N level.

RESULTS AND DISCUSSION

Copolymer Synthesis

A summary of our copolymerization experiments with propylene and ω -halo- α -olefins is presented in Tables II and III. For comparison, the effect of some additives on the polymerization of propylene is given in Table IV.

These results show that the yield and molecular weight* of the copolymer is always lower than that of polypropylene homopolymer obtained

TABLE II
Copolymerization of ω -Chloro- α -olefins with Propylene at 50°C.^a

| Run no. | ω -Chloro- α -olefin | Copolymer | | | ω -Chloro- α -olefin in copolymer, % |
|---------|------------------------------------|-----------|-------------------|-------|--|
| | | Yield, g. | $[\eta]$, dl./g. | Cl, % | |
| 1 | Allyl chloride | 0 | — | — | — |
| 2 | 5-Chloro-1-pentene | 8.0, 10.0 | 6.2 | 0.62 | 1.83 |
| 3 | 6-Chloro-1-hexene | 0, 0 | — | — | — |
| 4 | 8-Chloro-1-octene | 7.0, 8.3 | 5.0 | 0.77 | 3.19 |

^a Solvent: 100 ml. *n*-heptane; catalyst: 3 mmole $Al(C_2H_5)_2Cl$ + 1 mmole $TiCl_3$; monomers: 12 mmole ω -chloro- α -olefin + 50 psi propylene; temperature: 50°C.; time: 2 hr.

* It is assumed that the functional relationship between the average degree of polymerization and intrinsic viscosity is identical for polypropylene and for propylene/ ω -halo- α -olefin copolymers.

TABLE III
 Copolymerization of ω -Halo- α -olefins with Propylene at 70°C.^a

| Run no. | ω -Halo- α -olefin | Copolymer | | | ω -Halo- α -olefin in copolymer, % |
|---------|----------------------------------|----------------|-------------------|-------------|--|
| | | Yield, g. | $[\eta]$, dl./g. | Cl or Br, % | |
| 5 | Allyl chloride | 0 | — | — | — |
| 6 | 5-Chloro-1-pentene | 7.6, 6.6 | 2.1 | 0.73 | 2.15 |
| 7 | 6-Chloro-1-hexene | 0, 0 | — | — | — |
| 8 | 8-Chloro-1-octene | 0, 0 | — | — | — |
| 9 | 11-Chloro-1-undecene | 8.2 | 2.9 | 1.30 | 6.92 |
| 10 | Allyl bromide | 0 | — | — | — |
| 11 | 4-Bromo-1-butene | 2.2 | 1.5 | 1.44 | 2.43 |
| 12 | 5-Bromo-1-pentene | 5.6 | 2.8 | 1.94 | 3.62 |
| 13 | 6-Bromo-1-hexene | 0 ^b | — | — | — |
| 14 | 8-Bromo-1-octene | 5.6, 4.6 | 2.2 | 2.93 | 7.00 |

^a Solvent: 100 ml. *n*-heptane; catalyst: 3 mmole $\text{Al}(\text{C}_2\text{H}_5)_2\text{Cl}$ + 1 mmole TiCl_3 ; monomers: 12 mmole ω -halo- α -olefin + 50 psi propylene; temperature: 70°C.; time: 1 hr.

^b 11.54 g. of low molecular weight, tacky, semisolid was isolated ($[\eta] = 0.2$ dl./g.; Br = 0.63%).

 TABLE IV
 Effect of Additives on the Homopolymerization of Propylene^a

| Run no. | Temp., °C. | Time, hr. | Additive | Amt. additive, mmole | Polymer | | |
|---------|------------|-----------|----------------|----------------------|------------|-------------------|--------------------|
| | | | | | Yield, g. | $[\eta]$, dl./g. | Cl, % ^b |
| 15 | 50 | 2 | — | — | 16.1, 15.7 | 11.6 | <0.06 |
| 16 | 70 | 1 | — | — | 12.4, 11.7 | 4.9 | 0.13 |
| 17 | 50 | 2 | 1-Chlorooctane | 12 | 12.3, 14.5 | 9.5 | 0.07 |
| 18 | 70 | 1 | 1-Chlorooctane | 12 | 10.5, 12.9 | 2.8 | 0.04 |
| 19 | 70 | 1 | 1-Bromobutane | 12 | 7.8 | 3.8 | 0.09 |
| 20 | 70 | 1 | Pyridine | 1 | 12.6, 10.0 | 4.1 | 0.09 |
| 21 | 70 | 1 | 1-Bromobutane | 12 | | | |
| | | | Pyridine | 1 | 10.7 | 3.7 | 0.09 |
| 22 | 70 | 1 | 1-Octene | 12 | 11.5 | 4.2 | 0.09 |

^a Solvent: 100 ml. *n*-heptane; catalyst: 3 mmole $\text{Al}(\text{C}_2\text{H}_5)_2\text{Cl}$ + 1 mmole TiCl_3 ; propylene: 50 psi.

^b The chlorine content is probably due to catalyst residues.

under identical conditions (see runs 15 and 16 in Table IV). The decrease in yield is moderate with some of the ω -halo- α -olefins; however, it can be more drastic, completely preventing the formation of solid polymer, as was observed with the allyl halides, 6-chloro-1-hexene, 6-bromo-1-hexene, and also with 8-chloro-1-octene at 70°C.

We have found that by adding catalytic amounts of a Lewis base, e.g., pyridine, to the Ziegler catalyst the copolymer yields can be increased. In most cases the increased yield approximates that obtained in propylene homopolymerization. The effect is most striking in the cases where 6-

TABLE V
Copolymerization of ω -Halo- α -olefins with Propylene in the Presence of Pyridine^a

| Run no. | ω -Halo- α -olefin | Copolymer | | | ω -Halo- α -olefin in copolymer, % |
|---------|----------------------------------|-----------|-------------------|-------------|--|
| | | Yield, g. | $[\eta]$, dl./g. | Cl or Br, % | |
| 23 | Allyl chloride | 0 | — | — | — |
| 24 | 5-Chloro-1-pentene | 7.8 | 2.7 | 1.38 | 4.07 |
| 25 | 6-Chloro-1-hexene | 8.0 | 2.2 | 2.09 | 6.98 |
| 26 | 8-Chloro-1-octene | 6.7 | 2.4 | 2.51 | 10.53 |
| 27 | 11-Chloro-1-undecene | 8.6 | 2.4 | 2.46 | 13.10 |
| 28 | Allyl bromide | 0 | — | — | — |
| 29 | 4-Bromo-1-butene | 3.2 | 2.0 | 1.68 | 2.84 |
| 30 | 5-Bromo-1-pentene | 9.2 | 2.8 | 3.08 | 5.75 |
| 31 | 6-Bromo-1-hexene | 9.5, 8.6 | 2.6 | 2.84 | 5.80 |
| 32 | 8-Bromo-1-octene | 8.7, 9.7 | 2.0 | 5.10 | 12.19 |

^a Solvent: 100 ml. *n*-heptane; catalyst: 3 mmole $\text{Al}(\text{C}_2\text{H}_5)_2\text{Cl}$ + 1 mmole TiCl_3 ; additive: 1 mmole pyridine; monomers: 12 mmole ω -halo- α -olefin + 50 psi propylene; temperature: 70°C.; time: 1 hr.

TABLE VI
Copolymerization of Propylene with 5-Bromo-1-pentene in the Presence of Lewis Bases^a

| Run no. | Lewis base | Amt. Lewis base, mmole | Copolymer | | | 5-Bromo-1-pentene in copolymer, % |
|---------|-----------------|------------------------|-----------|-------------------|-------|-----------------------------------|
| | | | Yield, g. | $[\eta]$, dl./g. | Br, % | |
| 12 | — | — | 5.6 | 2.8 | 1.94 | 3.62 |
| 33 | Pyridine | 0.5 | 9.0 | 3.0 | 2.6 | 4.85 |
| 30 | Pyridine | 1.0 | 9.2 | 2.8 | 3.08 | 5.74 |
| 34 | Pyridine | 2.0 | 6.1 | 3.0 | 3.83 | 7.13 |
| 35 | Triethylamine | 1.0 | 8.0 | 3.5 | 3.32 | 6.18 |
| 36 | Tetrahydrofuran | 1.0 | 6.9 | 3.0 | 2.64 | 4.92 |

^a Solvent: 100 ml. *n*-heptane; catalyst: 3 mmole $\text{Al}(\text{C}_2\text{H}_5)_2\text{Cl}$ + 1 mmole TiCl_3 ; monomers: 12 mmole 5-bromo-1-pentene + 50 psi propylene; temperature: 70°C.; time: 1 hr.

chloro-1-hexene, 8-chloro-1-octene, and 6-bromo-1-hexene are used as comonomers. Nevertheless, no polymer is formed with allyl halides even in the presence of pyridine. These results are summarized in Table V.

The effect of pyridine concentration and the use of other Lewis bases in the copolymerization of 5-bromo-1-pentene and propylene is shown in Table VI.

These data show that the copolymer yield is probably maximum when the pyridine concentration is 1–2 moles/mole of TiCl_3 used. It is also evident that triethylamine and tetrahydrofuran are less effective than pyridine in raising the copolymer yields. The use of a Lewis base not only

TABLE VII
Effect of Pyridine on the Copolymerization
of 8-Bromo-1-octene with 4-Methyl-1-pentene^a

| Run no. | Pyridine, mmole | Copolymer | | | 8-Bromo-1-octene in copolymer, % |
|---------|-----------------|-----------|-------------------|-------|----------------------------------|
| | | Yield, g. | $[\eta]$, dl./g. | Br, % | |
| 37 | 0 | 2.5 | 1.3 | 8.84 | 21.12 |
| 38 | 1 | 9.1 | 4.1 | 11.30 | 27.00 |

^a Solvent: 100 ml. *n*-heptene; catalyst: 3 mmole $\text{Al}(\text{C}_2\text{H}_5)_2\text{Cl}$ + 1 mmole TiCl_3 ; monomers: 2.3 g. 8-bromo-1-octene + 25.2 g. 4-methyl-1-pentene; temperature: 50°C.; time: 2 hr.

TABLE VIII
Effect of Pyridine on the Preparation of
Propylene/Ethylene/8-Bromo-1-octene Terpolymer^a

| Run no. | 8-Bromo-1-octene, g. | Pyridine, mmole | Terpolymer | | | 8-Bromo-1-octene in terpolymer, % |
|---------|----------------------|-----------------|------------|-------------------|----------------|-----------------------------------|
| | | | Yield, g. | $[\eta]$, dl./g. | Br, % | |
| 39 | 0 | 0 | 12.9 | 2.8 | — ^b | — |
| 40 | 6.90 | 0 | Trace | — | — | — |
| 41 | 6.90 | 3 | 9.3 | 1.0 | 9.06 | 21.65 |

^a Solvent: 300 ml. *n*-heptane; catalyst: 6 mmole $\text{Al}_2(\text{C}_2\text{H}_5)_3\text{Cl}_3$ + 3 mmole VOCl_3 ; monomers: 426 ml./min. propylene + 129 ml./min. ethylene; temperature: 25–45°C.; time: 1 hr.

^b Contains 0.06% Cl.

increases the overall yield but also the incorporation of ω -halo- α -olefin (compare also the runs in Tables III and V).

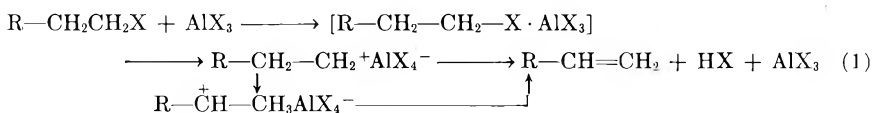
Other examples of ω -halo- α -olefin copolymerizations with and without an added Lewis base are summarized in Tables VII and VIII. These experiments furnish additional evidence that a Lewis base, such as pyridine, may substantially increase the yields in the copolymerization of ω -halo- α -olefins.

Cause of Catalyst Deactivation in ω -Halo- α -olefin Copolymerizations

To understand the role of ω -halo- α -olefins in copolymerizations the reactions of alkyl halides with aluminum halides will be considered briefly.

In the presence of Lewis acids, the 1-haloalkanes are unstable and undergo isomerization or hydrogen halide elimination.¹⁷ The first step in the reaction sequence leading to hydrogen halide elimination is a complex formation between the Lewis acid, e.g., aluminum halide and the alkyl halide. This complex may dissociate, giving an alkyl carbonium ion. The alkyl carbonium ion can lose a proton and form the appropriate hydrogen halide and olefin. The extent of elimination increases with the ionic nature of

the complex and will vary widely with the reactants. The reaction can be formulated as shown in eq. (1):

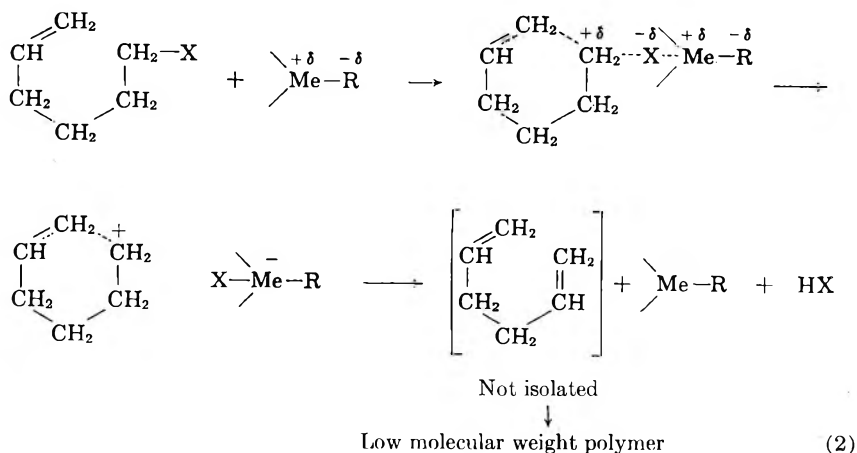


Analogous reactions involving alkylaluminum halides and alkyl halides have also been reported.^{11,13}

Since the Ziegler catalysts obtained from the reaction of aluminum alkyls and transition metal halides have a certain Lewis acid character, it is expected that they will also form complexes with halo compounds. If the complex ionizes and elimination takes place, then the hydrogen halide which is formed may deactivate a part of the catalyst resulting in lower yields. The hydrogen halides also lower the molecular weights by reacting with the growing chains.

Our experiments indicate that the copolymerization of propylene with 1-octene does not result in any substantial reduction of the yield (compare runs 16 and 22 in Table IV). Thus, the deactivation experienced with the ω -halo- α -olefins is due to the presence of a halogen atom in these monomers. Furthermore, reduction in the yield found with an equimolecular amount of 1-haloalkane is always less than with the corresponding ω -halo- α -olefins (compare runs 18 and 19 in Table IV with the runs in Table III). This observation indicates that the terminal double bond has some influence on the deactivating capacity of the halogen atom. The interaction of the double bond with the halogen atom in deactivating the catalyst is most strikingly demonstrated with allyl halides, 6-chloro-1-hexene, 8-chloro-1-octene, and 6-bromo-1-hexene (see Table III). We attribute the total lack of solid polymer formation to the strong tendency of these comonomers to dehydrohalogenate under polymerization conditions.

Dehydrohalogenation of the hexenes might be assisted by the double bonds as shown in eq. (2):



where $\text{Me}-\text{R}$ denotes Ziegler catalyst, Me is Al or Ti, and X is Cl or Br.

The driving force of the reaction is the formation of a resonance stabilized carbonium ion which, in the elimination step, loses a proton. Participation of the double bond in the ionization step will occur to a lesser degree with ω -halo- α -olefins which do not have the proper geometry for the formation of a cyclic intermediate. They will deactivate less efficiently in polymerization reactions.

Resonance-stabilized carbonium ion formation, without the necessity of invoking a cyclic intermediate, accompanied with the loss of hydrogen halide also explains the strong deactivation found with the allyl halides. The effect of temperature in promoting hydrogen halide elimination is evidenced by the fact that 8-chloro-1-octene copolymerizes readily at 50°C. but deactivates the catalyst completely at 70°C. (see runs 4 and 8 in Tables II and III, respectively). The difference observed in the deactivating capacity of 8-chloro-1-octene and 8-bromo-1-octene (see runs 8 and 14 in Table III) is presently not well understood.

Small amounts of impurities (such as isomeric allylic or secondary halides) in the higher ω -halo- α -olefins could not be responsible for the unusually strong deactivation found in some cases. Copolymerization of propylene and 5-chloro-1-pentene conducted in the presence of small amounts of added impurities proceeded readily; and the yields, chlorine contents, and intrinsic viscosities were only slightly affected. These results are shown in Table IX. In these experiments the concentration of the strongly deactivating additive was always higher than the amount of impurities detectable in the ω -halo- α -olefins.

Hydrogen halide formation, as a primary cause of the deactivation, was substantiated with homopolymerization experiments carried out with ω -halo- α -olefins. Allyl bromide, 5-bromo-1-pentene, allyl chloride, and 6-chloro-1-hexene were found to decompose in the presence of Ziegler catalysts $[\text{Al}(\text{C}_2\text{H}_5)_2\text{Cl} + \text{TiCl}_3]$. The gaseous products of the decomposition were hydrogen halides which could be absorbed in water. Analysis of the water

TABLE IX
Copolymerization of 5-Chloro-1-pentene with Propylene
in the Presence of Deactivating Additives^a

| Run no. | Additive | Additive concn., mole-% | Copolymer | | |
|---------|----------------|-------------------------|-----------|-------------------|-------|
| | | | Yield, g. | $[\eta]$, dl./g. | Cl, % |
| 6 | — | — | 7.6, 6.6 | 2.1 | 0.73 |
| 42 | 2-Chlorooctane | 2.12 | 6.0 | 2.0 | 0.93 |
| 43 | Allyl chloride | 2.65 | 4.2 | 2.0 | 0.98 |

^a Solvent: 100 ml. *n*-heptane; catalyst: 3 mmole $\text{Al}(\text{C}_2\text{H}_5)_2\text{Cl} + 1$ mmole TiCl_3 ; monomers: 12 mmole 5-chloro-1-pentene + 50 psi propylene; temperature: 70°C.; time: 1 hr.

solutions showed that they contain equivalent amounts of hydrogen and halide ions. The halide obtained from the decomposition of 5-bromo-1-pentene was 69.2 mole-% bromide and 30.8 mole-% chloride. The presence of both halides in the elimination product indicates the formation of an ion pair prior to elimination. The solid decomposition products of ω -halo- α -olefins are low molecular weight polymers containing only a fraction of the theoretically possible halogen. Efforts to isolate monomeric olefins or diolefins after the decomposition reaction were unsuccessful.

The deactivation reaction is also dependent on the Lewis acid strength of the catalyst components employed in the polymerization. Thus, it was found that by using a weak Lewis acid, such as $\text{Al}(\text{C}_2\text{H}_5)_3$, in combination with TiCl_3 , 6-chloro-1-hexene and propylene copolymerize readily. Under identical conditions a catalyst obtained from a stronger Lewis acid, such as $\text{Al}(\text{C}_2\text{H}_5)_2\text{Cl}$, and TiCl_3 did not produce any polymer. Similarly, by using a weak Lewis acid, such as $\text{Al}(i\text{-C}_4\text{H}_9)_3$, with VOCl_3 , a high molecular weight terpolymer of ethylene, propylene, and 8-bromo-1-octene could be obtained. The substitution of a stronger Lewis acid, such as $\text{Al}_2(\text{C}_2\text{H}_5)_3\text{Cl}_3$, for $\text{Al}(i\text{-C}_4\text{H}_9)_3$ produced no polymer.

The effect of Lewis bases in many of the described copolymerizations can also be interpreted in terms of decreasing the Lewis acid strength of the Ziegler catalyst used. The Lewis base, by coordinating with the electron-deficient Al or Ti compounds, will decrease the ionization of the Ziegler catalyst—haloolefin complex. Consequently, hydrogen halide formation will be suppressed, resulting in improved copolymer yields.

All our efforts to prepare copolymers from 7-chloro-1-octene were unsuccessful. This compound destroyed the Ziegler catalyst under all experimental conditions. The strong deactivating power of the secondary halides is probably due to the ease of carbonium ion formation followed by HCl elimination even in the presence of Ziegler catalysts having relatively weak

TABLE X
Polymerization Attempts in the Presence of Secondary Alkyl Chlorides^a

| Run no. | Chloro compound (12 mmole) | Catalyst | | | Temp., °C. | Time, hr. | Polymer yield, g. |
|---------|----------------------------|--|-----------------------|-----------------|------------|-----------|-------------------|
| | | Al compound (3 mmole) | Ti compound (1 mmole) | Other (1 mmole) | | | |
| 44 | 2-Chlorooctane | $\text{Al}(\text{C}_2\text{H}_5)_2\text{Cl}$ | TiCl_3 | | 50 | 2 | 0, 0 |
| 45 | 2-Chlorooctane | $\text{Al}(\text{C}_2\text{H}_5)_2\text{Cl}$ | TiCl_3 | | 70 | 1 | 0, 0 |
| 46 | 7-Chloro-1-octene | $\text{Al}(\text{C}_2\text{H}_5)_2\text{Cl}$ | TiCl_3 | | 50 | 2 | 0 |
| 47 | 7-Chloro-1-octene | $\text{Al}(\text{C}_2\text{H}_5)_2\text{Cl}$ | TiCl_3 | | 70 | 1 | 0 |
| 48 | 7-Chloro-1-octene | $\text{Al}(\text{C}_2\text{H}_5)_2\text{Cl}$ | TiCl_3 | Pyridine | 70 | 1 | 0 |
| 49 | 7-Chloro-1-octene | $\text{Al}(\text{C}_2\text{H}_5)_3$ | TiCl_3 | Pyridine | 70 | 1 | 0 |

^a Solvent: 100 ml. *n*-heptane; monomer: 50 psi propylene.

TABLE XI
Composition of Some Propylene/ ω -Halo- α -olefin Copolymers

| Run no. | ω -Halo- α -olefin in copolymer | Heptane-insoluble copolymer, % | Total copolymer | [η], dl./g. | | | Halogen (Cl or Br), % | | |
|---------|---|--------------------------------|-----------------|-----------------------------|---------------------------|-----------------|-----------------------------|---------------------------|-----------------|
| | | | | Heptane-insoluble copolymer | Heptane-soluble copolymer | Total copolymer | Heptane-insoluble copolymer | Heptane-soluble copolymer | Total copolymer |
| 20 | — | 78.5 | 4.1 | 4.8 | 1.0 | 0.09 | — | — | — |
| 30 | 5-Bromo-1-pentene | 71.0 | 2.8 | 3.7 | 0.81 | 3.08 | 2.10 | 4.54 | 4.54 |
| 32 | 8-Bromo-1-octene | 67.7 | 2.0 | 2.8 | 0.66 | 5.10 | 2.87 | 6.70 | 6.70 |
| 27 | 11-Chloro-1-undecene | 56.5 | 2.4 | 3.3 | 0.75 | 2.46 | 1.50 | 3.46 | 3.46 |

Lewis acid character. These results, together with some auxiliary experiments, are summarized in Table X.

Copolymer Characterization

Halogen contents and intrinsic viscosities of the α -olefin/ ω -halo- α -olefin copolymers are given in the respective tables describing the syntheses of these materials. From the halogen content the copolymer composition can be calculated.

The crystalline copolymers of propylene and ω -halo- α -olefins prepared with the highly stereospecific $\text{Al}(\text{C}_2\text{H}_5)_2\text{Cl} + \text{TiCl}_3$ catalyst are inhomogeneous with respect to haloolefin distribution and can be separated by extraction into fractions containing different amounts of halogen. The results of some extractions are shown in Table XI.

While the heptane-soluble fractions have a higher percentage of halogen than the total polymer, it is important to note that the heptane-insoluble fractions also contain a considerable amount of halogen. This can serve as a proof for copolymerization, since a homopolymer of the ω -halo- α -olefin (if it is formed at all) would be expected to be soluble in hot heptane. The fact of copolymerization is confirmed also by the increased heptane solubility of the copolymers compared to polypropylene prepared under identical conditions.

The infrared spectra of molded films of the propylene/ ω -halo- α -olefin copolymers exhibit distinct absorptions in the 720 cm^{-1} region. These bands observed both in the heptane-soluble and heptane-insoluble fractions are attributed to the $-(\text{CH}_2)_n-$ group^{19a} and are characteristic of the incorporated ω -halo- α -olefin. As is to be expected, the frequency of the $-(\text{CH}_2)_n-$ skeletal vibration increases in those copolymers where $n < 4$. In addition, absorption bands associated with the C—Cl and C—Br vibrations^{19b} and also those normally found in isotactic polypropylene are present in the infrared spectra. A summary of the absorption bands characteristic

TABLE XII
Infrared Absorption Bands Attributed to the Incorporated
 ω -Halo- α -olefin in Propylene/ ω -Halo- α -olefin Copolymers

| Run no. | ω -Halo- α -olefin in copolymer | Absorption band, cm^{-1} | | |
|---------|--|-----------------------------------|--------------------|---------------|
| | | $(\text{CH}_2)_n$ | C—X (X = Cl or Br) | |
| | | | <i>trans</i> | <i>gauche</i> |
| 24 | 5-Chloro-1-pentene | 754 | 726 | 655 |
| 25 | 6-Chloro-1-hexene | 733 ^a | 733 ^a | 654 |
| 26 | 8-Chloro-1-octene | 727 ^a | 727 ^a | 654 |
| 27 | 11-Chloro-1-undecene | 720 | 728 | 654 |
| 29 | 4-Bromo-1-butene | — | 650 | 564 |
| 30 | 5-Bromo-1-pentene | 748 | 649 | 563 |
| 31 | 6-Bromo-1-hexene | 732 | 648 | 562 |
| 32 | 8-Bromo-1-octene | 721 | 647 | 565 |

^a The $(\text{CH}_2)_n$ and C—Cl (*trans*) bands are not resolved.

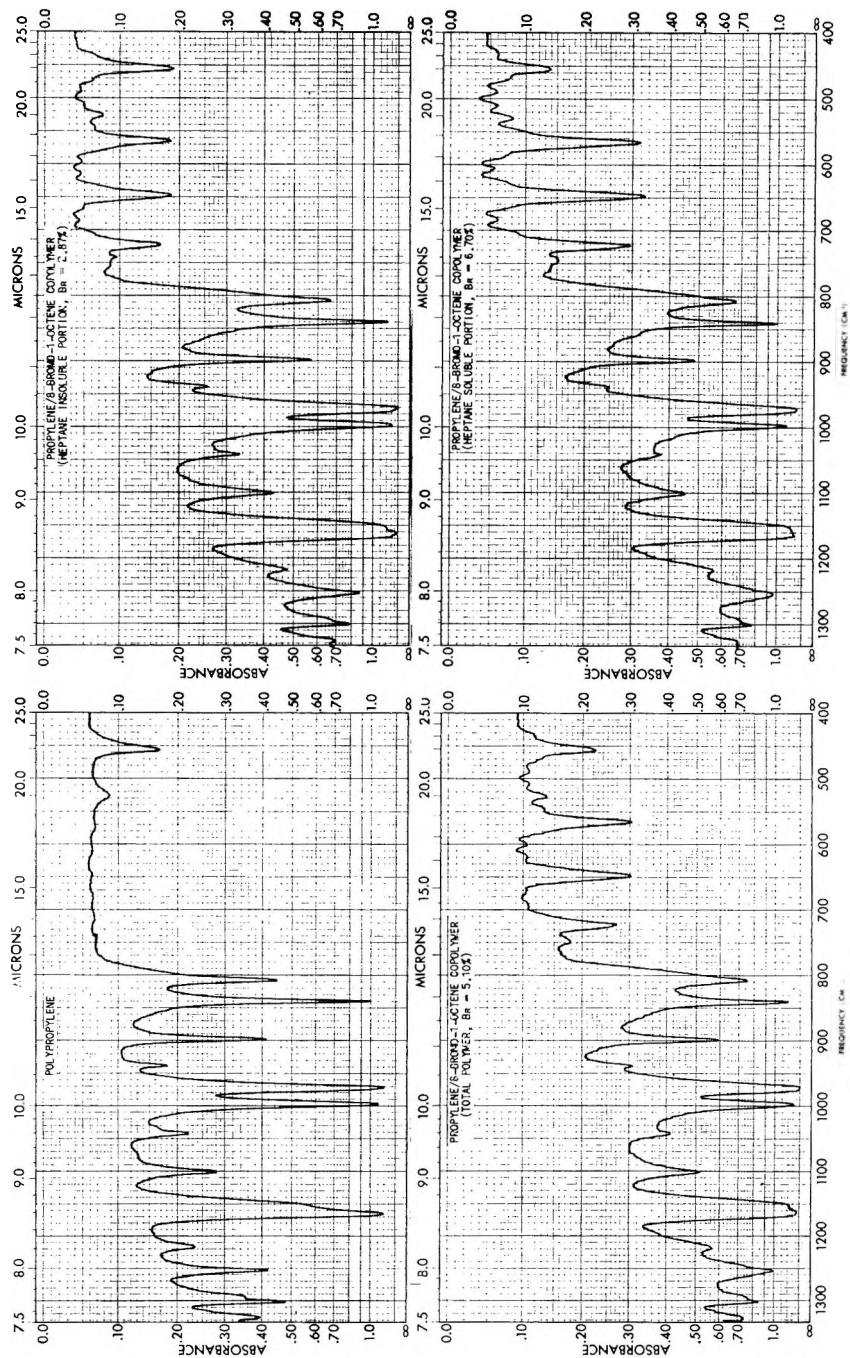


Fig. 1. Infrared spectra of propylene/8-bromo-1-octene copolymers.

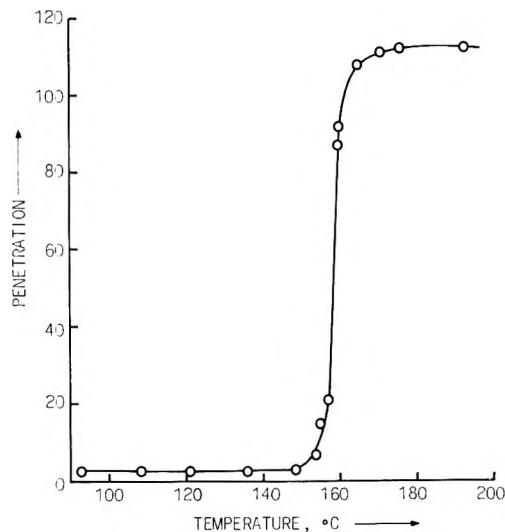


Fig. 2. Penetrometer melting point curve of a propylene/8-bromo-1-octene copolymer containing 3.03% 8-bromo-1-octene.

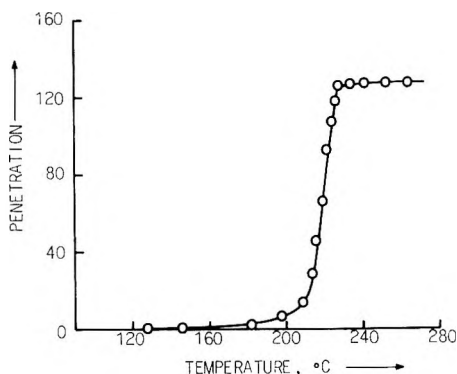


Fig. 3. Penetrometer melting point curve of a 4-methyl-1-pentene/5-chloro-1-pentene copolymer containing 9.23% 5-chloro-1-pentene.

of the incorporated ω -halo- α -olefin is presented in Table XII. Typical copolymer spectra are shown in Figure 1.

Propylene/ ω -halo- α -olefin copolymers containing relatively small amounts of ω -halo- α -olefin are crystalline solids which melt sharply but at somewhat lower temperature than isotactic polypropylene. For example, 3.03% or 5.33% 8-bromo-1-octene incorporation lowers the melting point from 174°C. to 162 or 145°C., respectively. The penetrometer melting point curve of one of these materials is presented in Figure 2.

The copolymerization of ω -halo- α -olefins with 4-methyl-1-pentene may lead to high molecular weight polymers soluble in many common organic solvents. A copolymer of 4-methyl-1-pentene and 5-chloro-1-pentene obtained by the $\text{Al}(\text{C}_2\text{H}_5)_2\text{Cl} + \text{TiCl}_3$ catalyst, and containing 9.23% 5-

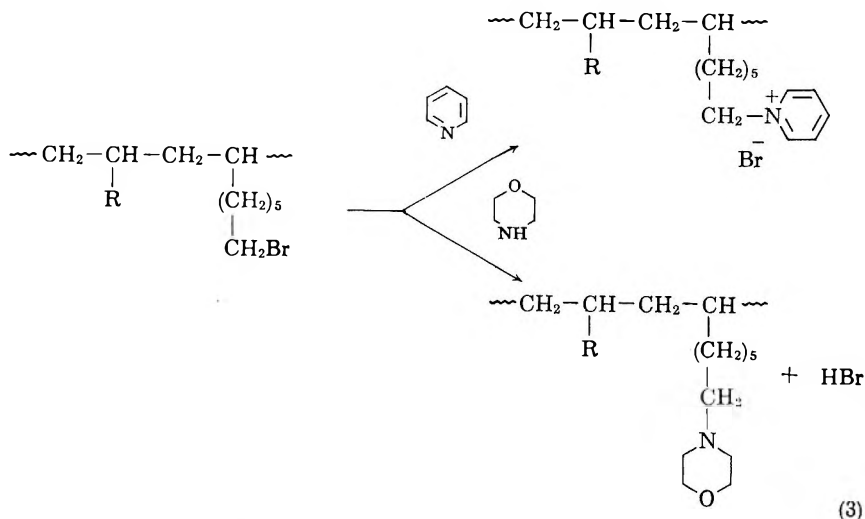
chloro-1-pentene, was soluble in boiling benzene, *n*-heptane, and chloroform. Since isotactic poly-4-methyl-1-pentene, prepared with the same catalyst, is insoluble in those solvents, this can be considered as an additional proof of copolymerization. This copolymer melts at 216°C., about 25°C. lower than poly-4-methyl-1-pentene (Fig. 3). It is also crystalline, showing the same x-ray diffraction pattern as poly-4-methyl-1-pentene (Fig. 4).

The copolymerization of ethylene, propylene, and 8-bromo-1-octene gave a completely amorphous, rubbery polymer which was soluble in heptane and benzene. The infrared spectrum of this terpolymer is similar to that reported for amorphous ethylene/propylene copolymers.²⁰

Some Reactions of α -Olefin/ ω -Halo- α -olefin Copolymers

The reactive halogen in α -olefin/ ω -halo- α -olefin copolymers provides a possible site for modifying the physical and chemical properties of these materials. We have found that certain nucleophilic substitution reactions proceed readily with the bromine-containing copolymers. As is to be expected, the chlorine-containing copolymers are much less reactive. The reactions investigated were carried out by heating the copolymer powder in pyridine or morpholine. Under the reaction conditions, the copolymers are swollen considerably by the amine. These experiments are summarized in Table XIII.

The elemental analyses of the products indicate that the copolymers probably react as shown in eqs. (3)



where R is CH₃ or CH₂CH(CH₃)₂.

The reaction with pyridine may be accompanied by degradation (see run 50). While the thermal instability of quaternary ammonium compounds is well known, this reaction leading to polymer degradation is not presently understood.

TABLE XIII
Reaction of α -Olefin/ ω -Halob- α -olefin Copolymers with Amines^a

| Run no. | Amine | Copolymer | Starting copolymer | | | Product | | | | | | | |
|---------|------------|-------------------------------------|--------------------|-------------------|-------------|-----------|-------------------|-----------------------|----------|----------|-----------------------|----------|------|
| | | | Wt. copolymer, g. | $[\eta]$, dl./g. | Br or Cl, % | Yield, g. | $[\eta]$, dl./g. | Calc., % ^b | Found, % | Br or Cl | Calc., % ^b | Found, % | N |
| 50 | Pyridine | Propylene/8-bromo-1-octene | 2 | 5.7 | 1.59 | 1.9 | 2.9 | 1.56 | 1.44 | 0.27 | 0.27 | 0.27 | 0.27 |
| 51 | Pyridine | Propylene/5-chloro-1-pentene | 2 | 6.2 | 0.62 | 1.9 | 6.0 | 0.61 | 0.61 | 0.24 | 0.24 | 0.10 | 0.10 |
| 52 | Morpholine | Propylene/8-bromo-1-octene | 1 | 5.7 | 1.59 | 0.96 | 5.8 | 0 | <0.1 | 0.28 | 0.28 | 0.33 | 0.33 |
| 53 | Pyridine | 4-Methyl-1-pentene/8-bromo-1-octene | 1 | 4.1 | 11.30 | 0.72 | — ^c | 10.15 | 8.76 | 1.78 | 1.78 | 1.36 | 1.36 |

^a 20 ml. amine, 100°C., 2 hr.

^b Calculated on the basis of reactions (3).

^c The product was insoluble in decalin.

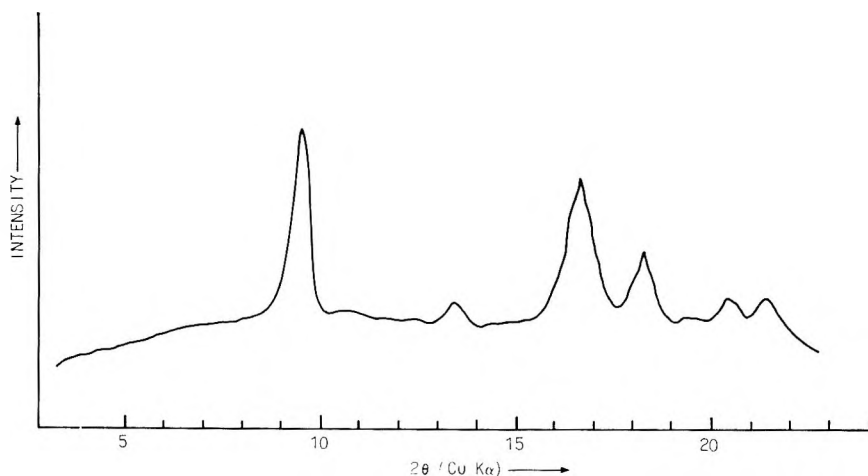


Fig. 4. X-ray diffraction pattern of a 4-methyl-1-pentene/5-chloro-1-pentene copolymer containing 9.23% 5-chloro-1-pentene.

The incorporation of tertiary amino or quaternary ammonium groups changes significantly the polarity of the α -olefin copolymers. This is reflected in the excellent dyeability of the polymers with acid dyes. The pyridine-treated propylene/8-bromo-1-octene copolymer powder (product of run 50) could be dyed rapidly to a deep blue shade with acidified aqueous solutions of Calcocid Alizarin Blue. The dyeing was permanent, and the color could not be removed by washing the dyed powder with hot aqueous detergent solution. The dyeability is apparently due to the presence of quaternary ammonium groups in the copolymer, since neither polypropylene nor the starting propylene/8-bromo-1-octene copolymer dye under the same conditions.

The author is indebted to Dr. J. E. Goodrich, Dr. S. J. Lapporte, and Dr. T. V. Liston for helpful discussions during this work. The 8-chloro-1-octene, 8-bromo-1-octene, and 7-chloro-1-octene were prepared by Dr. S. Suzuki and Dr. L. L. Ferstandig. Their help is gratefully acknowledged.

References

1. Natta, G., *J. Polymer Sci.*, **48**, 219 (1960).
2. Heller, J., D. O. Tieszen, and D. B. Parkinson, *J. Polymer Sci.*, **A1**, 125 (1963).
3. Hopkins, E. A., and M. L. Miller, *Polymer*, **4**, 75 (1963).
4. Gladding, E. K., B. S. Fisher, and J. W. Collette, *Ind. Eng. Chem. Prod. Res. Develop.*, **1**, No. 2, 65 (1962).
5. Natta, G., F. Danusso, and D. Sianesi, *Makromol. Chem.*, **28**, 253 (1958).
6. Etlis, V. S., K. S. Minsker, E. E. Rylov, and D. N. Bort, *Vysokomolekul. Soedin.*, **1**, 1403 (1959).
7. Giannini, U., and S. Cesca, *Chim. Ind. (Milan)*, **44**, 371 (1962); *Resins, Rubbers, Plastics*, **2**, 1915 (1962).
8. Sianesi, D., and G. Caporiccio, *Makromol. Chem.*, **60**, 213 (1963).
9. Overberger, C. G., and E. B. Davidson, *J. Polymer Sci.*, **62**, 23 (1962).
10. Natta, G., *J. Polymer Sci.*, **34**, 531 (1959).
11. Pozamantir, A. G., *Polymer Sci. USSR*, **3**, 217 (1962).

12. Murahashi, S., S. Nozakura, and K. Hatada, *Bull. Chem. Soc. Japan*, **34**, 631 (1961).
13. Salamatina, O. B., and P. S. Shantarovich, *Vysokomolekul. Soedin.*, **4**, 876 (1962).
14. Perrine, T. D., *J. Org. Chem.*, **18**, 1356 (1953).
15. Edgar, O. B., and E. Ellery, *J. Chem. Soc.*, **1952**, 2633.
16. Farley, L. L., and R. A. Winkler, *Anal. Chem.*, **35**, 772 (1963).
17. Olah, G. A., *Friedel-Crafts and Related Reactions*, Interscience, New York, 1963, p. 632.
18. Ziegler, K., in *Organometallic Chemistry*, H. Zeiss, Ed., Reinhold, New York, 1960, p. 198.
19. Bellamy, L. J., *Infra-Red Spectra of Complex Molecules*, Wiley, New York, 1958, (a) pp. 27, 28; (b) pp. 330, 331.
20. Natta, G., G. Mazzanti, A. Valvassori, and G. Pajaro, *Chim. Ind. (Milan)*, **39**, 733 (1957).

Résumé

On a étudié la copolymérisation des oléfines- α avec les oléfines- ω halogénées en ω au moyen des catalyseurs de Ziegler. On a trouvé que les oléfines- α halogénées en ω désactivent le catalyseur ce qui provoque un faible rendement en copolymère et réduit le poids moléculaire. La désactivation est provoquée par la formation d'halogénure d'hydrogène, grandement facilitée dans le cas des halogénures d'allyle et des 6-halo-1-hexènes. On interprète les différents degrés de désactivation en considérant la facilité de formation d'ion carbonium à partir des différentes oléfines- α halogénées en ω . Les rendements en copolymère sont fortement améliorés lorsqu'on ajoute une quantité catalytique d'une base de Lewis au système de polymérisation. On a proposé que la base de Lewis, en diminuant le caractère acide du catalyseur, supprime la décomposition des oléfines- α halogénées en ω conduisant à la formation d'hydracide halogéné. Suivant la nature du catalyseur de Ziegler employé, les copolymères des oléfines- α et des oléfines- α halogénées en ω peuvent être des solides soit cristallins, soit amorphes. L'halogène, surtout le brome dans les copolymères, est réactionnel dans les réactions de substitution nucléophile. La réaction avec les amines fournit des polymères qui peuvent être teintés au moyen de colorants acides.

Zusammenfassung

Die Kopolymerisation von α -Olefinen mit ω -Halogen- α -Olefinen mit Ziegler-Katalysatoren wurde untersucht. ω -Halogen- α -Olefine desaktivieren den Katalysator, was zu niedrigen Polymerausbeuten und zu herabgesetztem Molekulargewicht führt. Die Desaktivierung wird durch Halogenwasserstoffbildung verursacht, welche im Falle der Allylhalogenide und der 6-Halogen-1-Hexene stark begünstigt ist. Die verschiedenen Desaktivierungsgrade wurden als Folge der Leichtigkeit der Karboniumionbildung aus den verschiedenen ω -Halogen- α -Olefinen interpretiert. Die Polymerausbeute wurde durch Zusatz katalytischer Mengen einer Lewisbase zum Polymerisationssystem beträchtlich verbessert. Es wird angenommen, dass die zugesetzte Lewisbase durch Herabsetzung des Lewis-säuren-Charakters des Katalysators die zur Halogenwasserstoffbildung führende Zersetzung des ω -Halogen- α -Olefins unterdrückt. Je nach dem verwendeten Ziegler-Katalysator die Kopolymeren aus α -Olefinen und ω -Halogen- α -Olefinen entweder kristallisieren oder amorph sein. Das Halogen, besonders das Brom, in den Kopolymeren kann in nukleophilen Substitutionsreaktionen reagieren. Die Reaktion mit Aminen lieferte mit sauren Farbstoffen anfärbbare Polymere.

Received October 27, 1964

Revised December 3, 1964

(Prod. No. 4621A)

Fractionation of Polydienes by Means of Precipitation Chromatography

J. POLÁČEK, I. KÖSSLER, and J. VODEHNAL, *Institute of Physical Chemistry, Czechoslovak Academy of Sciences, Prague, Czechoslovakia*

Synopsis

The fractionation of polychloroprene, polyisoprene, and polybutadiene was carried out by a modified Baker-Williams chromatographic precipitation technique. The anomalous decrease of molecular weights of last fractions is explained as a result of oxidation processes leading to formation of peroxide bonds in the polymer. A correlation between the C=O group content and the value of the constant, k' , of the Schulz-Blaschke equation was found. The advantage of maintaining a relatively low temperature during the precipitation process and the influence of the method of preparation of the polymer film on the molecular weight distribution curve has been demonstrated.

I. INTRODUCTION

The method of precipitation chromatography of Baker and Williams,¹ is at present regarded as one of the best fractionation methods. The original apparatus requires the maintenance of a linear temperature gradient along the column. A modification of this method has been developed involving periodic variation of the temperature of the entire column.^{2,3} The modified method is simpler and seems to have other advantages.³ In a previous communication it was used for the fractionation of poly(methyl methacrylate).² In the present paper the fractionation of polydienes is described. It is shown that the anomalous decrease of molecular weights of the last fractions observed by other authors and interpreted in various ways⁴⁻¹³ is due to a destructive oxidation process.

II. EXPERIMENTAL

Polymers

Polychloroprene (Neoprene WRT) had $[\eta] = 1.245$ dl./g. in benzene at 25°C. *cis*-1,4-Polybutadiene was prepared by use of a cobalt catalyst: $[\eta] = 3.14$ dl./g. in benzene at 25°C.

Polyisoprene with a high content of the 3,4-structure was prepared by using phenylmagnesium bromide as catalyst;¹⁴ $[\eta] = 0.06$ dl./g. in benzene at 25°C.

Apparatus and Fractionation Conditions

The apparatus has been described previously.² The temperature range in the column was 28–35°C., the time of one cycle was 32–35 min., and the mean flow rate was 14 ml./hr. The column consisted of glass beads of 0.1 mm. diameter and the holdup in the column was 140 ml. A benzene-methanol mixture was the fractionation medium. The constant volume of the mixture in the mixing vessel was 500 ml. The concentrations of the methanol precipitant are given in Table I.

TABLE I
Methanol Concentration in the Benzene-Methanol Mixture

| Polymer | Methanol concentration, vol.-% | |
|-----------------|--------------------------------|--------------|
| | In mixing vessel (initial) | In reservoir |
| Polychloroprene | 50 | 11.5 |
| Polybutadiene | 50 | 0 |
| Polyisoprene | 100 | 17.5 |

Preparation of Polymer Films

Glass beads (150 g.) were either directly mixed with a solution of approximately 0.5 g. of polymer in 25 ml. of chloroform (procedure 1) or methanol was added with constant stirring until the first stable turbidity

TABLE II
Preparation of Polymer Films

| Experiment | Polymer | Method of film preparation ^a | Medium | Evaporation temperature, °C. | Remarks |
|------------|-------------------------------|---|---------------------|------------------------------|--|
| A | Neoprene WRT | 2 | N ₂ | 50 | 0.005 g. antioxidant added ^b |
| B | Neoprene WRT | 1 | Air | 60 | |
| C | Neoprene WRT | 1 | Air | 60 | Same as expt. B |
| D | Neoprene WRT | 2 | Air | 60 | |
| E | Neoprene WRT | 1 | Air, O ₂ | 60 | After evacuation of evaporation vessel with polymer O ₂ was introduced and the material dried for 1 hr. at 100°C. |
| F | Neoprene WRT | 2 | Air, O ₂ | 50 | Solvent was evaporated by a stream of O ₂ ; the material was then dried for 1 hr. at 100°C. |
| | 3,4-Polyisoprene | 1 | Air | 60 | |
| | <i>cis</i> -1,4-Polybutadiene | 1 | Air | 60 | |

^a See Experimental section.

^b Phenyl β -naphthylamine.

formed⁹ and the beads were then added (procedure 2). Other conditions of preparation of samples are given in Table II.

Preparation of the Column

The column was filled about three quarters full with glass beads, heated to 50°C., evacuated with a vacuum pump, cooled to 12–14°C., and under these conditions wetted with degassed methanol. The spaces above and below the column were opened to the atmosphere and air admitted. In the case of fractionation of Neoprene WRT (experiment A), pure nitrogen was used instead of air. Glass beads coated with polymer were then transferred to the space above the moistened column.

Viscosity Measurement and Determination of the Amount and Concentration of Polymer in the Fractions

Individual fractions were dried *in vacuo*, dissolved in benzene, dried again, and after redissolving in benzene, the quantity and concentration in the fractions as well as their limiting viscosity numbers were determined.

The concentration of polymer in the fraction was determined by means of the evaporation residue method. Aliquots were first evaporated at a slightly elevated temperature, and drying was completed in a vacuum oven at 45°C. for 4–6 hr.

The viscosity of benzene solutions of the fractions was measured at 25°C. in a Ubbelohde-type viscometer. Limiting viscosity numbers of the fractions were determined by measuring the dependence of viscosity on concentration for some fractions, and the limiting viscosity number as well as the $N = 1/k'$ value were determined by extrapolating the dependence $\eta_{sp}/c \rightarrow \eta_{sp}$.¹⁵ A calibration curve $N \rightarrow \eta_{sp}/c$ was then plotted,¹⁶ and from this the value of N was found for the remaining fractions whose limiting viscosity numbers were thus calculated from a single-point measurement (polychloroprene and polybutadiene). In the case of polyisoprene it was found that the value of $N = 0.18$ is applicable to the entire range of molecular weights.

Infrared Spectral Analysis of the Fractions

The Zeiss UR-10 instrument was used. Benzene solutions of fractions, containing approximately 3 mg. of the polymer, were mixed with 300 mg. KBr, dried at 50°C. *in vacuo*, and pressed into tablets.¹⁷ The content of C=O groups was determined from the density of the 1740 or 1710 cm.^{-1} bands; the content of C=C bonds from the density of the 1665 cm.^{-1} (polychloroprene, polybutadiene) or 1645 cm.^{-1} bands (polyisoprene). The influence of scattered radiation was eliminated by measuring the transmitted radiation at 1850 cm.^{-1} , where none of the polymers investigated show any specific absorption. This value was then used as I_0 in the relation $D = \log [I_0/I(\nu)]$.

III. RESULTS

A series of fractionations of Neoprene WRT were carried out under inert conditions (experiment A) as well as in the presence of air where the polymer was oxidized to different degrees. Oxidation was carried out simultaneously with the preparation of polymer films (see Experimental). Although the degree of oxidation cannot be expressed in a quantitative manner, it is possible to classify the degree of oxidation according to the conditions of polymer film preparation as A = unoxidized; F = most oxidized, and B-E = intermediate degrees of oxidation.

The fractionations of *cis*-1,4-polybutadiene and 3,4-polyisoprene were carried out under conditions which for polychloroprene should have caused slight oxidation.

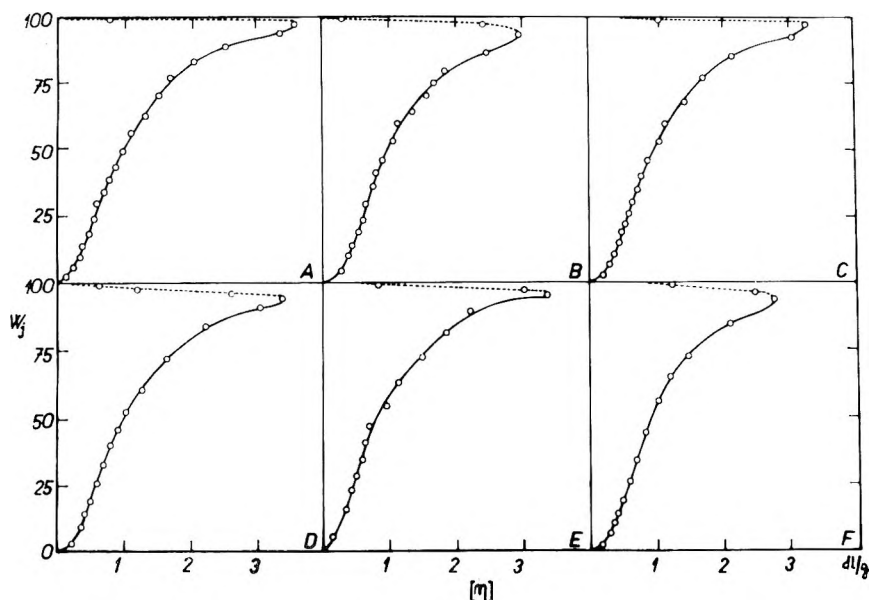


Fig. 1. Distribution curves of viscosities of Neoprene WRT (experiments A-F).

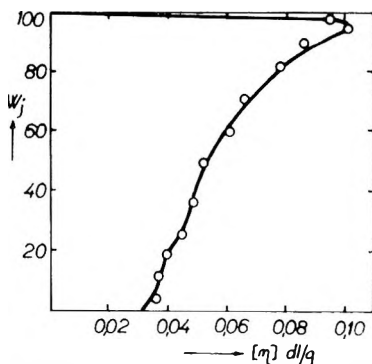


Fig. 2. Distribution curve of viscosities of 3,4-polyisoprene.

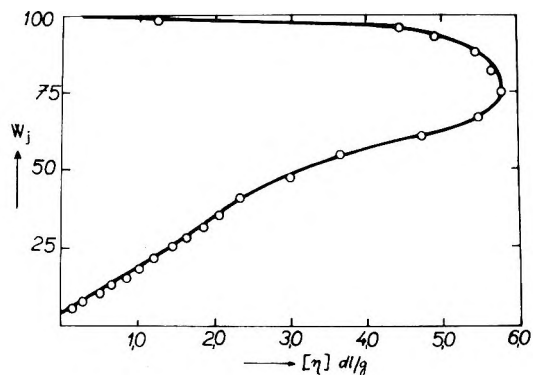


Fig. 3. Distribution curve of viscosities of *cis*-1,4-polybutadiene.

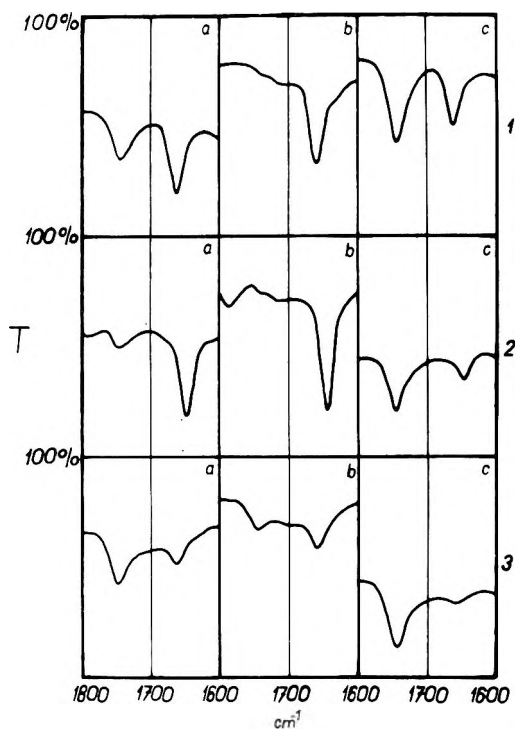


Fig. 4. Infrared spectra of some fractions in the range 1600–1800 cm^{-1} : (1) Neoprene WRT, experiment D (*c* = fraction 1, *b* = fraction 10, *c* = fraction 16); (2) 3,4-polyisoprene (*a* = fraction 2, *b* = fraction 9, *c* = fraction 14); (3) *cis*-1,4-polybutadiene (*a* = fraction 4, *b* = fraction 13, *c* = fraction 25).

Distribution curves of molecular weights for all samples fractionated are plotted in Figures 1–3. The corresponding fractionation data are summarized in Tables III–VII.

Infrared spectra of some samples are shown in Figures 4 and 5.

TABLE III
 Fractionation of Neoprene WRT by Precipitation Chromatography with Periodic
 Temperature Variation of the Column in the Range of 28–35°C.

| Experiment A, ^a [$\bar{\eta}$] _{fr.} = 1.240 dl./g. ^c | | | Experiment B, ^b [$\bar{\eta}$] _{fr.} = 1.217 dl./g. ^c | | |
|---|-------------|--------------------------|---|-------------|--------------------------|
| Fraction | % by weight | [$\bar{\eta}$], dl./g. | Fraction | % by weight | [$\bar{\eta}$], dl./g. |
| 1 | 4.73 | 0.143 | 1 | 7.89 | 0.296 |
| 2 | 2.62 | 0.265 | 2 | 3.45 | 0.395 |
| 3 | 4.57 | 0.360 | 3 | 4.12 | 0.451 |
| 4 | 1.90 | 0.390 | 4 | 5.40 | 0.548 |
| 5 | 1.93 | 0.397 | 5 | 3.34 | 0.614 |
| 6 | 4.88 | 0.496 | 6 | 8.53 | 0.646 |
| 7 | 6.34 | 0.576 | 7 | 5.45 | 0.770 |
| 8 | 4.54 | 0.623 | 8 | 4.34 | 0.805 |
| 9 | 4.37 | 0.715 | 9 | 5.24 | 0.933 |
| 10 | 4.70 | 0.818 | 10 | 8.85 | 1.072 |
| 11 | 5.44 | 0.901 | 11 | 4.60 | 1.137 |
| 12 | 6.27 | 1.010 | 12 | 5.26 | 1.374 |
| 13 | 7.08 | 1.133 | 13 | 5.69 | 1.577 |
| 14 | 6.90 | 1.344 | 14 | 4.27 | 1.679 |
| 15 | 7.15 | 1.550 | 15 | 5.16 | 1.845 |
| 16 | 6.88 | 1.720 | 16 | 7.82 | 2.481 |
| 17 | 5.55 | 2.089 | 17 | 6.03 | 2.953 |
| 18 | 5.04 | 2.550 | 18 | 3.25 | 2.425 |
| 19 | 4.88 | 3.390 | 19 | 1.41 | 0.310 |
| 20 | 2.77 | 3.610 | | | |
| 21 | 1.46 | 0.811 | | | |

^a Nitrogen atmosphere.

^b Air atmosphere.

^c [$\bar{\eta}$]_{fr.} = [$\bar{\eta}$] calculated from fractions.

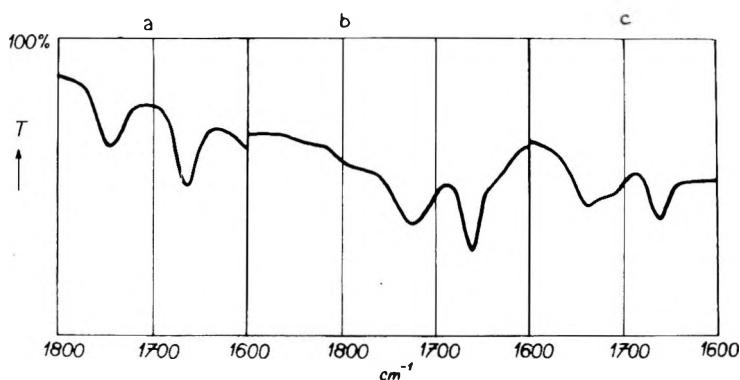


Fig. 5. Infrared spectra of some fractions of Neoprene WRT (experiment F) in the range 1600–1900 cm^{-1} : (a) fraction 1, (b) fraction 6, (c) fraction 16.

TABLE IV
 Fractionation of Neoprene WRT by Precipitation Chromatography with Periodic
 Temperature Variation of the Column in the Range of 28–35°C.

| Experiment C, [$\bar{\eta}$] _{fr.} = 1.204 dl./g. | | | Experiment D, [$\bar{\eta}$] _{fr.} = 1.210 dl./g. | | |
|---|-------------|--------------------|---|-------------|--------------------|
| Fraction | % by weight | [η], dl./g. | Fraction | % by weight | [η], dl./g. |
| 1 | 5.50 | 0.220 | 1 | 6.14 | 0.230 |
| 2 | 2.85 | 0.320 | 2 | 5.95 | 0.366 |
| 3 | 3.75 | 0.379 | 3 | 4.41 | 0.433 |
| 4 | 5.24 | 0.468 | 4 | 5.22 | 0.520 |
| 5 | 3.02 | 0.501 | 5 | 6.97 | 0.611 |
| 6 | 3.47 | 0.553 | 6 | 7.56 | 0.707 |
| 7 | 3.50 | 0.611 | 7 | 5.52 | 0.805 |
| 8 | 4.56 | 0.645 | 8 | 6.26 | 0.930 |
| 9 | 4.83 | 0.734 | 9 | 7.11 | 1.038 |
| 10 | 5.31 | 0.795 | 10 | 8.94 | 1.280 |
| 11 | 6.72 | 0.903 | 11 | 14.38 | 1.670 |
| 12 | 6.79 | 1.060 | 12 | 9.13 | 2.240 |
| 13 | 7.31 | 1.148 | 13 | 4.19 | 3.060 |
| 14 | 9.07 | 1.450 | 14 | 2.93 | 3.400 |
| 15 | 9.50 | 1.710 | 15 | 1.20 | 2.637 |
| 16 | 7.18 | 2.160 | 16 | 1.69 | 1.216 |
| 17 | 6.64 | 3.070 | 17 | 2.40 | 0.664 |
| 18 | 2.73 | 3.270 | | | |
| 19 | 1.47 | 1.053 | | | |

TABLE V
 Fractionation of Neoprene WRT by Precipitation Chromatography with Periodic
 Temperature Variation of the Column in the Range of 28–35°C.

| Experiment E, [$\bar{\eta}$] _{fr.} = 1.104 dl./g. | | | Experiment F, [$\bar{\eta}$] _{fr.} = 1.061 dl./g. | | |
|---|-------------|--------------------|---|-------------|--------------------|
| Fraction | % by weight | [η], dl./g. | Fraction | % by weight | [η], dl./g. |
| 1 | 4.58 | 0.178 | 1 | 9.67 | 0.155 |
| 2 | 3.91 | 0.297 | 2 | 6.39 | 0.348 |
| 3 | 2.98 | 0.356 | 3 | 4.18 | 0.441 |
| 4 | 4.08 | 0.405 | 4 | 5.26 | 0.507 |
| 5 | 5.68 | 0.484 | 5 | 6.80 | 0.604 |
| 6 | 7.42 | 0.581 | 6 | 4.48 | 0.350 |
| 7 | 8.44 | 0.680 | 7 | 5.70 | 0.642 |
| 8 | 11.27 | 0.825 | 8 | 7.10 | 0.707 |
| 9 | 11.88 | 1.020 | 9 | 8.00 | 0.981 |
| 10 | 7.85 | 1.194 | 10 | 8.90 | 1.147 |
| 11 | 7.49 | 1.470 | 11 | 9.80 | 1.500 |
| 12 | 16.23 | 2.100 | 12 | 8.26 | 1.870 |
| 13 | 2.26 | 2.775 | 13 | 8.21 | 2.220 |
| 14 | 2.81 | 2.480 | 14 | 3.10 | 3.400 |
| 15 | 2.49 | 1.235 | 15 | 1.37 | 3.036 |
| | | | 16 | 2.78 | 0.865 |

TABLE VI
 Fractionation of 3,4-Polyisoprene by Precipitation Chromatography with Periodic
 Temperature Variation of the Column in the Range of 28–35°C.

| Fraction | % by weight | $[\eta]$, dl./g. ^a |
|----------|-------------|--------------------------------|
| 1 | 6.64 | 0.040 |
| 2 | 8.24 | 0.037 |
| 3 | 7.24 | 0.036 |
| 4 | 6.78 | 0.045 |
| 5 | 7.45 | 0.049 |
| 6 | 8.48 | 0.049 |
| 7 | 9.55 | 0.052 |
| 8 | 10.67 | 0.061 |
| 9 | 10.72 | 0.066 |
| 10 | 11.48 | 0.078 |
| 11 | 5.08 | 0.086 |
| 12 | 4.36 | 0.108 |
| 13 | 1.64 | 0.095 |
| 14 | 1.67 | 0.000 |

^a $[\eta]_{fr.} = 0.057$ dl./g.

TABLE VII
 Fractionation of *cis*-1,4-Polybutadiene by Precipitation Chromatography with Periodic
 Temperature Variation of the Column in the Range of 28–35°C.

| Fraction | % by weight | $[\eta]$, dl./g. ^a |
|----------|-------------|--------------------------------|
| 1 | 5.51 | ^b |
| 2 | 2.15 | 0.146 |
| 3 | 2.31 | 0.277 |
| 4 | 2.88 | 0.507 |
| 5 | 1.94 | 0.650 |
| 6 | 2.35 | 0.839 |
| 7 | 2.86 | 1.013 |
| 8 | 4.23 | 1.190 |
| 9 | 2.68 | 1.425 |
| 10 | 2.91 | 1.619 |
| 11 | 3.53 | 1.849 |
| 12 | 4.75 | 2.037 |
| 13 | 6.09 | 2.318 |
| 14 | 7.33 | 2.986 |
| 15 | 6.77 | 3.638 |
| 16 | 5.51 | 4.734 |
| 17 | 5.60 | 5.480 |
| 18 | 5.35 | 5.780 |
| 19 | 5.36 | 5.780 |
| 20 | 3.75 | 5.654 |
| 21 | 2.86 | 5.450 |
| 22 | 4.95 | 5.450 |
| 23 | 2.85 | 4.912 |
| 24 | 3.35 | 4.460 |
| 25 | 1.17 | 1.277 |

^a $[\eta]_{fr.} = 3.014$ dl./g.

^b This fraction contained a high percentage of phenyl β -naphthylamine.

IV. DISCUSSION

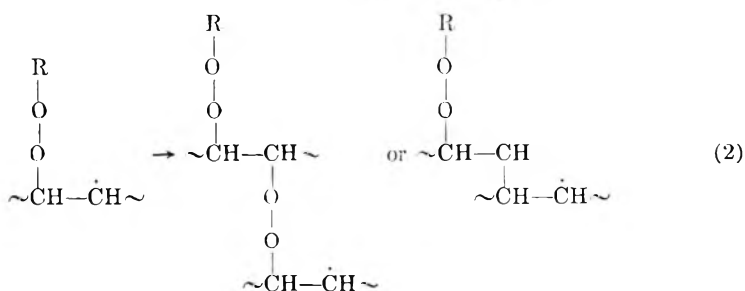
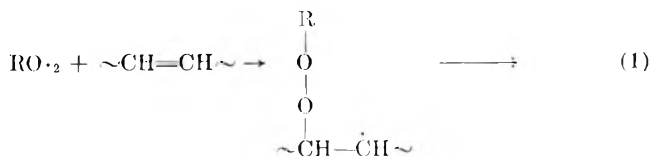
A number of workers have tried to explain the anomalous decrease of molecular weights of last fractions which often accompanies column fractionation methods.^{4,5,9,10,12,13} Their explanations, however, seem to us in some cases unconvincing and they do not explain all the observed effects. For example, neither Jungnickel and Weiss⁹ nor Cooper et al.¹² compared the average limiting viscosity number calculated from fractions with the limiting viscosity number of the unfractionated sample. Table III in the paper by Jungnickel and Weiss indicates that the limiting viscosity number of the unfractionated sample has the value 1.52 dl./g., whereas that calculated from the fractionation data has the value 1.41 dl./g. In the experiments described by Cooper, Vaughan, and Yardley,¹² again these values do not agree. In the latter case, however, the value of the limiting viscosity number calculated from data in columns A and B of their Table II is higher than the value for the unfractionated sample (1.71 and 1.67 dl./g.). The limiting viscosity number calculated from data in column C of this table is as high as 1.76 dl./g. We may therefore assume that in the course of the experiment the macromolecules were subjected to rupture, branching, and crosslinking. Further, a proof that no oxidative destruction takes place in the course of fractionation of *cis*-1,4-polybutadiene, is given by Hulme and McLeod,¹³ but it was not performed under the same conditions as the fractionation process itself.

On the basis of the results reported in the present paper and our earlier work dealing with the aging of polychloroprene¹⁸ we believe that the anomalies mentioned are connected with oxidative degradation processes, which take place in the polymer before, as well as during the fractionation itself. Anomalies are encountered mainly with those polymers which are easily oxidized (polydienes), whereas in the case of other polymers they do not occur at all or they occur very rarely. Further, Henry⁵ has found C=O groups in anomalously behaving polyethylene fractions and a simultaneous decrease of the limiting viscosity number calculated from the fractionation data. Additional evidence for such degradation of polydienes was observed during our study of the adsorption chromatography of polychloroprene solutions.¹⁹

We therefore regard rupture of peroxide groups, C—O—O—C, as the main reason for the anomalous decrease of molecular weights of the last fractions obtained by column fractionation methods. These groups may be present in some polymers in the main chain, such as when the polymerization is accompanied by copolymerization of the monomer with oxygen. These groups may, however, occur to a far greater extent in easily oxidizable polymers, where oxidation results in crosslinking of chains by the peroxide groups. Such polymers may be partially oxidized during their preparation or storage and possibly further oxidized during the preparation of the polymer film on the inert support. In the course of sample preparation the polymer is readily attacked by oxygen, which may diffuse into the

polymer film. The oxidation would be accelerated at the elevated temperature necessary for evaporation of the solvent.

In the course of the oxidation, primary radicals are formed in various ways, for instance by thermal cleavage of hydrogen from the tertiary carbon at the point of 3,4-addition or at a branching point. Polymeric radicals then react with molecular oxygen, forming peroxide radicals. These radicals may then react²⁰ with double bonds, eventually forming cross-linked structures.



However, with the most labile hydrogens, a hydroperoxide may be formed.²¹ The hydroperoxide, however, then decomposes to form two radicals. Details of the next steps are not quite clear. It is, however, evident, that on the one hand they may lead to the formation of various C=O groups as a result of scission of the macromolecule, while on the other hand they may lead to three types of crosslinks:



The peroxide bond [eq. (3)] is far weaker than the C—C or C—O—C bond [eqs. (4), (5)] and therefore its rupture takes place more readily.

The deposited polymer film therefore contains all of the types of crosslinks in various ratios. Some of the peroxide crosslinks may rupture when the film is dried; some, however, survive this operation and the rupture of C—O—O—C bonds continues in the column. The polymer film is relatively firmly fixed on the support at a number of points. In contact with the elution mixture it swells, its volume increases, and thus some of the weaker bonds are mechanically strained and finally broken. Additional cleavage may occur during passage of the polymer through the capillary of the column.^{22,23} Peroxide bond rupture decreases the molecular weight. Crosslinking and branching through C—C or C—O—C bonds on the other hand, increase the high molecular weight fraction.

Low molecular weight fractions, therefore, have an increased content of C=O groups formed by oxidative degradation reactions before fractionation begins and by mechanical rupture of peroxide groups in the first fractionation cuts. In later fractions the content of C=O groups decreases. Structures having a considerable amount of peroxide crosslinks behave, up to their dissolution, like very high molecular weight molecules, and they therefore dissolve last. On passage through the capillary medium of the column they disintegrate to low molecular weight fragments, with C=O groups being formed at the same time. In the last fractions, therefore, a sudden decrease of molecular weight and increase of C=O content is observed. The other modes of crosslinking [eqs. (4) and (5)] result in a variation of the slope of the dependence $\eta_{sp}/c \rightarrow \eta_{sp}$.

Influence of C—O—O—C Bonds on the Decrease of the Limiting Viscosity Number of the Last Fractions

As shown in Figure 1 and Table III, the decrease of the limiting viscosity number of the last fraction and sometimes also of the penultimate fraction occurred even when the fractionation of Neoprene WRT was carried out in the absence of the oxygen, indicating that the sample contained peroxide crosslinks formed before preparation of the film. The last fraction includes, however, only about 1.5% of the total initial amount, and therefore the limiting viscosity number calculated from fractionation data by means of Philipoff's relationship²⁴ is practically the same as the limiting viscosity number of the unfractionated sample. In other deliberately oxidized Neoprene WRT samples, the anomalies were more pronounced. At the same time, a decrease in the value of the limiting viscosity number calculated from fractionation data was observed.

This anomalous course of molecular weights of the last fractions was very clearly manifested in the fractionation of *cis*-1,4-polybutadiene when all operations were carried out in the presence of air (Fig. 3 and Table VII). In the fractionation of 3,4-polyisoprene (Fig. 2 and Table VI) anomalies were also observed, not only in the last fractions but also in the first ones, although this sample had a very low average molecular weight.

Infrared analyses of the fractions show (Figs. 4 and 5) that the first fractions really have, as expected, a relatively higher content of C=O groups, characterized by the absorption band at 1740 cm^{-1} . In later fractions its content decreases. In the last fractions, for which an anomalous decrease in viscosity was observed, the content of C=O groups rises sharply, usually reaching the highest values. Figure 6 shows the variation of magnitude of the absorption band at 1740 cm^{-1} for the individual fractions during the course of fractionation.

The magnitude of the 1710 cm^{-1} band, which corresponds to a different type of C=O group, does not change with fractions of samples oxidized to a low degree. A distinct variation is observed only for fractions of strongly oxidized Neoprene WRT (experiment F and partially in experiment E) and for some polybutadiene fractions.

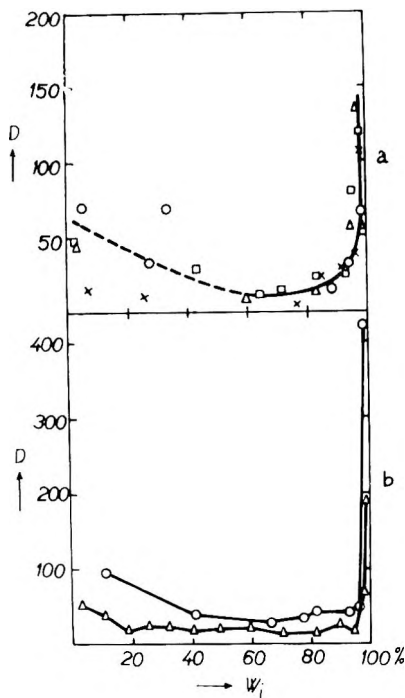


Fig. 6. Dependence of the density of the absorption band 1740 cm.^{-1} on the cumulative weight of the fractions: (a) Neoprene WRT, (\times) experiment C, (Δ) experiment D, (\square) experiment E, (\circ) experiment F; (b) (Δ) 3,4-polyisoprene, (\circ) *cis*-1,4-polybutadiene.

In terminal fractions having decreased molecular weights we have usually found a lower double bond content (bands at 1665 or 1645 cm.^{-1}) and an increased content of CH_3 endgroups (band at 1385 cm.^{-1}), which is in agreement with the higher concentration of degraded polymer in this fraction.

In 3,4-polyisoprene, which according to infrared analysis contained over 95% of 3,4 structure, an increased content of the 1,4 structure was found in the last two fractions (absorption bands at 572 , 840 , and 1130 cm.^{-1}). From this it may be assumed that 1,4-polyisoprene units are oxidized more readily than 3,4-polyisoprene units.

The explanation of the anomalous decrease of molecular weights based on the presence of peroxide bonds in the polymer is corroborated by the fact that in fractions of strongly oxidized Neoprene WRT (experiment F) absorption bands appear at 1785 cm.^{-1} and to a lesser degree at 1815 cm.^{-1} (Fig. 5). It has been shown by using dilauroyl peroxide as a model compound that these bonds correspond to $\text{C}=\text{O}$ groups in acyl peroxides. In this experiment we observed an anomalous decrease of molecular weight in a low molecular weight fraction also (see Table V), this fraction having the most intensive absorption at 1785 cm.^{-1} , and a high content of $\text{C}=\text{O}$ groups characterized by the 1710 cm.^{-1} absorption band.

Our explanation of the anomalous decrease of the molecular weight of the last fractions obtained by column fractionation methods is further supported by an observation made during the fractionation of an artificially aged polychloroprene by means of successive precipitations.¹⁸ The first, i.e., highest molecular weight, fraction was only partially soluble after precipitation. The reduced viscosity of a small, benzene-soluble portion, decreased during the course of the viscosity measurement, decreasing in 48 hr. from a value of 3.50 to a value of 2.84 dl./g. (at a concentration of 0.413 g./100 ml.), and continued to decrease after 48 hr. The next fraction showed a similar decrease of viscosity with time. It has been found by means of infrared spectroscopy that these fractions had a high content of C=O groups. This effect has been discussed previously.^{25,26}

Influence of C—C and C—O—C Crosslinks

Some crosslinks of this type are necessarily formed in chemical reactions involving oxidative degradation. Under the given conditions the amount of these crosslinks increases with increasing content of C=O bonds. Whereas in the case of polychloroprene the value of the limiting viscosity number calculated from fractionation data decreased considerably, this was not the case with polybutadiene. The limiting viscosity number of polybutadiene calculated for the fractions has a lower value than would correspond to an unfractionated sample, but with respect to the distinct anomalous decrease of the molecular weight of the last fractions, this difference is less than expected (3.14 for unfractionated sample, 3.014 calculated from fractions). This observation corresponds qualitatively to the results of Cooper, Vaughan, and Yardley.¹² In the case of polybutadiene, crosslinking by means of C—C or C—O—C bridges probably takes place to a greater extent than in the case of polychloroprene, and thus the value of the limiting viscosity number calculated from fractionation data may increase again. Another possible explanation is that in this case the rupture of the C—C bonds of the main chain takes place less frequently in the reaction of the polymer with oxygen. The results obtained do not yet permit a more precise explanation of the effect observed.

In addition to an influence on the limiting viscosity number calculated from fractionation data, the formation of branched or crosslinked structures also influences the value of the quantity k' in the Schulz-Blaschke equation. Plotting on the same set of axes the dependence of the density of the 1740 cm^{-1} absorption band and the value of the quantity $N = 1/k'$ for fractions of Neoprene WRT against their limiting viscosity number (with respect to the chronological order of the fractions), we see, that in all cases mentioned the maximum value of N is approximately identical with the density minimum of the 1740 cm^{-1} band (Fig. 7). Fractions having a low C=O group content are therefore little branched or crosslinked, and vice versa. The anomalously behaving low molecular weight fraction of Neoprene WRT (experiment F) for which a distinct absorption band was found at 1785 cm^{-1} , showing the presence of peroxides, has an unusually

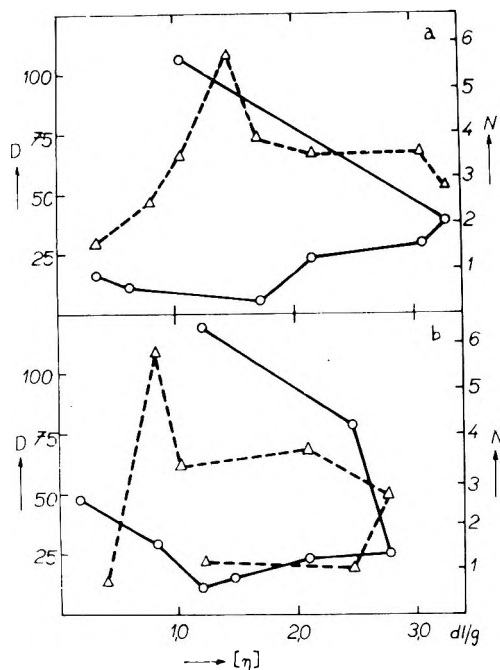


Fig. 7. Dependence of (O) the density of the 1740 cm.^{-1} and of (Δ) the value of $N = 1/k'$ of Neoprene WRT fractions on their limiting viscosity number (with respect to their chronological order): (a) experiment C; (b) experiment E.

steep dependence of $\eta_{sp}/c \rightarrow \eta_{sp}$. This is due to a high degree of branching or crosslinking, in this case, however, not only by C—C and C—O—C bonds, but also by unbroken peroxide bonds.

Influence of the Method of Preparation of the Polymer Film

We used two procedures for preparing the polymer film from solution (see Table II). As indicated in Tables III–V, in experiments A, D, and F the highest values of $[\eta]$ exceeded those in experiments B, C, and E, although, for instance, in experiment F the polymer was far more oxidized than in experiment B and about as much as in experiment E. It is therefore possible, that the mode of film preparation may have a great influence on the anomalies under discussion. Bresler et al.²⁷ found that, after evaporating a selective solvent from a styrene–isoprene block copolymer, in which the insoluble blocks form globules which are retained in solution only by the influence of soluble blocks, a coiled structure is retained for some time in the formed film. We may therefore assume that the polymer molecules in a film prepared from a solution to which a precipitant has been added till a stable weak turbidity is formed will have a shape closer to the globular one than in the case of film prepared from a solution in a good solvent. On contact with the precipitant which occurs at the beginning of the experiment in the column, the conformation of the

polymer molecules, mainly those of high molecular weight, remains nearly unchanged in the first case, whereas in the second case the molecules will tend to coil. At this stage rupture of chains may already occur in places where there is the weakest bonding. Therefore, when a polymer film is prepared after adding the precipitant to the solution before evaporation, we obtain for fractions having the highest limiting viscosity number, higher values of $[\eta]$ than if the film is prepared from a good solvent.

The results of polydiene fractionation show that the precipitation chromatography method with temperature variations of the whole column gives good results and that the method may be used to separate low molecular weight samples (in our case 3,4-polyisoprene) as well as samples with higher average viscosity number and a broader distribution of molecular weights (*cis*-1,4-polybutadiene). It is, however, necessary to work in strictly inert atmospheres in order to suppress oxidative degradation processes. When such conditions are not maintained, an undesirable decrease of the molecular weight of the last fractions will occur, and the molecular weight distribution will not represent the actual molecular weight distribution of the sample. The method of temperature variations of the whole column also permits fractionation at lower temperatures than the original method of Baker and Williams. This is another factor helpful in suppressing oxidative degradation processes.³

We thank Ing. Kálal of the College of Chemical Technology, Prague, for the polybutadiene sample.

References

1. Baker, C. A., and R. J. P. Williams, *J. Chem. Soc.*, **1956**, 2352.
2. Poláček, J., *Collection Czechoslov. Chem. Commun.*, **28**, 1838 (1963).
3. Poláček, J., *Collection Czechoslov. Chem. Commun.*, **28**, 3011 (1963).
4. Francis, P. S., R. C. Cooke, and J. H. Elliott, *J. Polymer Sci.*, **31**, 453 (1958).
5. Henry, P. M., *J. Polymer Sci.*, **36**, 3(1959).
6. Davis, T. E., and R. L. Tobias, *J. Polymer Sci.*, **50**, 227 (1961).
7. Schneider, N. S., J. D. Loconti, and L. G. Holmes, *J. Appl. Polymer Sci.*, **3**, 251 (1960); *ibid.*, **5**, 354 (1961).
8. Weakley, T. J., R. J. P. Williams, and J. D. Wilson, *J. Chem. Soc.*, **1960**, 3963.
9. Jungnickel, J. L., and F. T. Weiss, *J. Polymer Sci.*, **49**, 437 (1961).
10. Hall, R. W., in *Techniques of Polymer Characterization*, P. W. Allen, Ed., Butterworths, London, 1959.
11. Cooper, W., G. Vaughan, D. E. Eaves, and R. W. Madden, *J. Polymer Sci.*, **50**, 159 (1961).
12. Cooper, W., G. Vaughan, and J. Yardley, *J. Polymer Sci.*, **59**, S2 (1962).
13. Hulme, J. M., and L. A. McLeod, *Polymer*, **3**, 153 (1962).
14. Štolka, M., J. Vodehnal, and I. Kössler, *Collection Czechoslov. Chem. Commun.*, **28**, 1535 (1963).
15. Schulz, G. V., and F. Blaschke, *J. Prakt. Chem.*, **158**, 130 (1941).
16. Poláček, J., *J. Polymer Sci.*, **39**, 469 (1959).
17. Vodehnal, J., and I. Kössler, *Collection Czechoslov. Chem. Commun.*, **24**, 2428 (1964).
18. Poláček, J., *Collection Czechoslov. Chem. Commun.*, **25**, 2103 (1960).
19. Poláček, J., and B. Matyska, *Collection Czechoslov. Chem. Commun.*, **27**, 816 (1962).

20. Grassie, N., *Chemistry of High Polymer Degradation Processes*, Butterworths, London, 1956.

21. Emanuel, N. M., and D. G. Knorre, *Kurs khimicheskoi kinetiki*, Gosudarstvennoe Izdatel'stvo Vysshaya. Shkola, Moscow, 1962.

22. Morris, W. J., and R. Schnurmann, *Nature*, **160**, 674 (1947).

23. Bestul, A. B., and H. V. Belcher, *J. Appl. Phys.*, **24**, 1011 (1953).

24. Mussa, I. V. C., *J. Polymer Sci.*, **28**, 587 (1958).

25. Kössler, I., B. Matyska, and J. Poláček, *J. Polymer Sci.*, **53**, 107 (1961).

26. Kössler, I., and V. Novobilsky, *Collection Czechoslov. Chem. Commun.*, **28**, 578 (1963).

27. Bresler, S. E., L. M. Pyrkov, S. Ya. Frenkel, L. A. Laius, and S. I. Klenin, *Vysokomolekul. Soedin.*, **4**, 250 (1962).

Résumé

Le fractionnement du polychloroprène, du polyisoprène, et du polybutadiène, a été effectuée au moyen d'une technique modifiée de précipitation chromatographique suivant Baker-Williams. La diminution anormale des poids moléculaires des dernières fractions s'explique comme étant un résultat du processus d'oxydation conduisant à la formation de liaisons peroxydiques dans le polymère. On a trouvé une relation entre la teneur en groupement C=O et la valeur de la constante k' de l'équation de Schulz-Blaschke. On a démontré l'avantage de maintenir une température relativement basse pendant la précipitation et l'influence de la méthode de préparation du film de polymère sur la courbe de distribution du poids moléculaire.

Zusammenfassung

Die Fraktionierung von Polychloropren, Polyisopren, und Polybutadien wurde nach einem modifizierten chromatographischen Fällungsverfahren nach Baker-Williams durchgeführt. Die anomale Abnahme des Molekulargewichts bei den letzten Fraktionen lässt sich als Ergebnis von Oxydationsprozessen, die zur Bildung von Peroxybindungen im Polymeren führen, erklären. Eine Korrelation zwischen dem C=O-Gruppengehalt und dem Wert der Konstanten k' der Schulz-Blaschke-Gleichung wurde gefunden. Es ist vorteilhaft, während des Fällungsprozesses eine verhältnismässig niedrige Temperatur einzuhalten; der Einfluss der Darstellungsmethode des Polymerfilms auf die Molekulargewichtsverteilungskurve konnte nachgewiesen werden.

Received December 15, 1964

Prod. No. 4626A

Semiquantitative Aspect of Short Branch Detection by Using Polyelectrolyte Expansive Effects

W. M. PASIKA* and L. H. CRAGG†, *Department of Chemistry,
University of Alberta, Edmonton, Canada*

Synopsis

Linear and branched dextran polyelectrolyte reduced viscosity-concentration curves, obtained by employing a solvent which contained a low concentration of simple electrolyte, were characterized by means of a set of relative expansion ratios, R_{ncm} . The sets of R_{ncm} for branched and linear dextran polyelectrolyte samples of identical degree of substitution, whose reduced viscosity-concentration curves were determined in the same solvent, did not differ. This is interpreted as indicating that the same expansive mechanism operated in the linear and branched polyelectrolyte systems when they were diluted. Plots of R_{ncm} versus absolute concentration for linear and branched polyelectrolyte samples (of identical degrees of substitution, of different degrees of substitution and whose reduced viscosities were determined in solvents of different simple electrolyte concentrations) gave straight lines with a common intercept on the ordinate axis but with different slopes. It is suggested that the slope factor or p values of these lines might be employed as a means of detecting and measuring short branching in polymers convertible to polyelectrolytes.

Introduction

The viscometric method,¹ which has been extensively employed for the detection and estimation of branching in high polymeric compounds, is insensitive to short branches in low molecular weight (<100,000) polymer samples. Recently we have demonstrated^{2,3} that low molecular weight (<100,000) linear and branched dextran samples which exhibited small differences in viscosity behavior, when converted into polyelectrolytes, exhibited very marked differences in viscosity behavior. These differences were shown qualitatively to be due to the difference in the number of short branches existing between the two samples and did not arise as an artifact of the experimental technique.³ We now report on the semiquantitative aspect of using polyelectrolyte expansive effects to detect short branches in our model system—dextran.

Experimental

Preparation of the potassium dextran sulfate and the potassium carboxymethyl dextran samples was described previously.^{2,3} Only the curves for linear and branched dextran sulfate of identical degree of substitution

* Present address: Donnan Laboratories, University of Liverpool, England.

† Present address: Mount Allison University, Sackville, New Brunswick, Canada.

are reproduced here (Fig. 1) to facilitate discussion, since the data used in the present analyses have been recorded previously.^{2,3}

Results and Discussion

In order that the polyelectrolyte expansive effect be useful in the detection of branching in low molecular weight polymer samples it is desirable to isolate specifically some effect that branching has on the polyelectrolyte reduced viscosity-concentration curves and, if possible, to assign numerical values to this effect. Implicit in this is the need to correct for such factors as molecular weight, degree of substitution, and ionic strength of solvent.

One means of comparing polyelectrolyte reduced viscosity-concentration curves would be with the aid of a parameter dependent upon the expansion of the polyelectrolyte macromolecules as their solutions are diluted. Such a parameter can be obtained by taking the ratio of the maximum reduced viscosity $(\eta_{sp}/c)_{c_m}$, to the reduced viscosity at a concentration which is some multiple n of c_m , the concentration at which the maximum reduced viscosity occurs. This relative expansion ratio R_{nc_m} is, therefore, defined as

$$R_{nc_m} = (\eta_{sp}/c)_{c_m} / (\eta_{sp}/c)_{nc_m}$$

where $n = 2, 3, 4$, etc. Relative expansion ratios for a number of dextran polyelectrolytes are given in Table I. Close examination reveals some interesting relationships between the R_{nc_m} values of the polyelectrolyte reduced viscosity-concentration curves and the factors that affect them: R_{nc_m} is independent of molecular weight (compare samples a, b, c); R_{nc_m} increases with decreasing ionic strength of solvent (compare samples d and f, e, and g); R_{nc_m} decreases with increasing degree of substitution (compare samples a and i, d and h); R_{nc_m} is independent of branching (compare samples d and e, f and g).

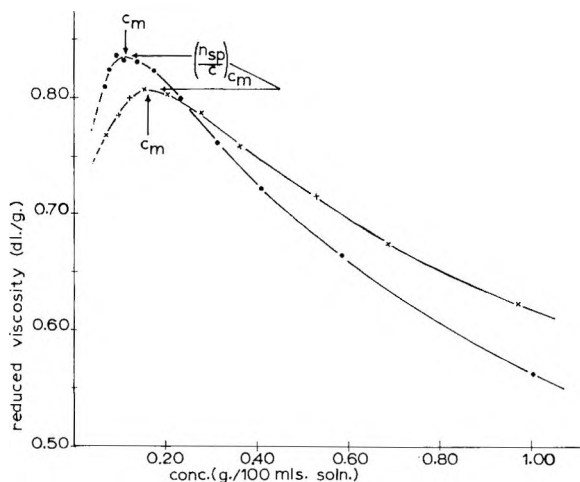


Fig. 1. Reduced viscosity-concentration curves of branched and linear potassium dextran sulfate samples (from dextran fractions of similar $[\eta]$) in aqueous 0.001*N* KCl: (×) branched (D.S. = 0.68); (●) linear (D.S. = 0.69).

TABLE I
Relative Expansion Ratios R_{ncm} for a Number of Linear and
Branched Polyelectrolyte Samples

| Sample no. | Sample (potassium salt) | Relative concentration | Absolute concentration, g./dl. | R_{ncm} |
|------------|--|------------------------|--------------------------------|-----------|
| a | Linear carboxymethyl dextran (D.S. 0.82); mol. wt. 73,100; 0.001 <i>N</i> KCl | $2c_m$ | 0.200 | 1.09 |
| | | $3c_m$ | 0.300 | 1.19 |
| | | $4c_m$ | 0.400 | 1.30 |
| | | $5c_m$ | 0.500 | 1.40 |
| b | Linear carboxymethyl dextran (D.S. 0.80); mol. wt. 119,400; 0.001 <i>N</i> KCl | $2c_m$ | 0.200 | 1.09 |
| | | $3c_m$ | 0.300 | 1.20 |
| | | $4c_m$ | 0.400 | 1.32 |
| | | $5c_m$ | 0.500 | 1.43 |
| c | Linear carboxymethyl dextran (D.S. 0.82); mol. wt. 135,000; 0.001 <i>N</i> KCl | $2c_m$ | 0.200 | 1.08 |
| | | $3c_m$ | 0.300 | 1.20 |
| | | $4c_m$ | 0.400 | 1.31 |
| | | $5c_m$ | 0.500 | 1.43 |
| d | Linear dextran sulfate (D.S. 0.69); 0.001 <i>N</i> KCl | $2c_m$ | 0.226 | 1.05 |
| | | $3c_m$ | 0.339 | 1.13 |
| | | $4c_m$ | 0.452 | 1.18 |
| | | $5c_m$ | 0.565 | 1.26 |
| e | Branched dextran sulfate, (D.S. 0.68); 0.001 <i>N</i> KCl | $2c_m$ | 0.330 | 1.05 |
| | | $3c_m$ | 0.495 | 1.12 |
| | | $4c_m$ | 0.660 | 1.19 |
| | | $5c_m$ | 0.835 | 1.26 |
| f | Linear dextran sulfate (D.S. 0.69); 0.0005 <i>N</i> KCl | $2c_m$ | 0.107 | 1.07 |
| | | $3c_m$ | 0.255 | 1.15 |
| | | $4c_m$ | 0.340 | 1.22 |
| | | $5c_m$ | 0.445 | 1.31 |
| g | Branched dextran sulfate (D.S. 0.68); 0.0005 <i>N</i> KCl | $2c_m$ | 0.120 | 1.07 |
| | | $3c_m$ | 0.180 | 1.12 |
| | | $4c_m$ | 0.240 | 1.24 |
| | | $5c_m$ | 0.300 | 1.31 |
| h | Linear dextran sulfate (D.S. 0.91); 0.001 <i>N</i> KCl | $2c_m$ | 0.130 | 1.02 |
| | | $3c_m$ | 0.195 | 1.06 |
| | | $4c_m$ | 0.260 | 1.11 |
| | | $5c_m$ | 0.325 | 1.16 |
| i | Linear carboxymethyl dextran (D.S. 1.22); 0.001 <i>N</i> KCl | $2c_m$ | 0.200 | 1.06 |
| | | $3c_m$ | 0.300 | 1.14 |
| | | $4c_m$ | 0.400 | 1.22 |
| | | $5c_m$ | 0.500 | 1.29 |
| j | Branched carboxymethyl dex- tran (D.S. 1.14); 0.001 <i>N</i> KCl | $2c_m$ | 0.364 | 1.04 |
| | | $3c_m$ | 0.546 | 1.11 |
| | | $4c_m$ | 0.728 | 1.18 |
| | | $5c_m$ | 0.910 | 1.24 |

The invariance of R_{ncm} at identical or near-identical degree of substitution for either the linear and branched dextran sulfate or carboxymethyl dextran samples suggests a basic similarity in the molecular expansions which can be made more evident by plotting η_{sp}/c against a concentration

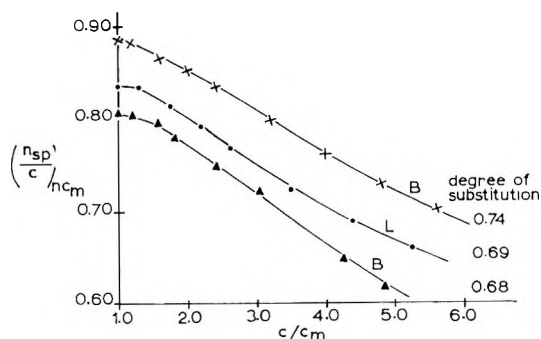


Fig. 2. Plot of reduced viscosity vs. reduced concentration c/c_m for linear (L) and branched (B) potassium dextran sulfate samples in 0.001N KCl.

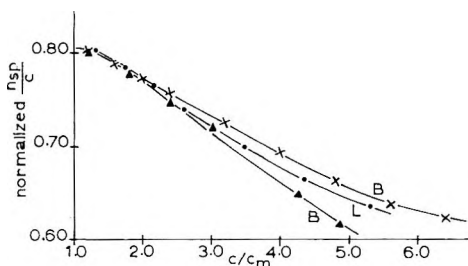


Fig. 3. Curves of Fig. 2 normalized by the application of a factor equal to the appropriate ratio of the maximum reduced viscosities: (\times) branched (D.S. = 0.74); linear (D.S. = 0.69); (\blacktriangle) branched (D.S. = 0.68).

suitably reduced, that is, against a concentration expressed as a function of c_m . Accordingly, in Figure 2 η_{sp}/c is plotted against c/c_m for linear and branched dextran sulfates of the same degree of sulfation (0.68 and 0.69). In the same figure is plotted the curve for dextran sulfate of higher degree of sulfation (0.74). This curve is nearly parallel to the others. However, if an attempt is made to make these three curves coincide by multiplying values of η_{sp}/c by the appropriate ratio of the $(\eta_{sp}/c)_{c_m}$ values,³ the results shown in Figure 3 are obtained. The curves coincide at values of c/c_m close to unity where normalization was effected but steadily diverge as c/c_m increases.

This near identity of the doubly reduced curves for linear and branched species indicates that the nature of the expansion of branched molecules with dilution is the same as that of linear molecules. The differences are in the "rate" of expansion with dilution.

The relative expansion ratio R_{nc_m} does not, therefore, reveal differences in branching. Any parameter that does so should relate expansion to absolute concentration changes rather than relative ones. Such a parameter was obtained by plotting R_{nc_m} for different values of n , i.e., at different concentrations $2c_m$, $3c_m$, $4c_m$, etc., against these concentrations expressed in

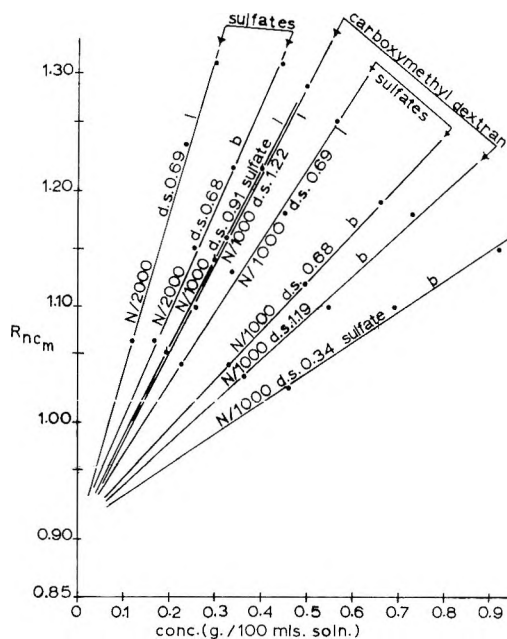


Fig. 4. Plots of the relative expansion ratio R_{ncm} vs. absolute concentration for various potassium dextran sulfate and potassium carboxymethyl dextran samples. Solvent was aqueous KCl (0.001*N* and 0.0005*N*).

absolute rather than relative units. Such plots are shown in Figure 4. All gave straight lines which satisfy the equation

$$R_{ncm} = 0.91 + pc \quad (1)$$

The significant parameter in the eq. (1) is p . Values of this slope factor for the different polyelectrolyte samples are listed in Table II. With the dextran sulfates it increases with increasing degree of substitution (samples d and e, f and g), but with the carboxymethyl dextrans it decreases with increasing degree of substitution (samples c and j). It increases with decreasing ionic strength of the solvent (samples d and h, g and i) and decreases very markedly with degree of branching (samples d and g, h and i, j and k).

The slope factor p has the advantage that it magnifies effects and permits quantitative comparisons which, though rough, are nevertheless interesting and suggest that the p factor has potential in the analysis of reduced viscosity-concentration curves obtained with the constant and simple salt dilution technique. For example, the ratio of p values for the linear dextran sulfate sample (D.S. 0.69) in 0.001*N* KCl and 0.0005*N* KCl is $0.65/1.30 = 0.50$, and for the branched dextran sulfate sample this ratio is $0.41/0.88 = 0.47$. The same change in ionic strength produced substantially the same relative change in p with the two different samples. An alternate comparison to show this fact can be obtained from the ratio of the p values for branched

TABLE II
Influence of Various Factors on the Slope Factor p

| Sample no. | Sample (potassium salt) | Degree of substitution | Solvent H ₂ O-KCl, N | p |
|------------|---|------------------------|-----------------------------------|------|
| a | Carboxymethyl dextran (linear); mol. wt. 135,000 | 0.82 | 0.001 | 1.09 |
| b | Carboxymethyl dextran (linear); mol. wt. 119,400 | 0.80 | 0.001 | 1.09 |
| c | Carboxymethyl dextran (linear); mol. wt. 73,100 | 0.82 | 0.001 | 1.09 |
| d | Linear dextran sulfate | 0.69 | 0.001 | 0.65 |
| e | Linear dextran sulfate | 0.91 | 0.001 | 0.82 |
| f | Branched dextran sulfate | 0.34 | 0.001 | 0.26 |
| g | Branched dextran sulfate | 0.68 | 0.001 | 0.41 |
| h | Linear dextran sulfate | 0.69 | 0.0005 | 1.30 |
| i | Branched dextran sulfate | 0.68 | 0.0005 | 0.88 |
| j | Linear carboxymethyl dextran | 1.22 | 0.001 | 0.77 |
| k | Branched carboxymethyl dextran | 1.14 | 0.001 | 0.37 |

and linear dextran sulfates; $0.41/0.65 = 0.63$ in $0.001N$ KCl and $0.88/1.30 = 0.68$ in $0.0005N$ KCl. Within the precision of the measurement, these ratios may be said to be the same and to indicate the ease with which solvent ionic strength calculations can be made if needed.

Molecular weight does not influence the p values (compare samples a, b, c of Table II).

The relationship between degree of substitution and p values is much more complicated and at present cannot be resolved simply. Nevertheless, some interesting observations can be made on this interdependence. The ratio of the degree of substitution of sample e (D.S. = 0.91) to that of sample d (D.S. = 0.69) of Table II is $0.91/0.69 = 1.31$ and the ratio of the p value of sample e to that of sample d is $0.82/0.65 = 1.26$. A similar comparison of ratios for sample g (D.S. = 0.68) and sample f (D.S. = 0.34) shows more of a difference between the ratios. The ratio of the degrees of substitution is $0.68/0.34 = 2.0$ and that of the p values $0.41/0.26 = 1.6$. However, with the highly substituted potassium carboxymethyl dextrans, whose p values run contrary to the trend of the p values of the potassium dextran sulfates, there exists an inverse linear relationship with respect to degree of substitution. The product of the degree of substitution and p value of sample a is $(0.82)(1.09) = 0.89$ and that of sample j is $(1.22)(0.77) = 0.94$. It would appear from these results that at high degrees of substitution (≤ 0.5) linear relationships between p values and degree of substitution might exist and that, in fact, simple corrections to p values concerning degree of substitution could be made.

Apart from the slope factor having potential in the detection of short branching in low molecular weight polyelectrolytes, it should be a useful experimental parameter as well in the more general theoretical calculations

and analysis of the types of polyelectrolyte curves we have been considering.

We are grateful to the Defence Research Board of Canada for financial assistance in the form of a research grant.

References

1. Thurmond, C. D., and B. H. Zimm, *J. Polymer Sci.*, **8**, 477 (1952).
2. Pasika, W. M., and L. H. Cragg, *J. Polymer Sci.*, **57**, 301 (1962).
3. Pasika, W. M., and L. H. Cragg, *J. Polymer Sci.*, **A3**, 1391 (1965).

Résumé

Les courbes de la viscosité réduite en fonction de la concentration pour le dextrane linéaire et ramifié, qui est un polyélectrolyte, ont été obtenues en employant un solvant contenant une faible concentration en électrolyte simple. Ces courbes ont été caractérisées au moyen d'une série de rapports d'extension relative, R_{ncm} . Les séries de rapports R_{ncm} pour les échantillons de dextrane linéaire et ramifié possédant le même degré de substitution et dont les courbes de viscosité réduite en fonction de la concentration ont été déterminées dans le même solvant, ne diffèrent pas. Cela indique que le même mécanisme d'extension se produit dans les systèmes de polyélectrolytes linéaires et ramifiés lorsqu'on les dilue. Les diagrammes de R_{ncm} en fonction de la concentration absolue (g/dl) pour des échantillons de polyélectrolytes linéaires et ramifiés possédant les mêmes degrés de substitution, des degrés de substitution différents et dont les viscosités réduites ont été déterminées dans des solvants contenant des concentrations différentes en électrolyte simple, donnent des lignes droites, possédant une même intersection à l'axe des ordonnées mais de pentes différentes. On suggère d'employer ce facteur de pente ou les valeurs de p de ces lignes pour détecter et mesurer une courte ramification dans les polymères convertissables en polyélectrolytes.

Zusammenfassung

Die Kurven reduzierte Viskosität gegen Konzentration für linearen und verzweigten Dextranpolyelektrolyten, die durch Verwendung eines Lösungsmittels mit einer niedrigen Konzentration an einfachen Elektrolyten erhalten wurden, konnten durch einen Satz relativer Expansionsverhältnisse R_{ncm} charakterisiert werden. Der R_{ncm} -Satz unterschied sich nicht für lineare und verzweigte Dextranpolyelektrolytproben mit identischem Substitutionsgrad, deren reduzierte Viskosität-Konzentrationskurven im gleichen Lösungsmittel bestimmt wurden. Das scheint zu zeigen, dass bei der Verdünnung linearer und verzweigter Polyelektrolytsysteme der gleiche Expansionsmechanismus wirksam ist. Die Auftragung von R_{ncm} gegen die absolute Konzentration (g/dl) lieferte für lineare und verzweigte Polyelektrolytproben (mit identischem Substitutionsgrad, mit verschiedenem Substitutionsgrad und bei Bestimmung der reduzierten Viskosität in Lösungsmitteln mit verschiedener Konzentration an einfachen Elektrolyten) gerade mit einem gemeinsamen Ordinatenabschnitt, aber mit verschiedener Steigung. Es wird vorgeschlagen, die Steigungsfaktoren oder p -Werte dieser Geraden zur Bestimmung der Kurzkettenverzweigung bei Polymeren, die in Polyelektrolyte umgewandelt werden können, zu verwenden.

Received December 23, 1964

Prod. No. 4628A

Studies in Condensed Phosphates. Part VIII. Complex Potassium Polymetaphosphates of Calcium, Zinc, and Cadmium

R. C. MEHROTRA and P. C. VYAS, *Chemical Laboratories, University of Rajasthan, Jaipur, India*

Synopsis

Derivatives with the formulas $[\text{K}_4\text{Ca}(\text{PO}_3)_6]_n$, $[\text{K}_4\text{Zn}(\text{PO}_3)_6]_n$, and $[\text{K}_4\text{Cd}(\text{PO}_3)_6]_n$ have been prepared by heating together mixtures of KH_2PO_4 , CaO , (or ZnO or CdO), and $(\text{NH}_4)_2\text{HPO}_4$ in the mole ratio of 4:1:2 at 800°C . for 1 hr. The number-average molecular weights of these derivatives have been measured by endgroup titration. Their conductance has been measured in aqueous solution of varying concentration, and their properties compared with those of Graham's salt and its complex derivatives prepared under similar conditions.

INTRODUCTION

In recent years the chemistry of polyphosphates has been the subject of extensive investigations because of the growing interest in inorganic polymers. The polyphosphates have been characterized as linear chain polymers by several investigators and a number of reviews¹⁻⁶ have appeared in the literature.

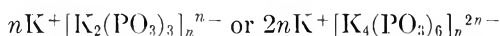
The complex-forming ability of polyphosphate chains has been reviewed by Van Wazer and Callis.⁷ Mehrotra and Gupta⁸⁻¹² prepared complex derivatives of Graham's salt with cations like Ca^{+2} , Sr^{+2} , Ba^{+2} , Zn^{+2} , Cu^{+2} , and Pb^{+2} . The properties of these derivatives with the composition $[\text{Na}_x\text{M}_{1-x/a}\text{PO}_3]_n$, where $x = 2/3$, $1/2$, or $1/3$, were similar to those of Graham's salt and were characteristic of polyelectrolytes. During their extensive investigations, latter workers also showed the existence of units of the type $n\text{Na}^+[\text{Na}_2(\text{PO}_3)_3]_n^{n-}$ or $2n\text{Na}^+[\text{Na}_4(\text{PO}_3)_6]_n^{2n-}$. These formulations were based on the observations of electrolytic studies by Wall and Dormeus¹³ and investigations of complex-forming behavior of Graham's salt with Ca^{+2} , Sr^{+2} , Ba^{+2} , Zn^{+2} , and Pb^{+2} ions by Dhar and Mehrotra.¹⁴

The potassium Karrol's salt also consists of a long chain of $(\text{PO}_3)^{n-}$ units, and its polymeric character has been established by various workers.¹⁵ It differs from Graham's salt in its insolubility and structure in the solid state.¹⁵ According to Madorsky and Clark,¹⁶ its solubility in water is less than 0.004 g./100 ml. at 25°C . Recently Ohashi et al.^{17,18} reported the solubility as 0.007-0.009 g./100 ml. at 20°C . The solubility is greatly increased in the salt solutions of alkali and alkaline earth metals.¹⁹ Mahm-

gren et al.²⁰⁻²⁴ studied the sedimentation velocity, dialysis, electrophoresis, and dilute solution viscosity of $(\text{KPO}_3)_n$ in the presence of a number of swamping electrolytes and found it to be a high molecular weight chain phosphate.

The process of dissolution of $(\text{KPO}_3)_n$ in salt solution of cations other than potassium is an ion-exchange process. Iler²⁵ has prepared its solution free of foreign anions by dissolving it in aqueous suspension of sodium-bound cation-exchange resin. Ohashi and co-workers^{17,18} observed an exchange of K^+ ion by bivalent and trivalent metal ions to the extent of 82-94% and 51.7%, respectively, in $(\text{KPO}_3)_n$ and also of sodium in sodium Kurrol's salt.

In view of the independence of the degree of dissociation and ionic mobility of the polyanion of the molecular composition and molecular weight, as borne out by the studies of Schindewolf²⁶ and Wall and Doremus,¹³ the existence of units of the type:



can be assumed for potassium polymetaphosphate also, as in the case of sodium polymetaphosphate. Gupta²⁷ has shown the existence of $\text{K}_x^+[\text{K}_y\text{Na}_z(\text{PO}_3)_{x+y+z}]^x-$ from the electrolytic conductance of the solution of sodium potassium polymetaphosphate of the composition $(\text{Na}^{2/3}\text{K}^{1/3}\text{PO}_3)_n$. It may be worthwhile to mention here that Thilo and co-workers^{28,29} have pointed out a close similarity between the ion-exchange phenomenon, exhibited by synthetic resins and complexation reactions of long-chain phosphates anions with polyvalent cations.

In view of the above observations, it was predicted that complex derivatives of composition $[\text{K}_x\text{M}_{1-x/a}\text{PO}_3]_n$ should be soluble and should have the properties of polyelectrolytes. On preparing complex derivatives of the type mentioned, the above prediction has come true. This paper describes the preparation of the derivatives $[\text{K}^{2/3}\text{M}^{1/6}(\text{PO}_3)]_n$, where M is calcium, zinc, and cadmium. The molecular weights of the derivatives have been determined by endgroup titrations.³⁰ Their conductance and molecular weights have been compared with those of the corresponding sodium derivatives.

EXPERIMENTAL

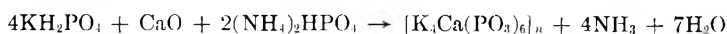
Materials and Apparatus

All reagents used were of Analar grade. Extra pure water was used for preparing the solutions. It was observed that the rate of dissolution of complex potassium polymetaphosphate derivatives is markedly more than that of the corresponding sodium derivatives. A R.L.C. Tesla bridge was employed for measuring resistances. For endgroup titrations a Cambridge pH meter having glass and calomel electrodes was employed. A Gallenkamp muffle furnace with thermostatic control to $\pm 25^\circ\text{C}$. was used for preparing samples. All the measurements were made after keeping the prepared solutions overnight in order to attain stability.⁵

Preparation of Complex Polymetaphosphates

The preparation of potassium polymetaphosphate by heating of the monopotassium orthophosphate at various temperatures for different lengths of time, has been described by a number of workers.^{21,31} Accordingly the complex polymetaphosphate derivatives have been prepared by heating a mixture of KH_2PO_4 , metal oxide, and diammonium hydrogen phosphate as follows.

A reaction mixture of 4 moles of KH_2PO_4 (K/P ratio = 0.9996),³² 1 mole of calcium oxide, and 2 moles of diammonium hydrogen phosphate in a platinum crucible was placed in a muffle furnace, and the temperature was slowly raised. Ammonia and water were slowly evolved, and after frothing had stopped the temperature was raised to 800°C ., at which it was maintained for 1 hr. The reaction could be represented as:



The product was a clear molten liquid which was chilled between cold stainless steel plates. Similar derivatives of zinc and cadmium were prepared by using stoichiometric quantities of zinc oxide and cadmium oxide in place of calcium oxide. In each case the weight of final product was found to be the same as calculated from corresponding equations. The corresponding sodium polymetaphosphate and its complex derivatives were prepared as described by Mehrotra and Gupta.⁸

Analysis

The complex polymetaphosphates were analyzed for phosphorus, as ammonium phosphomolybdate, and metals by standard procedures as described by Vogel.³³ Sodium and potassium were estimated with a Lang's flame photometer by the method of standard addition. The results of analysis are recorded in Tables I and II.

TABLE I
Analysis of Sodium Polymetaphosphate Derivatives

| Formula | Sodium, % | | Metal, % | | Phosphorus, % | |
|---|-----------|-------|----------|-------|---------------|-------|
| | Calcd. | Found | Calcd. | Found | Calcd. | Found |
| $(\text{NaPO}_3)_n$ | 21.96 | 21.82 | — | — | 30.37 | 30.35 |
| $[\text{Na}_4\text{Ca}(\text{PO}_3)_6]_n$ | 15.18 | 15.14 | 6.60 | 6.58 | 30.68 | 30.61 |
| $[\text{Na}_4\text{Zn}(\text{PO}_3)_6]_n$ | 14.54 | 14.50 | 10.36 | 10.32 | 29.46 | 29.34 |
| $[\text{Na}_4\text{Cd}(\text{PO}_3)_6]_n$ | 13.56 | 13.48 | 16.58 | 16.56 | 27.42 | 27.38 |

TABLE II
Analysis of Potassium Polymetaphosphate Derivatives

| Formula | Potassium, % | | Metal, % | | Phosphorus, % | |
|--|--------------|-------|----------|-------|---------------|-------|
| | Calcd. | Found | Calcd. | Found | Calcd. | Found |
| $[\text{K}_4\text{Ca}(\text{PO}_3)_6]_n$ | 23.33 | 23.12 | 5.98 | 5.94 | 27.72 | 27.70 |
| $[\text{K}_4\text{Zn}(\text{PO}_3)_6]_n$ | 22.49 | 22.28 | 9.40 | 9.38 | 26.73 | 26.68 |
| $[\text{K}_4\text{Cd}(\text{PO}_3)_6]_n$ | 21.07 | 21.05 | 15.10 | 14.98 | 25.05 | 25.04 |

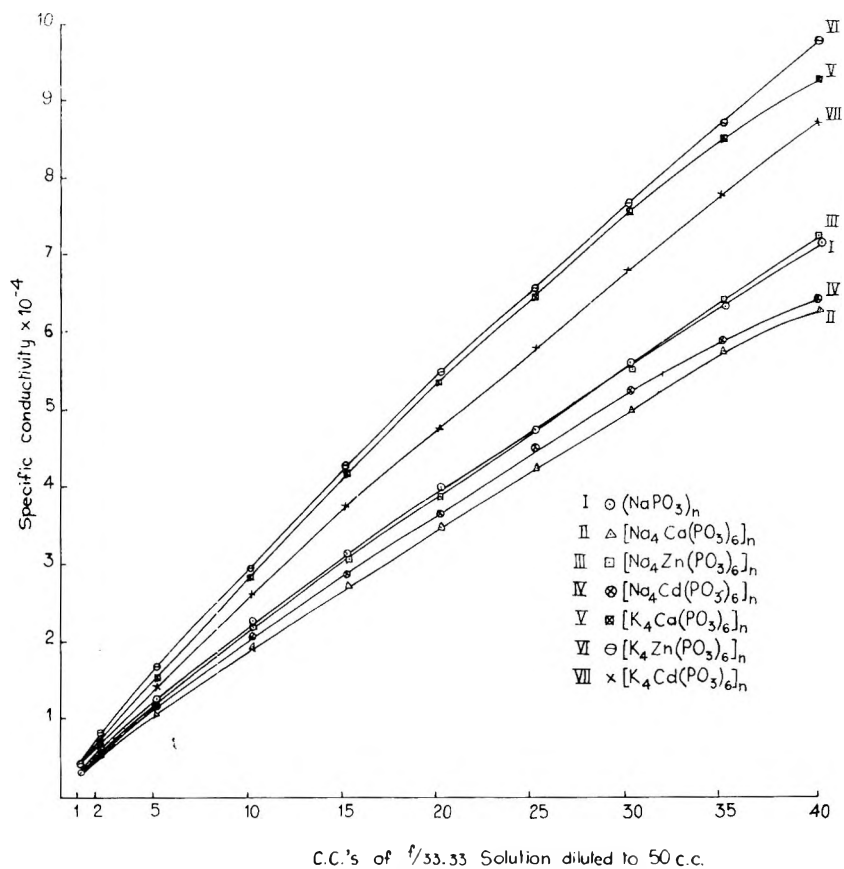


Fig. 1. Conductance of solutions.

Measurement of Molecular Weights and Conductivities

The molecular weights of the samples were determined by endgroup titrations. The values are given in Table III. The conductance of

TABLE III
Number-Average Molecular Weight of Complex Derivatives
of Sodium and Potassium Polymetaphosphates

| Formula | Number-average molecular weight \bar{M}_n |
|---|---|
| Na derivatives | |
| $(\text{NaPO}_3)_n$ | 8000 |
| $[\text{Na}_4\text{Ca}(\text{PO}_3)_6]_n$ | 5000 |
| $[\text{Na}_4\text{Zn}(\text{PO}_3)_6]_n$ | 3500 |
| $[\text{Na}_4\text{Cd}(\text{PO}_3)_6]_n$ | 5000 |
| K derivatives | |
| $[\text{K}_4\text{Ca}(\text{PO}_3)_6]_n$ | 3500 |
| $[\text{K}_4\text{Zn}(\text{PO}_3)_6]_n$ | 4000 |
| $[\text{K}_4\text{Cd}(\text{PO}_3)_6]_n$ | 4200 |

solutions of the complex polymetaphosphates of sodium and potassium and also of $(\text{NaPO}_3)_n$ are given in Table IV and Figure 1.

TABLE IV
Specific Conductivity

| Vol- ume of $f/33.33$ soln. diluted to 50 cc., cc. | Specific conductivity $\times 10^{-4}$ at $30 \pm 0.1^\circ\text{C}$. | | | | | | |
|---|--|---|---|---|--|--|--|
| | $(\text{NaPO}_3)_n$ | $[\text{Na}_4\text{Ca}(\text{PO}_3)_6]_n$ | $[\text{Na}_4\text{Zn}(\text{PO}_3)_6]_n$ | $[\text{Na}_4\text{Cd}(\text{PO}_3)_6]_n$ | $[\text{K}_4\text{Ca}(\text{PO}_3)_6]_n$ | $[\text{K}_4\text{Zn}(\text{PO}_3)_6]_n$ | $[\text{K}_4\text{Cd}(\text{PO}_3)_6]_n$ |
| 1 | 0.3555 | 0.3385 | 0.3745 | 0.3405 | 0.4322 | 0.4531 | 0.4162 |
| 2 | 0.5725 | 0.5202 | 0.6313 | 0.5792 | 0.7749 | 0.7803 | 0.6852 |
| 5 | 1.256 | 1.080 | 1.243 | 1.170 | 1.561 | 1.652 | 1.441 |
| 10 | 2.194 | 1.938 | 2.266 | 2.078 | 2.837 | 2.926 | 2.675 |
| 15 | 3.099 | 2.675 | 3.087 | 2.881 | 4.193 | 4.224 | 3.753 |
| 20 | 3.975 | 3.426 | 3.875 | 3.624 | 5.301 | 5.454 | 4.761 |
| 25 | 4.725 | 4.193 | 4.761 | 4.494 | 6.384 | 6.533 | 5.792 |
| 30 | 5.580 | 4.928 | 5.563 | 5.202 | 7.541 | 7.593 | 6.769 |
| 35 | 6.314 | 5.733 | 6.313 | 5.862 | 8.448 | 8.644 | 7.707 |
| 40 | 7.112 | 6.229 | 7.202 | 6.384 | 9.179 | 9.721 | 8.644 |

DISCUSSION

From the conductance data, the following conclusions are drawn. The plot of specific conductance against concentration is similar in nature to that reported by Davis and Monk,³⁴ Dhar and Mehrotra,¹⁴ and Mehrotra and Gupta⁸⁻¹² for sodium polymetaphosphate and its complex polymetaphosphates. The curves are also similar to those observed for other synthetic polyelectrolytes by Fuoss and Fitzgerald.³⁵

The conductance of solutions of $[\text{K}_4\text{Ca}(\text{PO}_3)_6]_n$, $[\text{K}_4\text{Zn}(\text{PO}_3)_6]_n$, and $[\text{K}_4\text{Cd}(\text{PO}_3)_6]_n$ are of the same order, indicating that the degree of dissociation and ionic mobility of polymeric anions are almost independent of molecular weights as well as composition.

The higher conductance of the solutions of complex potassium polymetaphosphates compared to the corresponding sodium derivatives can be attributed to the higher mobility of potassium in comparison to sodium ion and may also be due to stronger site bonding of sodium than of potassium ion on the anion chain.

The authors are grateful to the Council of Scientific and Industrial Research for the sanction of a school of Inorganic Polymers under the auspices of which the present work was carried out.

References

1. Terry, H., *Ann. Repts. Progr. Chem.*, **34**, 115 (1937).
2. Krabe, K., and G. Jander, *Kolloid-Bein.*, **54**, 1 (1942).
3. Quimby, O. T., *Chem. Revs.*, **40**, 141 (1947).
4. Topley, B., *Quart. Rev.*, **3**, 345 (1949).
5. Van Wazer, J. R., C. F. Callis, and P. G. Arvan, *Chem. Revs.*, **54**, 777 (1954).

6. Thilo, E., *Advan. Inorg. Radiochem.*, **4**, 1 (1962).
7. Van Wazer, J. R., C. F. Callis, *Chem. Revs.*, **58**, 1011 (1958).
8. Mehrotra, R. C., and V. S. Gupta, *J. Polymer Sci.*, **54**, 613 (1961).
9. Mehrotra, R. C., and V. S. Gupta, *J. Polymer Sci.*, **55**, 81 (1961).
10. Mehrotra, R. C., and V. S. Gupta, *Kolloid-Z.*, **184**, 1, 30 (1962).
11. Mehrotra, R. C., paper presented at International Macromolecular Conference, Montreal, July 1961.
12. Mehrotra, R. C., and V. S. Gupta, *J. Polymer Sci.*, **58**, 501 (1962).
13. Wall, F. T., and R. H. Dormeus, *J. Am. Chem. Soc.*, **76**, 868 (1954).
14. Dhar, N. R., and R. C. Mehrotra, *Proc. Natl. Inst. Sci. India*, **16**, 59 (1950); R. C. Mehrotra, Ph.D. Thesis, Allahabad University, 1948.
15. Thilo, E., *Angew. Chem.*, **64**, 510 (1952).
16. Madorsky, G. L., and K. G. Clark, *Ind. Eng. Chem.*, **32**, 244 (1940).
17. Ohashi, S., and K. Yamagishi, *Bull. Chem. Soc. Japan*, **33**, 1431 (1960).
18. Ohashi, S., and N. Takashi, *Bull. Chem. Soc. Japan*, **35**, 498 (1962).
19. Valkerding, C. C., R. Bradfield, *Soil. Sci. Soc. Am. Proc.*, **8**, 159 (1943).
20. Lamn, O., and H. Malmgren, *Z. Anorg. Allgem. Chem.*, **245**, 103 (1940).
21. Malmgren, H., and O. Lamn, *Z. Anorg. Allgem. Chem.*, **252**, 256 (1944).
22. Malmgren, H., *Acta Chem. Scand.*, **2**, 147 (1948).
23. Malmgren, H., *Acta Chem. Scand.*, **3**, 1331 (1949).
24. Malmgren, H., *Acta Chem. Scand.*, **6**, 1 (1952).
25. Iler, R. K., U. S. Pat. 2,557,109 (1951).
26. Schindewolf, U., *Z. Physik. Chem. (Frankfurt)*, **1**, 134 (1954).
27. Gupta, V. S., Ph.D. Thesis, University of Gorakhpur, India, 1962.
28. Thilo, E., A. Sorntag, and K. H. Ratty, *Z. Anorg. Allgem. Chem.*, **283**, 365 (1956).
29. Thilo, E., A. Winkler, and H. Hofsäss, *J. Prakt. Chem.*, [4] **7**, 46 (1958).
30. Gustavsson, K. H., and A. Lavsson, *Acta Chem. Scand.*, **5**, 1221 (1951).
31. Van Wazer, J. R., *Phosphorus and Its Compounds*, Interscience, New York, 1958, Vol. I, p. 666.
32. Pfanstiel, R., and R. K. Iler, *J. Am. Chem. Soc.*, **74**, 6059 (1952).
33. Vogel, A. I., *Textbook of Quantitative Analysis*, Longman-Gren London, 3rd Ed., 1961, pp. 402, 533, 495.
34. Davies, C. W., and C. B. Monk, *J. Chem. Soc.*, **1949**, 413.
35. Fuoss, R. M., and E. B. Fitzgerald, *J. Polymer Sci.*, **14**, 329 (1954).

Résumé

Des dérivés de formules $[K_4Ca(PO_3)_6]_n$, $[K_4Zn(PO_3)_6]_n$, et $[K_4Cd(PO_3)_6]_n$ ont été préparés en chauffant ensemble pendant une heure à 800°C des mélanges de KH_2PO_4 , CaO (ou ZnO, et CdO), et $(NH_4)_2HPO_4$ dans le rapport molaire 4:1:2. Les poids moléculaires moyens en nombre de ces dérivés ont été mesurés par la méthode de titration du groupement terminal. Leur conductance a été mesurée en solution aqueuse de différentes concentrations et leurs propriétés ont été comparées avec celles du sel de Graham et de ses dérivés préparés dans des conditions semblables.

Zusammenfassung

Derivate mit den Formeln $[K_4Ca(PO_3)_6]_n$, $[K_4Zn(PO_3)_6]_n$, und $[K_4Cd(PO_3)_6]_n$ wurden durch gemeinsames Erhitzen von Mischungen von KH_2PO_4 , CaO (oder ZnO und CdO), und $(NH_4)_2HPO_4$ im Molverhältnis von 4:1:2 auf 800°C während einer Stunde dargestellt. Das Zahlenmittelmolekulargewicht dieser Derivate wurde durch Endgruppentitration bestimmt. Ihre Leitfähigkeit wurde in wässriger Lösung bei verschiedenen Konzentrationen gemessen, ihre Eigenschaften mit denjenigen von Grahamsalz verglichen und dessen komplexe Derivate unter ähnlichen Bedingungen dargestellt.

Received December 28, 1964

Prod. No. 4629A

Studies on Melt Spinning. I. Fundamental Equations on the Dynamics of Melt Spinning

SUSUMU KASE and TATSUKI MATSUO, *Toyo Spinning Co., Ltd., Osaka, Japan*

Synopsis

The dynamics of melt spinning was analyzed by deriving a set of simultaneous partial differential equations.

Equation of heat balance:

$$v \frac{\partial t}{\partial x} + \frac{\partial t}{\partial \tau} = - \frac{2\sqrt{\pi} h(t - t^*)}{\rho C_p \sqrt{A}}$$

Equation of force balance:

$$\frac{\partial v}{\partial x} = \frac{E}{\beta A}$$

Equation of material balance:

$$v \frac{\partial A}{\partial x} + \frac{\partial A}{\partial \tau} = - A \frac{\partial v}{\partial x}$$

In the above equations, the distance x from the spinneret and time τ are the independent variables; temperature t , local velocity v , and cross-sectional area A are the dependent variables. It is assumed that tensile viscosity β is a function of temperature t alone, and the spinning tension F is a pure time function. Steady-state ($\partial/\partial\tau = 0$) solutions of the above equations showed a fairly good agreement with the experimentally measured values of temperature $t(x)$ and thickness $A(x)$.

1. INTRODUCTION

Ziabicki^{1,2} and Andrews,³ among others, studied how a polymer melt is stretched and cooled as it travels from the spinneret to the take-up roll in melt spinning. Ziabicki experimentally measured the diameter of a molten polymer filament, plotted it against the distance from the spinneret, and derived an equation relating the gradient of the filament diameter to the spinning tension acting on the filament. Point of solidification, local tensile viscosity etc. for a given spinning condition were also derived from the measured filament diameter.

Andrews, on the other hand, introduced a set of equations which make it possible to derive the distribution of temperature along the spinning thread when the filament diameter $A(x)$ is known as a function of the distance x from the spinneret.

The authors generalized the reasoning of Ziabicki and Andrews by relating all three quantities, filament diameter, spinning tension, and temperature by a set of simultaneous partial differential equations. The steady-state solution of these equations for given spinning conditions yields filament diameter, temperature, and spinning tension as functions of distance x from the spinneret.

The theories of Ziabicki and Andrews concern only steady-state conditions. The simultaneous partial equations proposed by the authors, on the other hand, include time as the second independent variable enabling the analysis of transients in melt spinning. Transients are closely related to the weight variation in the melt spun yarns.

Included in the present study are simultaneous partial equations consisting of the force balance equation, the heat balance equation and the equation of continuity. Also given are some steady state-solutions of these equations.

2. FORMULATION OF SIMULTANEOUS PARTIAL DIFFERENTIAL EQUATIONS

Partial Differential Equations (with a Few Simplifying Assumptions)

In introducing the partial differential equations we first make several assumptions as listed below: (1) the molten polymer filament is circular in cross section; (2) temperature is uniform across a particular cross section; (3) heat conduction in the longitudinal direction (x -direction) is negligible; (4) tensile viscosity β of the molten filament is dependent on local temperature t alone; (5) Elastic elongation of the filament is negligible in comparison to viscous flow (Fig. 1).

Additional assumptions will be made subsequently to eliminate those terms not significant in actual melt spinning.

Equation of Heat Balance: When a segment of unit length of the molten polymer filament is cooled by Δt degrees in $\Delta\tau$ seconds as the segment runs downwards, the equation of heat balance with respect to the segment is

$$-2\pi R h(t - t^*)\Delta\tau - 2\pi R \sigma \epsilon(t^4 - t^{*4})\Delta\tau = \pi R^2 \rho C_p \Delta t$$

where R is the local radius of the polymer filament, h is the coefficient of heat transfer at the filament surface, t is local temperature of the filament, t^* is temperature of ambient air, τ is time, σ is the Stefan-Boltzmann constant, ϵ is emissivity, ρ is the density of the polymer filament, and C_p is the isobaric specific heat of the molten filament.

Then, with

$$\lim_{\Delta\tau \rightarrow 0} \left(\frac{\Delta t}{\Delta\tau} \right) = \frac{Dt}{D\tau} = \frac{\partial t}{\partial \tau} + v \frac{\partial t}{\partial x}$$

we have

$$-2h(t - t^*) - 2\sigma\epsilon(t^4 - t^{*4}) = C_p \rho R \left(\frac{\partial t}{\partial \tau} + v \frac{\partial t}{\partial x} \right) \quad (1)$$

The first and second terms in the left-hand side of eq. (1), respectively, denote the convective and the radiant heat loss from the filament surface.

Equation of Force Balance. Tension F acting on the filament at point x is

$$F = F_w - G(v_w - v) + \int_x^{x_w} \rho A g dx \quad (2)$$

where

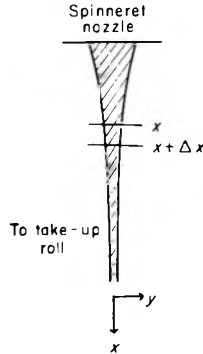


Fig. 1. Schematic diagram of melt spinning. Coordinates x and y .

x_w is the distance from the spinneret to the take-up roll, F_w is spinning tension at the take-up roll, G is mass velocity of the polymer filament, v is the local speed of the polymer filament, and A is the cross-sectional area of the filament. The second and the third terms on the right-hand side of eq. (2) are, respectively, components of spinning tension due to acceleration and that due to gravity. Air resistance acting on the filament surface and the surface tension are not included in eq. (2), but they are so small that they can be safely neglected.

Suppose a segment of the filament Δm in length and containing a fixed weight $\Delta G = \rho \Delta m A$ of polymer is stretched as it runs downward. Since the original length is Δm the increase in length must be $[D(\Delta m)/D\tau]\Delta\tau$. The rate of elongation, therefore, is $(1/\Delta m)[D(\Delta m)/D\tau]$.

We define the apparent tensile viscosity as the ratio of tensile stress acting on the segment of polymer melt over the rate of elongation resulting from that tensile stress (Fig. 2).

$$\frac{F}{A} = \beta \frac{1}{\Delta m} \frac{D(\Delta m)}{D\tau} \quad (3a)$$

By substituting the relation $\Delta G = \rho \Delta m A$ into eq. (3a) and noting that ΔG is a constant we get

$$\frac{F}{A} = \beta \left[-\frac{1}{A} \left(\frac{\partial A}{\partial \tau} + v \frac{\partial A}{\partial x} \right) - \frac{1}{\rho} \left(\frac{\partial \rho}{\partial \tau} + v \frac{\partial \rho}{\partial x} \right) \right] \quad (3b)$$

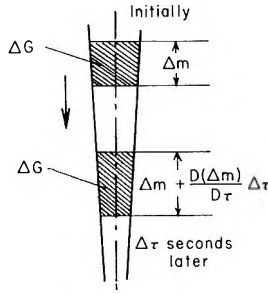


Fig. 2. Stretching of filament segment in melt spinning.

Substituting eq. (2) into eq. (3b) we get the general equation of force balance

$$F_w - G(v_w - v) + \int_x^{x_w} \rho A g dx = -\beta \left[\frac{\partial A}{\partial \tau} + v \frac{\partial A}{\partial x} + \frac{A}{\rho} \left(\frac{\partial \rho}{\partial \tau} + v \frac{\partial \rho}{\partial x} \right) \right] \tag{4}$$

If the derivatives of ρ are negligible, eq. (3b) takes the form (3c):

$$\frac{F}{A} = -\frac{\beta}{A} \left(\frac{\partial A}{\partial \tau} + v \frac{\partial A}{\partial x} \right) \tag{3c}$$

Equation of Continuity. Per unit time, polymer melt G in weight flows into the region bounded by cross sections x and $x + \Delta x$. During the same time interval, polymer $G + (\partial G/\partial x)\Delta x$ in weight flows out of the same region, resulting in a weight loss of $(\partial G/\partial x)\Delta x$ (Fig. 3).

Therefore, the equation of continuity is

$$\frac{\partial G}{\partial x} \Delta x = -\frac{\partial(A\rho)}{\partial \tau} \Delta x$$

Substituting the relation $G = \rho Av$ into the above equation we get

$$A\rho \frac{\partial v}{\partial x} + Av \frac{\partial \rho}{\partial x} + \rho v \frac{\partial A}{\partial x} = -\left(A \frac{\partial \rho}{\partial \tau} + \rho \frac{\partial A}{\partial \tau} \right) \tag{5a}$$

For a constant density ρ , eq. (5a) becomes

$$v(\partial A/\partial x) + (\partial A/\partial \tau) = -A(\partial v/\partial x) \tag{5b}$$

From eqs. (5b) and (3c) we get eq. (3d), $F/A = \beta(\partial v/\partial x)$, which shows that β is identical to the tensile viscosity as defined by other workers.

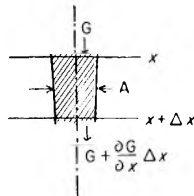


Fig. 3. Material balance for the region between x and $x \pm \Delta x$.

Partial Differential Equations (under Additional Assumptions)

Equations (1), (4), and (5a) can be simplified further by making several additional assumptions taking actual spinning conditions into consideration: (6) when the take-up speed is high as in most industrial melt spinning, the second and the third terms in the left-hand side of eq. (2) become insignificant in comparison to the first term, i.e., $F = Fw =$ a function of time τ alone; (7) derivatives of ρ in eq. (5a) are negligible in comparison to other terms; (8) the second term in the left-hand side of eq. (1), the term for radiant heat loss, is small in comparison to the first term for convective loss.

The above assumptions reduce eqs. (1), (4), and (5a) to the simultaneous partial equations (6), (7), and (8).

$$v \frac{\partial t}{\partial x} + \frac{\partial t}{\partial \tau} = \frac{2\sqrt{\pi}h(t - t^*)}{C_p \sqrt{A} \rho} \quad (6)$$

$$\partial v / \partial x = F / \beta A \quad (7)$$

$$v(\partial A / \partial x) + (\partial A / \partial \tau) = -A(\partial v / \partial x) \quad (8)$$

In steady-state conditions, the derivatives with respect to time drop out. Equation (8) then yields $G = \rho A v = \text{const.}$

Therefore, eqs. (6), and (7), become in a steady state:

$$dt/dx = (2\sqrt{\pi}/GC_p)(t^* - t)\sqrt{A}h \quad (9)$$

$$dA/dx = -(F\rho/G\beta)A \quad (10)$$

Simultaneous equations (9) and (10) can be solved analytically provided the tensile viscosity β and the coefficient h of heat transfer are given as functions of t , A , v , and x .

In eqs. (9) and (10), F appears as an unknown constant. In the final solution of the equations the value of F is determined to satisfy one of the given boundary conditions, i.e., the given take-up speed.

3. COEFFICIENT h OF HEAT TRANSFER AND POLYMER PROPERTIES ρ , C_p , AND β

Coefficient h of Heat Transfer

Numerous references are available on the coefficient h of heat transfer for gases flowing at right angles to a single cylindrical body. Many of these data are given by McAdams (Fig. 4).⁴

Coefficients of heat transfer for gases flowing outside and parallel to a cylindrical body are discussed by Simmons,⁵ and Mueller,⁶ and recently in detail by Sano and Nishikawa.⁷

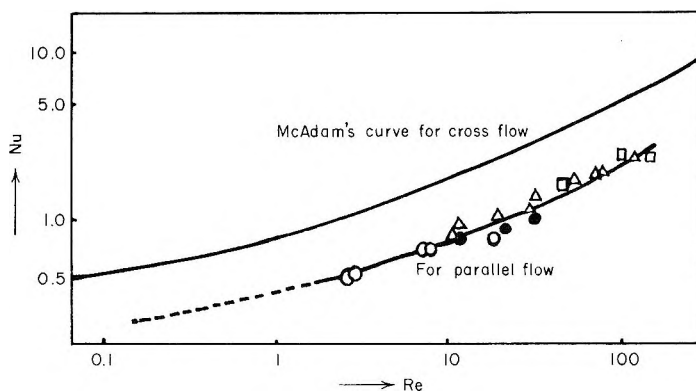


Fig. 4. Nu vs. Re in cooling by forced convection of cylindrical body; (●) data of Simmons⁵; (○) data of Mueller⁶; (△) data of Sano and Nishikawa⁷; (□) present work.

We measured h experimentally by subjecting a heated wire 0.2 mm in diameter to air flow, both parallel to the wire and at right angles to the wire, recording the cooling of the wire, the finally converting the cooling curves into Nu - Re relations (Fig. 4). Reynolds number Re is defined as $Re = 2vR/\nu_F$ and Nusselt number Nu as $Nu = 2hR/K_F$, where K_F and ν_F are heat conductivity and kinematic viscosity of ambient air, respectively. Figure 4 shows that h for parallel air flow is about half of that for cross flow. Figures 5 and 6 are the results of further experiments in which the air flow to the wire was at different angles ranging from 0° to 70° while the component of air velocity parallel to the filament axis v_x was kept constant.

In his calculation of filament temperature in melt spinning Andrews uses the relation $Nu = 0.764Re^{0.38}$ which is in close agreement with the curve for cross flow obtained in the present study (Fig. 4).

The experiments with the heated wire was an effort to simulate melt spinning, but, unlike melt spinning, the wire was kept stationary. Such differences give rise to several questions as to the validity of using Figures 4-6 in the analysis of melt spinning. (1) One possible interpretation of Figures 4-6 is to say that v_x is equal to the filament speed v and v_y is equal to the horizontal speed of the cooling air flowing into the spinning chamber. Whether this interpretation is valid is the first question.

(2) The possibility exists that the progressive thinning of the molten polymer filament in melt spinning and the accompanying increase in its speed may make Figures 4-6 not directly applicable to melt spinning. (3) In melt spinning the running surface of the filament tends to entrain a thin film of air. What effect does this air entrainment have on h ? (4) In melt spinning, filaments always exhibit a small transverse vibration. What effect does such a vibration have on h ?

The authors' interpretation of their own experimental data and the available literature on h are as follows.

In computing the coefficient h of heat transfer we use the air velocity relative to the running filament surface. The relative air velocity is as defined

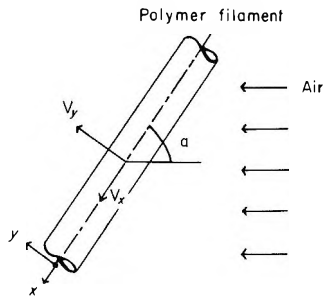


Fig. 5. Schematic diagram of x and y components of air velocity.

in question (1) above and in Figures 5. The Nu-Re curve for parallel flow as shown in Figure 4 is used as the basis of computation with the effect of transverse air velocity v_y taken into consideration by the coefficient $(1 + K)$. Reynolds number Re usually falls within the range 0.5–50 in melt spinning.

The Nu-Re relation for air flowing parallel to a cylinder is approximately

$$\text{Nu} = 0.42\text{Re}^{0.334} \quad (11)$$

within the above range of Re. Substituting the definitions of Nu and Re in eq. (11) and multiplying the right-hand side of the same equation with by the corrective coefficient $(1 + K)$ we get

$$h = 0.21k_F \sqrt{\frac{\pi}{A}} \left(\frac{2G}{\sqrt{\pi A} \rho v_F} \right)^{0.334} (1 + K) \quad (12)$$

The contribution of transverse air velocity on the coefficient K is computed with the aid of Figure 6 by equating $v_x =$ speed v of filament, and $v_y =$ transverse air velocity.

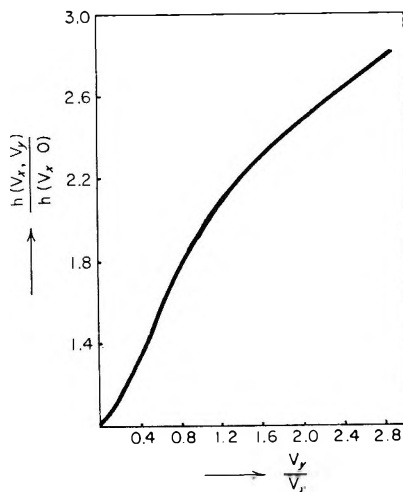


Fig. 6. Contribution of y component to the coefficient of heat transfer h .

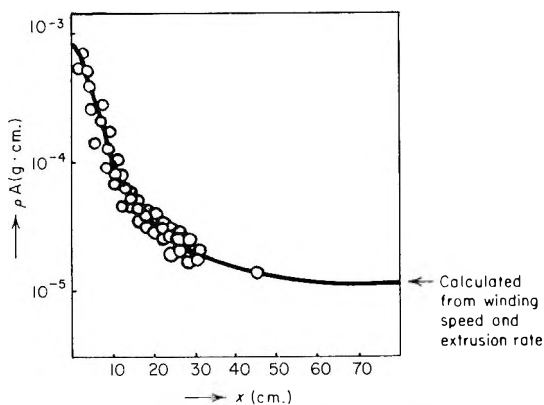


Fig. 7. Experimentally measured linear density of polymer filament vs. distance from nozzle x for copolymer of 90% poly(ethylene terephthalate) and 10% poly(ethylene isophthalate) having an intrinsic viscosity of 0.61 (in phenol-tetrachloroethane, 60/40, at 30°C.). Spinning conditions: spinneret temperature, 290°C.; take-up speed, 694 m./min; nozzle diameter, 0.3 mm.

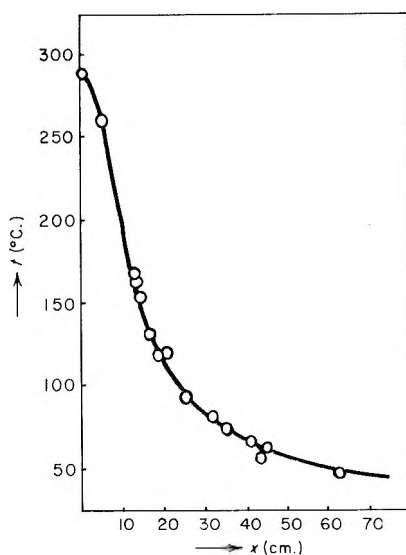


Fig. 8. Experimentally measured temperature of polyester filament vs. distance x . Spinning conditions same as in Fig. 7.

We measured the effect of filament vibration by placing a 0.2 mm. diameter wire under a parallel air flow of 20 cm./sec. and subjecting the wire to a vibration 0.3 cm. in amplitude and 4 cycles/sec. in frequency. The effect of the vibration on the coefficient h was found to be equivalent to $K = 0.3$.

Polymer Properties β , ρ , and C'_p

Ziabicki measured the cross-sectional area A of a filament experimentally, plotted A against distance x , measured spinning tension F_w , and derived by means of eq. (10) the tensile viscosity β as a function of x .

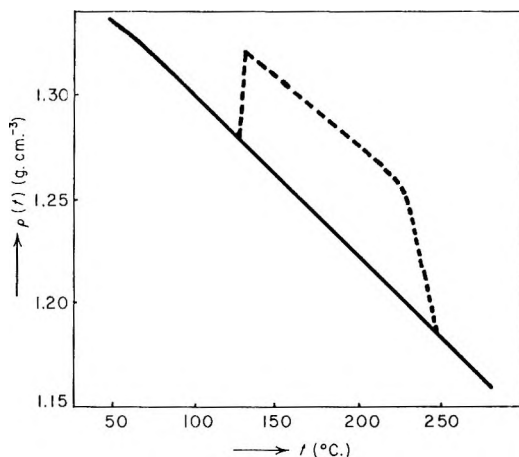


Fig. 9. Polymer density vs. temperature for copolymer of 90% poly(ethylene terephthalate) and 10% poly(ethylene isophthalate). Broken curve represents behavior when polymer is allowed to crystallize.

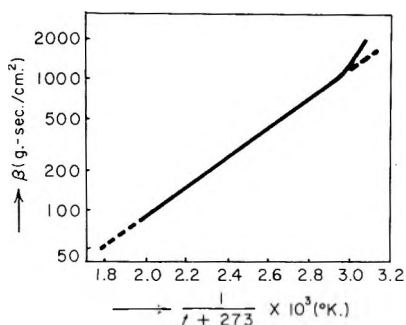


Fig. 10. Tensile viscosity of polyester filament derived from the experimental data in Figs. 7, 8, and 9. Intrinsic viscosity of polymer is 0.61 (in phenol-tetrachloroethane, 60/40, at 30°C.).

Such a β - x curve is not a unique polymer property since it is subject to changes depending on spinning conditions. Before eqs. (6), (7), (8), (9), or (10) can be solved for any spinning conditions, β must be determined. β as a polymer property is in general considered to be a function of temperature t and the rate of tensile strain dv/dx , but here we neglect the effect of dv/dx as relatively insignificant, leaving β as a function of temperature t alone.

To express β as a function of temperature t , we measured $t(x)$ and $A(x)$ experimentally. β was first expressed as a function of x by using eq. (10) in a slightly modified form:

$$\beta = -(F_w \rho / G) [d \log (\rho A) / dx] \quad (3e)$$

Then $\beta(x)$ obtained was compared against separately measured $t(x)$ to obtain the desired relation $\beta(t)$.

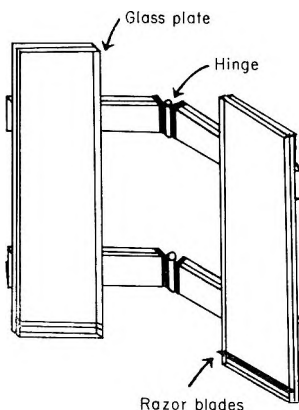


Fig. 11. Instrument for trapping molten polymer filament for measurement of linear density.

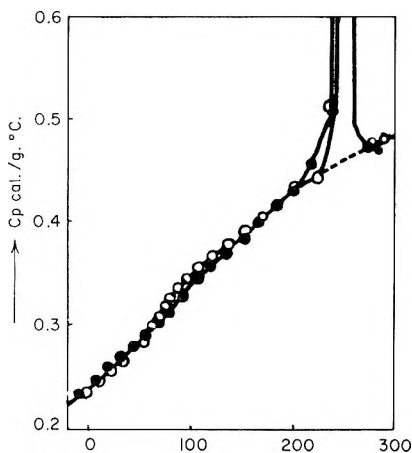


Fig. 12. Isobaric specific heat of poly(ethylene terephthalate): (O) melt-annealed Dacron; (●) pre-melt-annealed fiber.

Figures 7 and 8 show results of measuring $\rho A(x)$ and $t(x)$ for melt spinning of polyester fibers, i.e., copolymer of 90% poly(ethylene terephthalate) and 10% poly(ethylene isophthalate). $\beta(t)$ shown in Figure 10 was derived from the experimental data shown in Figures 7, 8, and 9. Figure 9 shows polymer density ρ with respect to temperature t . The solid line in Figure 9 obtains when the polymer does not exhibit appreciable crystallization, as in the industrial melt spinning of polyester fiber.

In measuring $\rho A(x)$ we used the instrument shown in Figure 11 to trap a segment of polymer melt. The molten polymer filament instantly solidified as it was trapped, leaving filament specimens ready for weighing.

The temperature t of the polymer melt was measured with a thermocouple similar to the one developed by Culpin, Madoc, and Jones.⁸

Ample literature is available on the isobaric specific heat C_p of various polymer materials. Figure 12 shows C_p for a polyester.⁹ Since polyester

develops little crystallinity in melt spinning, the sharp peak at the upper right corner of Figure 12 was neglected with the dotted curve used in place of the solid curve. The C_p shown in Figure 12 is that for 100% poly(ethylene terephthalate), but it is expected to be valid also for the 10% isophthalate copolymer now under discussion.

4. EXAMPLE SOLUTION

Substituting eq. (12) in eq. (9) and using the approximate value $k_{FVF}^{-0.334} = 1.22 \times 10^{-4}$ we get

$$\frac{dt}{dx} = 1.67 \times 10^{-4} C_p^{-1} G^{-0.666} \rho^{-0.334} (t^* - t) A^{-0.167} (1 + K) \quad (13)$$

Dividing eq. (10) by eq. (13) and integrating we get

$$F \int_t^{t_N} \frac{C_p \rho^{1.334}}{\beta(t - t^*)(1 + K)} dt = 1.00 \times 10^{-3} G^{0.334} (A^{-0.167} - A_N^{-0.167}) \quad (14a)$$

or

$$F \int_t^{t_N} \frac{C_p \rho^{1.334}}{\beta(t - t^*)} dt = +0.167 \times 10^{-3} G^{0.334} \int_A^{A_N} A^{-0.167} (1 + K) dA/A \quad (14b)$$

If K is given either as a function of t or A , eq. (14a) or (14b) can be integrated numerically, yielding A as a function of t . F , then, is determined to satisfy the given boundary conditions.

Shown in Figure 13 are polymer properties $C_p \rho^{1.334}/\beta$ and ρ/β derived from the experimental data in Figures 9, 10, and 12 and plotted against temperature t .

$A(t)$ obtained by integrating eq. (14) becomes a function of ρ/β by referring to Figure 13.

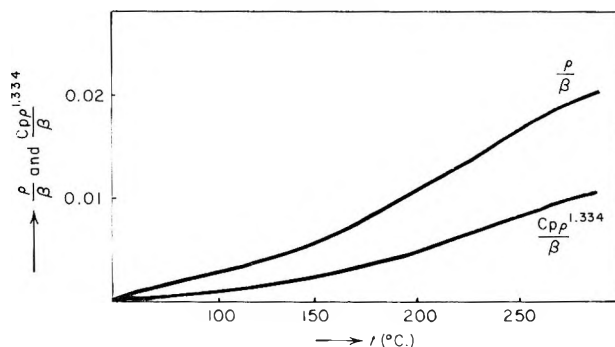


Fig. 13. ρ/β and $C_p \rho^{1.334}/\beta$ derived from Figs. 9, 10, and 12.

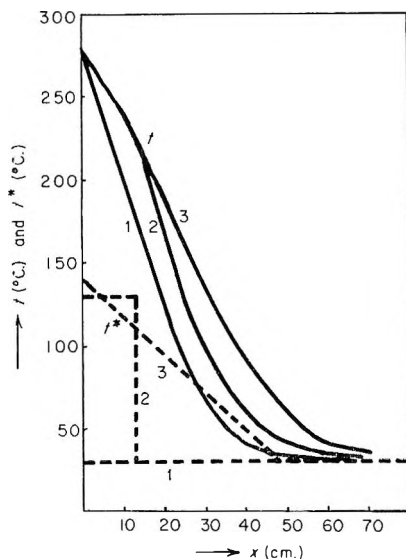


Fig. 14. Calculated temperature t of polyester filament vs. distance x under various ambient temperatures t^* : (1), (2), (3). Spinneret temperature, 280°C .; take-up speed, 600 m./min.

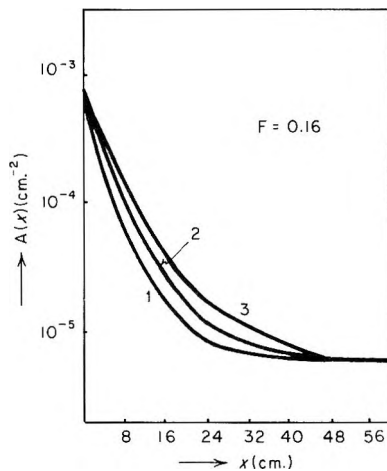


Fig. 15. Calculated cross-sectional area of polyester filament vs. distance x under various ambient temperatures: (1); (2); (3).

$A(\rho/\beta)$ then is substituted in eq. (10) and integrated to yield A as a function of x . Finally $t(x)$ is obtained by comparing $A(x)$ against $A(t)$.

Shown in Figures 14 and 15 are $A(x)$ and $t(x)$ computed for the melt spinning of the polyester copolymer shown in Figure 10 under the following conditions: spinneret temperature, 280°C .; take-up speed, 600 m./min.; nozzle diameter, 0.3 mm.; yarn denier as taken up, 7.5 den.; $K = 0$; ambient air temperature as shown in Figure 14.

While a uniform temperature across the cross section is assumed in the above calculations, the temperature differential across the filament cross section can be readily computed by referring to the table compiled by Heisler.¹⁰

The solid line in Figure 16 is identical with $t(x)$, curve (1) in Figure 14. Assuming that the solid line in Figure 16 gives the surface temperature of molten polymer filament in melt spinning, the corresponding temperature of filament core is computed with the aid of Heisler's chart as shown by the dotted line in Figure 16. Figure 16 reveals that the temperature differential between filament core and filament surface is less than 10% of that between filament surface and ambient air.

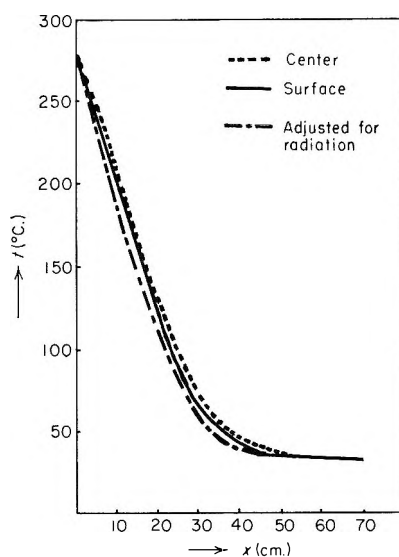


Fig. 16. Temperature differential between filament surface and filament core. Plot of t vs. x with radiant heat loss taken into consideration.

The broken line in Figure 16 is the filament temperature when the radiant heat loss is taken into consideration. Here the emissivity ϵ is assumed to be 0.9.

In computing $A(x)$ and $t(x)$ shown in Figures 14 and 15 the term $G(v_w - v)$ for acceleration and the term $\int_x^{x_w} \rho A g dx$ for gravity in eq. (2) are neglected. Values of the three terms in eq. (2) corresponding to the cross-sectional area $A(x)$ shown in Figure 14 are calculated as: $G(v_w - v) = 0.008$, $F = 0.16$, $\int_0^{x_w=500} \rho A g dx = 0.004$ at $x = 0$.

Since the first two terms in eq. (2) are much smaller in value than the third term F , it is valid to neglect them in deriving the differential equations.

We believe that the deformation of molten polymer filament in melt spinning due to elastic stretch is very slight in comparison to that due to viscous flow, since melt-spun filaments exhibit little contraction when quickly remelted.

References

1. Ziabicki, A., and K. Kedzierska, *Kolloid-Z.*, **171**, 51 (1960).
2. Ziabicki, A., *Kolloid-Z.*, **175**, 14 (1961).
3. Andrews, E. H., *Brit. J. Appl. Phys.*, **10**, 39 (1959).
4. McAdams, W. H., *Heat Transmission*, 3rd Ed., McGraw-Hill, New York, 1954, p. 259.
5. Simmons, A. C., *Trans. Am. Ind. Chem. Eng.*, **38**, 613 (1942).
6. Mueller, L. F. G., *Phil. Mag.*, [7] **3**, 81 (1927).
7. Nishikawa, and Sano, *Kagaku Kogaku*, **28**, 275 (1964).
8. Culpin, M. F., D. Madoc, and Jones, *J. Sci. Instr.*, **36**, 28 (1959).
9. Smith, C. W., and M. Dole, *J. Polymer Sci.*, **20**, 37 (1956).
10. Heisler, M. P., *Trans. ASME*, **69**, 227 (1947).

Résumé

La dynamique du filage à l'état fondu a été analysé au moyen d'une série d'équations différentielles partielles simultanées. (Voyez resume in anglais.) Dans les équations ci-dessus, la distance x à partir de la filière et le temps τ sont les variables indépendantes; la température t , la vitesse locale v et la surface de section A sont les variables dépendantes. On admet que la viscosité de tension β est une fonction uniquement de la température t , et que la tension de filage F est une fonction pure du temps. Les solutions des équations ci-dessus à l'état stationnaire ($\partial/\partial\tau = 0$) sont en bon accord avec les valeurs mesurées expérimentalement pour la température $t(x)$ et l'épaisseur $A(x)$.

Zusammenfassung

Die Dynamik des Schmelzspinnprozesses wurde durch Ableitung eines Systems simultaner partieller Differentialgleichungen analysiert. (Siehe englische Zusammenfassung.) In den obigen Gleichungen sind der Abstand von der Spinndüse und die Zeit die unabhängigen Variablen; die Zeit t , die lokale Geschwindigkeit v und die Querschnittsfläche A sind die abhängigen Variablen. Es wird angenommen, dass die Zugviskosität nur eine Funktion der Temperatur t , und die Spinnspannung F eine reine Zeitfunktion ist. Stationäre ($\partial/\partial\tau = 0$) Lösungen der obigen Gleichungen zeigen mit den experimentell gemessenen Temperatur $t(x)$ - und Dicke $A(x)$ - Werten ziemlich gute Übereinstimmung.

Received October 14, 1964

Revised December 15, 1965

(Prod. No. 4607A)

Potentiometric Study of the Conformational Transition in Poly(acrylic Acid)

A. R. MATHIESON and J. V. McLAREN, *Department of Chemistry, Ahmadu Bello University, Zaria, Nigeria*

Synopsis

Detailed potentiometric titration curves have been obtained for poly(acrylic acid) ($M_n = 2.6 \times 10^6$) in solution at four different ionic strengths at 25°C. When plotted as $\text{pH} + \log [(1 - \alpha)/\alpha]$ versus α (where α is the degree of dissociation), they reveal the presence of two different molecular conformations, denoted PAA(a) and PAA(b), with a transition between them. The proportion of the material present in the two conformations has been calculated for different degrees of dissociation and is found to be independent of ionic strength. PAA(a) is intact up to $\alpha = 0.22$ and is completely converted into PAA(b) by $\alpha = 0.75$. The free energy of transition from PAA(a) to PAA(b) when both forms are uncharged decreases numerically from -275 to -157 cal./mole monomer residues as the ionic strength increases from 0.02 to 0.20. The increase of the pH of solutions of the PAA(a) form over those of the PAA(b) form at a given value of α , is largely independent of α . This makes it possible to calculate the free energy of transition from PAA(a) to PAA(b) when both forms are charged to the same extent. This free energy is proportional to α and decreases numerically from -944α to -561α (cal.) as ionic strength increases from 0.02 to 0.20. The charge-independent part of the free energy of transition is a constant fraction of the total, at a given value of α , independent of the ionic strength. The PAA(a) form is the more compact, less contractile, and more ordered structure. The possibility is suggested that this conformation may be partly helical in nature.

INTRODUCTION

Potentiometric titration provides a method of investigating changes of conformation undergone by polyelectrolytes in solution, since the environment of the dissociating groups is dependent on the conformation of the polymer chain. Wada¹ has shown that the helix-coil transition of polyglutamic acid may be studied by this method, and this result has been confirmed by Nagasawa and Holtzer.² From the titration results, obtained in the presence of added salt, plots were made of $\text{pH} + \log [(1 - \alpha)/\alpha]$ versus α , where α is the degree of dissociation of the polyelectrolyte. The curves showed two main steps, corresponding to the titration of the helix and the coil respectively, with a transitional region between them. Leyte and Mandel³ have similarly found evidence of a transition between two conformations for poly(methacrylic acid), and Combet⁴ has reported a sharp break in the titration curve of poly(acrylic acid). Jacobson⁵ has interpreted her results on the binding of magnesium ions by poly(acrylic acid) in terms of two conformations for the polymer.

This paper presents precise potentiometric titration data for solutions of a sample of poly(acrylic acid) of high molecular weight, at constant ionic strength, which show similar features and indicate the presence of a conformational transition.

EXPERIMENTAL

Poly(acrylic acid) was prepared by the irradiation with the ultraviolet light from a 250-w. mercury arc of an aqueous solution of the monomer (under nitrogen, which had been previously outgassed). The monomer was purified by low-pressure distillation. The polymer, a stiff gel, was washed with water, then dissolved in water and freeze-dried. The molecular weight, determined by the method of Katchalsky and Eisenberg,⁶ was 2.6×10^6 . Water was double-distilled under nitrogen in an all-glass apparatus, and sodium chloride, sodium hydroxide, and hydrochloric acid were of AnalaR grade.

For potentiometric titration the cell consisted of hydrogen and silver-silver chloride electrodes separated by a saturated potassium chloride-agar salt bridge, kept at $25 \pm 0.01^\circ\text{C}$. Duplicate electrodes were employed, giving agreement to ± 0.005 of a pH unit. Titrations were made with the use of a micrometer syringe, and the EMF's were measured on a Tinsley potentiometer. Readings were obtained at intervals of the degree of dissociation of 0.02, covering the entire range. The titrations were carried out at constant ionic strength, using sodium chloride, by the method of Katchalsky, Shavit, and Eisenberg.⁷ A solution of poly-acid was neutralized with sodium hydroxide, and sodium chloride was added to bring the solution to the required ionic strength, taking the polymer ions into account. A solution of undissociated polyacid was then brought to the same ionic strength with sodium chloride, and titrated with the neutralized polyacid solutions, the volumes having been so arranged that the two solutions achieved the same concentration of poly(acrylic acid) of 9.23×10^{-3} base molar. The neutralized polyacid solution was also titrated with the solution of undissociated polyacid to the same point to make a complete titration curve. Results were obtained at the four constant ionic strengths 0.020, 0.065, 0.110, and 0.200.

RESULTS

Titration Curves

Figure 1 shows the titration results, plotted as $\text{pH} + \log [(1 - \alpha)/\alpha]$ versus α , as points connected by full curves. The four curves at the different ionic strengths all show the same features, which correspond closely with those obtained with poly(glutamic acid).^{1,2} The first short region, labelled *A* in the figure, is probably due to some instability in the solution, such as aggregation preceding precipitation, as suggested for poly(glutamic acid) by Wada.¹ In agreement with this suggestion it is

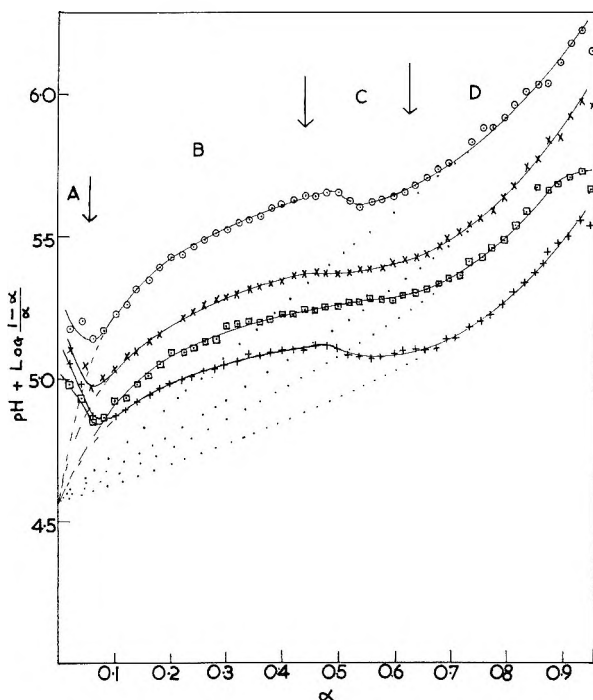


Fig. 1. Dependence of the function $\text{pH} + \log [(1 - \alpha)/\alpha]$ on α for poly(acrylic acid) at various ionic strengths μ : (\odot) $\mu = 0.02$; (\times) $\mu = 0.065$; (\square) $\mu = 0.11$; ($+$) $\mu = 0.20$.

found that this region extends to higher values of α at the higher ionic strengths. The second region, *B*, represents the ionization of the first conformation of the polymer, the third, *C*, the conformational transition, and the fourth, *D*, the ionization of the second conformation. The first conformation, which exists at the lower degrees of dissociation, has presumably the more tightly coiled structure, and will be denoted PAA(a). The second conformation, stable at high degrees of dissociation, and less tightly coiled, will be denoted PAA(b).

The four curves of PAA(a) in Figure 1 have been extrapolated (dashed curves) semiempirically to zero α , and they meet there at a value of $\text{pH} + \log [(1 - \alpha)/\alpha]$ of 4.58, which is the value of $\text{p}K'_0$, the intrinsic dissociation constant of the polyacid for ionic strengths of 0.06 and 0.11 found previously.⁸ This extrapolation is made with the help of plots of pH versus $\log [(1 - \alpha)/\alpha]$, shown in Figure 2. These plots, though almost linear over the whole range, as previously reported by Mandel and Leyte,⁹ are not quite so, and regions *A*, *B*, *C*, and *D* can be distinguished here also. Linear extrapolation of region *B*, which represents PAA(a), to higher values of $\log [(1 - \alpha)/\alpha]$ was used to obtain the extrapolations of the PAA(a) curves of Figure 1 to zero α . Figure 2 shows that pH is linear in $\log [(1 - \alpha)/\alpha]$ over regions *B* and *D*, with the lines for region *B* displaced

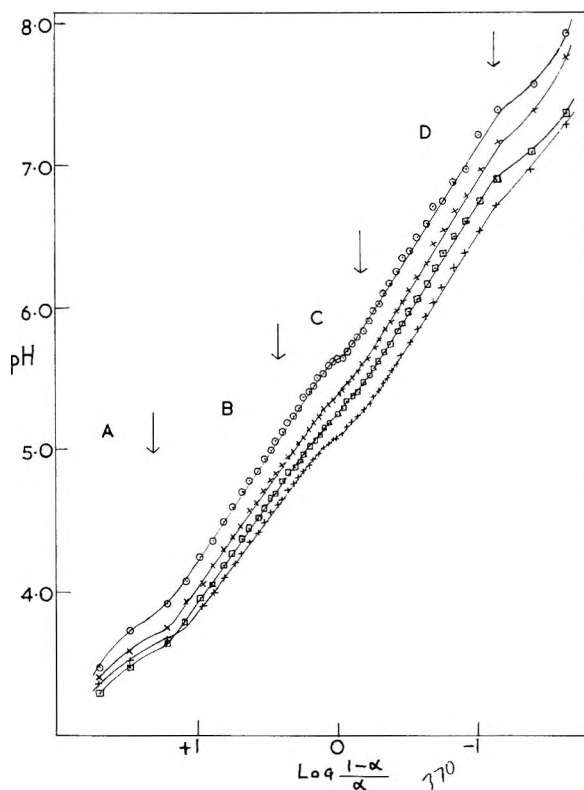


Fig. 2. pH versus $\log [(1 - \alpha)/\alpha]$ for poly(acrylic acid) at various ionic strengths μ :
 (O) $\mu = 0.02$; (X) $\mu = 0.065$; (□) $\mu = 0.11$; (+) $\mu = 0.20$.

slightly to regions of higher pH. This is similar to the result found for poly(methacrylic acid) by Leyte and Mandel,³ but here the effect is smaller. Extrapolations of the two linear regions B and D towards $\log [(1 - \alpha)/\alpha] = 0$ suggests that the value of pK'_0 for PAA(a) may be slightly higher than for PAA(b). If we represent the titration by the equation

$$pH = pK'_0 - \log [(1 - \alpha)/\alpha] + (0.4343/kT) (\partial G/\partial \nu)_\kappa \quad (1)$$

where G is the free energy of the polyanion carrying ν fixed charges and κ the inverse Debye-Hückel radius, it seems, however, that both conformations could have the same value of pK'_0 , if the free energy term was greater for PAA(a) than for PAA(b).

These two alternatives are discussed below. The extrapolation to zero α of the curves for PAA(b) in Figure 1 are somewhat uncertain because they are rather long, and because of this uncertainty in the value of pK'_0 for PAA(b). However, they can be extrapolated to the same pK'_0 , 4.58, as those for PAA(a) and these are shown as dotted curves in Figure 1. This extrapolation is almost linear for the lowest ionic strength.

Proportions of the Two Conformations

The method used by Nagasawa and Holtzer² to calculate the helix content of polyglutamic acid at different degrees of dissociation was used here, as it is quite general. The PAA(a) curves of Figure 1 are extrapolated to

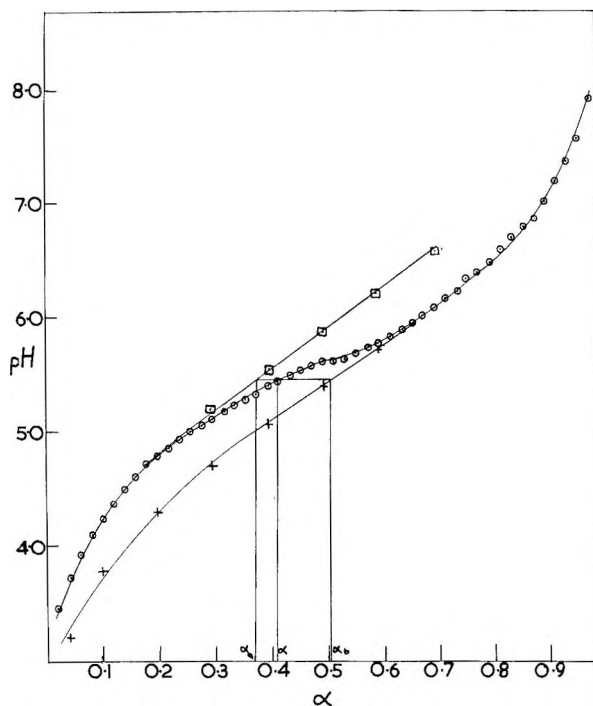


Fig. 3. Typical pH vs. α curve used for calculating the fraction of PAA(a) at $\mu = 0.02$: (\odot) actual titration curve; (\square) PAA(a) extrapolation curve; (+) PAA(b) extrapolation curve.

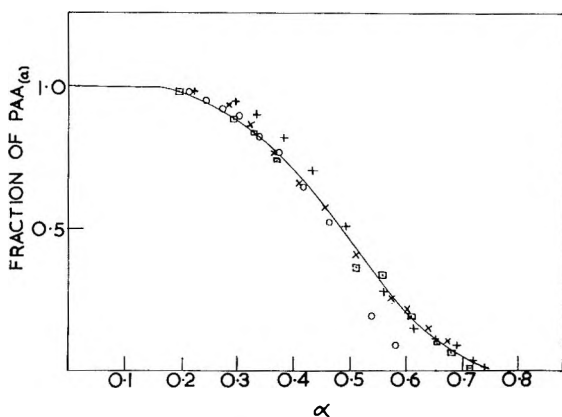


Fig. 4. Variation of the fraction of PAA(a) with degree of neutralization α at various ionic strengths: (\odot) $\mu = 0.02$; (\times) $\mu = 0.065$; (\square) $\mu = 0.11$; (+) $\mu = 0.20$.

higher as well as lower values of α , and plots are made of pH versus α , including the extrapolated curves. Figure 3 shows such a plot, for an ionic strength of 0.0200. The fraction of PAA(a) at any value of α is then given by

$$(\alpha_b - \alpha)/(\alpha_b - \alpha_a)$$

where α_a and α_b are the corresponding degrees of dissociation of PAA(a) and PAA(b), respectively. Figure 4 shows these results for the four ionic strengths, and it is clear that, within the errors introduced by the extrapolations, a single curve of F_a , the fraction of PAA(a), versus α can represent all the results. Within the accuracy obtainable, the proportion of the polymer present in the two conformations is independent of the ionic strength over the range studied, depending only on the degree of dissociation at constant temperature. PAA(a) remains intact up to $\alpha = 0.22$, and transformation to PAA(b) is complete at $\alpha = 0.75$.

Free Energy of Transition

Zimm and Rice¹⁰ have shown that for helix-coil transitions, the free energy of the transition from uncharged helix to uncharged coil, per mole of monomer residues, is simply given by

$$\Delta G^0/N = 2.303 RTA \quad (2)$$

where A is the area lying between the curves representing the two conformations on the plots of $\text{pH} + \log [(1 - \alpha)/\alpha]$ versus α . Nagasawa and Holtzer² have recalculated this expression in such a way as to show that eq. (2) is of general application to a polymeric conformational change in solution. Using this expression, values of $\Delta G^0/N$ were calculated for the change $\text{PAA(a)}^0 \rightarrow \text{PAA(b)}^0$, i.e., from uncharged PAA(a) to uncharged PAA(b). These are shown in Table I. They decrease numerically as ionic strength rises, over a similar range of values to that found for the helix-coil transition of poly(glutamic acid).²

TABLE I
Free Energies of the Conformational Transition

| Ionic strength | $\Delta G^2/N$, cal./mole | $(\Delta \text{pH})_\alpha$ | $\Delta G^v/N$, cal./mole | $\Delta G^0/(\Delta G^0 + \Delta G^v)$ | |
|----------------|----------------------------|-----------------------------|----------------------------|--|----------------|
| | | | | $\alpha = 0.1$ | $\alpha = 1.0$ |
| 0.020 | -275 | -0.49 | -944 α | 0.74 | 0.23 |
| 0.065 | -205 | -0.34 | -670 α | 0.75 | 0.23 |
| 0.110 | -165 | -0.32 | -593 α | 0.74 | 0.22 |
| 0.200 | -157 | -0.29 | -561 α | 0.74 | 0.22 |

The difference between the pH for PAA(a) and PAA(b), at constant degree of dissociation, $(\Delta \text{pH})_\alpha$, is also shown in Table I. Within the error of the estimations it is independent of α , as Figure 3 shows, over a wide range of α at least up to $\alpha = 0.7$. $(\Delta \text{pH})_\alpha$ varies linearly with the reciprocal

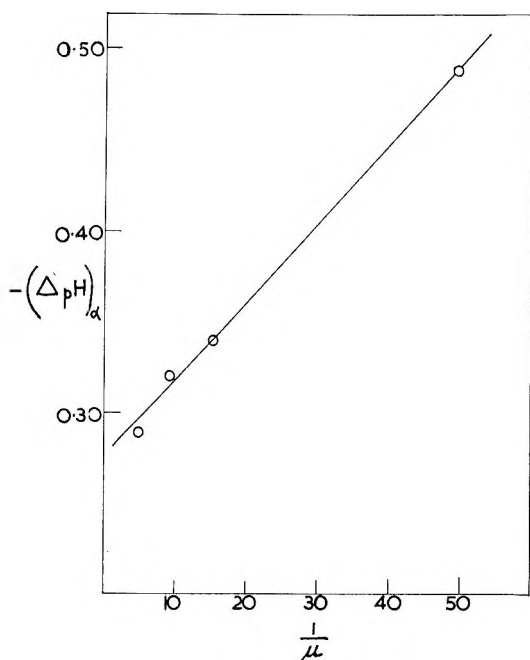


Fig. 5. Dependence of $(\Delta pH)_\alpha$ on ionic strength for poly(acrylic acid).

of the ionic strength over the range studied (Fig. 5). This $(\Delta pH)_\alpha$ can be equated to the difference in the free energy term of eq. (1) for PAA(a) and PAA(b), i.e.,

$$(\Delta pH)_\alpha = (0.4343/kT) \partial(G_b - G_a)_\alpha / \partial \nu \quad (3)$$

where G_a and G_b are the free energies of the a and b conformations, respectively, provided we assume that both forms have the same value of pK_0' .

The independence of $(\Delta pH)_\alpha$ of α , and hence of ν , allows us to evaluate the difference of free energy between PAA(a) and PAA(b) at various degrees of dissociation of these forms, in addition to that for the undissociated conformations. Writing simply

$$(\Delta pH)_\alpha = f(\mu) \quad (4)$$

where $f(\mu)$ is a function of ionic strength μ , and combining with eq. (3),

$$\partial(G_b - G_a)_\alpha / \partial \nu = 2.303 kT f(\mu)$$

Hence

$$\int_0^\nu \partial(G_b - G_a)_\alpha / \partial \nu = (G_b - G_a)_\nu - (G_b - G_a)_{\nu=0} = 2.303 kT \nu f(\mu)$$

and, expressing this as calories per mole of monomer residues, we have

$$\begin{aligned} [(G_b - G_a)_\nu / N] - [(G_b - G_a)_0 / N] &= (\Delta G^\nu / N) - (\Delta G^0 / N) \\ &= 2.303 RT \nu f(\mu) \end{aligned} \quad (5)$$

since $\alpha = \nu/N$. Here $\Delta G^0/N$ is the difference in free energy of the two uncharged conformations, already calculated, and $\Delta G^\nu/N$ is the difference for the two conformations when each carries ν charges, i.e., for $\text{PAA(a)}^\nu \rightarrow \text{PAA(b)}^\nu$. Values of $\Delta G^\nu/N$ are also shown in Table I, calculated on the assumption that both forms have the same $\text{p}K_0'$, and the empirical expression

$$-(\Delta\text{pH})_\alpha = 0.274 + 0.432/100\mu$$

derived from Figure 5. Equation (5) requires that $\Delta G^\nu/N$ is proportional to α .

DISCUSSION

Correlation with Other Evidence

The experiments of Jacobson⁵ on the release of hydrogen ions from poly(acrylic acid) at different degrees of dissociation by the addition of magnesium ions showed that a change of conformation takes place, roughly between values of α of 0.2 and 0.7, as found here. This was interpreted⁵ as a change from a spherical ball form to a winding chain form, as suggested earlier,¹¹ but it is not clear what structure is envisaged for the polymer chain within the spherical ball. Mandel and Leyte³ found that plots of pH versus $\log [(1 - \alpha)/\alpha]$ were linear for poly(acrylic acid) and suggested there was no conformational change for this polymer. Our results show that this is not so, at least for the sample used. Combet⁴ found a break in the titration curve at $\alpha = 0.25\text{--}0.375$, around the beginning of the transformation found here. It seems clear that the conformational change does take place, and the result of Mandel and Leyte may have arisen because the effect is quite small when represented on pH versus $\log [(1 - \alpha)/\alpha]$ plots, though not on plots of $\text{pH} + \log [(1 - \alpha)/\alpha]$ versus α . It is also quite possible that different samples, prepared by different methods, might behave differently, since it has been found that this polymer is a stronger acid when prepared in aqueous solution (as here) than in benzene, or by hydrolysis of its ester.¹²

Stabilization of the Conformations

It seems likely that PAA(a), the more tightly coiled structure, is also a more ordered structure than PAA(b). It also possesses, at a given value of α , a greater free energy and so must require some stabilization. This stabilization is sufficient to hold the structure intact until over 20% of the carboxyl groups are ionized, and under these conditions only a small proportion of ionized carboxyl groups carry associated sodium gegenions.^{13,14} It seems quite possible that carboxyl-carboxyl hydrogen bonding is responsible for this stabilization. However, our results provide no evidence that this is the case for poly(acrylic acid).

It can readily be shown that¹⁵ a hydrogen-bonded carboxyl group will titrate with a higher $\text{p}K_0'$ than will a nonhydrogen-bonded one. The $\text{p}K_0'$

values of hydrogen-bonded (pK_0',H) and nonhydrogen-bonded forms of the carboxyl group are related by¹⁶

$$pK_0',H = pK_0' + \log [1 + (\theta_H/\theta)] \quad (6)$$

where θ_H and θ are, respectively, the fractions of hydrogen-bonded and nonhydrogen-bonded (but unionized) carboxyl groups. If a significant fraction of the carboxyl groups is hydrogen-bonded in PAA(a), we might expect it to show a higher value of pK_0' than PAA(b). It is not possible to use the extrapolations of Figure 1 to test this, however, as they are not accurate enough, and the two linear regions of Figure 2 and $(\Delta pH)_\alpha$ can be explained by a difference of free energy between the two conformations without recourse to a difference in pK_0' . The use of eq. (1) to calculate pK_0' should lead, if PAA(a) has a different value of pK_0' than PAA(b), to values of pK_0' which decrease slowly with α . There is no evidence for this,¹⁷ but unfortunately the free energy term had to be calculated from electrophoretic measurements on the basis of a postulated model and with the assumption that all the free energy arose from electrostatic interaction, with no allowance for purely conformational free energy changes. Extra energy will be required to dissociate a hydrogen-bonded group, so that nonhydrogen-bonded groups will be preferentially ionized and the PAA(a) conformation may be disrupted rather by electrostatic repulsion of the ionized groups than by direct titration of its hydrogen-bonded links.

Free Energy of Transformation

$\Delta G^0/N$, the free energy of transformation of PAA(a) to PAA(b) when both are uncharged, falls with increased ionic strength, and so does $\Delta G^p/N$, the free energy of transformation at a particular state of charge. Also, the charge-independent free energy change is a constant fraction of the total free energy change for different ionic strengths, as shown on Table I for $\alpha = 0.1$ and 1.0. The variation of $\Delta G^0/N$ and $\Delta G^p/N$ with ionic strength implies that either or both conformations alter their detailed arrangements according to the ionic strength of the solution, the two conformations being less different at the higher ionic strengths. If it does alter a particular conformation, increased ionic strength will lead to a contraction of the molecule, and so PAA(b) is more contractile than PAA(a). Viscosity experiments show this quite clearly;⁸ at pH values of 3.0 and 3.5 increased ionic strength has only a small effect on the limiting viscosity number, but a much greater effect at pH 5.0, 7.0, 10.0, and 12.0.

It is tempting to suggest as a possibility that PAA(a) may be a partly helical structure. There is no direct evidence for this, but it would be in accord with the similarity of the results for poly(acrylic acid) to those for poly(glutamic acid). As the molecular weight is so high, the partly helical chain could easily be wound in such a way as to produce a nearly spherical molecule. Helical structures probably exist in tactic poly(acrylic acid).¹⁸

Correlation with Mobility and Viscosity Data

These results should be compared with those reported earlier on the electrophoretic mobility and viscosity of poly(acrylic acid).⁸ At the low ionic strengths (0.02 and 0.06), the mobility shows a rapid increase between pH 6 and 7, but this cannot correspond to the conformational transformation as this takes place at lower pH values (5–6). Over this range of pH the mobility continues its steady rise with pH which began at pH values where the PAA(a) structure is intact. At the higher ionic strengths (0.11 and 0.20) the steady increase of mobility with pH is maintained over the whole range. It seems that the conformational transformation has little direct effect on the mobility.

The limiting viscosity number, for all the ionic strengths studied, showed a rapid increase between pH 3.5 and 7.0, with little change outside this range. It is quite possible that this is related to the conformational transformation, but more detailed viscosity measurements between pH 3.5 and 5.0 are needed to verify this. The earlier paper⁸ promised that quantitative comparison of the predictions of polyelectrolyte theories with the mobility and viscosity data would be given later. As these theories generally describe the molecule using a single model it no longer seems profitable to do this. However, it may be stated that polyelectrolyte theories predict molecular extensions which are too large when compared with viscosity⁸ and light-scattering¹⁹ results. The existence of the more tightly coiled conformation PAA(a) over a wide range of degrees of dissociation could be one factor responsible for this. Results which showed maxima in the viscosity and dissymmetry coefficient, and a minimum extinction angle at 20–40% neutralization²⁰ could also be explained this way.

References

1. Wada, A., *Mol. Phys.*, **3**, 409 (1960).
2. Nagasawa, M., and A. Holtzer, *J. Am. Chem. Soc.*, **86**, 538 (1964).
3. Leyte, J. C., and M. Mandel, *J. Polymer Sci.*, **A2**, 1879 (1964).
4. Combet, S., *Compt. Rend.*, **254**, 2961 (1962).
5. Jacobson, A. L., *J. Polymer Sci.*, **57**, 321 (1962).
6. Katchalsky, A., and H. Eisenberg, *J. Polymer Sci.*, **6**, 145 (1951).
7. Katchalsky, A., N. Shavit, and H. Eisenberg, *J. Polymer Sci.*, **13**, 69 (1954).
8. Mathieson, A. R., and J. V. McLaren, *J. Chem. Soc.*, **1960**, 3581.
9. Mandel, M., and J. C. Leyte, *J. Polymer Sci.*, **56**, 823 (1962).
10. Zimm, B. H., and Rice, S. A., *Mol. Phys.*, **3**, 391 (1960).
11. Guinard, S., F. Boyer-Kawenoki, A. Dobry, and J. Tonnelat, *Compt. Rend.*, **229**, 143 (1949).
12. Sakurada, I., and Y. Sakaguchi, *Makromol. Chem.*, **61**, 1 (1963).
13. Huizenga, J. R., P. F. Greiger, and F. T. Wall, *J. Am. Chem. Soc.*, **72**, 2636 (1950).
14. Ikegami, A., *J. Polymer Sci.*, **A2**, 907 (1964).
15. Laskowski, M., and H. A. Scheraga, *J. Am. Chem. Soc.*, **76**, 6305 (1954).
16. Mathieson, A. R., and R. T. Slet, in preparation.
17. McLaren, J. V., Thesis, Nottingham, 1956.
18. Combet, S., *Compt. Rend.*, **254**, 2759 (1962).
19. Oth, A., and P. Doty, *J. Phys. Chem.*, **56**, 43 (1952).
20. Sakamoto, R., and K. Imahori, *Nippon Kagaku Zasshi*, **83**, 389 (1962).

Résumé

Des courbes de titration potentiométrique détaillées ont été obtenues pour l'acide polyacrylique ($M_n = 2.6 \times 10^6$) en solution à quatre différentes forces ioniques et à 25°C. Lorsqu'on porte $\text{pH} + \log [(1 - \alpha)/\alpha]$ en fonction de α (où α est le degré de dissociation) on remarque la présence de deux conformations moléculaires différentes, représentées par PAA(a) et PAA(b) avec une transition entre elles. La proportion du matériau présent dans les deux conformations a été calculée pour différents degrés de dissociation et on a trouvé qu'elle était indépendante de la force ionique. PAA(a) reste inchangé jusqu'à $\alpha = 0.22$ et est complètement transformé en PAA(b) pour $\alpha = 0.75$. L'énergie libre de transition depuis PAA(a) jusqu'à PAA(b), lorsque les deux formes sont non-chargées, diminue numériquement depuis -275 jusque -157 (cal par mole de résidu monomérique) alors que la force ionique augmente de 0.02 à 0.20. L'augmentation de pH des solutions de la forme PAA(a) à une valeur supérieure à celle de la forme PAA(b) pour une valeur donnée de α , est essentiellement indépendante de α , et permet de calculer l'énergie libre de transition depuis PAA(a) jusque PAA(b) lorsque les deux formes sont chargées de la même façon. Cette énergie libre est proportionnelle à α et diminue numériquement de -944 jusque -561 (cal) lorsque la force ionique augmente de 0.02 jusque 0.20. La partie, indépendante de la charge, de l'énergie libre de transition est une fraction constante de l'énergie totale, pour une valeur donnée de α , indépendante de la force ionique. La forme PAA(a) est la plus compacte, la moins contractile, possède la structure la plus ordonnée et est probablement stabilisée par la liaison hydrogène carboxyle-carboxyle. Il est possible que cette conformation soit de nature partiellement hélicoïdale.

Zusammenfassung

Genau potentiometrische Titrationskurven wurden für Polyacrylsäure ($M_n = 2,6 \times 10^6$) in Lösung bei vier verschiedenen Ionenstärken bei 25°C erhalten. Bei der Auftragung von $\text{pH} + \log [(1 - \alpha)/\alpha]$ gegen α (wo α der Dissoziationsgrad ist) zeigt sich das Vorhandensein von zwei verschiedenen Molekülkonformationen, als PAA(a) und PAA(b) bezeichnet, mit einer Umwandlung zwischen beiden. Das Verhältnis des Anteiles der beider Konformationen wurde für verschiedene Dissoziationsgrade berechnet und ergibt sich als unabhängig von der Ionenstärke. PAA(a) bleibt bis zu $\alpha = 0,22$ unverändert und wird bei $\alpha = 0,75$ in PAA(b) verwandelt. Die freie Umwandlungsenergie von PAA(a) zu PAA(b) für beide Formen im ungeladenen Zustand nimmt bei einem Anstieg der Ionenstärke von 0,02 auf 0,20 numerisch von -275 auf -157 (cal pro Mol Monomereinheit) ab. Die Zunahme des pH-Wertes von Lösungen der PAA(a)-Form über denjenigen der PAA(b)-Form ist bei einem gegebenen α -Wert weitgehend von α unabhängig, wodurch eine Berechnung der freien Umwandlungsenergie von PAA(a) zu PAA(b) für beide im gleichen Ausmass geladenen Polymeren ermöglicht wird. Diese freie Energie ist zu α proportional und nimmt bei einem Anstieg der Ionenstärke von 0,02 auf 0,20 numerisch von -944α auf -561α (cal) ab. Der lösungsunabhängige Teil der freien Umwandlungsenergie bildet bei gegebenem α -Wert unabhängig von der Ionenstärke einen konstanten Bruchteil des Gesamtwertes. Die PAA(a)-Form bildet die kompaktere, weniger kontraktile und höher geordnete Struktur und wird wahrscheinlich durch eine Carboxyl-Carboxyl-Wasserstoffbindung stabilisiert. Die Möglichkeit einer teilweisen Helixnatur für diese Konformation wird vorgeschlagen.

Received November 24, 1964
(Prod. No. 4618A)

Cationic Polymerization α,β -Disubstituted Olefins. Part I. Cationic Copolymerization of β -Methylstyrenes

A. MIZOTE, T. TANAKA, T. HIGASHIMURA, and S. OKAMURA,
Department of Polymer Chemistry, Kyoto University, Kyoto, Japan

Synopsis

Steric and electronic effects of the β -methyl group on monomer reactivity have been studied by copolymerization of styrenes and β -methylstyrenes. Steric hindrance of the β -methyl group in the transition state of homopolymerization is so great that the rate of the propagation reaction is considered to be depressed by as much as $1/10$ - $1/20$ of the corresponding styrene derivatives. In contrast to this, steric hindrance of the β -methyl group in cross propagation reactions with styrene is found to be very small. The monomer reactivity itself of β -methylstyrenes is a little lower than that of corresponding styrenes. This lowered reactivity of β -methylstyrenes is considered to be due to the electronic effect of the β -methyl group.

INTRODUCTION

It is well known that α,β -disubstituted olefins generally cannot be polymerized to high polymers, especially by a radical mechanism. This has been attributed to steric repulsion of the β -substituent in the transition state.¹

On the other hand, few experiments have been reported on polymerization of α,β -substituted olefins by a cationic mechanism from the view of effects of the β -substituent, except for some work on copolymerization of styrene and β -alkyl styrenes by Overberger and co-workers.² They presumed that introduction of alkyl group at the β -position increases the electron density of the carbon-carbon double bond and the olefin becomes more reactive in cationic polymerization. Experimental results, however, showed those monomers to have low reactivity. Thus Overberger et al. concluded that the steric effect of the β -alkyl group is so large that these monomers cannot be polymerized to high polymers by cationic or a radical mechanism, even if the β -alkyl group has electron-donating power (polar effect).

However, the electronic effect of β -substituents on monomer reactivity combines with the steric effect, and their separation has not been previously achieved.

Therefore, the studies of this sterics are intended to clarify the effect of the β -substituent.

In this paper the effect of the β -methyl group of β -methylstyrenes on

TABLE I
Physical Constants of Monomers

| Monomer | R | Boiling point, °C. | Refractive index n_D | Specific gravity d | Content of <i>trans</i> isomer, % | Reference |
|---|-------------------|--------------------|------------------------|----------------------|-----------------------------------|-------------------------------|
| Styrene derivatives | —CH ₃ | 74–75 (20 mm.) | 1.5420 (20°C.) | — | — | Present work |
| | —OCH ₃ | 82–83 (27 mm.) | 1.5395 (25°C.) | 0.891 (30°C.) | — | Overberger ⁴ |
| β -Methylstyrene derivatives | —OCH ₃ | 90–91 (10 mm.) | 1.5590 (20°C.) | — | — | Present work |
| | —H | 92–93 (12 mm.) | 1.5608 (20°C.) | 1.0023 (30°C.) | — | Okamura et al. ⁵⁻⁷ |
| | —H | 176–177 | 1.5450 (26°C.) | 0.9110 (25°C.) | 70 | Present work |
| $\text{CH}_2=\text{CH}-\text{C}_6\text{H}_4-\text{R}$ | —CH ₃ | 71 (25 mm.) | 1.5480 (25°C.) | 0.902 | 100 | Overberger |
| | —CH ₃ | 195–196 | 1.5463 (15.3°C.) | — | 85 | Present work |
| | —OCH ₃ | 195–197 | — | 0.9057 (13°C.) | — | Klages ⁸ |
| $\text{CH}_2=\text{CH}-\text{C}_6\text{H}_4-\text{R}$ | —OCH ₃ | 108–109 (11.5 mm.) | 1.5564 (24.2°C.) | 0.9788 (30°C.) | 99.8 | Present work |
| | —OCH ₃ | 112–114 (15 mm.) | 1.5614 (21°C.) | 0.9936 (15°C.) | — | Bert ⁹ |

monomer reactivity in copolymerization are studied. Steric and electronic effects could be estimated from the values of monomer reactivity ratios by choosing suitable monomer pairs.

The β -methylstyrene derivatives used in this experiment were mixtures of *trans* and *cis* isomers (except anethole) as differences in monomer reactivity between isomers may be assumed to be so small² as not to affect the present results.

It is found that the β -methyl group not only decreases the polymerizability of monomer sterically but also decreases the reactivity of the monomer itself electronically.

EXPERIMENTAL

Materials

β -Methylstyrene and *p*-methyl- β -methylstyrene were prepared from the corresponding allylbenzenes by refluxing with potassium butylate in butanol. Allylbenzenes were prepared from allyl bromide and phenylmagnesium bromide.³ The resulting β -methylstyrenes and commercial anethole (*p*-methoxy- β -methylstyrene) were purified by washing with 5% NaOH aqueous solution and water. After drying on sodium sulfate overnight and refluxing with calcium hydride, these monomers were distilled in a nitrogen atmosphere. These monomers were considered to be mainly *trans* isomer. Physical constants of monomers are listed in Table I.

Preparation and purification of styrene and styrene derivatives and purification of solvent and catalyst were by the usual methods.⁵⁻⁷

Procedure

Copolymerization. Copolymerization was carried out in a solution of ethylene dichloride at 30°C. in which total monomer concentration was 10 vol.-%; the catalyst was BF_3OEt_2 for all systems. The concentration of catalyst was chosen arbitrarily (in the range of 10^{-2} – 10^{-3} mole/l.) for various systems and batches in order to get moderate rates of polymerization.

The copolymer was precipitated in methanol and filtered, washed with methanol, and dried *in vacuo*. The polymerization reaction was stopped below 10% conversion.

A correction of monomer concentration for conversions of over 5% was made for each copolymerization.²

Rearrangement polymerization of β -methylstyrene was reported by Murahashi et al.¹⁰ and reviewed by Kennedy and Langer,¹¹ but from the infrared spectra, the poly- β -methylstyrenes obtained in our system seem not to be rearranged.

Normal polymerization (1,2-polymerization) of the more reactive *p*-methyl- β -methylstyrene and *p*-methoxy- β -methylstyrene (anethole) are more favored.

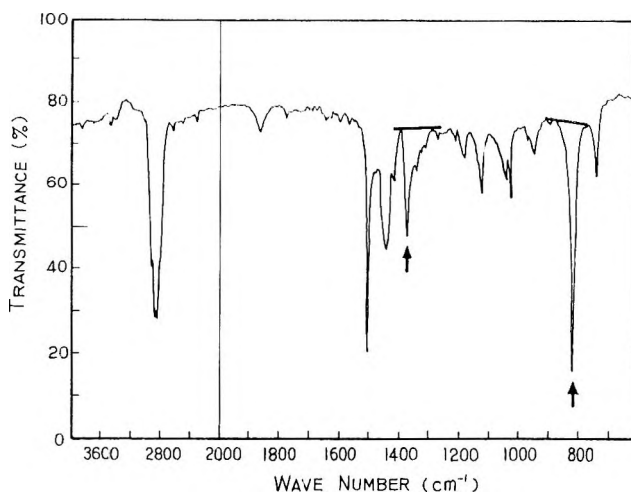


Fig. 1. Infrared spectrum of *p*-methylstyrene-*p*-methyl- β -methylstyrene copolymer. Mole fraction *p*-methylstyrene in copolymer $P_1 = 0.35$.

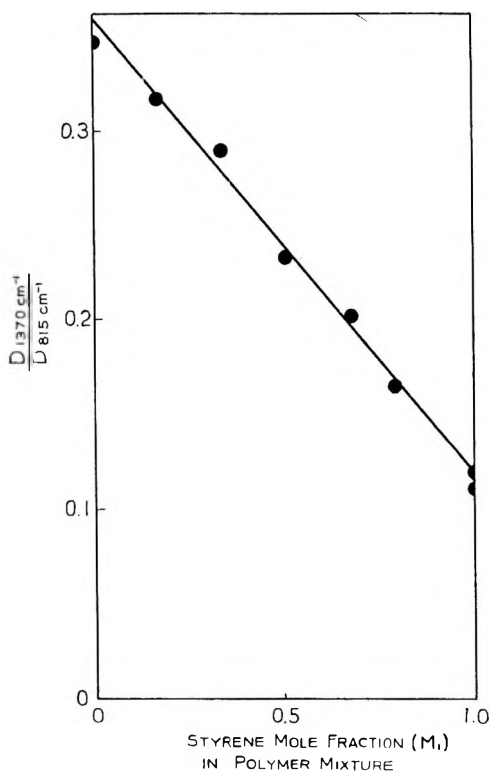


Fig. 2. Calibration curve for analysis of composition of *p*-methylstyrene (M_1)-*p*-methyl- β -methylstyrene copolymer.

Composition Analysis of Copolymers. Infrared methods^{12,13} were used to determine the composition of the copolymers. Calibration curves were obtained from infrared spectra of mixtures of fine powdery homopolymers mixed with KBr. Infrared spectra of copolymers and the calibration curve are shown in Figures 1 and 2 for the *p*-methylstyrene-*p*-methyl- β -methylstyrene pair.

Absorption bands for analysis of copolymer composition are listed in Table II.

TABLE II
Absorption Band of Infrared Spectra for Analysis of Copolymer Composition

| Monomer pair | Absorption frequency, cm. ⁻¹ |
|---|---|
| Styrene- β -methylstyrene | 1370, 1585 |
| Styrene- <i>p</i> -methyl- β -methylstyrene | 760, 810 |
| Styrene- <i>p</i> -methoxy- β -methylstyrene | 700, 830 |
| <i>p</i> -Methylstyrene- <i>p</i> -methyl- β -methylstyrene | 1375, 810 |
| <i>p</i> -Methoxystyrene- <i>p</i> -methoxy- β -methylstyrene | 1380, 830 |

The optical density of a functional group in infrared spectra is assumed not to be influenced by the penultimate monomer unit.

RESULTS

Copolymerization of Styrenes and Corresponding β -Methylstyrenes

In order to study the effect of the β -methyl group, we chose monomer pairs for which the propagating cations would be quite similar in structure to each other, that is, copolymerization was carried out of styrene derivatives which have a nuclear substituent and β -methylstyrenes for which the nuclear substituents, are the same as that of the corresponding styrene derivatives, as shown in eqs. (1).

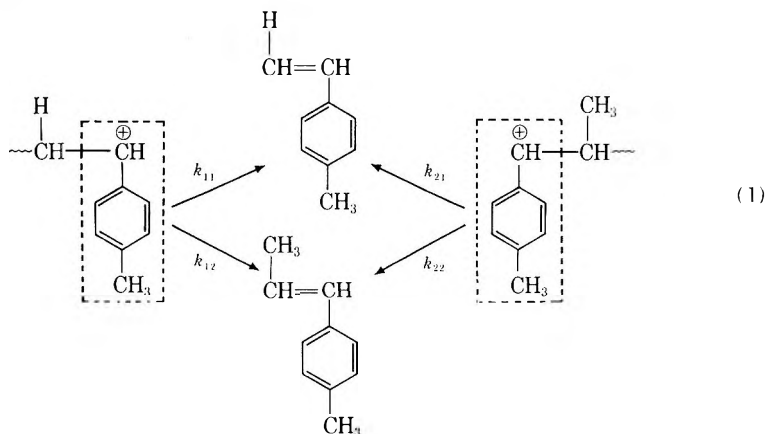
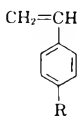
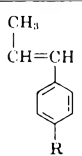
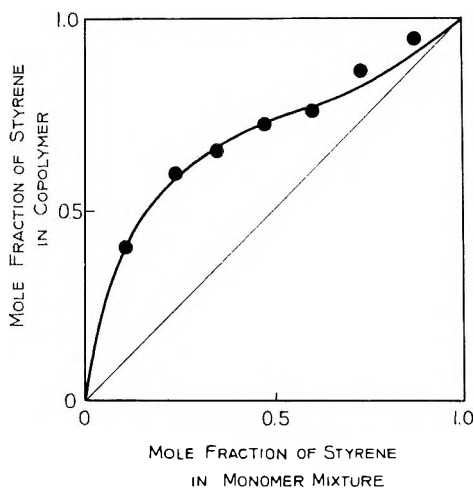
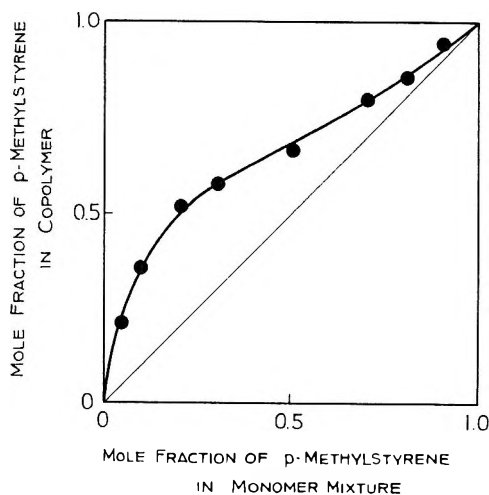


TABLE III
 Summary of Monomer Reactivity Ratios

| M_1 | M_2 | R | r_1 | r_2 |
|---|--|-------------------|---------------|-----------------|
| $\text{CH}_2=\text{CH}$  R | CH_3 $\text{CH}=\text{CH}$  R | -H | 1.8 ± 0.2 | 0.07 ± 0.02 |
| | | -CH ₃ | 1.3 ± 0.3 | 0.04 ± 0.04 |
| | | -OCH ₃ | 1.2 ± 0.2 | 0.04 ± 0.02 |


 Fig. 3. Copolymer composition curve for styrene (M_1) and β -methylstyrene (M_2). Solvent $(\text{CH}_2\text{Cl})_2$; catalyst BF_3OEt ; temperature 30°C .; monomer 10 vol.-%.

 Fig. 4. Copolymer composition curve for p -methylstyrene (M_1) and p -methyl- β -methylstyrene (M_2). Polymerization conditions as in Fig. 3.

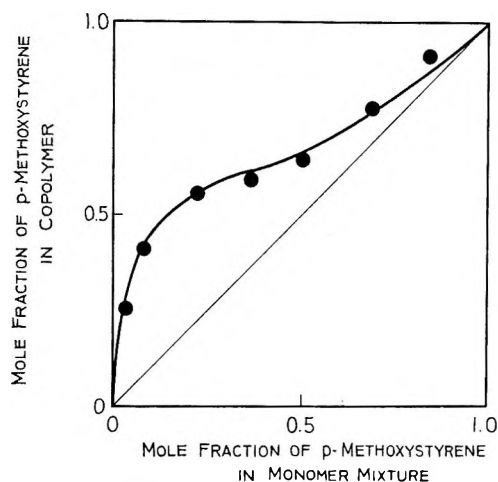


Fig. 5. Copolymer composition curve for *p*-methoxystyrene (M_1) and *p*-methoxy- β -methylstyrene. Polymerization conditions as in Fig. 3.

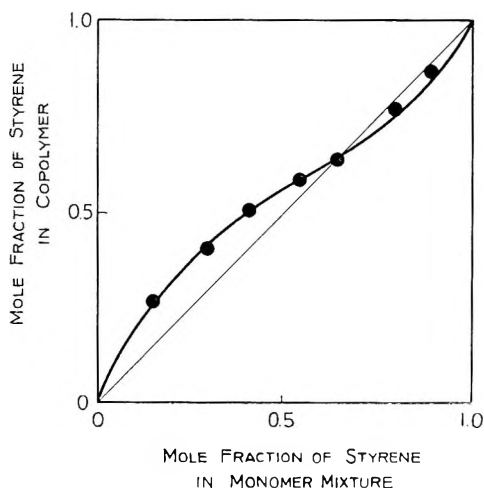


Fig. 6. Copolymer composition curve for styrene (M_1) and *p*-methyl- β -methylstyrene (M_2). Polymerization conditions as in Fig. 3.

As seen from eq. (1), the propagating cations of *p*-methylstyrene and *p*-methyl- β -methylstyrene can be considered quite similar because the inductive effect of the β -methyl group in the cation on the stabilizing charge is small. If the β -methyl group had no steric repulsion in the addition step, then k_{11}/k_{12} should be equal to k_{21}/k_{22} .

Figure 3 shows the copolymer composition curve for the styrene- β -methylstyrene copolymer for which monomer reactivity ratios are $r_1 = 1.8 \pm 0.3$; $r_2 = 0.07 \pm 0.02$ (as determined by the intersection method). From these values r_2 is found to be much smaller than expected (if $k_{11}/k_{12} = k_{21}/k_{22}$, then $r_2 = 1/r_1 = 0.56$).

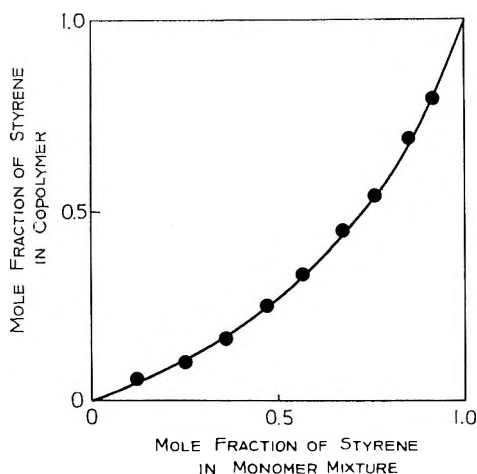


Fig. 7. Copolymer composition curve for styrene (M_1) and *p*-methoxy- β -methylstyrene (M_2). Polymerization conditions as in Fig. 3.

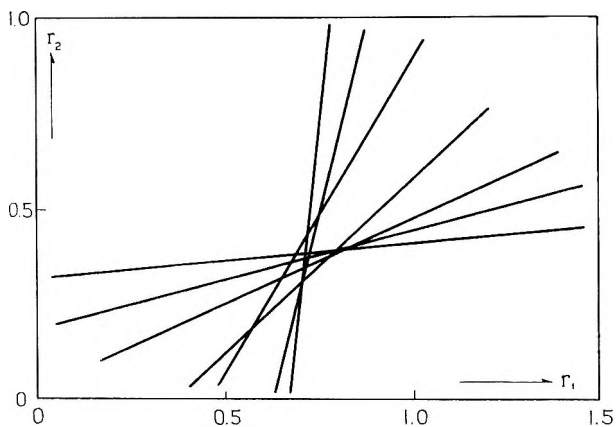


Fig. 8. Estimation of monomer reactivity ratio by intersection method from data of Fig. 6 for styrene (M_1) and *p*-methyl- β -methylstyrene (M_2).

Similar results were obtained with copolymerization of *p*-methylstyrene and *p*-methyl- β -methylstyrene and of *p*-methoxystyrene and *p*-methoxy- β -methylstyrene (anethole). Copolymer composition curves are shown in Figures 4 and 5. These results are summarized in Table III. The monomer reactivity ratios for three pairs obtained here are quite similar, although the reactivities of the monomers in each pair are so different from each other (*p*-methoxystyrene is 20–100 times more reactive than styrene). Furthermore, $r_1 < 2$ for all three pairs.

Copolymerization of Styrene (M_1) and β -Methylstyrenes (M_2)

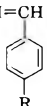
The influence of the nuclear substituent on monomer reactivity of β -methylstyrene derivatives was also investigated. Figures 6 and 7 show

copolymer composition curves for the monomer pairs styrene (M_1)-*p*-methyl- β -methylstyrene (M_2) and styrene (M_1)-*p*-methoxy- β -methylstyrene (M_2), respectively.

The copolymer composition curve obtained with the former pair shows an unusual shape for cationic copolymerization.

Monomer reactivity ratios were determined by the intersection method and the result is shown in Figure 8. Results are summarized in Table IV together with the results for the styrene (M_1)- β -methylstyrene (M_2) copolymer.

TABLE IV
Summary of Monomer Reactivity Ratios

| M_2 | R | r_1 | r_2 |
|--|-------------------|----------------|-----------------|
| $\text{CH}_3\text{-CH=CH}$  R | -H | 1.8 \pm 0.2 | 0.07 \pm 0.02 |
| | -CH ₃ | 0.75 \pm 0.1 | 0.36 \pm 0.05 |
| | -OCH ₃ | 0.45 \pm 0.2 | 2.8 \pm 0.2 |

Introduction of an electron-donating group (methyl or methoxy group) into the ring at the *para*-position increases monomer reactivity of β -methylstyrenes as well as styrene derivatives.

Even though the *p*-methyl group has a small effect with regard to increasing monomer reactivity, the monomer reactivity ratio r_1 of styrene-*p*-methyl- β -methylstyrene copolymer was less than unity. This fact implies that when a styrene cation attacks β -methylstyrenes, the β -methyl group has only a small steric influence on the course of polymerization. This seems to be reasonable, and is consistent with the previous results. The same phenomenon is found in the work of Overberger et al.²

In the case of the styrene (M_1)-*p*-methoxy- β -methylstyrene (anethole) (M_2) copolymer, the product of monomer reactivity ratios, r_1r_2 , is close to unity, as is usual in cationic copolymerization. Apparently, no steric effect can be recognized in this system.

DISCUSSION

Electronic Effect of β -Methyl Group

The monomer reactivity ratio (k_{11}/k_{12}), (relative reactivity of monomer toward the propagating styrene cation M_1^+ , having no β -methyl group) is a little larger than unity for all the three cases (Table III). It is well known that in radical copolymerization, the steric effect is not so important in alternating propagation of vinyl monomers and α,β -disubstituted olefins. A similar interpretation of this phenomenon is not valid in a discussion of the results in cationic copolymerization because of the difference of structure in the transition state of the propagation reaction. However, the

fact that reactivity of *p*-methyl- β -methylstyrene monomer is larger than that of styrene monomer implies that the steric effect of the β -methyl group is not so large in the cross propagation step for these systems.

If it can be assumed that there is no steric repulsion in the propagation step, $M_1^+ + M_2 \rightarrow M_2^+$, then the results of Table III showing $r_1 > 1$ for all cases can be interpreted as showing that the lowered reactivity of β -methylstyrene derivatives relative to the corresponding styrene derivatives is due to the electronic effect of the β -methyl group.

The introduction of an electron-donating group at the β -position as well as at the α -position has been presumed to increase monomer reactivity owing to increased electron density of the carbon-carbon double bond.² However, the results obtained here indicate the opposite is true. It is revealed that monomer reactivity of β -methylstyrenes is depressed by introduction of β -methyl group. This phenomenon can be interpreted as follows: introduction of an electron-donating group at β -position induces a partial negative charge at the α -position, not at β -position and depresses favorable polarization of the carbon-carbon double bond which is an important part of the propagation step in cationic polymerization.

While Overberger⁴ reported that *p*-methoxystyrene is 20–100 times more reactive than styrene toward the propagating styrene cation, the present study shows that the relative reactivity of styrene and *p*-methoxy- β -methylstyrene toward propagating styrene cation is only 2–3 times that of styrene (steric effect here for cross propagation is negligibly small). This fact also agrees with the above consideration of the effect of the β -methyl group on monomer reactivity.

A theoretical treatment (molecular orbital theory) of this phenomenon also confirms lowered reactivity of monomer on introduction of an electron-donating group at the β -position. The effect of β -substituents other than a methyl group were investigated by LCAO molecular orbital theory and will be discussed in a later report of this series.

Steric Effect of β -Methyl Group

All r_2 values for three pairs are very much smaller than unity, and monomer reactivity ratios for the three pairs are very close to each other. This fact indicates that the contribution of the steric effect of the β -methyl group on monomer reactivity can be discussed separately.

According to Branch and Calvin,¹⁴ the influence of variation of monomer structure on the activation free energy of the propagation reaction can be expressed as a sum of polar, resonance, and steric factors:

$$-\Delta F^\ddagger = P + R + S = RT \ln (k/k_0)$$

$$\log k/k_0 = F_p + F_r + F_s$$

Where F_p is the polar factor; F_r , the resonance factor, and F_s , the steric factor.

Applying this relation to copolymerization reaction yields

$$\begin{aligned}\log 1/r_1 &= \log k_{12}/k_{11} = F_P + F_R + F_S \\ \log r_2 &= \log k_{22}/k_{21} = F'_P + F'_R + F'_S\end{aligned}$$

In the copolymerization reaction both propagating cation M_1^+ and M_2^+ are the same; then

$$F_P + F_R = F'_P + F'_R$$

Furthermore the steric repulsion $H_{(\beta)} \cdots CH_{3(\beta)}$ ($H_{(\beta)}$ in the cation against $CH_{3(\beta)}$ in the monomer and $H_{(\beta)}$ in the monomer against $CH_{3(\beta)}$ in the cation) is negligibly small compared to steric repulsion between β -methyl groups ($CH_{3(\beta)} \cdots CH_{3(\beta)}$). This means that

$$F'_S \gg F_S$$

Thus we can estimate steric repulsion between β -methyl groups by the equation

$$F'_S = \log r_2 - \log 1/r_1$$

Estimated values of F'_S for the three pairs are around -1.0 to -1.3 . This means the rate constant of homopolymerization is depressed by a factor of $1/10^{-1/20}$ compared to the corresponding styrenes due to steric repulsion of the β -methyl group.

The steric course in the three pairs of copolymerization would not be so different that the F'_S value could be attributed to the steric effect of the β -methyl group.

Although possibilities for a penultimate effect may be expected, these are neglected in the discussion as this treatment is only a first approximation of the steric effect of the β -methyl group.

Although a steric effect of the β -methyl group of as much as $F'_S = -1.3$ should be also expected in homopropagation of anethole, it apparently can not be recognized in copolymerization of styrene and anethole. This can be interpreted to mean that the polar and resonance factors are much more important than the steric factor in this process.

References

1. Alfrey, T., Jr., J. J. Bohrer, and H. Mark, *Copolymerization*, Interscience, New York, 1952, p. 49.
2. Overberger, C. G., D. Tanner, and E. M. Pearce, *J. Am. Chem. Soc.*, **80**, 4566 (1958).
3. Hershberg, E. B., *Helv. Chim. Acta*, **7**, 351 (1934).
4. Overberger, C. G., L. H. Arnold, D. Tanner, J. J. Taylor, and T. Alfrey, Jr., *J. Am. Chem. Soc.*, **74**, 4848 (1952).
5. Matsushita, S., T. Higashimura, and S. Okamura, *Kobunshi Kagaku*, **17**, 465 (1960).
6. Okamura, S., and T. Higashimura, *Kobunshi Kagaku*, **13**, 262 (1956).
7. Okamura, S., T. Higashimura, and H. Yamamoto, *Kobunshi Kagaku*, **16**, 45 (1959).

8. Klages, *Ber.*, **35**, 2254 (1902).
9. Bert, L., *Compt. Rend.*, **213**, 873 (1941).
10. Murahashi, S., S. Nozakura, K. Tsuboshita, and Y. Kotake, *Bull. Chem. Soc. Japan*, **37**, 708 (1964).
11. Kennedy, J. P., and A. W. Langer, Jr.; *Fortschr. Hochpolymer. Forsch.*, **3**, 523 (1964).
12. Kubouchi, Y., H. Matsuo, and Yamamoto, *Kogyo Kagaku Zasshi*, **57**, 680 (1954).
13. Cross, L. H., R. B. Richards, and H. A. Willis, *Discussions Faraday Soc.*, **9**, 235 (1950).
14. Branch, G. E. K., and M. Calvin, *Theory of Organic Chemistry*, Prentice-Hall, New York, 1941, p. 192.

Résumé

On a étudié les influences stériques et électroniques du groupe méthyle en β sur la réactivité des monomères en copolymérisant des styrènes et des β -méthylstyrènes. L'empêchement stérique du groupement β -méthyle dans l'état de transition de l'homopolymérisation est si important que l'on considère que la réaction de propagation est diminuée de $1/10$ à $1/20$ par rapport à celles des dérivés correspondants du styrène. Contrairement à cela, l'empêchement stérique du groupement β -méthyle dans la réaction de propagation croisée avec le styrène est très petit. La réactivité des β -méthylstyrènes monomères est elle-même un peu plus faible que celle des styrènes correspondants. On considère que cette réactivité plus faible des β -méthylstyrènes est due à l'effet électronique du groupement β -méthyle.

Zusammenfassung

Sterische und elektronische Einflüsse der β -Methylgruppe auf die Monomerreaktivität wurden durch Kopolymerisation von Styrolen und β -Methylstyrolen untersucht. Die sterische Hinderung der β -Methylgruppe im Übergangszustand der Homopolymerisation ist so gross, dass eine Erniedrigung der Geschwindigkeit der Wachstumsreaktion bis auf $1/10$ - $1/20$ derjenigen der entsprechenden Styrolerivate angenommen wird. Im Gegensatz dazu erweist sich die sterische Hinderung der β -Methylgruppe bei der gekreuzten Wachstumsreaktion mit Styrol als sehr klein. Die Monomerreaktivität selbst von β -Methylstyrolen ist etwas kleiner als diejenige der entsprechenden Styrole. Diese erniedrigte Reaktivität der β -Methylstyrole wird auf den elektronischen Effekt der β -Methylgruppe zurückgeführt.

Received September 29, 1964

Revised January 27, 1965

Prod. No. 4637A

Solid-State Polymerization of Trioxane*

H. RAO† and D. S. BALLANTINE, *Brookhaven National Laboratory, Upton, New York*

Synopsis

Trioxane has been polymerized by irradiation with Co^{60} γ -rays in the temperature range 45–55°C. The data are extremely difficult to reproduce in spite of great precautions in sample preparation. The reaction reaches a limiting conversion, generally about 40%, but conversions as high as 96% have been observed. The viscosity of the polymer decreases with increasing conversion. Post-irradiation heating of monomer irradiated at low temperature (<30°C.) also leads to limiting conversions but much higher viscosity products. The polymerization has also been studied under pressure. Pressure applied to monomer prior to irradiation leads to higher conversions and higher viscosity polymers. In the post-irradiation polymerization technique, application of pressure after irradiation reduces the polymer yield to zero in almost every instance.

Considerable interest has been developed in the solid-state polymerization of nonvinyl type monomers following the disclosure by Okamura and co-workers that crystalline trioxane could be polymerized to a crystalline polymer.¹ The same group subsequently published additional findings on other cyclic monomers, and the reaction appears to be a fairly general one.²

It was concluded that the reaction probably proceeds by an ionic mechanism, since oxygen was found to have no effect and because the monomers investigated could not be polymerized in the liquid state by conventional free radical initiators. It has also been stated that the reaction is controlled by the crystal lattice, since the polymer is oriented in the same manner as the monomer. The present authors would agree that the crystalline arrangement of monomer units does affect the reaction to a marked degree. We should, however, like to present some recent findings which, while not in complete agreement with the results of previous workers, should be considered in any attempt to extrapolate data on trioxane to any other crystalline system.

Trioxane is a plastic crystal and is inherently disordered. It has also a high vapor pressure at the temperatures normally employed to polymerize it, i.e., 40–60°C. Because of its randomly disordered character it should be difficult to prepare identical samples. Conversely, it should be suscep-

* This work supported in part by the U. S. Atomic Energy Commission.

† Present address: Chemistry Division, Atomic Energy Establishment Trombay, Bombay, India.

tible to annealing, particularly when stored at room temperature, which is reasonably close to its melting point of 62°C. These considerations have prompted us to study the reaction under carefully controlled conditions of sample preparation. In spite of great precautions the reproducibility is so poor as to make difficult any definitive statements regarding the polymerization of trioxane.

EXPERIMENTAL PROCEDURE

Eastman Kodak trioxane was purified by vacuum sublimation or by a combination of recrystallization from methanol and sublimation.

The trioxane was degassed and sublimed a second time on a vacuum manifold. Samples of trioxane were placed in glass ampules and covered with a layer of silica gel. These were sealed on to one arm of a T-tube on the manifold; the other arm of each T-tube contained a final irradiation ampule. By suitable valving with stopcocks the final irradiation ampule was baked at 250°C. for several hours under high vacuum, the trioxane was degassed and in the last step sublimed into the final irradiation ampoule. The trioxane was sealed off under a pressure of 10^{-5} mm. In most experiments the trioxane was melted shortly before irradiation and quenched by immersing the irradiation ampule in liquid nitrogen. This final step was employed to attempt to standardize the state of the monomer during irradiation. If this was not done there was considerable difference in the size, shape, and appearance of the monomer crystals, particularly if there was a day's lapse between final sublimation and irradiation.

In the experiments on the effect of pressure, freshly sublimed trioxane was weighed into small polyethylene or nylon capsules cut specially to fit the die of the pressurizing apparatus. All the pressure studies were done in an air atmosphere.

Irradiations were performed in cobalt sources whose dosimetry was measured by Fricke dosimeters by using ASTM method D-1671-59T.

Polymer was determined gravimetrically after removing residual monomer by pumping or by solution of monomer in methanol. The polymer viscosities were determined at 60°C., 0.5 g. in 100 ml. of chlorophenol solvent containing 2% α -pinene being used. It was established that polymer solutions were stable at 60°C. for at least 8 hr.

EXPERIMENTAL RESULTS

The plots of conversion versus time are shown in Figures 1-3, from which one can deduce readily the magnitude of the reproducibility problem. Figure 4 is an Arrhenius plot of the rate data from which an activation energy of 29 kcal./mole was calculated. Also shown in Figure 3 is the conversion rate at 55°C. of trioxane crystals which were obtained by slow cooling rather than the usual quick quench in liquid nitrogen.

The viscosity of the polymers resulting from γ -induced polymerization of trioxane are shown in Figure 5. The general trend is toward lower vis-

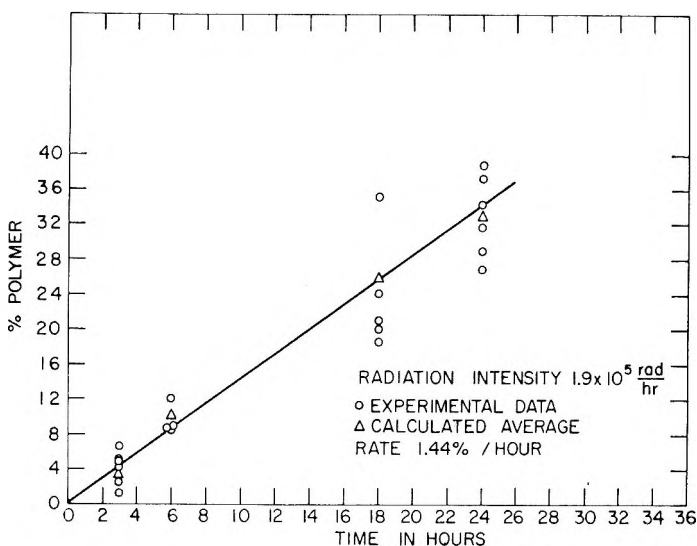


Fig. 1. Polymerization of trioxane at 45°C.

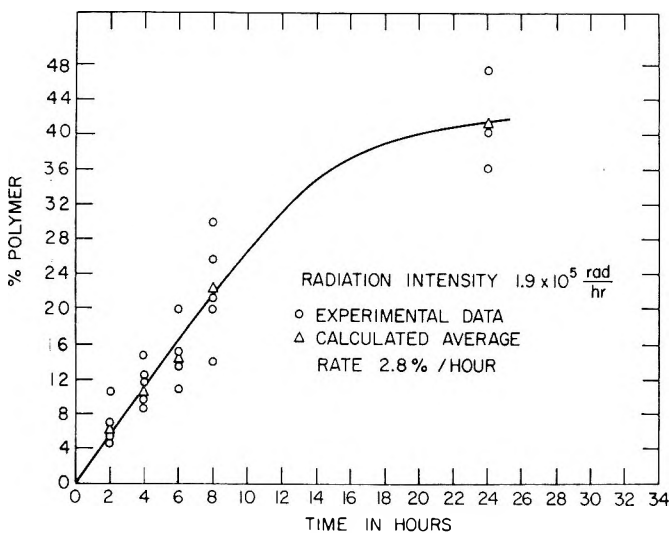


Fig. 2. Polymerization of trioxane at 50°C.

cosities at higher doses. Such a trend could be due to direct radiation decomposition of polymer formed or could be related to the kinetics of solid-state polymerization. Figure 5 also shows the change in viscosity with radiation dose of trioxane polymer which had been formed by radiation. These data suggest that radiation degradation is at least partially responsible for the decreasing viscosity. However, Table I contains data on polymer viscosities which suggest that viscosity is related to conversion. In general, for equal irradiation doses where different polymer yields were

obtained, the viscosities were lower for the sample obtained in higher yield. Such a result is more easily understood in terms of the kinetics of solid-state reaction.

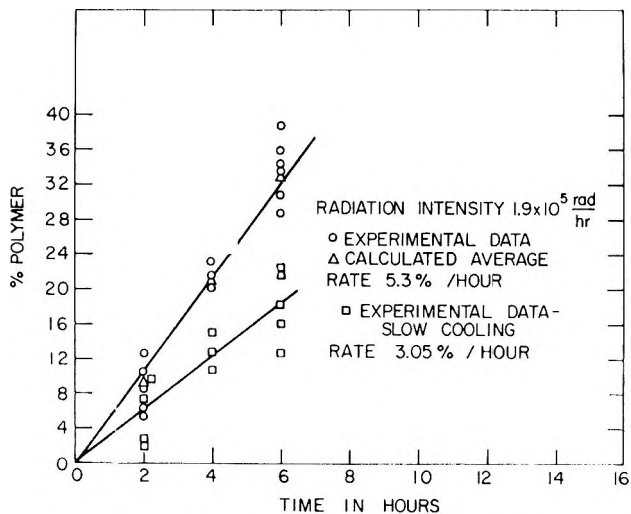


Fig. 3. Polymerization of trioxane at 55°C.

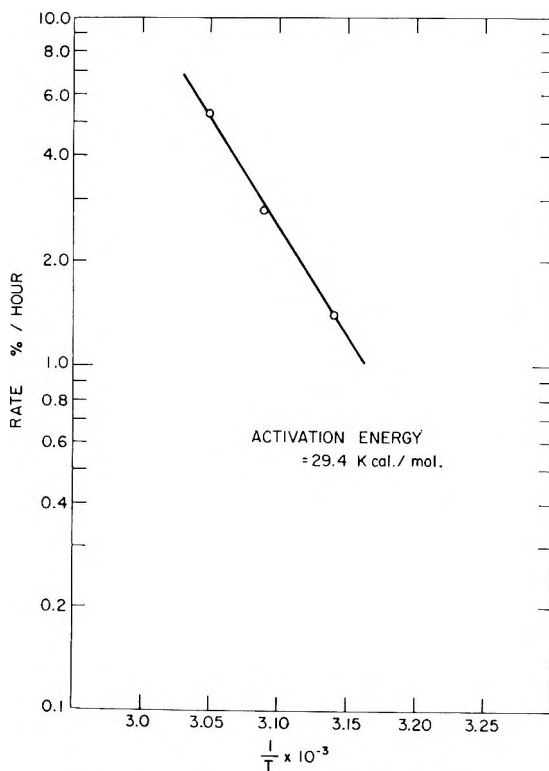


Fig. 4. Arrhenius plot of trioxane data.

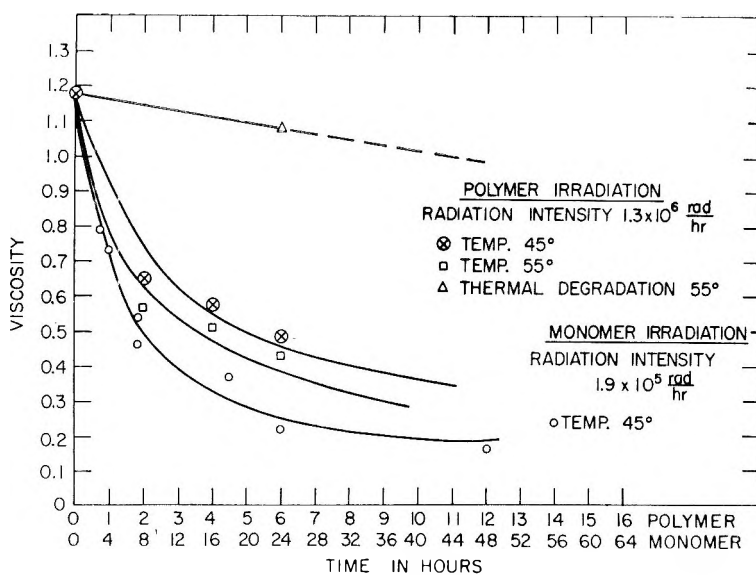


Fig. 5. Viscosity of trioxane polymers.

TABLE I
Radiation-Induced Polymerization of Trioxane^a

| Irradiation dose, rads $\times 10^5$ | Polymer yield, % | Specific viscosity, dl./g. |
|---|------------------|-------------------------------|
| 3.8-7.6 | 70-76 | 0.18 |
| 3.8-7.6 | 8.8-15 | 0.53 |

^a Temperature, 55°C.; source intensity, 22×10^5 rad/hr.

TABLE II
Post-Irradiation Polymerization of trioxane

| Irradiation temperature, °C. | Dose, Mrad | Post-irradiation heating time, at 55°C., hr. | Polymer yield, % | Specific viscosity, dl./g. |
|------------------------------------|---------------|--|---------------------|-------------------------------|
| 0 | 1 | 2 | 11.1 | 2.00 |
| 0 | 1 | 2 | 21.5 | 1.97 |
| 0 | 1 | 4 | 20.9 | 2.11 |
| 0 | 1 | 4 | 18.6 | 2.29 |
| 0 | 1 | 2 | 20.2 | 2.29 |
| 0 | 2 | 2 | 28.0 | 2.48 |
| 0 | 3 | 2 | 26.8 | 1.89 |
| -78 | 1 | 2 | 5.4 | 1.99 |
| -78 | 1 | 2 | 7.1 | 1.99 |
| -78 | 1 | 18.5 | 11.1 | 2.02 |
| -78 | 1 | 18.5 | 9.6 | 2.02 |
| -78 | 1 | 2 | 21.8 | 1.87 |
| -78 | 2 | 2 | 25.6 | 2.28 |
| -78 | 3 | 2 | 27.4 | 1.94 |

Post-Irradiation Studies

In these experiments the trioxane was irradiated at low temperatures where polymerization does not occur. After irradiation the samples were heated in thermostatted baths and the polymer isolated. The results of these studies in which the irradiation temperature, irradiation dose, and post-irradiation heating times were varied are summarized in Table II. All the samples reported in Table II were irradiated in an air atmosphere. It has been noted that when samples were irradiated in vacuum, little or no polymer was formed in the post-irradiation heating process. Even after 3.6 Mrad at 0°C. and heating for 4 hr. at 55°C. only traces of polymer were obtained. A decrease in yield was similarly reported by Japanese workers for irradiations in vacuum.³

Effect of Pressure

Since trioxane is a plastic crystal and is pliable, some experiments were conducted in which the monomer was placed under high pressures. The results summarized in Table III are for the situation where the samples were pressurized prior to irradiation and the irradiation carried out at 55°C. The general conclusion is that samples which are pressurized to 500,000 psi prior to irradiation give a higher yield and higher molecular weight than unpressurized controls. The variation of time of pressurization from 0.5 to 4 hr. had little effect on either the degree of conversion or the viscosity of the polymer. It is also evident from Table IV that there was also no significant difference between samples pressurized at 45°C. and samples pressurized at 55°C.

TABLE III
Effect of Pressurization on Trioxane Polymerization^a

| Time of pressurization, hr. | Polymer yield, % | Specific viscosity, dl./g. |
|--------------------------------|---------------------|-------------------------------|
| 0 | 14.6 | 0.55 |
| 0.5 | 18.8 | 0.91 |
| 0.5 | 11.3 | 0.96 |
| 1.0 | 17.3 | 0.93 |
| 1.0 | 18.8 | 0.97 |
| 2.0 | 17.3 | 1.02 |
| 2.0 | 16.8 | 0.93 |
| 4.0 | 11.5 | 0.91 |
| 4.0 | 8.5 | 0.92 |

^a Pressure, 5×10^5 psi; pressurization temperature, 55°C.; irradiation intensity, 1.23×10^6 rad/hr.; irradiation time, 2 hr.; irradiation temperature, 55°C.

Table V presents the results obtained when samples were first pressurized at 55°C. and 500,000 psi and subsequently polymerized by the post-irradiation technique. The most definite difference due to pressure is a significant increase in the polymer viscosity.

TABLE IV
Effect of Pressurization Temperature on Trioxane Polymerization^a

| Temperature of pressurization, °C. | Irradiation time, hr. | Polymer yield, % | Specific viscosity, dl./g. |
|--|--------------------------|---------------------|-------------------------------|
| 45 | 1 | 12.05 | 1.09 |
| 45 | 2 | 26.3 | 0.99 |
| 45 | 4 | 41.4 | 0.63 |
| 55 | 1 | 14.4 | 1.29 |
| 55 | 2 | 30.7 | 1.06 |
| 55 | 4 | 35.7 | 0.64 |

^a Pressure, 0.5×10^6 psi; pressurization time, 0.5 hr.; irradiation intensity, 191×10^6 rad/hr.; irradiation temperature, 55°C.

TABLE V
Effect of Pressure on Post-Irradiation Polymerization of Trioxane^a

| Dose, Mrad | Post-irradiation heating time, at 55°C., hr. | Polymer yield, % | Specific viscosity, dl./g. |
|----------------|--|---------------------|-------------------------------|
| 1 ^b | 2 | 11.1 | 2.00 |
| | | 21.5 | 1.97 |
| 1 | 1 | 19.5 | — |
| 1 | 1 | 20.8 | 2.83 |
| 1 | 2 | 20.2 | 2.68 |
| 1 | 2 | 26.3 | 2.75 |
| 1 | 3 | 29.4 | 3.68 |
| 1 | 3 | 26.4 | — |

^a Pressure, 5×10^6 psi; time of pressurization, 0.5 hr.; temperature of pressurization, 55°C.; irradiation temperature, 0°C.; irradiation intensity, 2.2×10^6 rad/hr.; total radiation dose, 1 Mrad.

^b Unpressurized control.

TABLE VI
Effect of Pressure Studied on Trioxane Polymerization^a

| Pressure, psi $\times 10^{-3}$ | Pressurization temperature, °C. | Polymer yield, % |
|-----------------------------------|------------------------------------|---------------------|
| 5 | 55 | 0 |
| 5 | 55 | 0 |
| 24 | 55 | 0 |
| 24 | 55 | 0 |
| 5 | 20 | 1.04 |
| 5 | 20 | 1.77 |
| 24 | 20 | 3.54 |
| 24 | 20 | 1.34 |
| 5 | -78 | 1.4 |
| 5 | -78 | 1.0 |

^a Radiation intensity, 2.2×10^6 rad/hr.; irradiation dose, 3.5 Mrad; irradiation temperature, 0°C.; pressurization time, 0.5 hr.; post-irradiation heating time, 1 hr.; post irradiation temperature, 55°C.

Another series of experiments included the operational sequence of irradiation at 0°C., pressurization at varying temperatures, and post-irradiation heating at 55°C. These results are summarized in Table VI.

Finally, Table VII contains results for samples irradiated at 0°C. and pressurized to 500,000 psi during the post-irradiation heating step.

The effect of pressure on the decomposition of separated polymer is shown in Table VIII. The trioxane polymer used was prepared by irradiation, any unreacted monomer being removed by sublimation.

TABLE VII
Pressure Effect on Post-Irradiation Polymerization of Trioxane^a

| Pressure, psi $\times 10^{-3b}$ | Post-irradiation heating and pressurization time, hr. | Polymer yield, % |
|------------------------------------|---|---------------------|
| — | 0.5 | 10.0 |
| — | 0.5 | 8.1 |
| — | 1.0 | 11.1 |
| — | 1.0 | 12.2 |
| 500 | 0.5 | 0 |
| 500 | 0.5 | 0 |
| 500 | 1.5 | 0 |

^a Irradiation intensity, 2.2×10^5 rad/hr.; irradiation dose, 3.2 Mrad; irradiation temperature, 0°C.; post-irradiation heating and pressurization temperature, 55°C.

^b Pressure applied during the post-irradiation heating.

TABLE VIII
Effect of Pressure on Trioxane Polymer Decomposition^a

| | Viscosity | |
|---------------|-----------|----------------------|
| | Initial | After 2 hr. at 55°C. |
| Unpressurized | 0.8 | 0.55 |
| Pressurized | 0.73 | 0.63 |
| Pressurized | 0.71 | 0.59 |

^a Pressure, 5×10^5 psi; time of pressurization, 1½ hr.; temperature of pressurization, 55°C.; radiation intensity, 1.23×10^5 rad/hr.; irradiation time, 2 hr.; irradiation temperature, 55°C.

DISCUSSION

One of the salient and disturbing features of the polymerization of trioxane is the great difficulty in obtaining reproducibility. Trioxane has an appreciable vapor pressure at room temperature and recrystallizes very quickly on standing. It is also known that the monomer crystal is inherently disordered. It seems obvious that the character of the monomer crystal will be affected by its manner of preparation. In the present study great care has been taken to reproduce the condition of the monomer at the time of irradiation. Therefore, monomer samples were melted and

quenched shortly before irradiation in the hope that a reproducible initial state would be obtained. In spite of the precautions, the scattered data in Figures 1-3 are typical, yet no mention is made in previous papers on this subject of reproducibility.

In this study monomer samples have been analyzed by gas chromatography and found to be >99.9% pure. Since formaldehyde is known to initiate polymerization of trioxane⁴ a special effort was made to identify it, but only trace quantities were detected after the usual method of monomer purification.

We feel that the reproducibility problem is more a reflection of the disordered character of the monomer itself, since it is known that there is a tendency toward random disorder in forming crystals of this type. The role of disorder is suggested, in spite of the scatter of experimental results, in Figure 3, where results of slowly cooled and shock-cooled thioxane are compared. The rate is consistently higher for the shock-cooled material. This result is somewhat opposite to the findings of Okamura, who reported higher yields for slowly grown large crystals.³ The present results are consistent with previous work on acrylamide for which case it was suggested that sites of defects were favored locations for initiation of the polymerization process.⁵

Another characteristic of this system which has also been observed by previous workers is the failure of the trioxane to undergo complete polymerization. Some limiting conversion is normally reached, usually in the range 40-50%. However, in occasional instances, conversions of about 90% are observed without any clearcut correlation to manner of preparation. It has been suggested that beyond a certain radiation exposure depolymerization occurs, and that the limiting conversion can be attributed to this reverse reaction. In fact, a reduction in yield for radiation exposure beyond this "limiting conversion" has been reported and attributed to depolymerization.⁶ The present studies do not indicate any significant degradation to monomer over the time scale of the radiation exposures employed. In this experiment samples of polymer were irradiated at 55°C. for doses of about 3 Mrad and the weight loss determined by weighing the irradiated polymer after lengthy evacuation. The loss was limited to less than 5%. We do confirm the decrease in viscosity with increasing conversion or exposure. It is possible that the decreased viscosity is due to polymer degradation, since exposure of separated polymer resulted in decreased viscosities, as shown in Figure 5. However, we do feel that this is only part of the explanation. Invariably, in any single series of experiments, higher conversion samples give lower viscosity polymers. Therefore, on numerous occasions several samples given similar doses had widely different yields. In each case the higher conversion sample gave lower viscosity. This suggests a kinetic effect due to a higher initiation rate in the case of high conversion and low viscosity. Such a result is easy to explain in terms of an initiation step which is related to disorder or crystalline defects.

The effects of pressure on the reaction of trioxane are interesting, since opposite effects are obtained depending on whether pressure is applied before or after irradiation. If the samples are first pressurized and then irradiated, the general effect is a trend toward higher yields and higher viscosity polymers. These results are shown in Tables III and IV.

If samples are pre-irradiated at low temperature and pressure applied during the post-irradiation heating step, then no polymer is observed, as the data in Table VII indicate. Similarly, if the pressure is applied after low temperature irradiation but before the post-irradiation heating step, no polymer is obtained. This is indicated in Table VI.

In the absence of definitive physical structure measurements one can only speculate on the reasons for the pressure effect.

If we consider the situation where trioxane is preirradiated at 0°C. (Table II), it is certain that the radiation produces a stable reactive intermediate, presumably a radical pair or an ion pair. When such species are subsequently heated, a propagation reaction occurs and polymer is formed. However, if pressure is applied before or during the heating process, the original ion or radical pair can recombine (Tables VI and VII). This recombination and the mobility of active species which this necessarily implies could be associated with a phase change induced by application of pressure. Such a phase change, if it exists, is easy to effect, since there is little difference in results whether samples are pressurized for 0.5 or 1.5 or 4 hr. (Table VII). Also, as little as 5000 psi seems to be sufficient to inhibit the reaction in the experiments noted in Table VI. Bamford et al.⁷ have shown an effect of pressures as small as 50 psi in the solid-state polymerization of acrylic and methacrylic acid.

One could attribute the inhibiting effect of pressure in these cases to a transformation of the crystal under pressure to a nonreactive orientation of monomers. However, this is difficult to reconcile with the significant positive effect of pressure that is found when the samples are pressurized prior to irradiation.

It may be misleading to compare the preirradiation experiments with the others, since it has been suggested recently that the reactions resulting from the two techniques proceed via different mechanisms.³ The evidence for this rests primarily on the fact that oxygen has little effect during the in-source reaction but is essential for the preirradiation case.

The application of pressure before irradiation can be pictured as a physical orienting or ordering force acting to align molecules in a manner conducive for propagation. This is not necessarily a contradiction of the previous comments which suggested that higher rates and lower viscosity might be related to the number of defects present in the monomer. The observed rate and viscosity are actually a function of the number of growing chains and the length to which a chain grows before it terminates. Pressure can affect the initiation in a negative sense by removing defect sites, but, contrawise, the order imposed may permit the chain to grow to a greater degree before terminating.

The authors wish to express their gratitude to Drs. M. Prince and C. Marsel of the College of Engineering of New York University for their generous cooperation in making available the use of high pressure equipment. We also wish to acknowledge the advice and assistance of Dr. G. Adler of Brookhaven National Laboratory in the discussion of this work.

References

1. Okamura, S., K. Hayashi, and Y. Nakamura, *Isotopes Radiation*, **3**, 510 (1960).
2. Okamura, S., and K. Hayashi, *Makromol. Chem.*, **47**, 230 (1961).
3. Hayashi, K., H. Ochi, and S. Okamura, *J. Polymer Sci.*, **A2**, 2929 (1964).
4. Jaacks, V. K., and W. Kean, *Makromol. Chem.*, **52**, 37 (1962).
5. Adler, G., *J. Chem. Phys.*, **31**, 848 (1959).
6. Okamura, S., K. Hayashi, and Y. Kitamishi, *J. Polymer Sci.*, **58**, 925 (1962).
7. Bamford, C. H., G. C. Eastmond, and J. C. Ward, *Nature*, **192**, 1036 (1961).

Résumé

Le trioxane a été polymérisé par irradiation au moyen des rayons gamma du Co^{60} dans un domaine de température situé entre 45 et 55°C. Les résultats sont très difficiles à reproduire en dépit des grandes précautions prises dans la préparation de l'échantillon. La réaction atteint une conversion limite, généralement située aux environs de 50%, mais on a observé des conversions de 96%. La viscosité du polymère diminue lorsque la conversion augmente. La chaleur dégagée par la post-irradiation du monomère irradié à basse température (<30°C) conduit également à des conversions limitées mais les produits formés possèdent une viscosité beaucoup plus élevée. On a également étudié la polymérisation sous pression. La pression appliquée au monomère avant l'irradiation donne des conversions plus élevées et des polymères possédant une viscosité plus élevée également. Dans la technique de polymérisation par post-irradiation l'application de pression après irradiation réduit le rendement en polymère à zéro dans la plupart des cas.

Zusammenfassung

Trioxan wurde durch Bestrahlung mit Co^{60} γ -strahlung im Temperaturbereich 45–55°C polymerisiert. Trotz grosser Vorsichtsmassnahmen bei der Probenherstellung sind die Ergebnisse nur äusserst schwierig zu reproduzieren. Die Reaktion erreicht einen Grenzumsatz, im allgemeinen etwa 80%, es wurden jedoch auch Umsätze bis zu 96% beobachtet. Die Viskosität des Polymeren nimmt mit steigendem Umsatz ab. Erhitzung des bei tiefer Temperatur (<30°C) bestrahlten Monomeren nach der Bestrahlung führt ebenfalls zu einem Grenzumsatz, jedoch zu Produkten mit viel höherer Viskosität. Die Polymerisation wurde auch unter Druck untersucht. Druckbelastung des Monomeren vor der Bestrahlung führt zu höheren Umsätzen und zu Polymeren mit höherer Viskosität. Bei der Nachbestrahlungspolymerisation setzt die Anwendung von Druck nach der Bestrahlung die Polymerausbeute in fast allen Fällen auf Null herab.

Received January 6, 1965

Prod. No. 4646A

Polymer Production from Aqueous Solutions of D-Glucose by High-Energy Radiation

JOHN B. SNELL, *The Institute of Paper Chemistry,
Appleton, Wisconsin*

Synopsis

Polymeric material was produced by passing aqueous glucose solutions under a beam of high energy electrons. The yield of polymer increased with dose and dose rate. The weight-average molecular weights of polymers formed at 40 Mrad, measured by light scattering, ranged from 9,800 to 5,000,000. The polymers exhibited very low intrinsic viscosities in water, and are therefore thought to be highly branched. Measurement of the number-average molecular weight of one of the polymers by osmometry established an \bar{M}_w/\bar{M}_n ratio of 4.9, indicating a fairly broad distribution of molecular weights within the polymer. One polymer was fractionated on Sephadex and the chemical composition of the fractions compared. The carboxyl content increased regularly with molecular weight, suggesting that the carboxyl groups were the result of secondary oxidative attack. Hydrogen and oxygen contents decreased with increasing molecular weight. Elemental analysis and infrared spectral data on the fractions were consistent with the hypothesis that gluconolactone was incorporated into the polymer in the early stages of formation. Chromophoric groups, perhaps of the endiol type, were formed, and oxygen-rich fragments were apparently lost as the molecular weight of the polymer increased. Oxygen contents, on the other hand, decreased with increasing molecular weight. The regularity observed in the fraction analyses suggested that the polymerization followed a pattern, and was not the result of the random joining of unlike fragments. Elemental analysis and infrared spectral data on the fractions were consistent with the hypothesis that gluconolactone was incorporated into the polymer in the early stages of formation. Chromophoric groups, perhaps of the enediol type, were formed, and oxygen-rich fragments were apparently lost as the molecular weight of the polymer increased.

INTRODUCTION

Recent work by Barker et al.¹ indicated that a high yield of nondialyzable material could be obtained by irradiating deaerated aqueous solutions of glucose with γ -rays from a Co⁶⁰ source. Treatment of a 0.1% solution to 7.10 Mrad at 610 rad/min. gave 45% nondialyzable material.* No physical measurements were made on the material; instead the authors devoted their work to a chemical characterization of the polymer. They found the material to be acidic, having an equivalent weight of 328, or a carboxyl content of 13.7%. The polymer was resistant to acid hydrolysis,

* A rad is defined as the absorption of 100 ergs of energy per gram of material irradiated; a megarad is 10⁶ rads.

and in fact, a portion of it precipitated in the hot acid. The precipitate had an infrared absorption spectrum similar to that of the original polymer, and the soluble portion showed no mobile components upon paper chromatography.

From the above information the authors concluded that the polymeric linkage was neither that of a glycoside nor an ester. Instead, they proposed a carbon-carbon linkage similar to that formed upon irradiation of alcohols.^{2,3} The proposed mechanism involved the production of hydrogen and hydroxyl free radicals from the water, which in turn abstracted hydrogen atoms from the carbohydrate. Coupling of the sugar free radicals was then thought to produce the polymer. A similar mechanism has been used to explain polymer production from mannose,⁴ sorbitol,⁵ and glycolic acid.⁶

Since a high yield of gluconic acid was obtained from glucose in another study,⁷ and a high yield of polymer was obtained from gluconolactone, Barker et al.¹ suggested that the main route of polymerization was through gluconic acid. In a later paper, Barker, Lloyd, and Stacey⁸ proposed that in the early stages of polymerization, the repeating unit was gluconic acid, which upon further irradiation would undergo radiation damage to give a heterogeneous polymer.

This paper concerns the size and shape of the molecules produced upon irradiation of aqueous glucose solutions. In addition, one of the polymers was fractionated by molecular weight and the chemical composition of the fractions compared to yield information on the structure of the polymer.

EXPERIMENTAL

Radiation Source

All irradiations were conducted by the High Voltage Engineering Corporation. A linear accelerator was used for most of the work, but a Van de Graaff accelerator was used for one run. The linear accelerator produced a pulsed beam of 8.5 M.e.v. electrons, while the Van de Graaff produced a steady beam of 1.5 M.e.v. electrons. With both machines, the samples were placed on a conveyor belt and repeatedly passed under a magnetically scanned beam until the desired dose was built up.

Cobalt glass dosimetry, which had previously been calibrated by Argonne National Laboratories, was used with the linear accelerator. Blue cellophane, poly(vinyl chloride), and the Faraday cup were used with the Van de Graaff.

Preparation of Solutions for Irradiation

Polyethylene bag "pillows" were used as containers for the solutions in most of the work because they enabled treatment of a large volume of solution at a minimum sample thickness. The deaerated glucose solutions were prepared by boiling 1.0% glucose solutions at 100°C. for about 5 min. The flasks were stoppered, cooled to room temperature, and placed in a

nitrogen box. Oxygen was removed from the atmosphere of the box until the atmosphere gave an Orsat analysis for oxygen of approximately zero. The polyethylene bags, which had previously been placed in the nitrogen box, were each filled with 400 ml. of solution and closed by heat sealing. Since lower energy electrons were used with the Van de Graaff accelerator, 100 ml.-portions were placed in these bags to reduce the sample thickness. Before the bags were removed from the nitrogen box, they were sealed in larger polyethylene bags. This provided an atmosphere of nitrogen around the small bags and therefore cut down the rate of diffusion of oxygen into the solutions enroute to the radiation source. Also, just before the bags were removed from the nitrogen box, one bag was opened, and the oxygen content of the solution measured by the short Theriault modification of the Winkler test.⁹ The oxygen content of the deaerated solutions was generally less than 1 ppm.

In the study of the effect of oxygen on the yield of polymer, glass tubes were used for containers since polyethylene is known to be somewhat permeable to oxygen. The glass tubes were alternately evacuated and filled with nitrogen three times, and then filled with 75 ml. of deaerated solution. The tubes were then sealed off in a gas flame.

Yield of Nondialyzable Material

To determine the yield of nondialyzable material, 25-ml. aliquots of the irradiated solutions were placed in bags of dialyzer tubing (seamless cellulose tubing; Fischer Scientific Company). All dialyzer tubing was taken from the same roll to minimize the variation of pore size between pieces of tubing. The bags were immersed in 300 ml. of water which was changed daily.

Isolation of Polymers

The polymers were isolated for characterization by precipitation with ethanol. The 500-ml. aliquots of the whole irradiated solution were concentrated almost to dryness, and then redissolved in approximately 10 ml. of water. Then 450 ml. of absolute ethanol was added to precipitate the polymer. The 45/1 ratio of ethanol to water was used to maximize the yield of polymer without precipitating glucose. The resulting flocculent precipitate was separated by centrifugation and then washed twice with 20 ml. of each of the following: 45/1 ratio of ethanol-water solution, absolute ethanol, absolute diethyl ether, and low boiling petroleum ether. A few drops of hydrochloric acid were added to aid precipitation during the washing steps.

Light Scattering

Water was used as a solvent for most of the light-scattering work because a suitable organic solvent could not be found. In order to investigate the possibility of aggregation in water, one measurement was made in

dimethyl sulfoxide containing 2% water to reduce the rate of moisture absorption.

The solvent was clarified by repeated filtration under pressure through a 2500 A. pore size Polypore filter. For the highest molecular weight polymer, the solvent exhibited a turbidity less than 1% of the turbidity of a 0.1% solution. For the lowest molecular weight polymer, the turbidity of the solvent was usually about 6% that of a 1.0% solution. The dissymmetry of the clarified water was generally in the range of 1.2 to 1.8. The dissymmetry of the polymer solutions lay in the range 1.05-1.20.

Solutions of the polymers were made up to approximately 1.0% in distilled water and then centrifuged in a laboratory centrifuge equipped with a high-speed head which produced a centrifugal force of about 12,000*g*. The solutions were carefully removed from the centrifuge cells with a syringe, and placed in the Polypore filtering apparatus. The solutions were filtered through 4500 A. pore size Polypore filters five times, the last filtration being made directly into the light-scattering cell.

Light-scattering measurements were made on Brice-Phoenix photometer (Series 1937) with 546 m μ wavelength light. The performance of the instrument was checked with a sample of polystyrene of known molecular weight.

The refractive index gradient was measured, in most cases, on a Rayleigh interferometer (Baird Associates, Cambridge, Mass.) at 546 m μ . Interference fringes were matched at four concentrations. The refractive index gradient of the highest molecular weight polymer was measured with a Bausch and Lomb dipping refractometer, since these solutions exhibited too much color for accurate alignment of the fringes on the Rayleigh interferometer.

Molecular weights were calculated by Debye's method of dissymmetry.^{10,11} Values of $1/P_{90}$ were obtained from the tables of Beattie and Booth.¹² A spherical model was chosen because the viscosity data suggested a highly branched, compact molecule, and a model for such a polymer was not available. Since the lowest molecular weight polymer exhibited appreciable fluorescence, the scattering ratio in this case was corrected for fluorescence by Brice's method.¹³

Osmometry

A Mechrolab Model 501 high speed membrane osmometer was used for all osmotic pressure measurements. In addition to greatly increasing the speed of measurement, it is believed the dynamic method increases the accuracy of measurement where molecules are present which can permeate the membrane.^{14,15} In order to minimize the effects of diffusion, readings were taken within 5 min. after introduction of the sample, and the reference reading for the solvent was redetermined after each measurement. A B-20 membrane (50 A. pore size) from the Schleicher and Schuell Company, Keene, New Hampshire was used.

In order to reduce the polyelectrolyte effect, the polymers were dissolved in 0.33*N* potassium chloride and neutralized to approximately pH 7 with a few drops of 0.1*N* potassium hydroxide. All solutions were made up by weight.

Molecular weights were calculated from van't Hoff's law using values of π/c extrapolated to zero concentration.

Viscometry

Viscosities were measured at $30.0 \pm 0.005^\circ\text{C}$. in an Ubbelohde viscometer, Cannon size 50, of the small volume type. Since the difference in efflux time between the solutions and solvent was a mere 2–3 sec. for most solutions, it was necessary to scrupulously clean the viscometer before each measurement in order to obtain reproducible results.

Fractionation

Fractionation was performed on Sephadex, manufactured by AB Pharmacia, Uppsala, Sweden. A 100-ml. aliquot of an aqueous solution containing 1.56 g. of polymer 1 (see Table I) was placed on a $4\frac{1}{2} \times 15$ in. column of Sephadex G-25 and elution started with distilled water. Solute started to appear in the effluent after 1260 ml., the void volume of the column. Ten 200-ml. fractions were collected, which accounted for 95.4% of the solids placed on the column.

Analysis of the Fractions

The solids content of each fraction was determined by evaporation of an aliquot to dryness. The polymers in each fraction were isolated by freeze-drying and the molecular weights measured by light scattering and osmometry.

Carbon and hydrogen were measured on the fractions as carbon dioxide and water, respectively. Oxygen was calculated by difference.

Infrared absorption spectra were run in KBr pellets on a Perkin-Elmer Model 21 recording spectrophotometer.

Ultraviolet absorption spectra were measured in aqueous solution on a Beckman DK-2 recording spectrophotometer.

Carboxyl groups were measured by potentiometric titration with 0.01*N* NaOH at room temperature. Nitrogen was passed over the solutions during titration.

RESULTS AND DISCUSSION

Effect of Dose

The yield of polymer, measured as either the amount of nondialyzable material, the amount of ethanol precipitate, or the amount of immobile material on a paper chromatogram, increased with dose. Work on polymers isolated by ethanol precipitation indicated that the average molecular

weight increased as the yield of ethanol precipitate increased. Therefore, it appears that the molecular weight of the polymer increases with dose.

Infrared absorption spectra showed the carbonyl absorption in the region 1760–1720 cm.^{-1} to increase with dose also.

Dose Rate

The effect of different dose rates on the yield of polymer is shown in Table I. It can be seen that increasing the dose rate by increasing the frequency of the passes under the electron beam increased the yield of polymer. Increasing the dose rate would be expected to increase the concentration of hydrogen and hydroxyl free radicals in solution, which in turn would increase the concentration of sugar free radicals. This would make coupling of the free radicals more likely, and hence increase the yield of polymer. The high yield of polymer from the Van de Graaff treatment can be accounted for by a similar explanation. The steady beam of the Van de Graaff would tend to give a higher concentration of free radicals than a pulsed beam, and also the rate of energy loss per unit path length is greater for the 1.5 M.e.v. electrons of the Van de Graaff than for the 8.5 M.e.v. electrons of the linear accelerator.

TABLE I
Effect of Dose Rate on Yield

| Sample no. | Dose rate | Total dose, Mrad | Nondialyzable material, % |
|----------------|-------------------------------|------------------|---------------------------|
| 4 | 1 Mrad/pass; 1 pass/5.5 min. | 20 | 0.8 |
| 5 | 1 Mrad/pass; 1 pass/0.78 min. | 20 | 2.7 |
| 6 | 4 Mrad/pass; 1 pass/3.12 min. | 20 | 2.8 |
| 1 | 1 Mrad/pass; 1 pass/5.5 min. | 40 | 3.8 |
| 7 | 2 Mrad/pass; 1 pass/5.5 min. | 40 | 3.2 |
| 2 | 1 Mrad/pass; 1 pass/0.77 min. | 40 | 21.3 |
| 8 | 2 Mrad/pass; 1 pass/0.6 min. | 40 | 28.7 |
| 3 ^a | 1 Mrad/pass; 1 pass/0.64 min. | 40 | 60.0 |

^a Irradiation conducted on the Van de Graaff accelerator; all others on the linear accelerator.

The other factor that must be considered in analyzing the effect of dose rate is that the heat built up in the samples was greater at the higher dose rates. All irradiations were conducted at ambient temperature, with no temperature control. Higher temperatures would be expected to increase the mobility of the sugar radicals, and thus make coupling more likely.

The molecular weights of three polymers each made at 40 Mrad but at different dose rates are given in Table II. The same explanation concerning the concentration of free radicals used for the effect on yield can be used to explain the effect of dose rate on molecular weight.

TABLE II
Effect of Dose Rate on Yield and Molecular Weight

| Polymer | Dose rate | Total dose, Mrad | Yield (ethanol ppt.), % | Light-scattering molecular weight |
|----------------|-------------------------------|------------------|-------------------------|-----------------------------------|
| 1 | 1 Mrad/pass; 1 pass/5.5 min. | 40 | 10.2 | 9,800 |
| 2 | 1 Mrad/pass; 1 pass/0.77 min. | 40 | 16.6 | 140,000 |
| 3 ^a | 1 Mrad/pass; 1 pass/0.64 min. | 40 | 41.8 | 5,000,000 |

^a Irradiation conducted on the Van de Graff accelerator.

Oxygen Content of the Solutions

Small amounts of dissolved oxygen in the solution (i.e., up to 8 ppm) did not affect the yield of nondialyzable material significantly under the irradiation conditions used in this work. Apparently, at the high doses and dose rates employed, the small amounts of dissolved oxygen were used up early in the process, and subsequent reactions occurred as if oxygen were absent.

Glucose Concentration

The per cent yield dropped by a factor of approximately 10 in going from a 1% to a 10% glucose solution. This is the result predicted for an indirect mechanism where the radiation decomposes the solvent molecules and the resulting products attack the solute molecules.¹⁶

Molecular Weight

The molecular weights, along with the intrinsic viscosities, for three of the polymers formed at 40 Mrad are given in Table III. The light-scattering measurements indicated that the polymers were of much higher molecular weight than had been anticipated from earlier work. Barker, Lloyd, and Stacey¹⁷ suggested that, on the basis of viscosity measurements, their polymer had a molecular weight in the range of 1200–4000. This was a very rough approximation, for, as they pointed out, no reliable constants were available for estimation of molecular weight from viscosity data.

A typical light-scattering plot is presented in Figure 1. Very low second virial coefficients were obtained for the polymers in water, indicating very

TABLE III
Molecular Weight and Viscosity Data on Whole Polymers

| Polymer | dn/dc | Z | Molecular weight (light scattering) | $[\eta]$, dl./g. |
|---------|---------|------|-------------------------------------|-------------------|
| 1 | 0.166 | 1.1 | 9,800 | 0.024 |
| 2 | 0.200 | 1.6 | 140,000 | 0.026 |
| 3 | 0.215 | 2.35 | 5,000,000 | 0.205 |
| 3 | -0.135 | 1.6 | 2,500,000 ^a | |

^a Measured in 98% dimethyl sulfoxide; all others in water.

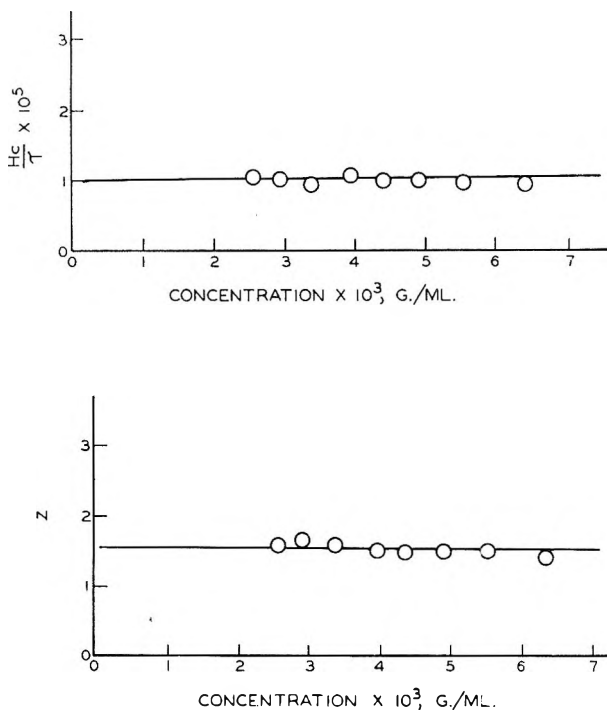


Fig. 1. Typical light-scattering results (polymer 2 in water).

little polymer-solvent interaction. In fact, in many plots a slightly negative second virial coefficient was obtained, suggesting the possibility of aggregation.¹⁸ In order to check this possibility, the molecular weight of polymer 3 was measured in 98% dimethyl sulfoxide. The fact that a molecular weight of 2,500,000 was obtained in 98% dimethyl sulfoxide in comparison to 5,000,000 in water indicates that although aggregation did occur in water, the polymer is indeed of very high molecular weight. A higher second virial coefficient was also obtained in 98% dimethyl sulfoxide.

The values of dn/dc in Table III are seen to increase with molecular weight, reflecting a change in the chemical composition with molecular weight. The same result was found with the fractions of polymer 1, which will be discussed later.

A test on polymers 2 and 3 indicated a negligible amount of fluorescence. However, polymer 1, the lowest molecular weight polymer, exhibited a great deal of fluorescence. Therefore, for this polymer, the 90° scattering ratios were corrected for fluorescence by the method of Brice et al.¹³ The fact that polymer 1 exhibited fluorescence and polymers 2 and 3 did not is puzzling, although Moacanin et al.¹⁹ did notice that fluorescence was greater for low than for high molecular weight lignosulfonate molecules. This appears to be true for the present system.

The number-average molecular weight of polymer 1, measured on the membrane osmometer, was 2000. This value is far below that usually

measured on a membrane osmometer, but its accuracy was confirmed by measurement on a vapor pressure osmometer.²⁰ Since the weight-average molecular weight was 9800, this gives an \bar{M}_w/\bar{M}_n ratio of 4.9, which is quite reasonable for branched molecules.²¹⁻²²

Evidence for Branching

Although the polymers had high light-scattering molecular weights, they had very low intrinsic viscosities, as shown in Figure 2. Similar results have been found by other workers. For example, Goring²⁴ obtained an intrinsic viscosity of 0.08 dl./g. for a dioxane-hydrochloric acid lignin molecule of 50,000 molecular weight in pyridine. Similarly, Greenwood and Robertson²⁵ report an intrinsic viscosity of 0.10 dl./g. for glycogen of 4,800,000 molecular weight in 1.0*N* potassium hydroxide.

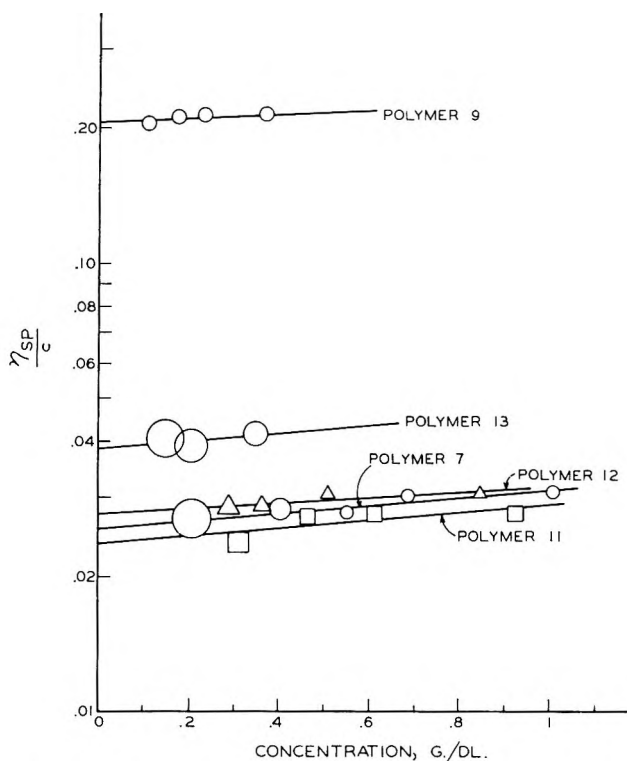


Fig. 2. Viscosity data on polymers in water at $30.000 \pm 0.005^\circ\text{C}$.

Polyelectrolyte Behavior

A marked polyelectrolyte effect was encountered in osmometry as shown in Figure 3. When polymer 1 was dissolved in water, the π/c versus c curve increased with dilution and became asymptotic to the ordinate at low concentrations. Apparently, hydrogen ions dissociated from the carboxyl groups as dilution proceeded and acted as separate osmotic species.

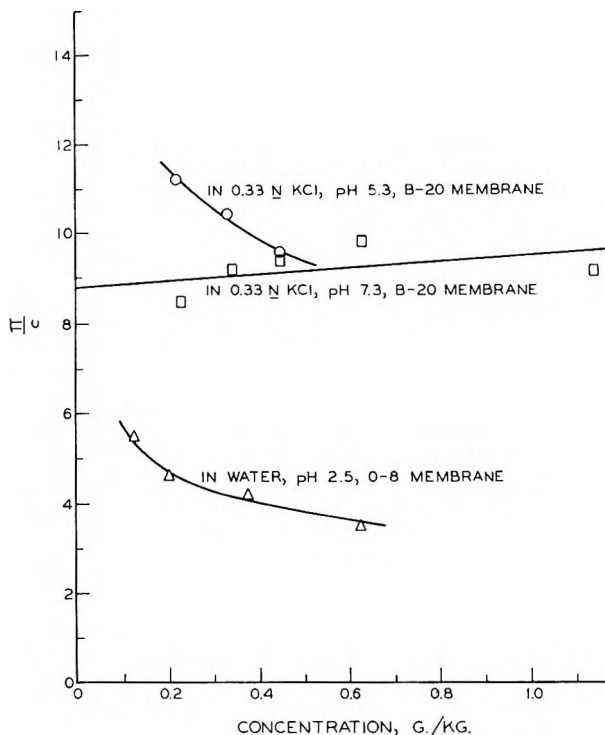


Fig. 3. Osmotic pressure data on polymer 1, fraction 3. The curve for the water solution is below the others because a more porous membrane was used which led to diffusion and a large Staverman effect.

When the polymer was dissolved in 0.33*N* potassium chloride and neutralized to approximately pH 7, normal π/c versus c curves were obtained.

Light-scattering measurements were taken on fraction 2 of polymer 1 under three conditions: (1) dissolved in water, (2) dissolved in 0.33*N* potassium chloride, and (3) dissolved in 0.33*N* potassium chloride and neutralized to pH 7.8. Since the molecular weights obtained in the presence of salt were not greatly different than those in the absence of salt and greater negative second virial coefficients were obtained, the use of salt was discontinued.

Although no attempt was made to suppress the polyelectrolyte effect with salt, the linear plots in Figure 2 suggest that polyelectrolyte effects upon viscosity were negligible. Apparently, the molecules are too highly branched and compact to expand significantly during dilution.

Fractionation

The solids distribution obtained upon fractionation of polymer 1 is shown in Figure 4.

The molecular weights of the fractions were measured by light scattering and osmometry. The results are summarized in Table IV, and the osmom-

etry data are given in Figure 5. The fractions after fraction 5 contained too little material for molecular weight determinations, but it is anticipated that they would follow the same trend established in the first five fractions. The high dissymmetry found for fraction 4 is thought to be due to the fact

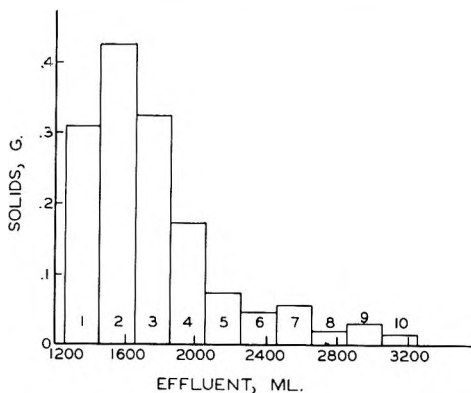


Fig. 4. Fractionation of polymer 1 on Sephadex G-25.

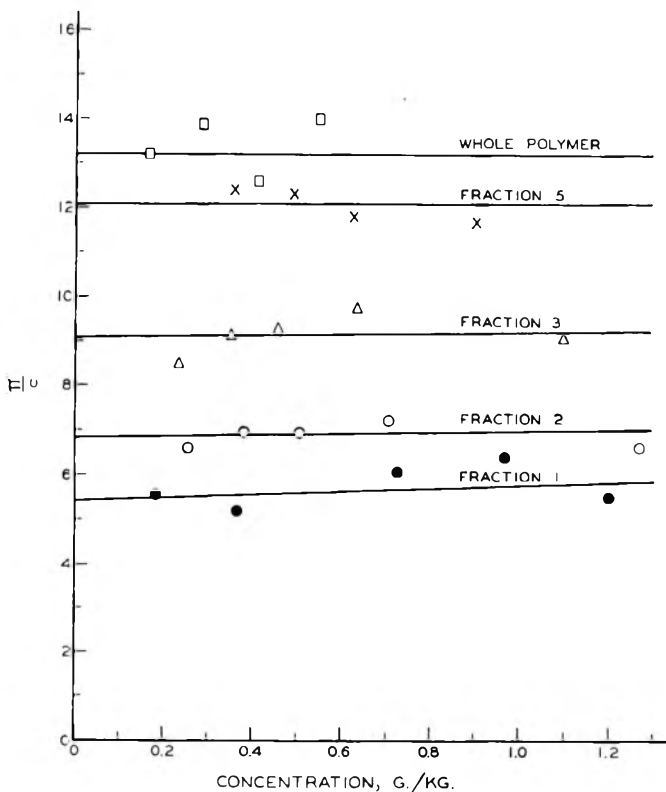


Fig. 5. Osmotic pressure data on fractions of polymer 1. All solutions were in 0.33N KCl and neutralized to approximately pH 7.

that very high sensitivity settings were required for this low molecular weight material, thus making the readings very sensitive to small amounts of dust. The light-scattering molecular weight for fraction 4 should therefore be discounted.

TABLE IV
Molecular Weight Determinations on Fractions of Polymer 1

| Fraction | Yield, g. | dn/dc | Z | \bar{M}_w (light scattering) | \bar{M}_n (osmometry) |
|------------------|--------------|---------|------|--------------------------------------|----------------------------|
| 1 | 0.3100 | 0.185 | 1.10 | 13,000 | 4,900 |
| 2 | 0.4260 | 0.167 | 1.25 | 12,000 | 3,800 |
| 3 | 0.3240 | 0.165 | 1.05 | 4,200 | 2,900 |
| 4 | 0.1740 | 0.163 | 2.00 | 21,000 | |
| 5 | 0.0780 | | | | 2,200 |
| Whole polymer | | 0.166 | 1.10 | 9,800 | 2,000 |

The values of dn/dc in Table IV increase with molecular weight, reflecting a consistent variation in chemical composition among the fractions. These changes will be discussed later.

The osmometry data of Table IV clearly indicate that fractionation by molecular weight was obtained on the Sephadex column. The ratios of \bar{M}_w/\bar{M}_n for the fractions are in the range of about 1.4–3.2, and are therefore less than the ratio of 4.9 for the whole polymer.

The chemical properties of the fractions were studied in an attempt to further elucidate the structure of the polymer. It is assumed that the higher molecular weight material was formed by accretion of smaller units

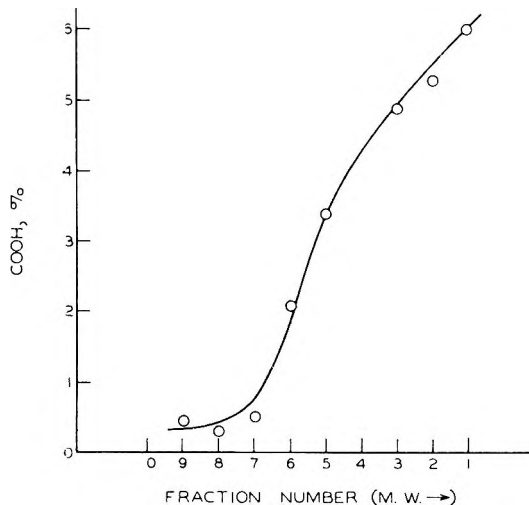


Fig. 6. Carboxyl content of the fractions of polymer 1.

to the growing molecule. Since the molecular weight of the product increases with the severity of radiation, this assumption seems valid.

Carboxyl Content

The carboxyl content of the fractions is plotted in Figure 6. The fraction numbers are plotted in reverse order so that the molecular weight increases in the plot from left to right. The carboxyl groups are seen to be associated mainly with the higher molecular weight material, and hence are thought to be the result of a secondary reaction which takes place on the molecule as it grows in size. Apparently, the repeating unit in the early stages of polymerization is not gluconic acid, as proposed earlier.¹

Infrared Absorption Spectra

The infrared absorption spectra of the fractions showed that as the molecular weight of the polymer increased, the carbonyl absorption band increased in intensity and gradually split into two peaks. One peak was at approximately 1720 cm.^{-1} and the other at approximately 1760 cm.^{-1} . The peak at 1720 cm.^{-1} falls into the range of $1725\text{--}1700\text{ cm.}^{-1}$ quoted by Bellamy²⁶ for saturated aliphatic acids. The peak at 1760 cm.^{-1} is too high to be in the normal aldehyde or ketone range, but is in the range of esters and lactones. Bellamy gives $1740\text{--}1720$ and $1725\text{--}1705\text{ cm.}^{-1}$ as the position for saturated aldehydes and ketones, respectively, and $1750\text{--}1735$ and $1780\text{--}1760\text{ cm.}^{-1}$ for δ - and γ -lactones, respectively. The lactone is considered more likely than an ester because the polymer is resistant to acidic and alkaline hydrolysis,¹ and because Barker, Lloyd, and Stacey⁸

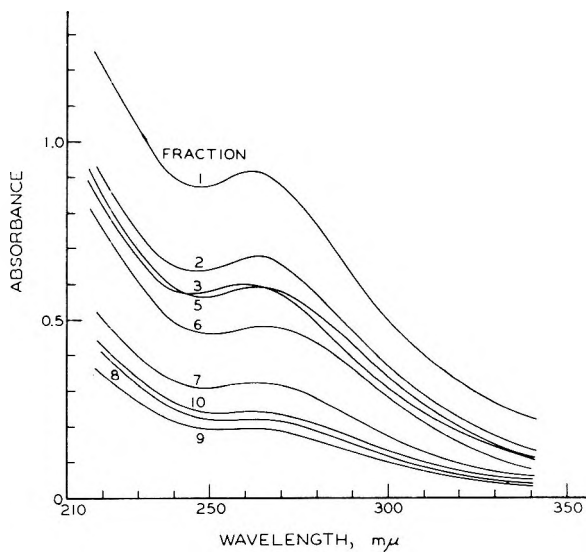


Fig. 7. Ultraviolet absorption spectra of the fractions of polymer 1 (concentration = 1.8×10^{-4} g./ml.).

found evidence of lactone formation in the polymer. Sodium borohydride reduction by the method for lactones²⁷ reduced the intensity of the peak at 1760 cm.^{-1} , but left the peak at 1720 cm.^{-1} , supporting the theory that this peak is due to the carboxyl carbonyl.

Ultraviolet Absorption Spectra

The absorption of the fractions in the ultraviolet is shown in Figure 7. The specific extinction coefficient at $265\text{ m}\mu$ increases with molecular weight. If the absorption at $265\text{ m}\mu$ is due to an enediol structure as suggested by Grant and Ward,⁷ the production of the enediol increases with molecular weight. Most likely this is the result of radical attack on the polymer molecule as it grows in size.

Elemental Analyses

The results of the elemental analyses are given in Figure 8. The oxygen content of the fractions decreases with molecular weight, in spite of the fact that the carboxyl content increases. The rate of oxygen loss is too

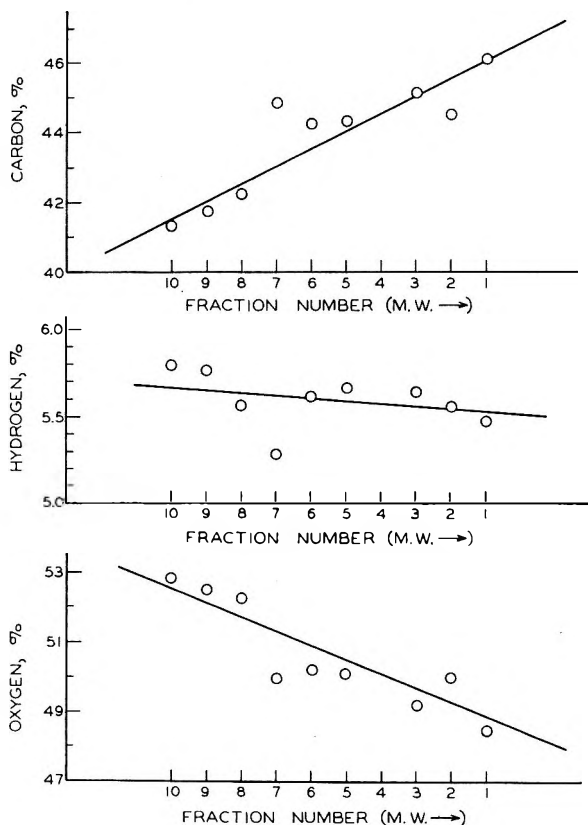


Fig. 8. Elemental analyses of the fractions of polymer 1.

great to be accounted for by dehydration alone. Apparently, oxygen-rich fragments such as carbon dioxide or formic acid are lost from the molecule as polymerization proceeds.

The elemental analyses of the low molecular weight fractions come close to fitting the composition of gluconolactone. The elemental analysis and infrared spectral data, therefore, are both consistent with the hypothesis that gluconolactone is incorporated into the polymer in the early stages of formation. Although neither gluconic acid nor gluconolactone were isolated as products of irradiation in this study, other workers have established gluconic acid as a product.^{7,28} Also, Barker et al.¹ obtained a slightly higher yield of polymer from gluconolactone than from glucose.

Comparison of the Polymers with those of Barker et al.

Determination of the infrared absorption spectra of a polymer sample obtained from Barker showed that the polymers formed in this work are similar in overall nature to those formed by Barker et al.¹⁷ Differences in properties such as molecular weight and degree of oxidation would naturally be expected. The polymers formed in this study were also resistant to acid hydrolysis, as noted by Barker et al.¹

CONCLUSIONS

Irradiation of aqueous glucose solutions with high energy electrons produces a highly branched, high molecular weight, acidic polymer. Molecular weights can be produced which are much higher than previously predicted and are definitely in the high polymer range.

A wide range of molecular weights may be produced, depending on the conditions of irradiation. For example, the weight average molecular weights of the polymers produced in this work ranged from 9,800 to 5,000,000. Increasing either the dose or the dose rate appears to increase the molecular weight of the product.

In addition to being heterogeneous with respect to molecular weight, the polymers are heterogeneous in chemical composition. The carboxyl content increases with molecular weight and is therefore thought to be the result of secondary attack on the molecule which takes place as it grows in size. This is opposed to the earlier hypothesis that the repeating monomer unit during the initial stages of polymerization was gluconic acid. Infrared spectroscopy and elemental analysis data are consistent with the hypothesis that gluconolactone is incorporated into the polymer in the early stages of formation. Secondary attack then results in the formation of carboxyl groups,enediol groups, and the loss of oxygen-rich fragments.

The author sincerely appreciates the helpful advice of Drs. E. J. Jones and J. W. Green, and of E. E. Dickey and H. A. Swenson. Thanks are also expressed to Dr. S. A. Barker of the University of Birmingham for the gift of a sample of his polymer, and to High Voltage Engineering Corp., Rockford, Ill. and Burlington, Mass., for the irradiation work.

A portion of a thesis submitted in partial fulfillment of the requirements of The Institute of Paper Chemistry for the degree of Doctor of Philosophy from Lawrence College, Appleton, Wis., June, 1964. This work was carried out under the direction of Edward J. Jones.

References

1. Barker, S. A., P. M. Grant, M. Stacey, and R. B. Ward, *J. Chem. Soc.*, **1959**, 2648.
2. Burr, J. G., *J. Phys. Chem.*, **61**, 1477 (1957).
3. McDonnell, W. R., and A. S. Newton, *J. Am. Chem. Soc.*, **76**, 4651 (1954).
4. Phillips, G. O., and W. J. Criddle, *J. Chem. Soc.*, **1962**, 2733.
5. Phillips, G. O., and W. J. Criddle, *J. Chem. Soc.*, **1961**, 3763.
6. Grant, P. M., and R. B. Ward, *J. Chem. Soc.*, **1959**, 2654.
7. Grant, P. M., and R. B. Ward, *J. Chem. Soc.*, **1959**, 2871.
8. Barker, S. A., I. R. L. Lloyd, and M. Stacey, *Radiation Res.*, **17**, 619 (1962).
9. American Public Health Association, American Water Works Association, and Water Pollution Control Federation, *Standard Methods for the Examination of Water and Wastewater*, 11th Ed., New York, American Public Health Association, 1960, p. 316.
10. *The New Brice-Phoenix Light Scattering Photometer, Operation Manual OM-1000*, Phoenix Precision Instrument Company, Philadelphia, Pa., 1955.
11. Debye, P., *J. Appl. Phys.*, **15**, 338 (1944).
12. Beattie, W. H., and C. Booth, *J. Phys. Chem.*, **64**, 696 (1960).
13. Brice, B. A., G. C. Nutting, and M. Halwer, *J. Am. Chem. Soc.*, **75**, 824 (1953).
14. *The Mechrolab Model 501 High Speed Membrane Osmometer, Operation Manual*, Mechrolab, Inc., Mountain View, California, 1962.
15. Bruss, D. B., and F. H. Stross, *J. Polymer Sci.*, **A1**, 2439 (1963).
16. Bovey, F. A., *The Effects of Ionizing Radiation on Natural and Synthetic High Polymers*, Interscience, New York, 1958.
17. Barker, S. A., I. R. L. Lloyd, and M. Stacey, *Radiation Res.*, **16**, 224 (1962).
18. Tanford, C., *Physical Chemistry of Macromolecules*, Wiley, New York, 1961.
19. Moacanin, J., V. F. Felicetta, W. Haller, and J. L. McCarthy, *J. Am. Chem. Soc.*, **77**, 3470 (1955).
20. Rankin, J., Mechrolab, Inc., Mountain View, California, personal communication, 1964.
21. Peebles, L. H., Jr., *J. Am. Chem. Soc.*, **80**, 5603 (1958).
22. Muus, L. T., and F. W. Billmeyer, *J. Am. Chem. Soc.*, **79**, 5079 (1957).
23. Stacy, C. J., and J. F. Foster, *J. Polymer Sci.*, **25**, 39 (1957).
24. Goring, D. A. I., in *Proceedings of the Wood Symposium (I.U.P.A.C.)*, Montreal, Canada, Aug., 1961, London, Butterworths, 1962, p. 233.
25. Greenwood, C. T., and J. S. M. Robertson, *J. Chem. Soc.*, **1954**, 3769.
26. Bellamy, L. J., *The Infra-Red Spectra of Complex Molecules*, Wiley, New York, 1954, 323 p.
27. Frush, H. L., and H. S. Isbell, *J. Am. Chem. Soc.*, **78**, 2844 (1956).
28. Phillips, G. O., G. J. Moody, and G. L. Mattok, *J. Chem. Soc.*, **1958**, 3522.

Résumé

Lorsqu'on soumet des solutions aqueuses de glucose à un rayonnement d'électrons d'énergie élevée, il se forme du polymère. Le rendement en polymère augmente avec la dose et la vitesse de dose. Les poids moléculaires moyens en poids des polymères formés à 40 Mrad, mesurés par diffusion lumineuse, se situent entre 9.800 et 5.000.000. Les polymères présentent de très faibles viscosités intrinsèques dans l'eau et on pense par conséquent qu'ils sont fortement ramifiés. La mesure par osmose du poids moléculaire moyen en nombre de l'un des polymères donne un rapport \bar{M}_w/\bar{M}_n de 4.9 ce qui indique une distribution assez large des poids moléculaires dans le polymère. Un polymère a été fractionné sur Sephadex et on a comparé la composition chimique des frac-

tions. La teneur en carboxyle augmente régulièrement avec le poids moléculaire, ce qui suggère que les groupes carboxyles sont le résultat d'une attaque oxydante secondaire. La teneur en hydrogène et oxygène diminue avec l'augmentation du poids moléculaire. Les résultats de l'analyse élémentaire et ceux de l'analyse infrarouge sur les fractions sont en accord avec l'hypothèse de l'incorporation de gluconolactone dans le polymère lors des stades préliminaires de sa formation. Il se forme des groupements chromophores, peut-être du type énediol, et les fragments riches en oxygène disparaissent apparemment lorsque le poids moléculaire du polymère augmente.

Zusammenfassung

Durch Einwirkung hochenergetischer Elektronen auf wässrige Glukoselösungen wurden polymere Stoffe erhalten. Die Ausbeute an Polymerem nahm mit Dosis und Dosisleistung zu. Die durch Lichtstreuung bestimmten Gewichtsmittelmolekulargewichte der bei 40 Mrad gebildeten Polymeren lagen im Bereich von 9800 bis 5,000,000. Die Polymeren besaßen in Wasser sehr niedrige Viskositätszahlen und scheinen daher sehr stark verzweigt zu sein. Die Messung des Zahlenmittelmolekulargewichts eines der Polymeren durch Osmometrie führt zu einem \bar{M}_w/\bar{M}_n -Verhältnis von 4,9, was eine ziemlich breite Molekulargewichtsverteilung im Polymeren erkennen lässt. Ein Polymeres wurde an Sephadex fraktioniert und die chemische Zusammensetzung der Fraktionen verglichen. Der Carboxylgehalt nahm mit dem Molekulargewicht stetig zu, was auf eine Entstehung der Carboxylgruppen durch einen sekundären oxydativen Angriff hinweist. Der Wasserstoff- und der Sauerstoffgehalt nahm mit steigendem Molekulargewicht ab. Elementaranalyse und Infrarotdaten der Fraktionen lieferten eine Stütze für die Hypothese, dass Gluconolacton in die Polymeren in einem frühen Bildungsstadium eingebaut wurde. Bei Zunahme des Molekulargewichts der Polymeren wurden chromophore Gruppen, vielleicht vom Endioltyp, gebildet und sauerstoffreiche Bruchstücke offenbar abgespalten.

Received October 16, 1964

Revised January 7, 1965

Prod. No. 4630A

Chemical Scission of Poly(methyl Acrylate)

JESSE C. H. HWA* and LEON MILLER, *Research Laboratory, Rohm & Haas Company, Philadelphia, Pennsylvania*

Synopsis

By copolymerizing methyl acrylate with methyl α -chloroacrylate at various ratios, the resulting poly(methyl acrylate) backbone had reactive chlorine sites. The poly(methyl acrylate-co-methyl α -chloroacrylate) was dehydrochlorinated by amine. After hydrolysis to convert methyl ester to sodium salt of the acid, the unsaturated bonds introduced by dehydrochlorination were oxidized to glycol by potassium permanganate and cleaved by periodic acid. The resulting poly(sodium acrylate) was converted to the free acid by ion exchange and reesterified with diazomethane. Degraded fragments having number-average molecular weights of 5,000-12,000 were obtained at 83% polymer recovery. Based on the original chlorine content, the efficiency of overall degradation was 20-26% and perhaps somewhat higher.

INTRODUCTION

Polyacrylates can be degraded by a variety of "physical" methods involving the scission of the backbone carbon-carbon covalent bonds. High energy^{1,2} and ultraviolet³ irradiations are capable of degrading polyacrylates with simultaneous crosslinking. Pyrolysis of poly(methyl acrylate) *in vacuo* gave largely volatile products,^{4,5} while thermal-oxidative degradation of poly(ethyl acrylate) appeared to be more efficient with little weight loss.⁶ Techniques involving ultrasonic waves⁷ and high shear⁸ are also known.

We undertook this present work in order to develop a chemical method for degrading the backbone of poly(methyl acrylate) to shorter fragments. The approach is as follows. A few reactive sites were introduced along the backbone chain and then, by a series of chemical reactions, the chains were cleaved at the indicated sites and the degraded fragments isolated and characterized. The present method is lengthy, but the techniques described may serve as a useful background whereby some portion may be adapted advantageously by others to other problems.

The scope of this work consisted of (a) preparation of a series of methyl α -chloroacrylate-methyl acrylate copolymers having varying chlorine contents, (b) development of oxidation and isolation procedures, (c) application of the best procedure to these copolymers, and (d) comparison of the molecular weights of the degraded polymers with those calculated assuming scission of backbone occurred at each chlorine site.

* Present address: Eastern Research Center, Stauffer Chemical Company, Dobbs Ferry, New York.

The degradative scheme consisted of the steps shown in eqs. (1) on facing page.

EXPERIMENTAL

Preparation of Polymer

Poly(methyl acrylate-co-methyl α -chloroacrylate) was prepared by conventional solution polymerization. A mixture of 430 g. (5.0 mole) of uninhibited methyl acrylate (Rohm & Haas Company), 6.0 g. (0.049 mole) of methyl α -chloroacrylate⁹ (freshly distilled, b.p. 54.5–55°C./50 mm.), 12.42 g. of azobisisobutyronitrile (recrystallized from methanol, m.p. 100–101°C.) and 430 g. of reagent grade benzene was heated at 50°C. under nitrogen atmosphere for 110 min. The solution was cooled rapidly and added with agitation to 3 liters of *n*-hexane. The white polymer was isolated by filtration and dried at 65°C. *in vacuo* overnight. It weighed 58.3 g. (13.3% conversion), 1.88% Cl, $[\eta] = 0.731$ dl./g. (in benzene at 30°C.). Based on the equation¹⁰

$$[\eta] = 4.5 \times 10^{-5} \bar{M}_v^{0.78} \quad (2)$$

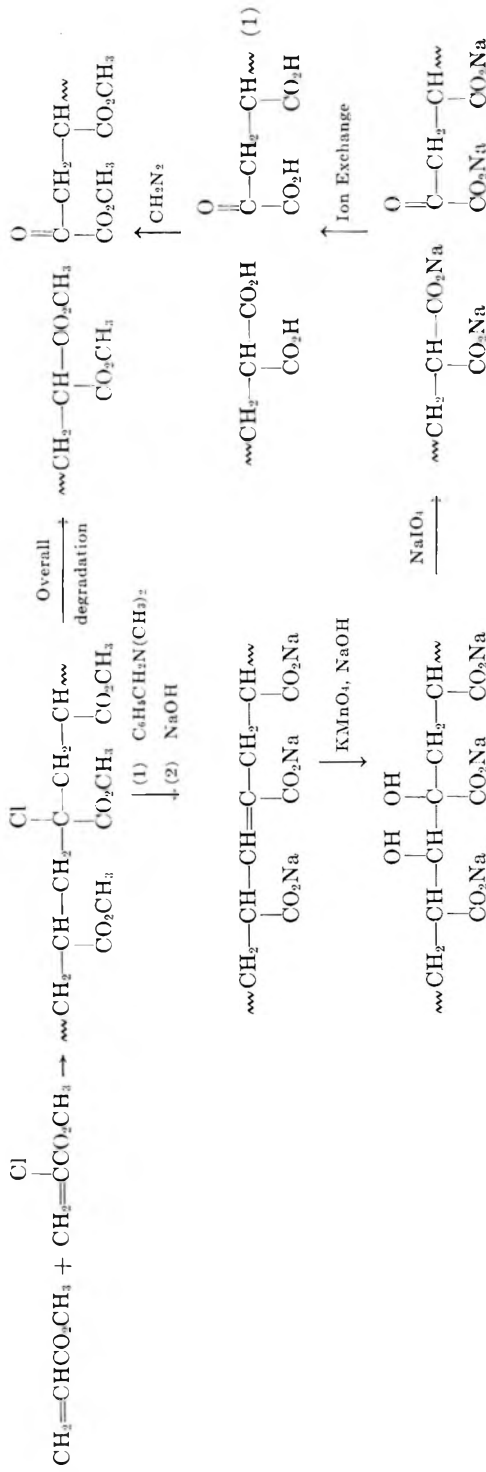
the calculated \bar{M}_v was 245,000.

Degradation and Isolation

A mixture of 20.0 g. of the above copolymer and 180 ml. of benzyldimethylamine (freshly distilled, b.p. 178–179°C.) was heated at 150–155°C. for 1.5 hr. On cooling to room temperature the polymer that separated was isolated by decantation. The polymer was cut into small pieces and washed with three 500-ml. portions of 5% sulfuric acid over a period of 24 hr. and with excess deionized water until the water wash was neutral. The product, after drying at 65°C. for 2 hr. and over anhydrous calcium chloride *in vacuo*, weighed 18.1 g. It contained no chlorine and 0.72% nitrogen.

A portion (15 g., 0.174 mole of ester groups containing 7.96 meq. of reactive sites) of the dehydrochlorinated polymer was hydrolyzed by heating in a solution of 7.00 g. (0.175 mole) of sodium hydroxide and 133 ml. of deionized water at 95–100°C. for 18 hr. No provision to exclude air was made. About 200 ml. of water was added, and the mixture was steam-distilled for 4 hr. to remove methanol. The homogeneous aqueous solution weighed 237 g. By titration of a small aliquot for residual alkali with 0.1*N* hydrochloric acid in 1*N* sodium chloride solution, the hydrolysis was found 94.8% complete.

To the alkaline hydrolyzate a solution of 3.36 g. (21.1 mmole) of potassium permanganate in 100 ml. of water was added and the mixture stirred at 25–28°C. for 16 hr. The voluminous precipitate of manganese dioxide that separated was removed by filtration, first through coarse-grade paper and then through a Celite packing (Johns-Manville Co., grade 545). The latter was obtained by depositing 5–7 g. of Celite with water in a suction funnel to form a 1/4-in. thick wet cake. The filtrate was mixed with 9.05 g.



(39.6 mmole) of paraperiodic acid ($\text{HIO}_4 \cdot 2\text{H}_2\text{O}$) and 2.0 g. of sodium hydroxide, and the solution was heated at 50–60°C. for 2.5 hr. and then allowed to stand at room temperature for 19 hr. The inorganic precipitate that separated during this step was removed by filtration.

To effect complete conversion of the degraded polyelectrolyte from the salt to the free acid form and to remove selectively the inorganic salts, two separate beds of ion-exchange resins were made ready in the following way. Amberlite IR-120 (Rohm & Haas Co., hydrogen form, sulfonic type) was freshly regenerated by passing in succession 2 bed-volumes of 8% hydrochloric acid and 10 bed-volumes of deionized water (specific resistance of 550,000 ohm-cm.) at a rate of 0.13 ml./ml./min. Amberlite IR-45 (Rohm & Haas Co., weak base type) was freshly regenerated by passing successively 2 bed-volumes of 4% sodium hydroxide and 10 bed-volumes of deionized water. The effluent was neutral.

The clear amber solution containing the polymer and inorganic salts was passed first through 700 ml. of Amberlite IR-120 (H) in a column at a rate of 0.07 ml./ml./min. followed by 700 ml. of deionized water. This amount of resin corresponded to 1.40 mole, which was about 500% in excess of the expected amount of alkali metal ions present in the liquor. (Without this large excess of resin the metal ions would not be substantially removed from the polymer and would subsequently block complete esterification of the polyac.d.) The pH of the final effluent was 4–5. The liquor was then passed through 80 ml. of Amberlite IR-45 at the same rate. The amount of the resin used was 300% in excess of the calculated iodate content present in the solution (39.6 meq.). The clear filtrate was then freeze-dried to yield 9.7 g. of polymer. With allowance for aliquots consumed in titrations, the recovery based on the starting material was 82.8%.

To 4.0 g. of the degraded polyacid was added a solution of 110 meq. of diazomethane in 200 ml. of benzene which was prepared from 14.9 g. of *N*-nitrosomethylurea by a modified procedure.¹¹ After standing at room temperature overnight some unreacted flocculent material, weighing 0.7 g. dry, was removed by filtration. [This residue, amounting to 17.5% of the product, was caused by incomplete exchange of sodium ions. If the polyacid were passed through another bed of fresh Amberlite IR-120 (H), the residue after esterification could be reduced to 2–5% of the esterified material.] The clear straw yellow solution was freeze-dried. After further drying at 50°C. *in vacuo* for 16 hr. the degraded poly(methyl acrylate) weighed 4.3 g. and had an intrinsic viscosity of 0.0885. Because of the near randomness of the molecular weight distribution of the isolated, degraded product, one could assume:¹²

$$\bar{M}_v = 1.90\bar{M}'_n \quad (3)$$

where \bar{M}'_n is the apparent \bar{M} number-average molecular weight. The \bar{M}'_n for the degraded product was 8,300. The overall efficiency of the degradation based on the original chlorine content of the copolymer was 21.6%.

RESULTS AND DISCUSSION

Labeling of the Backbone with Reactive Chlorine Atoms

The most direct way of attaching reactive chlorine atoms at the α -carbon position of poly(methyl acrylate) was to copolymerize methyl acrylate with methyl α -chloroacrylate. Depending on the amount of the latter used, the copolymer would have a range of reactive sites, the length of the degraded fragments being inversely proportional to the concentration of these sites.

A series of methyl α -chloroacrylate-methyl acrylate copolymers having 2-16 mole-% of chlorine was prepared by a solution polymerization at 8-16% conversions. The results are shown in the first three columns in Table I.

TABLE I
Chemical Degradation of Poly(methyl Acrylate-co-Methyl α -Chloroacrylates)

| Conversion, % | MACA, mole-% ^a | | [η], dl./g. ^c | | Molecular weights $\bar{M}_n \times 10^{3d}$ | | Efficiency, % ^e | |
|------------------|---------------------------|--------------------|-------------------------------------|--------|---|-------|-------------------------------|--|
| | In feed | Found ^b | Initial | Final | Initial | Final | | |
| 8.2 | 0.41 | 2.49 | 0.752 | 0.128 | 264 | 25.3 | 25.3 | |
| 13.3 | 0.97 | 4.66 | 0.731 | 0.0885 | 245 | 15.8 | 21.6 | |
| 14.2 | 0.99 | 4.72 | 0.472 | 0.0769 | 143 | 13.1 | 26.1 | |
| 13.6 | 1.96 | 8.15 | 0.714 | 0.0583 | 240 | 9.5 | 20.0 | |
| 15.2 | 3.84 | 17.3 | Gelation during dehydrochlorination | | | | | |

^a A run based on poly(methyl acrylate) having no MACA was run as a control to test if the chemical reactions used would degrade poly(methyl acrylate) itself which did not contain reactive sites. No definite conclusions could be reached, however.

^b Based on chlorine analysis.

^c In benzene at 30°C.

^d By eq. (2).

^e Number-average molecular weight between the chlorine atoms present in the original copolymer divided by \bar{M}'_n , which is calculated from final \bar{M}_n by using eq. (3).

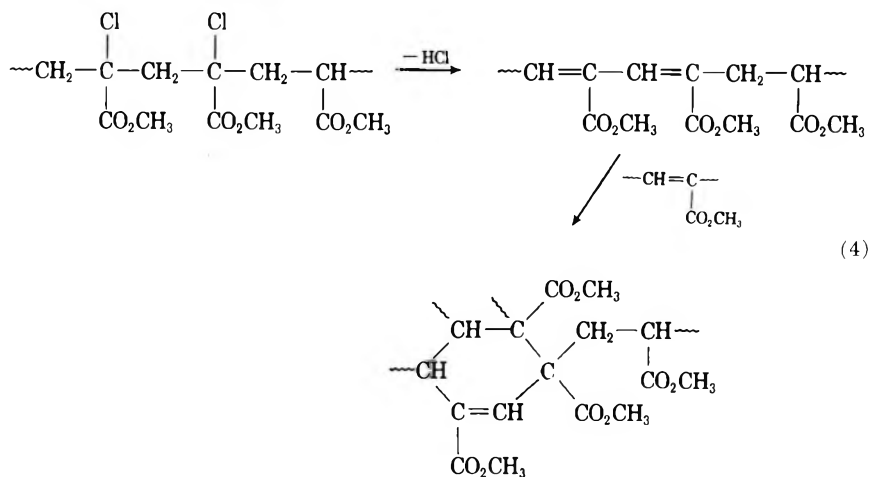
From reactivity ratio considerations, the chlorine atoms were probably not randomly distributed along the poly(methyl acrylate) backbone chains. From the Q and e values of methyl α -chloroacrylate (3.69 and 1.41)¹³ and methyl acrylate (0.42 and 0.6),¹⁴ the reactivity ratios of these two monomers were calculated to be 2.80 and 0.19, respectively.¹⁵ The amounts of chloro monomer incorporated in the copolymer at low conversions were greater than those of the feed. One would also expect that the chlorine content found in the copolymer was an average of some compositional heterogeneity. Machine computations (Bendix G-15) based on these reactivity ratios were in support of this view (data not shown).

Dehydrochlorination and Hydrolysis

To find a reagent capable of effective dehydrochlorination, insoluble methyl α -chloroacrylate-divinylbenzene beads were reacted with different chemicals under a variety of conditions and assayed for the residual chlorine content. Both hot (155°C. for 2 hr.) benzyl-dimethylamine and refluxing 20% alcoholic potassium hydroxide were found to be effective: practically no chlorine was left in the product. The former reagent was adopted for all the preparations because the caustic method could also lead to partial replacement of the chlorine with a hydroxyl group.

A sample of the amine-treated product derived from soluble poly(methyl acrylate-co-methyl α -chloroacrylate) had no residual chlorine. The formation of olefinic unsaturation along the polymer backbone was supported qualitatively by the appearance of an infrared absorptive band at 1642 cm^{-1} (C=C stretch). Polarographic measurement of the dehydrochlorinated ester (0.16% in dimethylformamide solution with the use of 0.1M tetra-*n*-butylammonium iodide as supporting electrolyte versus a mercury pool) showed definite reduction potential although insufficient data were available to verify the particular structure postulated.

It was also found that one copolymer sample containing 17.3 mole-% of methyl α -chloroacrylate resulted in gelation during the dehydrochlorination step with benzyldimethylamine. Those polymers having a lower chlorine content did not. Apparently the compositional drift resulted in a significant concentration (0.1–0.5 mole-%) of adjacent methyl α -chloroacrylate units. These double units would result in conjugated dienes which conceivably could cause crosslinking by reacting with other polymer chains in the Diels-Alder manner [eq. (4)].



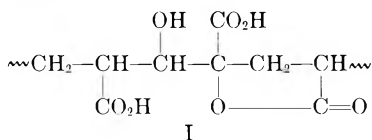
To be ready for the subsequent oxidation steps in aqueous media the dehydrochlorinated polymers were rendered water-soluble by hydrolysis with 2.5–5% aqueous sodium hydroxide at equimolar ratios. The extent of hydrolysis was 90–94% by titration with dilute acids.

Hydroxylation and Periodate Cleavage

Hydroxylation of the backbone unsaturation was effected by alkaline permanganate at room temperature.¹⁶ The decolorization of the permanganate proceeded steadily without notable viscosity drop of the polymer solution, while under the same conditions a separate sample of poly(acrylic acid) was not affected. At the end of the reaction period the majority of the unsaturation was presumed to be hydroxylated, although it was possible that a small fraction of the glycol groups was oxidized further and that some unwanted oxidation of the neighboring acrylic acid units could also have taken place.

The presence of glycol groups in the polymers was strongly indicated by the ease of the subsequent periodate oxidation step.¹⁷ The progress of the periodate oxidation in alkaline medium was followed by a modified iodimetry¹⁸ and by viscosity change as determined with an Ubbelohde viscometer. It was found that after 19 hr. practically all the periodate ions were reduced to iodate ions and that substantial reduction in the viscosity of the aqueous solution took place. Since periodate is known to cleave 1,2-diols specifically,¹⁷ the above findings support the belief that the majority of chain degradations occurred at the glycol sites as shown in the reaction scheme.

It was interesting to observe that when the reaction mixture resulting from the permanganate oxidation was acidified, no oxidation by periodate was observed in 18 hr. under the same conditions. This was surprising, since it is known that the rate of periodate oxidation is several times faster in acid media than that in alkaline media.¹⁹ A possible explanation is that at low pH the glycol and the neighboring acid groups formed lactones (I) which blocked periodate cleavage.



(A copolymer of methyl methacrylate and methyl α -chloroacrylate was subjected to similar dehydrochlorination and hydroxylation steps. On acidification the isolated polymer was found to have a weak carbonyl band at 1785 cm.^{-1} which corresponded to a five-membered lactone.)

Ion Exchange and Polymer Isolation

Separation of the degraded polymer from other ionic contaminants present in the aqueous reaction liquor was achieved by ion exchange. Passage of the reaction mixture through a bed of sulfonic ion-exchange resin in the hydrogen form converted practically all of the ingredients to the free acid form, and a subsequent passage through a bed of weak-base type ion-exchange resin removed preferentially inorganic anions such as iodate; the polyacid, being a weak acid, emerged in the effluent.

In the ion-exchange step it was found important to purify the sulfonic resin carefully by regeneration prior to use and to use a large excess of the resin (5–10-fold excess of the theoretical equivalents needed). With these precautions it was possible to obtain polyacid sufficiently free from trapped alkali metal ions that 83–98% of the polyacid could be converted to its methyl ester by diazomethane.

It was also found that only 83% of the expected polyacid was actually recovered. Apparently the balance of the polymer was lost during the anion exchange step. Possibly some low molecular weight polyacid was lost by adsorption on the surface of the weak-base resin.

CONCLUSIONS

After completing the entire cycle: dehydrochlorination, hydrolysis, oxidation, ion exchange, and esterification, one was now able to compare the chain length of the initial and the degraded poly(methyl acrylates). The results, listed in Table I, show that short-chain fragments of 5,000–13,000 number-average molecular weight were obtainable by the chemical degradation of poly(methyl acrylate) having active chlorine sites. The weight recovery of the degraded product in a typical case was 83%. The overall efficiency of degradation, as measured, was about 20–26%.

The actual degradation efficiencies probably were appreciably higher than those shown in Table I. Because of the compositional drift in the copolymerization step occasional diene groups would result and become consumed in a Diels-Alder reaction even though the whole sample had not gelled. Such wastage of active sites, if any, would mean that the degradation was in fact more efficient than that found. Furthermore, the degraded product probably would have a somewhat wider molecular weight distribution than a random one. Since it was found that about 13% of the degraded product was actually lost, very likely the material lost was the very short fragments. The apparent number-average molecular weights calculated from viscosity measurements could be on the high side. Hence for these reasons the real efficiencies could well be between 40 and 50%.

In view of these results, the chemical degradation method, though lengthy, certainly seemed to be capable of cleaving a polymeric backbone according to the scheme devised. Since the pertinent reactions were centered on the methyl α -chloroacrylate functional group, possibly the present scheme of degradation, with appropriate modification or improvement, can be adapted to several other polymeric backbones. Such an application of the present method would be useful if no other suitable physical methods are readily available.

References

1. Shultz, A. R., and F. A. Bovey, *J. Polymer Sci.*, **22**, 485 (1956).
2. Bovey, F. A., *The Effects of Ionizing Radiation on Natural and Synthetic High Polymers*, Interscience, New York, 1958, Chap. VI.
3. Jacobs, H., and R. Steele, *J. Appl. Polymer Sci.*, **3**, 239, 245 (1960).

4. Straus, S., and S. L. Madorsky, *J. Res. Natl. Bur. Std.*, **50**, 165 (1953).
5. Madorsky, S. L., *J. Polymer Sci.*, **11**, 491 (1953).
6. Steele, R., and H. Jacobs, *J. Appl. Polymer Sci.*, **2**, 86 (1959).
7. Schmid, G., and O. Rommel, *Z. Physik. Chem.*, **A185**, 97 (1939).
8. Larsen, H. A., and G. H. Drickamer, *J. Phys. Chem.*, **61**, 1643 (1957).
9. Barnes, C. E. (to General Aniline & Film Corp.), U. S. Pat. 2,476,528 (July 19, 1949).
10. Rohm & Haas Company, unpublished information.
11. Bachmann, W. E., and W. S. Struve, in *Organic Reactions*, Vol. I, Wiley, New York, 1942, pp. 47-51.
12. Fox, T. G., J. B. Kinsinger, H. F. Mason, and E. M. Schuele, *Polymer*, **3**, 71 (1962).
13. Alfrey, T., Jr., J. Bohrer, H. Haas, and C. Lewis, *J. Polymer Sci.*, **5**, 719 (1950).
14. Young, L. J., *J. Polymer Sci.*, **54**, 411 (1961).
15. Alfrey, T., Jr., J. Bohrer, and H. Mark, *Copolymerization*, Interscience, New York, 1952.
16. Polgar, A., and J. L. Jungnickel, in *Organic Analysis*, Vol. III, Interscience, New York, 1956, p. 203.
17. Jackson, E. L., in *Organic Reactions*, Vol. II, Wiley, New York, 1944, p. 341.
18. Hillenbrand, E. F., Jr., in *Glycols*, G. O. Curme, Jr. and F. Johnston, Eds., Reinhold, New York, 1952, p. 337.
19. Price, C. C., and M. Knell, *J. Am. Chem. Soc.*, **64**, 552 (1942).

Résumé

En copolymérisant dans des rapports différents de l'acrylate de méthyle avec de l' α -chloroacrylate de méthyle, la chaîne principale de polyacrylate de méthyle qui en résulte possède des chlorures réactionnels. Le copolymère acrylate de méthyle- α -chloroacrylate de méthyle est déshydrochloré par une amine. Après hydrolyse en vue de transformer l'ester méthylique en sel sodique de l'acide, les liaisons non-saturées introduites par déshydrochloration sont oxydées en glycol par le permanganate de potassium et sont cassées par l'acide periodique. Le polyacrylate de sodium résultant est transformé en acide libre par échangeur d'ion et réstérifié avec le diazométhane. On a obtenu, à raison de 83% du polymère de départ, des fragments dégradés, possédant des poids moléculaires moyens en nombre se situant entre 5.000 et 12.000. En se basant sur la teneur initiale en chlore, l'efficacité de la dégradation est de 20-26% et peut-être plus.

Zusammenfassung

Durch Kopolymerisation von Methylacrylat mit Methyl- α -chloracrylat in verschiedenem Molverhältnis wurde eine Polymethylacrylathauptkette mit reaktionsfähigem Chloratom erhalten. Das Poly(methylacrylat-ko-methyl- α -chloracrylat) wurde mit Amin dehydrochloriert. Nach Hydrolyse zur Umwandlung des Methylesters in das Natriumsalz der Säure wurden die durch Dehydrochlorierung eingeführten Doppelbindungen mit Kaliumpermanganat zu Glykol oxydiert und mit Perjodsäure gespalten. Das erhaltene Natriumpolyacrylat wurde durch Ionenaustausch in die freie Säure umgewandelt und mit Diazomethan wieder verestert. Abbaubruchstücke mit einem Zehnmittelmolekulargewicht von 5000 bis 12000 wurden bei 83% iger Polymerrückgewinnung erhalten. Bezogen auf den ursprünglichen Chlorgehalt war die Bruttoabbauausbeute 20 bis 26% und vielleicht etwas höher.

Received September 21, 1964

Revised January 18, 1965

Prod. No. 4636A

Relaxation Response of Polyurethane Elastomers

P. S. THEOCARIS, *The National Technical University, Athens, Greece*

Synopsis

The transient extension relaxation modulus $E(t)$ and the lateral contraction ratio $\nu_r(t)$ for a polyurethane elastomer have been simultaneously measured in the transition region from the glassy to the rubbery consistencies of the material. The differential moiré method was used in these measurements and yielded simultaneous values of the longitudinal extension and the lateral contraction principal strains of the tension specimen. Composite curves of $E(t)$ and $\nu_r(t)$ reduced to a standard temperature were obtained by applying the method of reduced variables. The time factors K_T in both curves were coincident and they followed the WLF equation. The shear and bulk modulus characteristic functions were determined from the extension modulus and lateral contraction ratio functions. The values of the lateral contraction ratio in relaxation were determined by using data of the extension relaxation modulus along the whole viscoelastic range and the initial value of the lateral contraction ratio at the rubbery state and applying an indirect method. The results obtained by the indirect method coincided with the experimental values. The shear modulus function was evaluated from the extension relaxation modulus and the lateral contraction ratio functions and compared with the shear dynamic compliance determined by Landel. The experimental data indicated that a linear relationship holds between the lateral contraction ratio in relaxation and the bulk modulus along the whole response spectrum. The same relationship was previously shown to hold for a series of various polymeric substances.

Introduction

The general features of the viscoelastic properties of various elastomers were extensively studied in recent years. These studies were referred to a particular function describing the viscoelastic behavior of a polymer or elastomer in creep or relaxation. The theory of linear viscoelasticity guarantees the uniqueness of the characterization of the mechanical properties and its independence of the type of test used to determine them. This implies the possibility to interconvert data obtained from various types of tests. Several inversion methods were developed for the determination of any one characteristic creep or relaxation function from its corresponding function in transient or dynamic creep or relaxation. Moreover, numerical and other approximation methods were developed yielding any one of these characteristic functions from the corresponding retardation or relaxation spectra. Considerable literature has been accumulated on this subject.^{1,2}

It has been generally accepted that the behavior of a linear isotropic viscoelastic material is completely determined if two independent charac-

teristic functions are determined along the whole viscoelastic response, provided that the temperature dependence of the material has been properly specified. The two characteristic functions may be expressed by two independent linear differential or integral operator relations. For totally incompressible materials, as is essentially the case of all linear polymers at the rubbery region, the mean normal stress is independent of the vanishing dilation and only one relation is needed. But the incompressibility assumption is a coarse approximation, which may lead to misconceptions, especially in cases where molecular parameters must be deduced from the existing limited viscoelastic data or in cases where the viscoelastic behavior in regions of time or frequency scale, which are not experimentally accessible, is to be predicted.

It was recently shown experimentally³ that instead of a pair of independent operator relationships along the whole viscoelastic spectrum, only one characteristic function is needed and an initial value of another independent function. In other words, it was shown for a series of polymeric substances covering the whole range from low molecular uncrosslinked to high molecular crosslinked polymers that all operator relations expressing the mechanical behavior of linear viscoelastic substances are uniquely inter-related.⁴

Moreover, it has been shown that a linear relationship holds along the whole viscoelastic spectrum between the bulk relaxation modulus and the lateral contraction ratio function in relaxation. This relationship may be used instead of the incompressibility or the constancy of Poisson's ratio assumptions in problems of the praxis, where more than one operational modulus or compliance is involved in a complicated mode. When the solution of such problems is sought by the method of the Laplace or Fourier transforms and the associated elastic solution is found analytically, the problem of the transform inversion may be reduced considerably by using this simple relationship.

On the other hand, the common practice of running successive series of tests to determine either the extension and shear, or the extension and bulk, or the shear and bulk characteristic functions leads to considerable discrepancies and significant errors and, in some cases, to results incompatible with the basic laws of mechanical behavior of any substance. This is due to the fact that the mechanical properties of different specimens made from different batches or the same batch may vary, and, in the case of a single specimen, the environmental conditions of each test cannot be guaranteed to remain the same. Moreover, measurements of the bulk characteristic functions, which are weakly dependent on time or frequency, require elaborate apparatus and skillful technique to obtain accurate measurements of the volume variation of the specimen and to separate and exclude the bulk change due to the variation of the free volume of the material. It has been established that the curve of variation of free volume with temperature presents different average slopes below and above the glass transition temperature T_g .^{1,5} Measurements of the bulk modulus at various steps of

temperature will necessarily include the variation of the free volume. Since the transient bulk modulus master curve is derived from individual bulk relaxation curves at various steps of temperature, knowledge of the values of free volume at different steps of temperature is necessary for the determination of the transient bulk modulus, which depends only on the phenomenon of contraction due to the distortion of the molecular domains of the polymer. Measurements of the free volume collapse with temperature are delicate and subject to errors which influence considerably the values of the bulk modulus. This has been the main cause of contradictions and discrepancies in determining the lateral contraction ratio function with time of various polymers in cases where this function has been derived from data of the extension or shear moduli and the bulk modulus of the material.^{6,7}

The necessity of a compound test yielding simultaneously all the data needed for the complete determination of the viscoelastic behavior of the material seems obvious from the above discussion. In this manner errors due to variations in environmental conditions can be significantly reduced. In the case of crosslinked amorphous polymers, which do not present any type of flow, it is possible to use the same specimen for all steps of temperature, provided that sufficient rest time is allowed to elapse between loading periods in order to permit the specimen to recover completely from the previous loading. In this case the variability of samples from the same batch of the material may be eliminated.

In this paper a method yielding simultaneously all the necessary data for the complete characterization of a polymeric substance was used for the study of the mechanical viscoelastic properties of a typical elastomer, Hysol 8705. The method is based on the so-called image interference of zonal gratings of a density of 20 lines per millimeter and yields the values of the longitudinal extension as well as of the lateral contraction principal strains of a tension specimen tested in transient relaxation. The same method was used previously for the characterization of the viscoelastic properties of a high molecular weight crosslinked polymer.⁸

Relaxation Lateral Contraction Ratio Characteristic Function

If a longitudinal extension strain ϵ_0 , constant with time, is applied to a specimen of a linear elastomer, a lateral contraction strain $-\epsilon_y(t)$ varying with time will be produced. The variation in time of the lateral strain $-\epsilon_y(t)$ normalized to the constant applied longitudinal strain is a new material function and is called the relaxation lateral contraction ratio $\nu_r(t)$. This function is associated with Poisson's ratio for the corresponding elastic behavior. Then, we have for a relaxation tension test that

$$\nu_r(t) = -\epsilon_y(t)/\epsilon_0 \quad (1)$$

The lateral contraction ratio function $\nu_r(t)$ is related to the extension, shear, and bulk moduli functions $[E(t), G(t), K(t)]$ by the following equations

$$\nu_r(t) = [E_0/2G(t) - 1] + 1/2 \int_0^t \dot{E}(t - \tau)/G(\tau) d\tau \quad (2)$$

$$\nu_r(t) = 1/2 [1 - E_0/3K(t)] - 1/6 \int_0^t \dot{E}(t - \tau)/K(\tau) d\tau \quad (3)$$

Similarly, the shear and bulk moduli are related to the extension modulus and the lateral contraction ratio in relaxation by the following relationships, which are the solutions of eqs. (2) and (3).

$$G(t) = \frac{E_0}{2[1 + \nu_r(t)]} + 1/2 \int_0^t \frac{\dot{E}(t - \tau)}{[1 + \nu_r(\tau)]} d\tau \quad (4)$$

$$K(t) = \frac{E_0}{6[1/2 - \nu_r(t)]} + 1/6 \int_0^t \frac{\dot{E}(t - \tau)}{[1/2 - \nu_r(\tau)]} d\tau \quad (5)$$

Where E_0 is the value of the relaxation modulus of the material at the instant of application of the loading and τ the relaxation time.

The first two relations express explicitly the lateral contraction ratio function as integral over two other characteristic functions, while the two last relations express the shear and bulk moduli as integrals over the other two characteristic functions. It may be worthwhile noting the simplicity of these relations where either the quantity $\nu_r(t)$ or the quantities $G(t)$ and $K(t)$ do not occur in the integrands.

For the uniaxial tension test, both the lateral strain $-\epsilon_y(t)$ and the mean normal strain are positive, and the inequalities (6) are valid.

$$\begin{aligned} E(t)/2 > G(t) &\geq E(t)/3 \\ 1/2 > \nu_r(t) &> 0 \end{aligned} \quad (6)$$

Although the variation of the relaxation lateral contraction ratio function is limited between the glassy state value ν_{r0} and 0.5, it cannot be claimed on theoretical grounds that $\nu_r(t)$ is a monotonic function. However, there is sufficient experimental evidence covering the whole range of high polymers according to which the relaxation lateral contraction ratio (as well as the corresponding creep function) is a monotonically increasing function with time.⁴ Both functions exhibit a smooth transition between glassy and rubbery consistencies with the creep function preceding in time from the relaxation function.⁷

Differential Moiré Method with Zonal Gratings

The moiré method was used for the simultaneous measurement of the displacements along both principal directions of the tension specimen. The displacement components measured along the two principal directions of the tension specimen for constant applied deformation and various temperature steps and time intervals yielded the components of strain along the longitudinal and transverse directions. Measurement of the applied load

which varied with time in order to keep the longitudinal strain constant gave the instantaneous value of applied stress and subsequently the instantaneous values of the relaxation modulus and the lateral contraction ratio functions.

A zonal grating of a density of 20 lines/mm. was reproduced on the surface of a large tension specimen by using an Ozalid template lacquer as photosensitive material and exposing the specimen in contact with the negative grating to a intense ultraviolet light (Kodak Photo Resist, K.P.R. Developer, and K.P.R. dye supplied by the Eastman Kodak Co., Rochester, N. Y.). After developing the copy of the grating in ammonia vapor and fixing, a grating of 50% transmissivity was reproduced on the surface of the specimen, which gave sharp moiré fringes when it was superimposed to the reference grating. This method of reproducing gratings is suitable for elastomers and rubbers because in this manner, there is no stiffening effect from the emulsion.

Similar zonal gratings were used as reference gratings. The density of these gratings was changed by very small quantities $\pm\lambda$ so that, when superimposed on the model grating, they gave an initial moiré pattern. The displacements due to this initial pattern were algebraically added to the loaded pattern displacements, which contained both the initial and true displacement components. The Cartesian components of strains along the two principal axes of the specimen were expressed by the relation

$$\epsilon_{xij} = (\partial u_i / \partial x_j) - \lambda_j \delta_{ij} \quad (7)$$

where $\partial u_i / \partial x_j$ are the gradients of the displacement curves along the principal directions ($x = i = j = 1, y = i = j = 2$), δ_{ij} is the Kronecker delta, and λ_j the contribution of the initial moiré pattern in both directions ($j = 1, 2$). In this relation the summation convention is not holding. The contribution of λ_j is given by the relation

$$\lambda_j = e_j / (f_j + e_j) \quad (8)$$

where e_j are the pitches of each master grating along each principal direction ($j = 1, 2$) and f_j is the initial interfringe spacing produced by each reference grating and the underformed model grating. It was decided to use enlarged zonal gratings as reference gratings because with these gratings the contraction displacements, which were smaller than the longitudinal extension displacements, were more accurately determined. Strains of the order of 10^{-3} on a 10-mm. gage length were easily and accurately measured with such gratings and the differential moiré method.

Materials and Methods

The material selected for study was a sample of a polyurethane elastomer designated commercially as Hysol 8705 and provided by the Hysol Corporation, Olean, New York. The liquid epoxy prepolymer was mixed at 95°C. with 24 parts of a diisocyanate to produce a soft rubber after curing for 1½ hr. at 140°C. and 4 hr. at 100°C.

Tensile specimens were cut from a plate of the material 6 mm. thick. These specimens, which had a "dogbone" shape, had a width at their reduced section equal to $w = 7.5$ mm. and a length $l = 150$ mm. along the reduced section, which was considered as uniformly loaded.

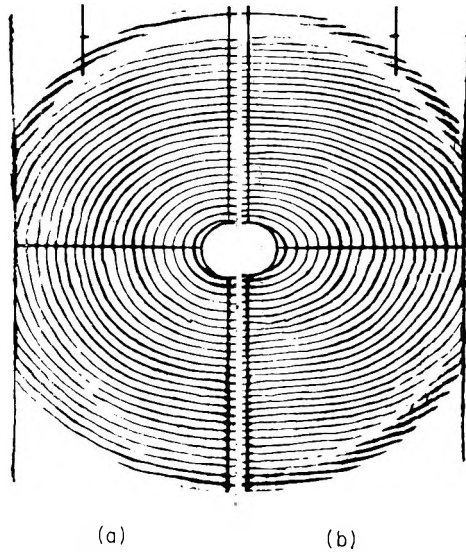


Fig. 1. Moiré patterns of zonal gratings in a tension specimen of polyurethane elastomer: (a) original pattern with the specimen unloaded; (b) loaded pattern from a relaxation test at 293°K. and $t = 16$ min.

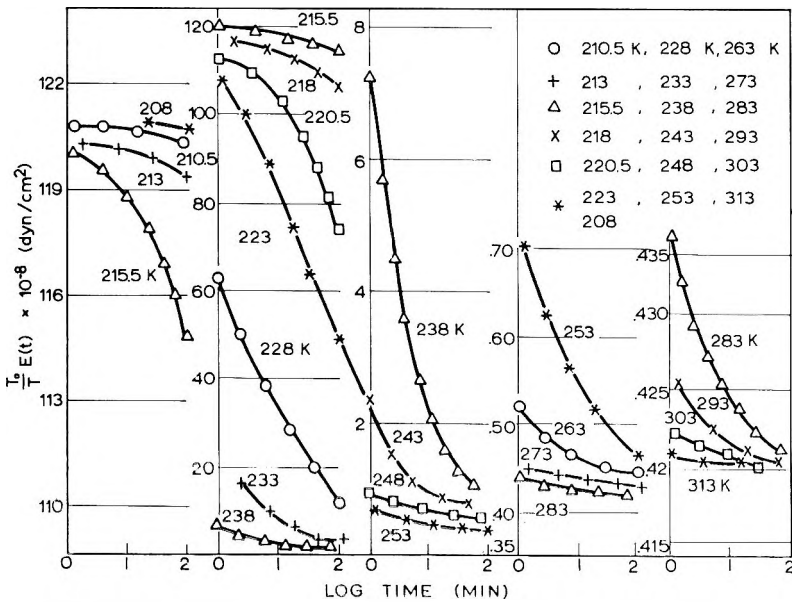


Fig. 2. Individual extension relaxation modulus curves for polyurethane elastomer for various steps of temperature.

The test equipment used in the experiments has been previously described.⁹

Measurements of both principal components of strain and the corre-

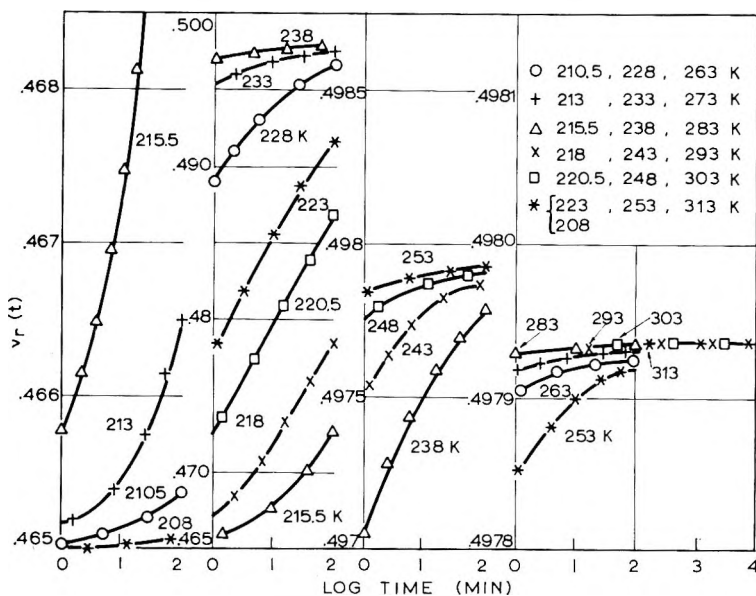


Fig. 3. Individual lateral contraction ratio curves for a polyurethane elastomer at relaxation for various steps of temperature.

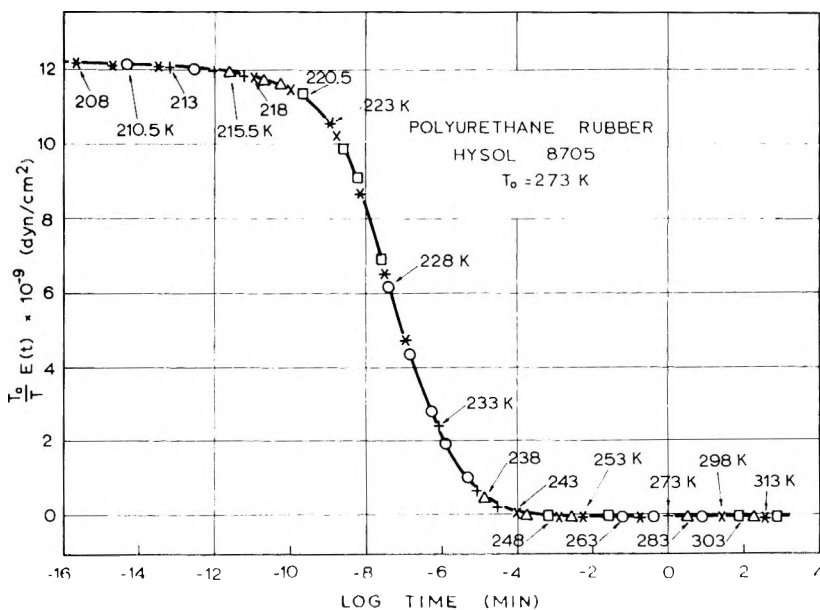


Fig. 4. Composite curve of the extension relaxation modulus for a polyurethane elastomer ($T_0 = 273^\circ\text{K.}$).

sponding stress were taken at equal intervals in a logarithmic scale from 1 to 100 min. for each step of temperature.

The relaxation tests were carried out at various steps of temperature from the glassy up to the rubbery state of the material in order to yield the extension relaxation modulus as well as the relaxation lateral contraction ratio functions along the whole viscoelastic range. For this purpose the method of reduced variables or time-temperature superposition principle was applied for the formation of the composite curves of these functions.

Since the material did not present any kind of flow for the range of deformations applied during the experiments the technique of using a single sample for all steps of temperature was practiced. This has the advantage

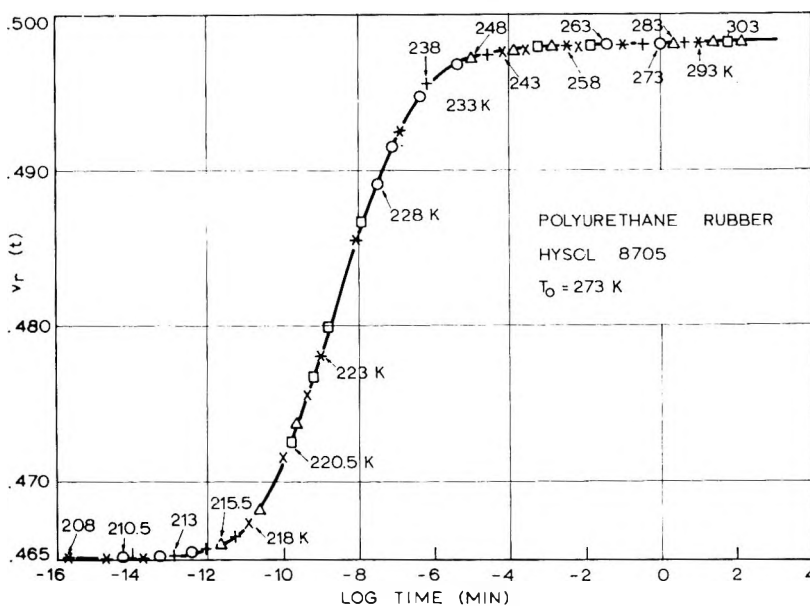


Fig. 5. Composite curve of the lateral contraction ratio for a polyurethane elastomer in relaxation ($T_0 = 273^\circ \text{K}$).

of eliminating the errors due to the variability of samples from the same batch. The specimen was allowed to recover completely after each loading period and the next loading step started only when the specimen returned to its initial condition. The whole experiment was repeated with different specimens in the same manner and the composite curves derived from each specimen were compared. All composite curves coincided with each other, yielding a master composite curve for the material.

Figure 1 shows the moiré patterns of a tension specimen. The original pattern with the specimen unloaded is shown in Figure 1a, while in Figure 1b the loaded pattern is presented after 16 min. of relaxation loading at $T = 293^\circ \text{K}$. The individual relaxation curves for the extension modulus and the lateral contraction ratio at various steps of temperature are shown in

Figures 2 and 3. The range of temperatures covers the whole response spectrum of the material from the glassy to the rubbery state.

The composite curves of these two characteristic functions are shown in Figures 4 and 5, as they derived from the corresponding individual curves by applying the principle of reduced variables. The temperature $T_0 = 273^\circ\text{K}$. was taken as reference temperature.

Results

The values of the time factor K_T were determined in order to derive the temperature dependence of the viscoelastic functions of the material. The factor K_T was derived from the amount of shifting of each individual relaxation curve along the log time scale to meet the corresponding position in the composite curve. The values of $\log K_T$ fitted well the WLF equation:¹⁰

$$\log K_T = -K_1(T - T_R)/[K_2 + (T - T_R)] \quad (9)$$

where the near universal constants are $K_1 = 8.86$ and $K_2 = 101.6$ for temperature expressed in degrees Centigrade. T_R is a reference temperature which was found to be approximately 50°C . above the glass transition tem-

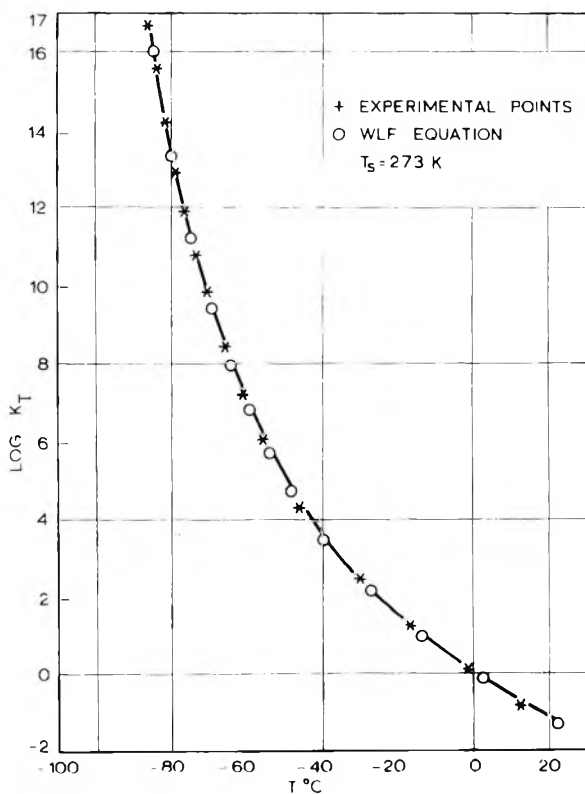


Fig. 6. Logarithm of the time-shift factor vs. temperature curve for a polyurethane elastomer referred to the reference temperature $T_0 = 273^\circ\text{K}$.

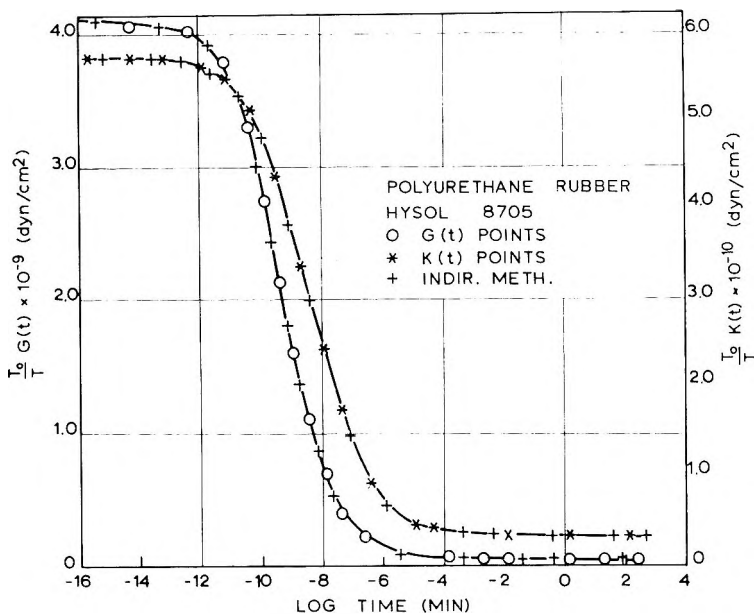


Fig. 7. Shear and bulk relaxation modulus composite curves for a polyurethane elastomer ($T_0 = 273^\circ\text{K}$).

perature T_0 . Since T_0 for the material was found to be 223°K , T_R was taken equal to 273°K . Figure 6 presents the values of $\log K_T$ versus the temperature as they derived from the shifting of the experimental individual curves of the extension relaxation modulus. These values compared favorably with the corresponding values derived from relation (9). An almost coincident curve may be obtained from the shifting factors of the lateral contraction ratio individual curves, since these factors were approximately equal to the corresponding factors of the extension relaxation modulus curves.

Figure 7 shows the shear and bulk relaxation modulus composite curves as they derived from the values of the extension relaxation modulus and the corresponding lateral contraction ratio. As was expected, all relaxation moduli characteristic functions are monotonically decreasing. The shear relaxation modulus relaxes more rapidly than the extension modulus, and the bulk modulus relaxes more slowly than the other two moduli. This results in a relaxation lateral contraction ratio function which is a monotonically increasing function, the shape of which resembles the strain-optical coefficient characteristic function.³

The experimental values of all relaxation characteristic functions were compared with the values obtained by applying an indirect method.⁴ This method uses the experimental values of one characteristic function all over the whole viscoelastic range of the material and an initial arbitrary value of a second characteristic function. The extension relaxation modulus function and an initial value of the lateral contraction ratio at the rubbery

state were used as the necessary data to determine the values of all the other functions.

For this purpose eqs. (3) and (5), which are nonhomogeneous Volterra integral equations of the second kind were solved by using finite differences. In this case they may be changed into a set of simultaneous algebraic equations. The procedure was similar to the approximation method developed by Hopkins and Hamming¹¹ and used by Lee and Rogers.¹² If we divide the log time interval into a number of n subintervals between 1 and $(n + 1)$ so that the maximum variation of the known function $E(t)$ in any of these subintervals is considered small, then, for a stronger reason, the variations of the $K(t)$ and $\nu_r(t)$ functions in the same interval may be considered as constant. In this case the values of the function $\nu_r(t)$ may be written in the form

$$\nu_r(t_{n+1}) = 1/2 \left[1 - \frac{E_0}{3K(t_n)} \right] - 1/6 \int_{t_i}^{t_{n+1}} \frac{\dot{E}(t_{n+1} - \tau)}{K(\tau)} d\tau \quad (10)$$

or

$$\nu_r(t_{n+1}) = 1/2 \left[1 - \frac{E_0}{3K(t_n)} \right] + 1/6 \sum_{i=1}^n \int_{t_i}^{t_{i+1}} \frac{1}{K(\tau)} \frac{\partial E(t_{n+1} - \tau)}{\partial \tau} d\tau$$

If we use the approximation that in the interval between t_i and t_{i+1} the weak function with time $K(\tau)$ remains constant, we obtain

$$\nu_r(t_{n+1}) = 1/2 \left[1 - \frac{E_0}{3K(t_n)} \right] - \frac{1}{6K(t_n)} \sum_{i=1}^n \int_{t_i}^{t_{i+1}} \frac{\partial E(t_{n+1} - \tau)}{\partial \tau} d\tau$$

or

$$\nu_r(t_{n+1}) = 1/2 \left[1 - \frac{E_0}{3K(t_n)} \right] + \frac{1}{6K(t_n)} \sum_{i=1}^n [E(t_{n+1} - t_{i+1}) - E(t_{n+1} - t_i)] \quad (11)$$

Similarly we can find for the bulk modulus function the following relation

$$K(t_{n+1}) = \frac{E_0}{6[1/2 - \nu_r(t_n)]} - 1/6 \sum_{i=1}^n \frac{E(t_{n+1} - t_{i+1}) - E(t_{n+1} - t_i)}{[1/2 - \nu_r(t_n)]} \quad (12)$$

The initial values $E_0 = E(t_1)$, $\nu_{r0} = \nu_r(t_1)$, and $K_0 = K(t_1)$ are the values of these quantities at the glassy or rubbery state. They are interrelated by the well known elastic relationships, since the time dependence at these states is insignificant. Moreover, the quantities $E(t_{n+1} - t_n)$ express the values of the extension modulus at the interval $(t_{n+1} - t_n)$, and they are replaced by the values of this function at the end of the interval.

Taking $n = 1, 2, 3, \dots$, in the set of eqs. (11) and (12) successively we obtain relations from which we evaluate the pairs of quantities $\nu_r(t_2)K(t_2)$, $\nu_r(t_3)K(t_3)$, \dots , each equation determining the next value of either of these quantities in terms of the values of the other quantity and the values of the

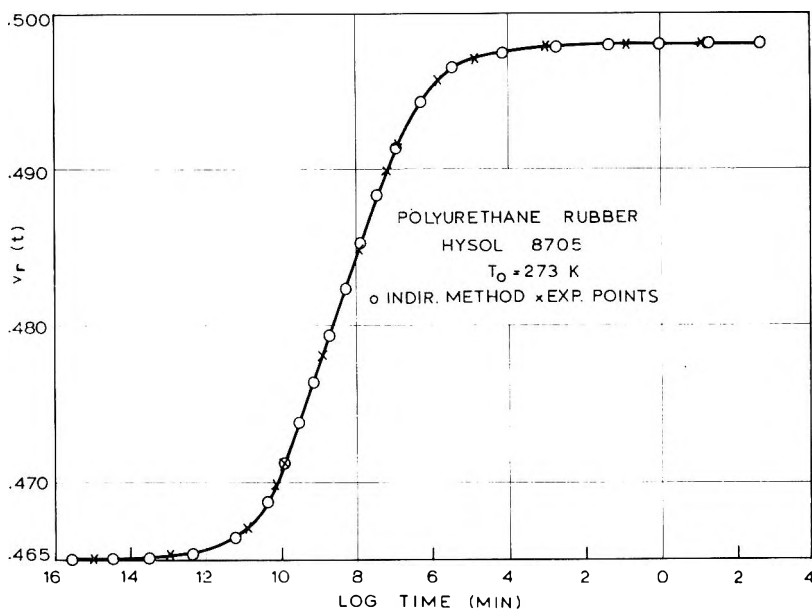


Fig. 8. Lateral contraction ratio composite curve for a polyurethane elastomer in relaxation as derived by the indirect method.⁴

function $E(t)$ at the points t_n of the relaxation spectrum, which are evaluated experimentally.

Relations (11) and (12) yield lower and upper bounds for the functions $\nu_r(t)$ and $K(t)$. The one bound was generated by starting the calculation process with the one initial value (say, K_0) and the other bound by starting with the initial value of the other function (ν_{r0}).

This finite difference approximation found to be extremely stable by the results obtained in cases where the $E(t)$ function is a smooth, positive decreasing function, as it is the case for all crosslinked polymers.⁴ The evaluation of the bounds of both characteristic functions was programmed for the IBM 7074 computer at Pennsylvania State University Computing Laboratory. Flexibility of the number of log-time subintervals was so provided that discrepancies between bounds could be minimized by an appropriate choice of the time increment.

The values of the lateral contraction ratio obtained by this indirect method were compared with experimental values. They are plotted in Figures 7 and 8. The coincidence of the results is remarkable and proves the validity of the indirect method. Moreover, the experimental data for the extension relaxation modulus and the values of shift factor K_T compared well with similar data given recently by Williams and co-workers.¹³

Landel¹⁴ has studied the viscoelastic behavior of polyurethane elastomers and used a sample of Vulcollan 18/40. Although this material belonged to the same family of polyurethane elastomers it was different from the Hysol sample used in our experiments because it was prepared from a

low molecular weight polyester crosslinked by reacting with naphthalene 1,4-diisocyanate and 1,4-butanediol, while the Hysol elastomer was prepared from a high molecular weight liquid epoxy prepolymer in which the

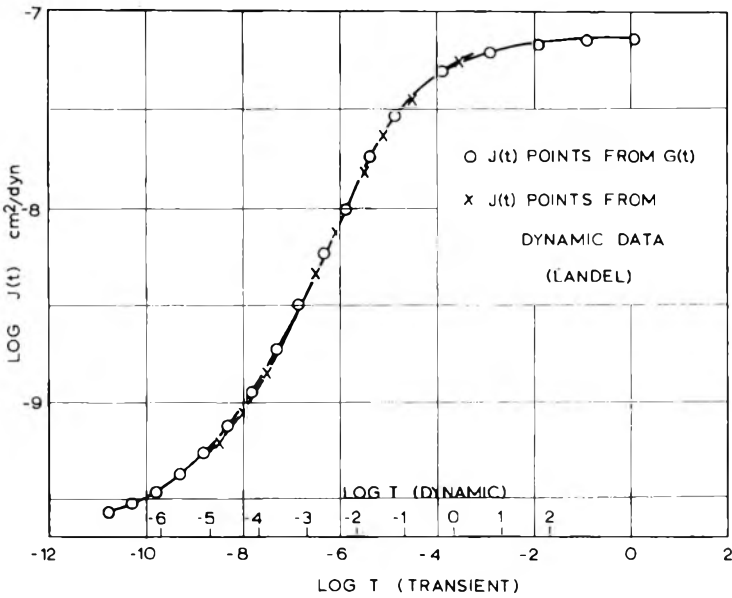


Fig. 9. Transient shear compliance composite curves for a polyurethane elastomer as derived from a numerical inversion of the corresponding shear modulus curve and from the complex shear compliance of the material.

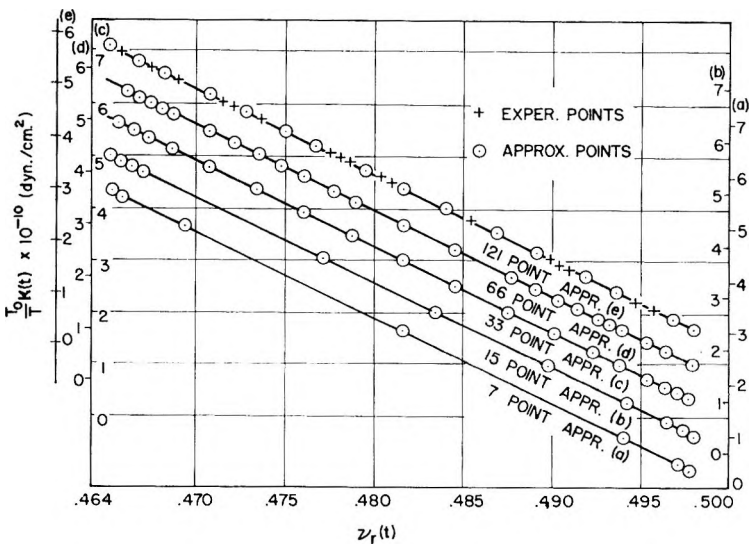


Fig. 10. Bulk relaxation modulus vs. lateral contraction ratio curves for a polyurethane elastomer (Hysol 8705).

hydroxyl groups of the chain were reacted with a diisocyanate to provide crosslinking.

In spite of the differences in the molecular structure of the two materials their viscoelastic behavior was expected to be similar since both substances belong to the same general type of polymers. Landel has measured the complex shear compliance in the transition region from rubbery to glasslike states. The values of the transient shear compliance $J(t)$ were determined from the real and imaginary parts of the complex shear compliance by using Ninomiya and Ferry's approximation method.¹⁵ These values are plotted in Figure 9. The values of the transient shear compliance were plotted in the same figure, as they were determined from the values of the transient shear modulus by a numerical inversion of the Duhamel integral relating the two functions. For this purpose the numerical method introduced by Hopkins and Hamming¹¹ was used. The comparison of the two groups of values shows a satisfactory agreement.

The bulk and the lateral contraction functions are the only functions which depend uniquely on the change of volume. Then, it is reasonable to seek interrelations between these two functions. For this purpose the bulk modulus was plotted versus the lateral contraction ratio in Figure 10.

It may be derived from this figure that a linear relationship connects these two characteristic functions in relaxation to a high degree of approximation. The same linear relation between these two functions derived from the indirect method and this relationship held for every step of approximation. In Figure 10 the lines $K = f(\nu_r)$ were plotted for various steps of approximation from 7 points up to 121 points along the whole viscoelastic range of the material.

The same linear relationship was shown previously to hold for a series of polymeric substances.⁴

Since this linear relationship between the bulk modulus and the lateral contraction ratio in relaxation seems to hold to a high degree of approximation it may replace any other assumption, such as the incompressibility and the constancy of bulk, along the whole viscoelastic spectrum, and it will yield results closer to the exact values. This relationship may be used in problems of applications where more than one operational modulus or compliance is involved in a complicated form. The solution of viscoelastic problems in such cases is sought by using the Laplace or Fourier transform operation with respect to time. This eliminates time from the equation in favor of the transform parameter, and the system is converted to a set of partial differential equations in the space variables only for transformed components of stresses, which corresponds to an elastic analysis problem. Inversion of the transformed elastic solution presents insuperable difficulties in cases in which the associated elastic solution is a complicated function where the material properties are contained in a complicated form, as is usually the case in actual systems. In this case the linear relationship between two characteristic functions of the materials may simplify the problem and permit solution of the inversion by reducing the unknown operational moduli to one function.

Moreover, this linearity between $K(t)$ and $[^{1/2} - \nu_r(t)]$ implies that the contributions of the variations of the bulk modulus and the complementary lateral contraction ratio to the variation of the extension modulus function are equivalent. Indeed, from the linearity between these two functions we have the relation

$$K(t)/[^{1/2} - \nu_r(t)] = K_0/(^{1/2} - \nu_{r0}) \quad (13)$$

which, by differentiation with respect to time, yields,

$$dK(t)[^{1/2} - \nu_r(t)] = K(t)d\nu_r(t) \quad (14)$$

If we consider a double subinterval ($n, n + 2$) of the log-time scale where, for the first subinterval ($n, n + 1$), the function $K(t)$ is held constant while, for the second subinterval ($n + 1, n + 2$) the function $\nu_r(t)$ is held constant, then for the first subinterval it is valid that

$$dE(t_{n+1}) = -6K(t_n)d\nu_r(t) \quad (15)$$

while, for the second subinterval it is valid that

$$dE(t_{n+2}) = 6dK(t)[^{1/2} - \nu_r(t_{n+1})] \quad (16)$$

Relation (14) implies that $dE(t_{n+1}) = dE(t_{n+2})$, that is, the variation of extension modulus function at the subinterval ($n, n + 2$) is equally distributed between the variations of $K(t)$ and $[^{1/2} - \nu_r(t)]$.

Conclusions

The transient extension relaxation modulus $E(t)$ and the lateral contraction ratio $\nu_r(t)$ for a polyurethane elastomer Hysol 8705 were measured simultaneously in the transition region by using the differential moiré method and zonal gratings of a density of 20 lines/mm.

The composite curves of $E(t)$ and $\nu_r(t)$ were traced by using the method of reduced variables. It was shown that the transient lateral contraction ratio in relaxation is a monotonically increasing function. This experimental evidence, together with previously obtained data^{3,4} concerning other types of polymers, elucidates the controversial arguments of previous investigators⁶ concerning the shape of this master curve.

The lateral contraction ratio function was also determined by an indirect method by using data of the extension relaxation modulus function and an initial value of the lateral contraction ratio at the rubbery state. The comparison of results showed a remarkable agreement which indicates the near universality of the method.

The experimental results revealed that a linear law relates the bulk modulus and the lateral contraction ratio functions of the substance along the whole viscoelastic region. The same law was previously found to hold for a series of polymers of various values of molecular weight.

The experimental method of the differential moiré with the use of zonal gratings, yielding simultaneously values of the longitudinal extension and the transverse contraction in a transient extension specimen proved by its

results to be very efficient for the determination of the mechanical properties of amorphous polymers.

References

1. Ferry, J. D., *Viscoelastic Properties of Polymers*, Wiley, New York, 1961.
2. Tobolsky, A. V., *Properties and Structure of Polymers*, Wiley, New York, 1960.
3. Theocaris, P. S., *J. Mech. Phys. Solids*, **12**, 125 (1964).
4. Theocaris, P. S., *Rheol. Acta*, **4**, 3, 299 (1964).
5. Kovacs, A. J., Thesis, Fac. Sci. Paris, 1954.
6. Heydemann, P., *Kolloid Z.*, **193**, 12 (1963).
7. Theocaris, P. S., and C. HadjiJoseph, *Kolloid Z.*, in press.
8. Theocaris, P. S., and H. H. Kuo, *J. Appl. Mech.*, in press.
9. Theocaris, P. S., and C. HadjiJoseph, *Proc. Intern. Congr. Rheology, 4th Congr., Providence, 1963*, 322 (1963).
10. Williams, M. L., R. F. Landel and J. D. Ferry, *J. Am. Chem. Soc.*, **77**, 3701 (1955).
11. Hopkins, I. L., and R. W. Hamming, *J. Appl. Phys.*, **28**, 906 (1957).
12. Lee, E. H., and T. G. Rogers, *J. Appl. Math. Phys.*, **30**, 127 (1963).
13. Arenz, R. J., G. W. Ferguson, T. Kunio, and M. L. Williams, *Galcit Report SM 63-31*, (1963).
14. Landel, R. F., *J. Colloid Sci.*, **12**, 308 (1957).
15. Ninomiya, K., and J. D. Ferry, *J. Colloid Sci.*, **14**, 36 (1959).

Résumé

Le module de relaxation en extension $E(t)$ et le rapport de la contraction latérale $\nu_r(t)$ d'un élastomère de polyuréthane, ont été mesurés simultanément dans la région de transition de l'état vitreux à l'état caoutchouteux. La méthode différentielle de Moiré a été employée pour ces mesures et elle fournit simultanément des valeurs de l'allongement longitudinal et de la contraction latérale qui sont les principales déformations de l'échantillon sous tension. Les courbes maîtresses de $E(t)$ et $\nu_r(t)$, réduites pour une température standard ont été obtenues en appliquant la méthode des variables réduites. Les facteurs de glissements K_T coïncident pour les deux courbes et suivent l'équation WLF. Le module de cisaillement et le module de compression sont déterminés à partir du module d'allongement et du rapport $\nu_r(t)$ de contraction latérale. Les valeurs du rapport de contraction latérale dans la relaxation sont déterminées en utilisant les résultats du module de relaxation à l'extension dans tout le domaine viscoélastique et de la valeur initiale du rapport de contraction latérale à l'état caoutchouteux et en appliquant une méthode indirecte. Les résultats obtenus par la méthode indirecte coïncident avec les valeurs expérimentales. La fonction du module de cisaillement a été évaluée à partir du module de relaxation à l'extension et des fonctions du rapport de contraction latérale et a été comparée avec l'inverse du module de cisaillement dynamique déterminé par Landel. Les résultats expérimentaux montrent qu'il y a une relation linéaire entre le rapport de la contraction latérale dans la relaxation et le module pour tout le spectre. On a montré antérieurement que la même relation existait pour une série de substances polymériques diverses.

Zusammenfassung

Der momentane Ausdehnungsrelaxationsmodul $E(t)$ und das seitliche Kontraktionsverhältnis $\nu_r(t)$ wurden gleichzeitig an einem Polyurethanelastomeren im Umwandlungsbereich vom Glas- zum Kautschukzustand gemessen. Die differentielle Moirémethode wurde bei diesen Messungen angewendet und lieferte Simultanwerte für die longitudinale Dehnung und die seitliche Kontraktion bei der Hauptverformung der Zugprobe. Mit der Methode der reduzierten Variablen wurden die auf eine Standardtemperatur re-

duzierten zusammengesetzten Kurven für $E(t)$ und $\nu_r(t)$ erhalten. Die Zeitfaktoren K_T koinzidierten in beiden Kurven und befolgten die WLF-Gleichung. Die charakteristischen Funktionen des Scher- und Kompressionsmoduls wurden aus dem Dehnungsmodul und dem seitlichen Kontraktionsverhältnis erhalten. Die Werte des seitlichen Kontraktionsverhältnisses bei der Relaxation wurden mit Daten für den Dehnungsrelaxationsmodul über den ganzen viskoelastischen Bereich und den Anfangswert des seitlichen Kontraktionsverhältnisses im Kautschukzustand unter Anwendung einer indirekten Methode bestimmt. Die mit der indirekten Methode erhaltenen Ergebnisse stimmten mit den experimentellen Werten überein. Die Funktion für den Schermodul wurde aus dem Dehnungsrelaxationsmodul und dem seitlichen Kontraktionsverhältnis bestimmt und mit der von Landel bestimmten dynamischen Schernachgiebigkeit verglichen. Die Versuchsergebnisse zeigen, dass zwischen dem seitlichen Kontraktionsverhältnis bei der Relaxation und dem Kompressionsmodul über das ganze Reaktionsspektrum eine lineare Beziehung besteht. Schon früher wurde gezeigt, dass die gleiche Beziehung für eine Reihe verschiedener polymerer Substanzen gilt.

Received October 1, 1964

Revised December 18, 1964

(Prod. No. 4611A)

Effect of Crosslinking Density on the Viscoelastic Properties of Unsaturated Polyesters

K. SHIBAYAMA and Y. SUZUKI, *Central Research Laboratories, Mitsubishi Electric Corporation, Amagasaki, Japan*

Synopsis

Viscoelastic properties of unsaturated polyesters were investigated in the glass-rubber transition region in relation to the temperature dependence of specific volume. Polyesters which are homologous with respect to crosslinking density were prepared by using mixtures of succinic and fumaric acid as the dibasic acid component. The temperature dependence of the specific volume was determined by refractive index measurement, the specific refractivity being assumed to be independent of temperature. The temperature dispersion of dynamic viscoelasticity was measured at a constant frequency. Results are summarized as follows. Specific volume and glass temperature are linearly related to the logarithm of crosslinking density. The thermal expansion coefficient and steepness of viscoelastic dispersion decrease with increasing crosslinking density. Fractional free volume and expansion coefficient of free volume, both of which were calculated by WLF equation, are in good agreement with the temperature dependence of specific volume. The results indicate that the effect of crosslinking is largely attributable to the change in amount and distribution of free volume in polymer networks.

INTRODUCTION

In general, solid polymers usually considered to exist in the form of three-dimensional network structures, because their molecular chains are aggregated by various junctions, e.g., chemical crosslinking, chain entanglement, and other intermolecular couplings. The statistical theory of rubberlike elasticity, which has been derived directly from the above concept, has been the basis for considerable progress in polymer science. Recently, studies on fine structure and properties of crystalline polymers have greatly advanced. In contrast with this, very few studies have been made of the effects of network structure, except for polymers in rubbery states. It has been usual to consider that the changes in properties due to network structure are negligible when a polymer goes from the rubbery to glassy region where segmental motions are restricted in some short ranges. It would seem, however, necessary to examine more carefully the possible effects of network structure on properties of polymers in the so-called glass to rubber transition region, in view of the fact that the glass temperature is an increasing function of network density.

In this paper, viscoelastic properties and glass transition phenomena are investigated for unsaturated polyesters as typical amorphous polymers which have permanent networks. Several investigations of these polymers by viscoelastic,¹ dielectric,² and nuclear magnetic resonance³ methods have been reported. However, the effects of network structure have not been the principal subject in these investigations. As the first step in elucidating the effects of network structure, it is necessary to study the effects of network density in a homologous series of polymers. In this study, an attempt was made to obtain a series of polymers each of which differs in network density but which are otherwise identical as far as possible, though this requirement can be never satisfied completely because introduction of permanent network junctions (chemical crosslinks) is always accompanied by a change in chemical structure.

MATERIALS AND EXPERIMENTAL METHODS

Polyesters having different concentrations of unsaturated groups were prepared and copolymerized with vinyl monomers as summarized in Table I. In this way, we can derive a series of polymers homologous with respect to crosslinking density, provided fumaric and succinic acid in co-

TABLE I
Compositions of samples

| Sample no. | Polyester ^a | | | Vinyl monomer ^b | | $\rho \times 10^3$, mole/g. ^c |
|------------|------------------------|---------------------|-------------------------|----------------------------|---------------------|---|
| | Fumaric acid, mole | Succinic acid, mole | Diethylene glycol, mole | Styrene, mole | Vinyl acetate, mole | |
| S-1 | 0.30 | 0.70 | 1.05 | 1.00 | 0.00 | 1.71 |
| S-2 | 0.35 | 0.65 | 1.05 | | | 2.00 |
| S-3 | 0.50 | 0.50 | 1.05 | | | 2.86 |
| S-4 | 0.60 | 0.40 | 1.05 | | | 3.44 |
| S-5 | 0.70 | 0.30 | 1.05 | | | 4.02 |
| SA3-1 | 0.30 | 0.70 | 1.05 | 0.70 | 0.30 | 1.71 |
| SA3-2 | 0.35 | 0.65 | 1.05 | | | 2.00 |
| SA3-3 | 0.50 | 0.50 | 1.05 | | | 2.86 |
| SA3-4 | 0.60 | 0.40 | 1.05 | | | 3.44 |
| SA3-5 | 0.70 | 0.30 | 1.05 | | | 4.02 |
| SA5-1 | 0.30 | 0.70 | 1.05 | 0.50 | 0.50 | 1.71 |
| SA5-2 | 0.35 | 0.65 | 1.05 | | | 2.00 |
| SA5-3 | 0.50 | 0.50 | 1.05 | | | 2.86 |
| SA5-4 | 0.60 | 0.40 | 1.05 | | | 3.44 |
| SA5-5 | 0.70 | 0.30 | 1.05 | | | 4.02 |

^a Esterification carried out in the usual manner at 170–200°C. to acid number of 20 mg. KOH/g. resin.

^b Resin solution (70 wt.-%) in vinyl monomer. Cure schedule: 1% BPO; 2 hr. at 80°C.; 2 hr. at 100°C.; 5 hr. at 130°C.; 8 hr. at 150°C./0.1 mm. Hg.

^c Number of moles of fumaric acid units per unit weight of cured resin.

polymer networks are identical chain members except for crosslinking ability of the former.

Careful operations are usually required to determine the thermal expansion coefficient of polymers by an immersion type dilatometer. We have attempted to get equivalent information from refractive index measurements. Specific volume v can be expressed on the basis of the Lorenz-Lorentz equation as

$$v = (n^2 + 2)r/(n^2 - 1) \quad (1)$$

where n is refractive index and r is specific refractivity, which is assumed to be independent of temperature. The value of r was calculated by eq. (1) by using the value of v measured at 30°C. in a density gradient tube. Measurement of refractive index was carried out by the usual Abbé type refractometer. Dimensions of a typical specimen were 3×3 mm. and 0.1 mm. in thickness. It is recommended that the specimen be so cut that one side is smooth while other three sides are rough. The specimen must be smaller than the prism face of the refractometer.

Dynamic modulus and $\tan \delta$ were measured at a constant frequency (138 cycles/sec.) by a mechanical $\tan \delta$ meter of the direct-reading type⁴ at temperatures from -20 to 180°C. It has been reported in an earlier paper⁵ that the temperature dependence of $\tan \delta$ can be expressed as eq. (2) when the frequency dependence of the dynamic modulus, E' , is fitted by an empirical eq. (3) which is analogous to the one proposed by Tobolsky⁶ for the relaxation modulus and is readily transcribed into a form of temperature dependence by using the WLF⁷ equation,

$$\tan \delta(T) = \frac{\sqrt{\pi}}{2} h \log \frac{E'_1}{E'_2} \exp \left\{ - \left[\frac{hC_1(T - T_m)}{C_2 + T - T_m} \right]^2 \right\} \quad (2)$$

$$\log E'(\omega) = \frac{1}{2} \left(\log E'_1 E'_2 + \log \frac{E'_1}{E'_2} \operatorname{erf} \left\{ h \log \frac{\omega}{k} \right\} \right) \quad (3)$$

where E'_1 and E'_2 are upper and lower equilibrium values of dynamic modulus, h is a parameter representing steepness of frequency dispersion, C_1 and C_2 are characteristic constants appearing in the WLF equation, T_m is the temperature at which $\tan \delta$ exhibits its maximum value, ω is angular frequency, and k is frequency when $\log E' = 1/2 (\log E'_1 E'_2)$. Derivation of eq. (2) from eq. (3) is essentially identical to Schwarzl-Staverman's approximation.⁷ It is possible to evaluate C_1 , C_2 and h from the measurement of temperature dispersion at a single frequency. Equations (4) and (5), derived from eq. (2), can be used conveniently for this purpose,

$$h = 2 \tan \delta(T_m) / \left[\sqrt{\pi} \log (E'_1/E'_2) \right] \quad (4)$$

$$hC_1(T - T_m)/(C_2 + T - T_m) = \left\{ \ln \left[\tan \delta(T_m)/\tan \delta(T) \right] \right\}^{1/2} \quad (5)$$

Crosslinking density ρ_E can be evaluated by eq. (6) from the observed value of rubbery modulus E'_2 for lightly crosslinked systems:

$$\rho_E = vE'_2/3RT \quad (6)$$

In this experiment, however, values of E'_2 can be as high as 10^9 dyne/cm.², as will be discussed below. For such high degrees of crosslinking, Gaussian statistics are obviously invalid, so the applicability of eq. (6) is open to question. It is, therefore, preferable to use ρ , defined as the number of moles of fumaric acid units per unit weight of cured resin, as a relative measure of crosslinking density, assuming that the conversions of fumaric acid units in polyester primary chains into crosslinkages are quantitative.

RESULTS

Figures 1, 2, and 3 show specific volume versus temperature curves for the three series. In each case, experimental points may be fitted by three straight lines, giving two apparent transition points. The lower one, denoted T_{θ_1} , is always in the range of -20° to -10°C ., irrespective of the

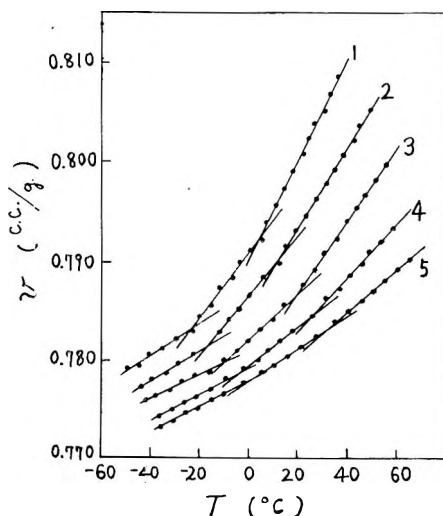


Fig. 1. Specific volume vs. temperature curves for series S.

kind of series, while the upper one, denoted as T_{θ_2} , appears at higher temperature as we proceed from series SA-3 to S. In one series, both T_{θ_1} and T_{θ_2} increase with crosslinking density. There is no other inflection point on specific volume versus temperature curves up to 100°C . in all cases. Values of parameters which characterize the temperature dependence of specific volume are listed in Table II; values of thermal expansion coefficient below T_{θ_1} are omitted because of experimental uncertainty. The value of specific refractivity is roughly constant in a series. This might be a neces-

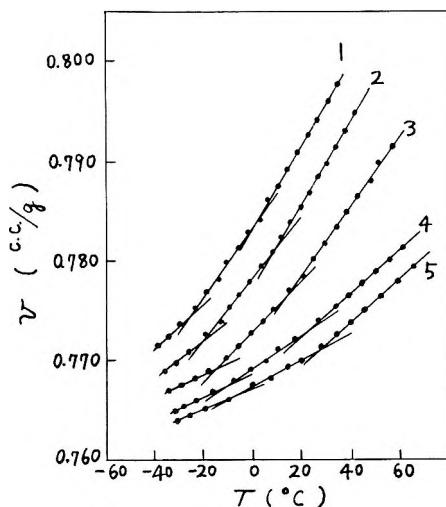


Fig. 2. Specific volume vs. temperature curves for series SA3.

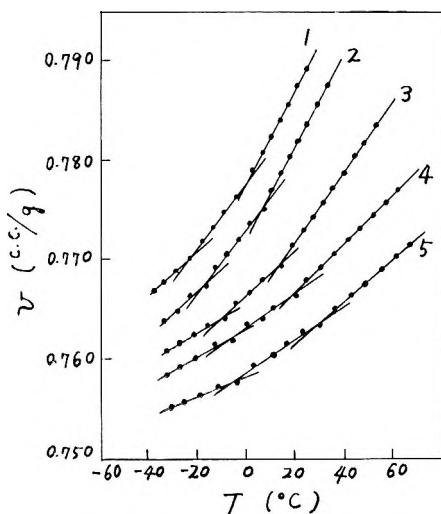


Fig. 3. Specific volume vs. temperature curves for series SA5.

sary condition for regarding each series as a chemically homologous one. Wiley and Brauer⁸ have determined the glass temperature directly by plotting the refractive index against temperature. Hookway⁹ has used the Gladstone-Dale relationship instead of the Lorenz-Lorentz equation for relating refractive index and specific volume. As for the glass temperatures, the results of Figures 1-3 are not altered in any significant way by these alternatives.

Figures 4, 5, and 6 show storage and loss moduli and $\tan \delta$ versus temperature curves for the three series. The dispersion region was found to

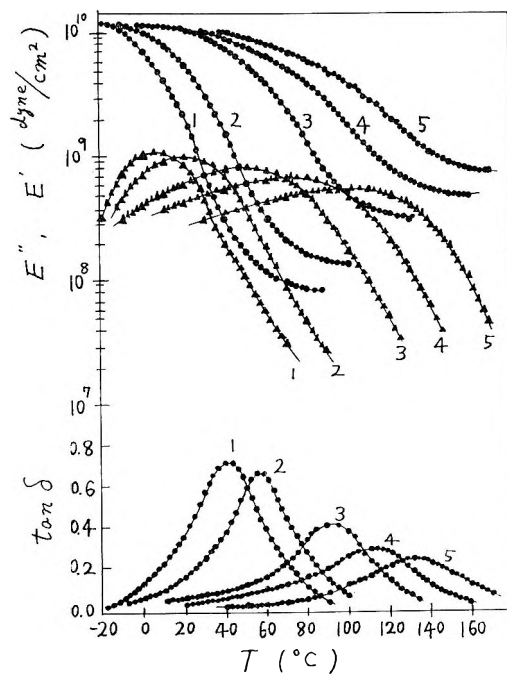


Fig. 4. Plots of E' , E'' , and $\tan \delta$ vs. temperature for series S (138 cycles/sec.).

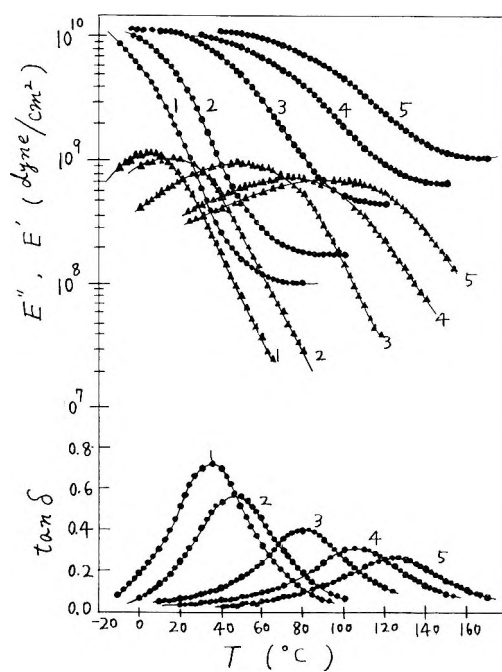


Fig. 5. Plots of E' , E'' , and $\tan \delta$ vs. temperature for series SA3 (138 cycles/sec.).

extend toward the higher temperature region when the crosslinking density was increased. Single broad dispersion was observed in each case but no secondary dispersion was apparent in the range of this experiment. The validity of eq. (5) is illustrated in Figure 7. From these plots, values of

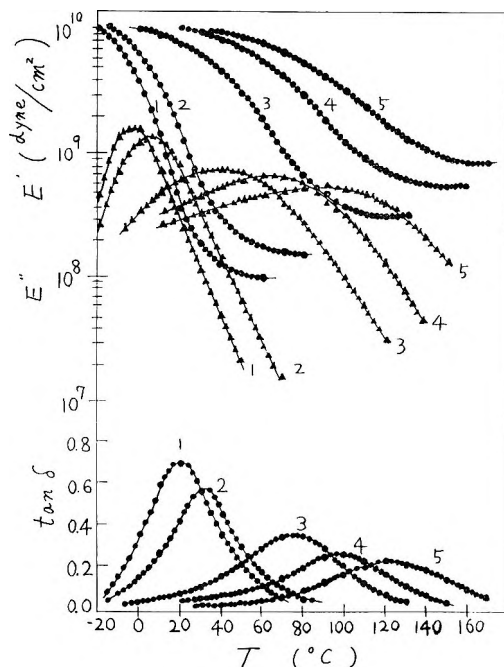


Fig. 6. Plots of E' , E'' , and $\tan \delta$ vs. temperature for series SA5 (138 cycles/sec.).

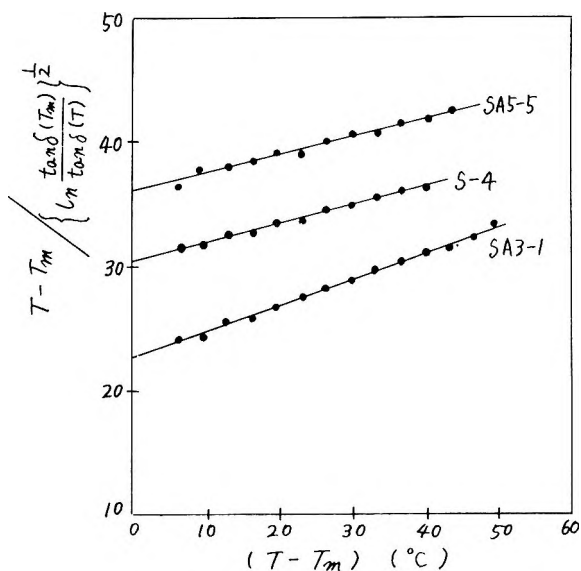


Fig. 7. Examples of WLF plots.

TABLE II
 Parameters Characterizing Temperature Dependence of Specific Volume

| Sample no. | $T_{g1}, ^\circ\text{C.}$ | $T_{g2}, ^\circ\text{C.}$ | $v_g, \text{cc./g.}$ | $\alpha_a \times 10^4$ | r |
|------------|---------------------------|---------------------------|----------------------|------------------------|--------|
| S-1 | -23 | 4 | 0.783 | 4.69 | 0.2453 |
| S-2 | -19 | 11 | 0.790 | 4.50 | 0.2443 |
| S-3 | -16 | 20 | 0.787 | 3.48 | 0.2445 |
| S-4 | -13 | 28 | 0.785 | 2.73 | 0.2440 |
| S-5 | -11 | 32 | 0.784 | 2.25 | 0.2442 |
| SA3-1 | -22 | 2 | 0.785 | 4.76 | 0.2391 |
| SA3-2 | -18 | 8 | 0.782 | 4.35 | 0.2386 |
| SA3-3 | -14 | 16 | 0.778 | 3.91 | 0.2381 |
| SA3-4 | -11 | 24 | 0.773 | 2.42 | 0.2386 |
| SA3-5 | -10 | 27 | 0.772 | 2.38 | 0.2385 |
| SA5-1 | -22 | 1 | 0.779 | 4.58 | 0.2351 |
| SA5-2 | -18 | 6 | 0.776 | 4.41 | 0.2344 |
| SA5-3 | -13 | 14 | 0.771 | 3.57 | 0.2341 |
| SA5-4 | -11 | 19 | 0.767 | 2.67 | 0.2343 |
| SA5-5 | -7 | 25 | 0.763 | 2.08 | 0.2337 |

C_1 and C_2 were determined. Evidently C_1 and C_2 are the WLF constants referred to T_m , which were then transformed to C_1^g and C_2^g appropriate to T_g by the relations

$$C_1^g = C_1 C_2 / (C_2 + T_g - T_m)$$

$$C_2^g = C_2 + T_g - T_m$$

 TABLE III
 Parameters Characterizing Viscoelastic Properties

| Sample no. | h | C_1 | C_2 | f_g | $\alpha_f \times 10^4$ |
|------------|-------|-------|-------|--------|------------------------|
| S-1 | 0.397 | 18.1 | 78.5 | 0.0233 | 3.07 |
| S-2 | 0.415 | 18.9 | 73.5 | 0.0230 | 3.13 |
| S-3 | 0.323 | 30.5 | 93.7 | 0.0142 | 1.52 |
| S-4 | 0.266 | 41.0 | 105.5 | 0.0105 | 1.00 |
| S-5 | 0.250 | 51.3 | 267.0 | 0.0085 | 0.31 |
| SA3-1 | 0.374 | 18.6 | 82.0 | 0.0233 | 2.86 |
| SA3-2 | 0.333 | 22.1 | 88.5 | 0.0197 | 2.23 |
| SA3-3 | 0.307 | 30.7 | 110.3 | 0.0141 | 1.28 |
| SA3-4 | 0.250 | 45.7 | 147.8 | 0.0095 | 0.65 |
| SA3-5 | 0.238 | 55.3 | 256.0 | 0.0079 | 0.31 |
| SA5-1 | 0.384 | 15.2 | 79.3 | 0.0286 | 3.63 |
| SA5-2 | 0.341 | 16.8 | 79.5 | 0.0258 | 3.25 |
| SA5-3 | 0.286 | 31.2 | 74.1 | 0.0139 | 1.88 |
| SA5-4 | 0.252 | 40.0 | 104.0 | 0.0109 | 1.05 |
| SA5-5 | 0.234 | 50.2 | 171.5 | 0.0085 | 0.51 |

Finally the values of f_θ , fractional free volume at T_θ , and α_f , the thermal expansion factor of free volume, were calculated by the relations

$$f_\theta = (1/2.303)C_1^\theta$$

$$\alpha_f = (1/2.303)C_1^\theta C_2^\theta$$

To permit the above calculations to be carried out, T_θ has to be known. Values of T_θ , which is considered as the temperature of the onset of the freezing-in process as will be shown later, were used for this purpose.

Value of parameters which characterize the temperature dispersions of viscoelastic functions are listed in Table III.

DISCUSSION

Glass Temperature

It has been shown in earlier papers^{8,9} that a change in specific volume, Δv , caused by an increase in crosslinking density from ρ_0 to ρ can be expressed as eq. (7), assuming the network restriction is localized near crosslinking points,

$$\Delta v = -a \ln (\rho/\rho_0) \quad (7)$$

where a is a proportionality constant having a value in the range of 0.02–0.04 which is in reasonable agreement with the estimated value of fractional free volume in usual polymers. From the data of Figures 1–3 Δv is plotted against the logarithm of ρ as shown in Figure 8. A straight line can be drawn for each series, as predicted from eq. (7). The value of a is found to increase with increasing ratio of vinyl acetate in the monomer mixture. This indicates that the volume contraction accompanied by crosslinking is

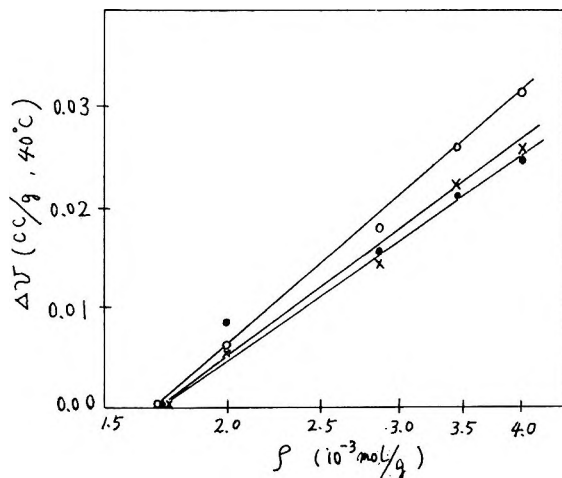


Fig. 8. Change in specific volume Δv , vs. crosslinking density ρ : (●) series S; (×) series SA3; (○) series SA5.

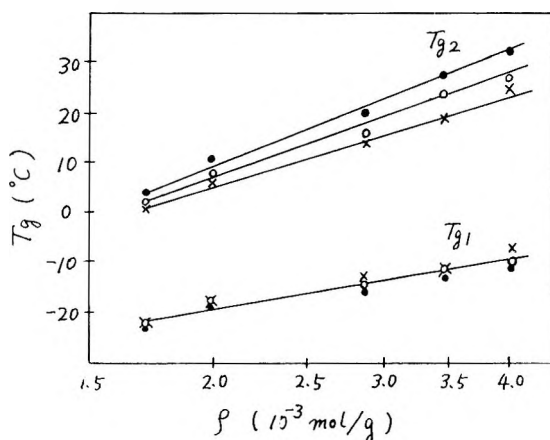


Fig. 9. Glass temperatures T_g -vs. crosslinking density ρ : (●) series S; (×) series SA3; (○) series SA5.

dependent on the nature of the molecular chain. For the poly(vinyl acetate) series, near the crosslinking points, more close packing of molecular chains may be sterically favored than for the polystyrene series.

It has been found for several types of polymers that the dependence of glass temperature on crosslinking density can be predicted by eq. (8):^{8,9}

$$T_g = K_1 \ln K_2 \rho \quad (8)$$

where K_1 and K_2 are characteristic constants for a homologous series of polymers. Dependence of both T_{g1} and T_{g2} on crosslinking density can be expressed by eq. (8) as shown in Figure 9. As for T_{g1} , values of K_1 and K_2 are almost identical for the three series. On the contrary, T_{g2} shows different ρ dependences for the three series. This difference in ρ dependence, principally in the value of K_2 , seems to agree with usual observations on copolymer systems. Though T_{g1} and T_{g2} show somewhat different dependences on crosslinking density as mentioned above, we can hardly conclude that, at these two temperatures, transitions of different mechanisms take place, since difference between T_{g1} and T_{g2} are not so large that two distinct mechanisms are necessarily considered. Hideshima¹² has pointed out that the transition occurs through a range of temperature owing to the nature of relaxational phenomenon and at both ends of the range the specific volume changes rather abruptly. According to this scheme, T_{g2} and T_{g1} can be considered as temperatures of onset and completion of the freezing-in process, respectively. Further support for this idea can be derived from the fact that $\tan \delta$ or E'' goes through a single smooth maximum. It is plausible that the onset and completion of the freezing-in process are affected by the presence of the rigid polystyrene sequence and the composition of the polyester primary chain, respectively.

As is seen from Table III, f_g , the fractional free volume at T_{g2} , decreases with increasing ρ . This dependence of f_g on ρ is consistent with a previous

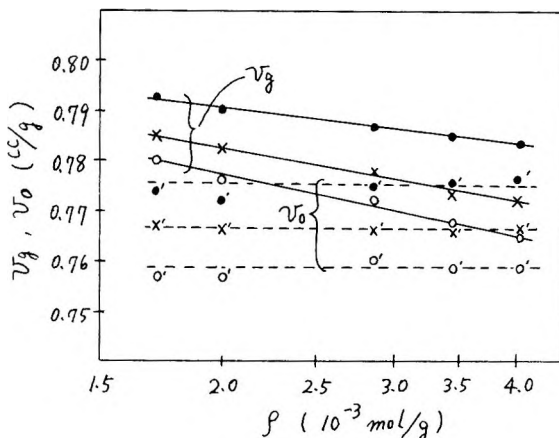


Fig. 10. Specific volume at T_{g2} , v_g , and occupied volume v_0 vs. crosslinking density ρ : (●) series S; (×) series SA3; (○) series SA5.

view⁹ which is based on the isofree volume concept modified by assuming local distribution of free volume along a chain.

Values of occupied volume, v_0 , calculated by $v_0 = v_g (1 - f_g)$ are constant in one series, as shown in Figure 10. It is concluded from this that the primary effect of crosslinking, in the present case, is to reduce the amount of free volume.

Thermal Expansion

The thermal expansion coefficient, α_a , decreases regularly with increasing ρ , as shown in Figure 11. The expansion coefficient of the free volume α_f , calculated from the WLF equation, shows a similar dependence on ρ . Subtracting α_f from α_a , we obtain a value about 1.8×10^{-4} which agrees with the expansion coefficient below T_g generally observed for polymers. The thermal expansion above T_g is thus attributed to the increase in free

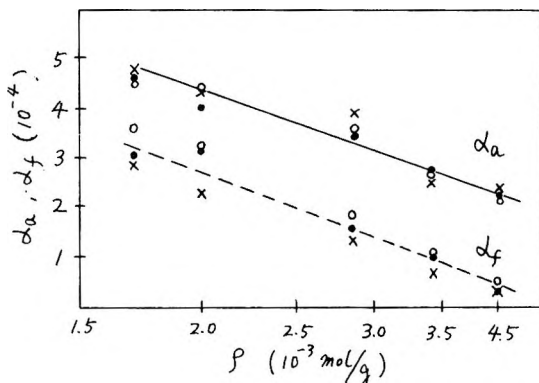


Fig. 11. Thermal expansion coefficient α_a and expansion coefficient of free volume α_f vs. crosslinking density ρ : (●) series S; (×) series SA3; (○) series SA5.

volume, as is the usual practice. Gibbs and Dimarzio¹³ have developed a quasi-lattice theory for amorphous linear polymers. According to their theory, the most probable value of the number of vacant sites n_0 is expressed as follows

$$\ln (\bar{V}_0^{(z/2)-1}/S_0^{z/2}) - (z\epsilon S_r^2/2kT) = 0 \quad (9)$$

where

$$S_r = [(z-2)x+2]n_x/[(z-2)x+2](n_x+zn_0)$$

$$S_0 = 1 - S_r$$

$$\bar{V}_0 = n_0/(xn_x + n_0)$$

z is the coordination number of lattice, ϵ is the energy of interaction between a pair of neighboring segments, x is the degree of polymerization, and n_x is the number of polymer molecules. An expression for the temperature dependence of fractional free volume f is derived from eq. (9) assuming $x \gg 1$, $xn_x/n_0 \gg 1$, and $z = 4$:

$$f \simeq n_0/xn_x = 1/4 \exp \{ -2\epsilon/kT \} \quad (10)$$

Equation (10) is essentially identical with an earlier result derived by Hirai.¹⁴ Comparing eq. (10) with the usual expression of fractional free volume, $f = f_g + \alpha'_f(T - T_g)$, we obtain

$$\alpha'_f T_g = -f_g \ln (4f_g) \quad (11)$$

The left-hand side of eq. (11) is expected to be constant, provided f_g is constant, as observed for most linear polymers.^{15,16} In the present case, f_g is not constant but depends on ρ , as seen in Table III. It is plausible that the energy required to increase the free volume becomes larger for a crosslinked system because molecular chains are coupled together by covalent bonds. Values of ϵ were readily calculated by eq. (10) by using the values of f_g and T_g listed in Table III, and were found to increase with ρ .

If eqs. (9) and (10) are valid for the present system, or in other words if the effect of crosslinking can be presumed to be given entirely by the increase in energy ϵ , calculation of α'_f by eq. (11) by using the values of T_g and f_g listed in Table III will give the same values with α_f . As shown in Table IV, α'_f thus calculated does not coincide with α_f . The latter decreases more rapidly than the former with increasing ρ . Lack of agreement must mean that either the Gibbs-Dimarzio theory does not apply or the WLF equation does not hold, provided the approximations used in deriving eq. (10) from eq. (9) were appropriate. It is, however, more likely to consider that the Gibbs-Dimarzio theory should be so modified as to be valid for crosslinked systems, since the relationship between α_f and α_a was found to be a reasonable one and the WLF equation seems to hold as mentioned earlier. It is conceivable that the crosslinking may affect not only the energy ϵ but also the configurational entropy of the system. One possible explanation for the discrepancy between α_f and α'_f is that the in-

crease in number of possible arrangements of polymer molecules in a lattice with increasing n_0 is suppressed by network restrictions in crosslinked systems, and thus α_f would decrease more rapidly than α'_f calculated by eq. (11), where only the energy ϵ is taken into consideration.

TABLE IV
Comparison of α_f and α'_f

| Sample no. | $\alpha_f \times 10^4$ | $\alpha'_f \times 10^{-4}$ |
|------------|------------------------|----------------------------|
| S-1 | 3.07 | 1.99 |
| S-2 | 3.13 | 1.92 |
| S-3 | 1.52 | 1.38 |
| S-4 | 1.00 | 1.09 |
| S-5 | 0.31 | 0.94 |
| SA3-1 | 2.86 | 2.00 |
| SA3-2 | 2.23 | 1.77 |
| SA3-3 | 1.28 | 1.40 |
| SA3-4 | 0.65 | 1.05 |
| SA3-5 | 0.31 | 0.91 |
| SA5-1 | 3.63 | 2.26 |
| SA5-2 | 3.25 | 2.09 |
| SA5-3 | 1.88 | 1.39 |
| SA5-4 | 1.05 | 1.16 |
| SA5-5 | 0.51 | 0.96 |

Frequency Dispersion of Viscoelasticity

The parameter h , which represents the steepness of frequency dispersion, decreases regularly with increasing ρ , as shown in Figure 12. Increasing values of h correspond qualitatively to increasing upward curvature in the relaxation spectra.¹⁵ It has been shown that the shapes of the relaxation spectra are not altered on introducing a regular network structure according to Rouse's theory.¹⁶

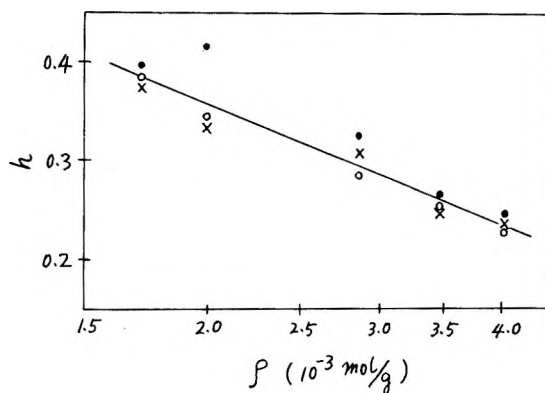


Fig. 12. Steepness of frequency dispersion h vs. crosslinking density ρ : (●) series S; (×) series SA3; (○) series SA5.

The dependence of h on ρ must be interpreted in terms of structural specialities which are cumulative with increasing ρ and have not been taken into consideration in Rouse's theory. As a possible explanation of this behavior, one may suppose that the distribution of chain length between crosslinking points becomes broader with increasing ρ . However, the broadening of chain length distribution is not required as an inevitable consequence of increasing degree of crosslinking. The author^{19,20} has shown from analog computer analysis of a modified ladder network model that the steepness of frequency dispersion is affected strongly by distribution of segmental mobilities along a chain. The distribution of segmental mobilities may serve as an alternative concept in interpreting the effect of crosslinking density on the shape of viscoelastic function in the glass-rubber transition region.

References

1. Ueki, K., N. Yoshioka, H. Maki, and Y. Inoue, *Kogyo Kagaku Zasshi*, **62**, 1135 (1959).
2. Shito, N., *Nippon Kagaku Zasshi*, **82**, 1578 (1961).
3. Tanaka, K., *Bull. Chem. Soc. Japan*, **33**, 1705 (1960).
4. Takayanagi, M., *Zairyo Shiken*, **8**, 350 (1959).
5. Shibayama, K., *Kobunshi Kagaku*, **19**, 543 (1962).
6. Tobolsky, A. V., *J. Am. Chem. Soc.*, **74**, 3786 (1952).
7. Staverman, A. J., and F. Schwarzl, in, *Die Physik der Hochpolymeren*, H. A. Stuart, Ed., Springer-Verlag, Berlin 1956, Vol. IV, Cyap. 1.
8. Wiley, R. H., and G. M. Brauer, *J. Polymer Sci.*, **3**, 455 (1948).
9. Hookay, D. C., *J. Textile Inst.*, **49**, 292 (1958).
10. Shibayama, K., *Kobunshi Kagaku*, **18**, 183 (1961).
11. Shibayama, K., *Kobunshi Kagaku*, **19**, 219 (1962).
12. Hideshima, M., *Zairyo Shiken*, **10**, 246 (1961).
13. Gibbs, J. H., and E. A. Dimarzio, *J. Chem. Phys.*, **28**, 373 (1958).
14. Hirai, N., *Nippon Kagaku Zasshi*, **75**, 683 (1954).
15. Boyer, R. F., and R. S. Spencer, *J. Appl. Phys.*, **15**, 389 (1944).
16. Simha, R., and R. F. Boyer, *J. Chem. Phys.*, **37**, 1003 (1962).
17. Ferry, J. D., *Viscoelastic Properties of Polymers*, Wiley, New York, 1961, p. 269.
18. Takemura, T., *J. Polymer Sci.*, **28**, 185 (1958).
19. Shibayama, K., *Kobunshi Kagaku*, **20**, 221 (1963).
20. Shibayama, K., *Mitsubishi Denki Lab. Repts.*, **5**, 91 (1964).

Résumé

On a étudié les propriétés viscoélastiques des polyesters non-saturés, dans la région allant depuis la transition vitreuse jusqu'à la transition caoutchouteuse, en relation avec la dépendance du volume spécifique vis-à-vis de la température. Des polyesters homologues quant à la densité de pontage ont été préparés en employant des mélanges d'acides succinique et fumarique comme acides bibasiques. La dépendance du volume spécifique vis-à-vis de la température a été déterminée par mesure de l'indice de réfraction, en admettant que la réfractivité spécifique est indépendante de la température. La dispersion de température de la viscoélasticité dynamique a été mesurée à une fréquence constante. Les résultats se résument de la façon suivante; le volume spécifique et la température vitreuse sont en relation linéaire avec le logarithme de la densité de pontage. Le coefficient de dilatation thermique et la pente de la dispersion viscoélastique diminuent avec l'augmentation de la densité du pontage. Le volume libre partiel et

le coefficient de dilatation du volume libre, qui sont calculés au moyen de l'équation WLF, sont en bon accord avec la dépendance du volume spécifique vis-à-vis de la température. On peut conclure des résultats ci-dessus que l'influence du pontage est fortement attribuée au changement de la quantité et de la distribution du volume libre dans les réseaux de polymères.

Zusammenfassung

Die viskoelastischen Eigenschaften ungesättigter Polyester wurden im Glas-Kautschuk-Umwandlungsbereich in Beziehung zur Temperaturabhängigkeit des spezifischen Volumens untersucht. In Bezug auf die Vernetzungsdichte homologe Polyester wurden mit Bernstein- und Fumarsäuremischungen als zweibasische Säurekomponente dargestellt. Die Temperaturabhängigkeit des spezifischen Volumens wurde durch Brechungsindexmessung unter Annahme einer temperaturunabhängigen, spezifischen Refraktivität bestimmt. Die Temperaturdispersion der dynamischen Viskoelastizität wurde bei konstanter Frequenz gemessen. Die Ergebnisse werden in folgender Weise zusammengefasst: Spezifisches Volumen und Glastemperatur stehen zum Logarithmus der Vernetzungsdichte in linearer Beziehung. Der thermische Expansionskoeffizient und die Steilheit der viskoelastischen Dispersion nehmen mit steigender Vernetzungsdichte ab. Freier Volumbruchteil und Expansionskoeffizient des freien Volumens, beide mit der WLF-Gleichung berechnet, zeigen eine gute Korrelation zur Temperaturabhängigkeit des spezifischen Volumens. Die oben angeführten Ergebnisse erlauben den Schluss, dass der Vernetzungseffekt zu einem grossen Teil der Änderung des Betrages und der Verteilung des freien Volumens im Polymernetzwerk zuzuschreiben ist.

Received October 19, 1964

Revised January 22, 1965

(Prod No. 4633A)

Polymerization of Adsorbed Monolayers.

I. Preparation of the Clay-Polymer Complex

ALEXANDRE BLUMSTEIN,* *Department of Chemistry, University of Delaware, Newark, Delaware*

Synopsis

Monomolecular layers of methyl methacrylate adsorbed on the surface of sodium montmorillonite clay were prepared by saturation of the clay with the monomer, followed by desorption of the excess monomer by means of repeated washings with nonpolar hydrocarbons. No spontaneous polymerization was observed. The polymerization of these monolayers was initiated with γ -ray irradiation or by free radical catalysts. The doses of γ -rays and the concentration of free radical catalysts required to initiate polymerization are much higher than for the polymerization of methyl methacrylate in bulk. Complexes containing 25% MMA gave inserted polymer only; complexes containing more than 25% of MMA gave inserted and external polymer. The yields of polymerization of the inserted polymer were found to be below 50%. The inserted polymer is strongly retained by the surface of the clay. X-ray data show that its segments are oriented horizontally (lying flat) on the surface.

In recent years, considerable research has been devoted to the study of various types of heterogeneous polymerizations. Among them interfacial polycondensation has received a great deal of attention; little work, however, has been devoted to the interfacial polymerization of monolayers of monomers.

The first problem arising in a study of the polymerization of an adsorbed monolayer of monomer molecules is the choice of a convenient substrate. An ideal substrate should have a well characterized structure, it should be chemically unreactive toward the monomer, and its surface should be known and be as large as possible. While no substrate is ideal, two different types of surfaces can be utilized in practice: (1) undivided surfaces, such as air/water or oil/water interfaces; (2) finely divided surfaces, such as those of crystallites of colloidal size, emulsions, suspensions, aerosols.

Polymerizations on surfaces of the first type have been studied somewhat.¹⁻⁴ The results of these studies, however, have not been conclusive. This was due in part to the delicate measurements required to follow the conversion of monomer to polymer, but mostly to the fact that the quantities of the polymer which were obtained were too small to allow an analysis

* Present address: Department of Chemistry, Lowell Technological Institute, Lowell, Mass.

of the product. [In order to obtain 1 mg. of poly(methyl methacrylate) adsorbed on a surface in a monomolecular layer, an area of at least 3.5 m.^2 is necessary.]

Nature of the Substrate Used

The substrate used in the present work is montmorillonite clay, a silico-aluminate having a lamellar structure. The structure of montmorillonite has been established by Hoffmann,⁵ Marshall,⁶ and Hendricks⁷ (Fig. 1). The crystallite of montmorillonite is composed of superposed lamellae, which bear a diffuse negative charge due to different substitutions in the crystal lattice of the lamellae. This negative charge is compensated by adsorption of cations such as H^+ , Na^+ , K^+ , Ca^{++} , Mg^{++} , which can be easily exchanged. The cohesion between lamellae is insured by water or other polar molecules, which may penetrate between the lamellae. This effect may be easily followed by the increase of the basal (001) spacing.

Electron microscopy has made possible direct observation of various clays.^{8, 9} Montmorillonite is formed of units called aggregates, whose size ranges often between 0.1 and 10μ . An aggregate is made up of a number of structural units or primary particles, a primary particle being in turn composed of a number of superposed lamellae (Fig. 1*b*). Mering⁸ suggests 300 Å. for the diameter and 80–100 Å. for the height of the primary particle. The thickness of the lamella is 9.6–10 Å.; thus each primary particle contains approximately eight lamellae or 16 (001) planes. The primary particles are almost always associated with other primary particles of a

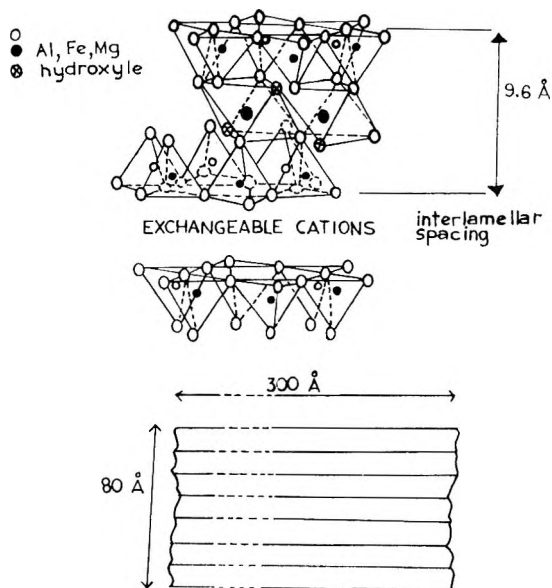


Fig. 1. Structure of montmorillonite: (a) structure according to Hendricks⁷ and Hoffmann;⁵ (b) schematic view of a primary particle of montmorillonite.

given aggregate, mainly through (001) planes, but sometimes also through sides or edges. One can easily see that any molecules which are adsorbed on the internal surface (the term internal surface is used to designate the surface available for adsorption inside the aggregate) are arranged in regular layers, the thickness of which may be determined by the (001) x-ray spacings. On the other hand, the layers adsorbed on the external surface can be very irregular, and their thickness is difficult to estimate. Fortunately, the ratio S_{int}/S_{ext} (where S_{int} and S_{ext} are the internal and external surface areas, respectively) is very large in most cases, and the contribution of the external surface to the adsorption may be neglected. In the case of the sodium montmorillonite used in this work, S_{int} constitutes at least 95% of the total surface available for adsorption, the Na^+ cation causing strong aggregation between primary particles. The total surface of different samples is considerable (780 m.²/g. of clay) and is quite constant from sample to sample.

The solvation of montmorillonite has been studied by McEwan¹⁰ and other authors.^{11,12} Various organic molecules can form mono-, bi-, or tri-molecular layers between the lamellae. X-rays show that the molecules lie "flat" on the surface. At high concentrations, however, the molecules may in some cases orient in a manner favoring the closest packing.¹² Only polar molecules can penetrate between the lamellae. Thus, aliphatic hydrocarbons, for instance can only be adsorbed on the external surface. According to McEwan¹⁰ the forces to which the adsorbed molecules are subjected are dipolar attractions and van der Waals forces, but Bradley¹¹ found evidence for some hydrogen bonding between the oxygens of the external face of the lamellae and the hydrogens of the hydrocarbon backbone of a molecule. These forces seem to be too diffuse to prevent the movement of the molecules on the surface of a lamella. This results from the easy conversion of one solvation complex to another by a simple contact of the complex with an excess of molecules of another type.

Bearing in mind the properties of montmorillonite which have just been briefly described, it is easy to see that a liquid adsorbed on a surface of montmorillonite exists as mono- or bimolecular layers covering the enormous surface of the lamellar planes. The individual molecules retain relative freedom of movement in the plane of the lamella and it may be reasonably expected that the chemical reactivity of the adsorbed molecules is not drastically modified.

In the present work a sodium montmorillonite has been used as substrate for the polymerization of monomolecular layers of acrylic monomers.

Preparation of Monomolecular Layers

Solvation complexes of montmorillonite with various organic compounds have been prepared by several authors.^{10,11} A saturated solvation complex is prepared by shaking the dehydrated clay with an excess of the organic liquid. An increase of temperature favors the solvation. Table I shows the manner in which some monomers are inserted between the

lamellae of the crystallites. Δd represents the difference between the (001) x-ray spacing of the saturated complex and 9.6 Å., which is the (001) spacing of the dehydrated clay. Δd is zero if there is no monomer adsorbed between the lamellae, which remain in contact with each other. Table I shows that a "horizontal" orientation of molecules adsorbed on the lamellae agrees well with the x-ray spacings. Furthermore the adsorption depends on the dipole moment of the molecule. Methyl methacrylate is adsorbed, giving one monomolecular layer on each lamella (or two monomolecular layers sandwiched between two lamellae). No evidence of adsorption of styrene or isoprene was found.

Polymerization can be effected in a saturated complex prepared by contact of the dehydrated clay with liquid monomer. It is, however, impossible to avoid the presence of some monomer occluded in the microvoids between the aggregates. The polymer resulting from the polymerization of monomer "inserted" in monolayers between the lamellae, which will be called "insertion polymer" is then accompanied by a certain amount of polymer formed outside the lamellae ("external polymer").

TABLE I
Insertion of Monomers between the Lamellae of Montmorillonite

| Monomer | Δd , Å. | Approx. minimum thickness of molecule, Å. | Number of layers | Dipole moment, debyes |
|---------------------|-----------------|--|---------------------|--------------------------|
| Acrylonitrile | 8.7 | 2.8 | 3 | 3.88 |
| Methyl methacrylate | 7.6 | 3.8 | 2 | 1.7 |
| Vinyl acetate | 7.6 | 3.8 | 2 | 1.7 |
| Styrene | 0 | 3.5 | 0 | 0.37 |
| Isoprene | 0 | 3.8 | 0 | 0.38 |

The inclusion of monomer between the aggregates can be minimized by the use of one of the following techniques: (a) the substrate can be exposed to monomer vapor at relative pressures $P/P_0 < 0.9$ (P is the vapor pressure used and P_0 is the corresponding saturation pressure); (b) the occluded "external" monomer can be eliminated by treating the insertion complex with a nonpolar solvent, which does not penetrate between the lamellae and thus cannot displace the inserted monomer. A monomolecular layer of monomer remains therefore "retained" on the surface of the lamellae.

The first method was successfully applied to the polymerization of methyl acrylate.¹³ The adsorption isotherm of this monomer is given in Figure 2; here τ_a is the yield of adsorption or weight of monomer adsorbed per unit weight of dehydrated clay. Saturation occurs for values of τ_a between 0.22 and 0.24, which corresponds almost exactly to a monomolecular layer of molecules of methylacrylate oriented "flat" on the lamella and covering the total surface available for adsorption. The molecule of

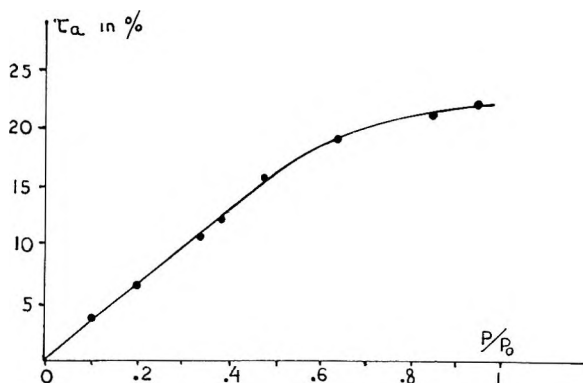


Fig. 2. Adsorption isotherm of methyl acrylate on sodium montmorillonite at 25°C. Yield of adsorption vs. the relative vapor pressure P/P_0 .

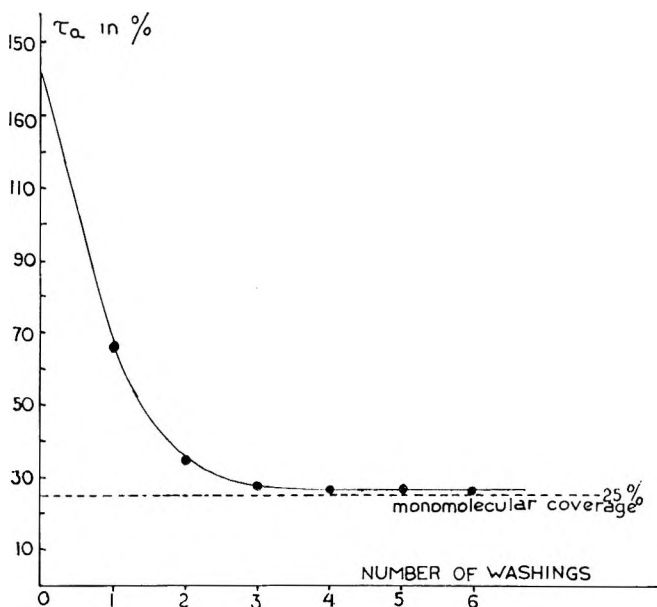


Fig. 3. Desorption of methyl methacrylate from sodium montmorillonite saturated with monomer. Yield of adsorption τ_a vs. number of washings with heptane.

methyl acrylate (MA) lying flat covers approximately 44–45 Å². One gram of clay, having a surface of 780 m.²/g. adsorbs $n = 7.8 \times 10^{21}/44 = 1.78 \times 10^{21}$ molecules of MA or $1.78 \times 10^{21} \times 86/6.0 \times 10^{23} = 0.24$ g. of methyl acrylate. The disadvantage of this method is that it is difficult to apply to nonvolatile monomers and that special adsorption equipment is necessary.

The second method, which was utilized in the present series of experiments, can easily yield a complex without external monomer by simple saturation of the substrate with liquid monomer followed by repeated

washings of the saturated complex with an aliphatic hydrocarbon, in order to displace the external monomer. Figure 3 gives the yield of adsorption of methyl methacrylate (MMA) as a function of the number of washings with heptane. After five washings τ_a is approximately 0.25 and decreases only very slowly with further washings. The complex contains a monomolecular layer of MMA molecules in horizontal packing and will be called the "retention complex," although this term is not quite appropriate in the case of five or six washings. (Strictly speaking, the clay mineralogists¹⁴ reserve the term retention complex for a system from which no organic molecules can be desorbed at room temperature in vacuum. This would correspond to an infinite number of washings.)

Experimental

The montmorillonite used was a Fisher U.S.P. bentonite with a typical approximate analysis: silica (SiO_2), 64.32%; alumina (Al_2O_3), 20.74%; ferric oxide (Fe_2O_3), 3.03%; ferrous oxide (FeO), 0.46%; titanium oxide (TiO_2), 0.14%; lime (CaO), 0.50%; magnesia (MgO), 2.3%; soda (Na_2O), 2.6%; potash (K_2O), 0.39%; sulfur trioxide (SO_3), 0.35%; chemically held water (H_2O), 5.14%; minor constituents 0.03%. The exchange capacity is approximately 0.9 meq./g.

The methyl methacrylate, kindly supplied by the Rohm and Haas Company, was freed of inhibitor, methyl hydroquinone, by washing with a 1–2% sodium hydroxide solution, followed by repeated washings with distilled water. The monomer was then dried over CaCl_2 and distilled.

The clay was dehydrated by drying for 4 hr. at 100°C. The saturated complex was prepared by shaking the sample of dehydrated montmorillonite with $2\frac{1}{2}$ times its weight of monomer for 30 min. The sample was then centrifuged and the supernatant replaced with the same weight of heptane. This procedure was repeated as many times as necessary to attain the desired yield of adsorption. The quantity of MMA was determined in the centrifugate by means of ultraviolet spectrophotometry (absorption at 250 $m\mu$). The yield of adsorption was obtained by subtracting the weight of MMA remaining in the centrifugate from the total weight of MMA.

Polymerization of the Monolayers

Monomolecular layers of MMA adsorbed on the surface of montmorillonite were polymerized by initiating the reaction with free radical catalysts or with γ -rays.

Free Radical Initiators. Benzoyl peroxide (BPO) or azobisisobutyronitrile can be used. The catalyst is either dissolved in the monomer or predeposited on the clay from a solution in pentane. The technique by which the presence of polymer inserted between the lamellae can be detected has been previously described^{13,14} and will be only briefly recalled here. As already mentioned, the molecules of MMA adsorbed between the lamellae of the crystallites can move in the interlamellar plane with relative free-

TABLE II
 Polymerization of Clay-MMA Complexes

| Nature of the complex | Temperature, °C. | Catalyst | Δd , A. | |
|--------------------------|---------------------|----------|----------------------------|---------------------------|
| | | | Before polymeriza- tion | After polymeriza- tion |
| Saturated complex of MMA | 25 | None | 7.6 | 0 |
| " | 100 | None | 7.6 | 0 |
| " | 25 | 0.5% BPO | 7.6 | 0 |
| " | 100 | 0.5% BPO | 7.6 | 7.3-7.6 |
| Retention complex of MMA | 100 | 0.5% BPO | 7.6 | 0 |

dom; they can escape if the temperature is raised, and they can also be replaced by other polar molecules. An adsorbed layer of the polymer, on the other hand, cannot easily be removed, and its presence can be detected by x-ray measurements ($\Delta d = 7.6$ A. for PMMA). The sample believed to contain polymer is extracted with methanol and heated above 80°C . to constant weight. When no polymer is present the monomer-montmorillonite complex becomes a methanol-montmorillonite complex, which dissociates upon heating to the anhydrous clay ($\Delta d = 0$). The quantity of polymer present can be determined by calcination at 1000°C . of the sample previously extracted with methanol and dried to constant weight at 100°C . Table II gives the results of some experiments of polymerization of MMA complexes performed in sealed tubes. No spontaneous polymerization was observed; the presence of catalyst is necessary, even at 100°C . The retention complex refused to polymerize under the conditions described in Table II.

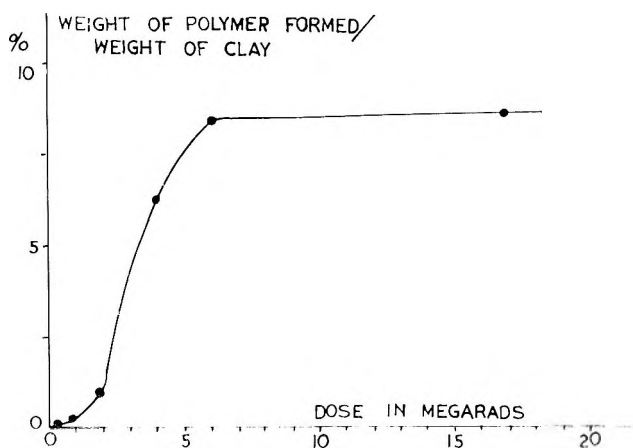


Fig. 4. Polymerization with γ -rays. Amount of polymer formed as a function of the irradiation dose for a retention complex of methyl methacrylate with sodium montmorillonite.

γ -Irradiation. Using γ -rays as initiator one can obtain polymerization even in the case of the retention complex, but the intensities required to initiate the polymerization are very high. While an intensity of 0.1 Mrad is sufficient to polymerize MMA in bulk to almost complete conversion,

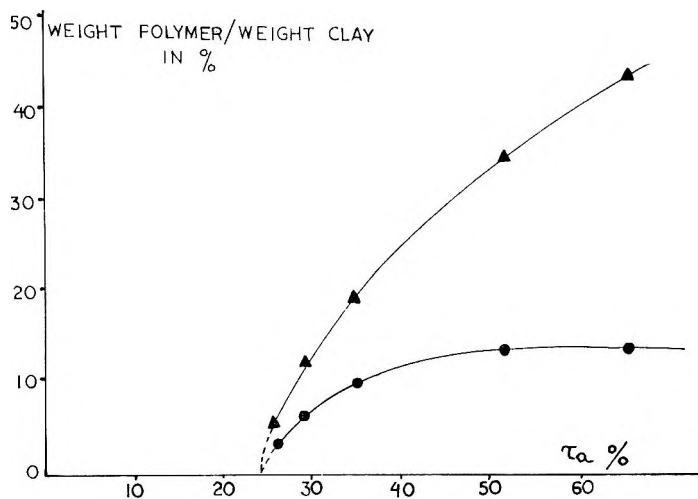


Fig. 5. Relative amounts of total and unextracted polymer as a function of the yield of adsorption τ_a of the methyl methacrylate-clay complex polymerized with azoisobutyronitrile at 100°C.: (I, ▲) total amount of polymer; (II, ●) unextracted inserted polymer.

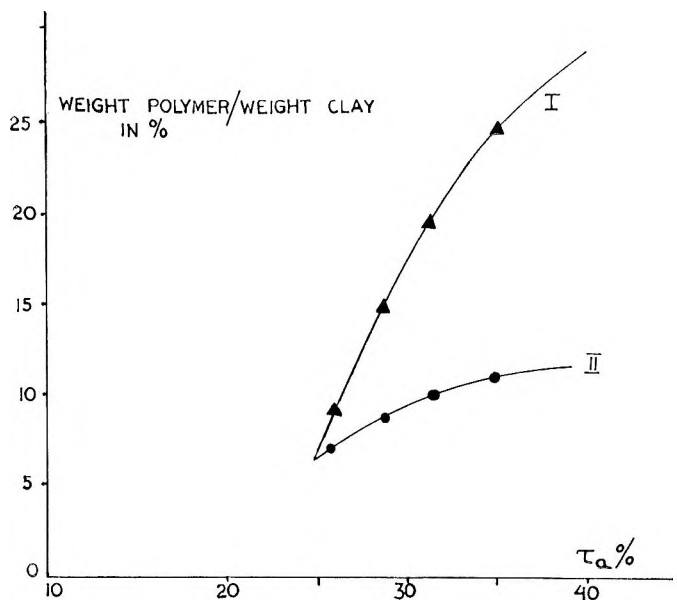


Fig. 6. Relative amounts of total and unextracted polymer as a function of the yield of adsorption τ_a of the methyl methacrylate-clay complex, polymerized with γ -rays (4 Mrad) at 25°C.: (I) total amount of polymer; (II) unextracted inserted polymer.

much higher doses are necessary in this case. Figure 4 shows the quantity of polymer formed as a function of the dose applied to a retention complex.

Results and Discussion

X-ray measurements of the interlamellar spacings after polymerization show that the inserted polymer molecule is lying "flat" on the surface of the lamellae (Tables II and III).

TABLE III
Extraction of a PMMA-Clay Complex Containing 44-wt.-% of PMMA

| Solvent | Polymer extracted/total polymer, % | Weight of remaining polymer per unit weight of clay (%) | Δd , A. |
|------------------------------|------------------------------------|---|-----------------|
| Methanol | 0 | 44 | 7.6 |
| Benzene | 26 | 32.6 | 7.6 |
| Acetone or dimethylformamide | 74 | 11.4 | 3.6 |

When γ -rays were used to initiate polymerization, complexes having adsorption yields of 0.25, corresponding to a monomolecular coverage, could be polymerized. When benzoyl peroxide or azobisisobutyronitrile were used, however, significant amounts of polymer could be obtained only by polymerization of complexes with yields of adsorption of 0.30 or more, which resulted in formation of various amounts of external polymer, contaminating the inserted polymer. External polymer can, however, be extracted with appropriate solvents. Table III shows typical extraction values for a polymer-clay complex, containing 44 wt.-% poly(methyl methacrylate), formed by polymerizing a monomer-clay complex with an adsorption yield of 0.60-0.65. Extraction was effected with various solvents until no more polymer could be detected in the refluxing solvent. Table III shows that two monomolecular layers are present between two lamellae.

Benzene does not extract the inserted polymer, nor does it extract all of the external polymer. Polar solvents such as acetone or dimethylformamide can penetrate between the lamellae, washing out part of the adsorbed polymer.

One can distinguish in the inserted polymer two types of material: one which can be extracted with polar solvents and another which is impossible to extract. The amount of inserted polymer extracted depends on the conditions of polymerization and on the yield of adsorption of the initial monomer-clay complex.

Table III indicates that approximately 50% of the inserted polymer is extracted and that only one monomolecular layer remains retained between the two lamellae. On the other hand, it was found that less than 10% of the polymer can be extracted from a polymerized retention complex.

Figures 5 and 6 give the relative amounts of total and unextracted polymer as a function of the yield of adsorption of the monomer-clay complex. The upper curves were obtained from weight losses of samples extracted with hexane and dried to constant weight. The curves corresponding to the retained polymer level off at 12–13% of inserted unextracted polymer, which represents one molecular layer inserted between two lamellae.

We have seen that γ -ray and free radical initiators can catalyze the polymerization of monolayers of MMA adsorbed on montmorillonite, but that high γ -ray doses or high catalyst concentrations and temperatures are necessary to induce the polymerization. No spontaneous polymerization of methyl methacrylate adsorbed on montmorillonite was observed. The spontaneous polymerization of MMA on sodium montmorillonite reported by Uskov¹⁵ for samples subjected to a mechanical treatment termed "vibrodesintegration" most probably takes place by a free radical type of initiation, through mechanical bond breaking. This view is supported by the reported inhibition of the polymerization by an increase in the viscosity of the system.

Friedlander and Frink,¹⁶ on the other hand, have reported the spontaneous polymerization on sodium montmorillonite of monomers such as butadiene and other olefins. These monomers are of the electron-repelling type susceptible to cationic initiation, and the experimental evidence strongly suggests an ionic mechanism for which no evidence could be found in our case. The complexity of the substrate makes it difficult to ascertain, even qualitatively, the factors causing the decreased reactivity observed for the monomer sandwiched between the lamellae (as compared to its reactivity in the polymerization in bulk or in solution). The mobility of the molecules of monomer which are confined between the lamellae and oriented with their principal axis parallel to the surface of the substrate is certainly restricted when compared to the mobility of molecules in a free liquid.

On the other hand, the exchangeable cations of the surface of the clay have a tendency to interact with the nucleophilic groups of the inserted molecules, the stoichiometry being one molecule for one cation in the case of bulky monovalent cations localized in the hexagonal cavities of the surface and more than one molecule to one cation in the case of cations such as H^+ or of bivalent cations such as Ca^{2+} .¹⁷ These interactions also contribute to the decrease of the overall mobility of the monomer molecules contained in the monolayer.

Although the molecules of monomer are by no means attached to the surface of the clay, their restricted mobility suggests that the collision frequency between monomer molecules will strongly depend on their surface concentration. This concentration does not vary much and corresponds to the saturation of surface available for adsorption in all complexes studied here, which differ mainly by the amount of external monomer present. Nevertheless, the amount of polymer formed between the lamellae strongly depends on the initial yield of adsorption τ_a , that is on the amount of external monomer present in the monomer-clay complex. Complexes with

higher yields of adsorption give two monomolecular layers of polymer sandwiched between two lamellae, which indicates complete polymerization of the inserted monomer (Table III).

For retention complexes, which have adsorption yields $\tau_a = 0.25$, only a fraction of the monomer sandwiched between the lamellae can be polymerized (Fig. 6). The extent of this fraction can vary with the conditions of polymerization, but it was found to be always below 50%.

It may be that, as the initial yield of adsorption decreases, a very small decrease of surface pressure of the inserted molecules produces a strong decrease of the collision frequency, thus leading to an abrupt decrease in the yield of polymerization between the lamellae. This might also be the reason why the retention complex, which begins to dissociate at 100°C., did not polymerize at this temperature.

From the above it seems that the main factor causing the decrease in reactivity observed is entropic in nature and is due to the specific two-dimensional organization of the polymerizing assembly. This view is also supported by the noticeably increased thermal stability observed for the inserted polymer.¹⁸ The importance of steric factors does not, however, preclude the possible influence of energetic factors (interactions between monomer and substrate influencing the activation energy of the individual reaction steps).

The author wishes to express his thanks to Dr. E. Dyer, Dr. L. Scolnick, and Dr. C. Trumbore who kindly let him use their instruments.

The support of the National Science Foundation (Grant No. GP 652) is gratefully acknowledged.

References

1. Gee, G., *Proc. Roy. Soc. (London)*, **A153**, 129 (1935).
2. Gee, G., C. B. Davies, and H. W. Melville, *Trans. Faraday Soc.*, **35**, 1928 (1939).
3. Bresler, S., M. Judin, and D. Talmud, *Acta Physicochim. URSS*, **14**, 71 (1941).
4. Scheibe, G., and H. Schuller, *Z. Elektrochem.*, **59**, 861 (1956).
5. Hoffmann, U., K. Endell, and D. Wilm, *Z. Krist.*, **A86**, 340 (1933).
6. Marshall, C. E., *Z. Krist.*, **A91**, 433 (1935).
7. Hendricks, S. B., *J. Geology*, **50**, 276 (1942).
8. Mering, J., *Trans. Faraday Soc.*, **42B**, 219 (1946).
9. Mathieu-Sicaud, A., J. Mering, and I. Perrin-Bonnet, *Bull. Soc. Min. Cristal.*, **74**, 439 (1951).
10. McEwan, D. M. C., *Trans. Faraday Soc.*, **44**, 349 (1948).
11. Bradley, W. F., *J. Am. Chem. Soc.*, **67**, 975 (1945).
12. Green-Kelly, R., *Trans. Faraday Soc.*, **51**, 412 (1955).
13. Blumstein, A., *Bull. Soc. Chim. France*, **1961**, 899.
14. Blumstein, A., J. Herz, V. Sinn, and C. Sadron, *Compt. Rend.*, **246**, 1856 (1958).
15. Uskov, A., *Vysokomolekul. Soedin.*, **2**, 926 (1960).
16. Friedlander, H. Z., and C. R. Frink, *J. Polymer Sci.*, **B2**, 475 (1964).
17. Glaeser, R., Thesis, Univ. of Paris (1953).
18. Blumstein, A., *J. Polymer Sci.*, **A3**, 2665 (1965).

Résumé

Des couches monomoléculaires de méthacrylate de méthyle adsorbées à la surface de montmorillonite de sodium ont été préparées par saturation du support argileux avec le

monomère, suivie de la désorption du monomère en excès par lavages répétés au moyen d'hydrocarbures non polaires. On n'observe pas de polymérisation spontanée. La polymérisation de ces couches monomoléculaires a été initiée par rayonnement γ ou par des radicaux libres. Les doses de rayonnements γ et de la concentration en radicaux libres nécessaires pour initier la polymérisation sont beaucoup plus élevées que pour la polymérisation du méthacrylate de méthyle en bloc. Des complexes contenant 25% de MMA donnent uniquement du polymère d'insertion; des complexes contenant plus de 25% de MMA donnent du polymère d'insertion et du polymère externe. On trouve que les rendements de la polymérisation en polymère d'insertion sont inférieurs à 50%. Le polymère d'insertion est fortement retenu à la surface de l'argile. Les résultats d'analyse aux rayons-X montrent que les segments sont orientés horizontalement sur la surface.

Zusammenfassung

Monomolekulare, auf der Oberfläche von Natriummontmorillonitton adsorbierte Methylmethacrylatschichten wurden durch Sättigung des Tones mit dem Monomeren und darauffolgende Desorption des Überschussmonomeren durch wiederholtes Waschen mit unpolaren Kohlenwasserstoffen dargestellt. Es wurde keine spontane Polymerisation beobachtet. Die Polymerisation der Monoschichten wurde durch γ -Bestrahlung oder mit radikalischen Katalysatoren gestartet. Die zum Polymerisationsstart erforderlichen γ -Dosen und Konzentrationen an radikalischem Katalysator sind viel höher als bei der Polymerisation von Methylmethacrylat in Substanz. Komplexe mit 25% MMA lieferten nur eingelagertes Polymeres; Komplexe mit mehr als 25% MMA lieferten eingelagertes und nicht eingelagertes Polymeres. Die Polymerisationsausbeute an eingelagertem Polymeren lag unter 50%. Das eingelagerte Polymeres wird durch die Tonoberfläche stark festgehalten. Röntgendaten zeigen, dass seine Segmente auf der Oberfläche horizontal ("flach") liegend orientiert sind.

Received November 20, 1964

Revised January 19, 1965

Prod. No. 4639A

Polymerization of Adsorbed Monolayers. II. Thermal Degradation of the Inserted Polymer*

ALEXANDRE BLUMSTEIN,† *Department of Chemistry, University of Delaware, Newark, Delaware*

Synopsis

Monomolecular layers of methyl methacrylate inserted between the lamellae of montmorillonite clay were polymerized. Finely divided complexes of poly(methyl methacrylate)-montmorillonite were suspended in boiling hydrocarbons and subjected to thermal degradation at 215°C. and above, under air and nitrogen, with constant vigorous stirring. Aliquots were regularly withdrawn, centrifuged, and extracted with appropriate solvents. The weight losses upon calcination at 1000°C. were determined, and from them the rates of reversal to monomer were followed. Complexes containing inserted and external polymer were studied. The inserted polymer was found to resist thermal degradation under conditions at which complete degradation of the external polymer was found. This effect seems to be due to steric factors hindering the thermal motion of the segments of the polymer sandwiched between the lamellae of the crystallites. The insertion polymer isolated from the polymer-clay complexes, had a greater thermal stability than poly(methyl methacrylate) made in a conventional free radical system without the presence of clay.

The preparation and polymerization of monomolecular layers of methyl methacrylate (MMA) adsorbed on the surface of montmorillonite clay have been described previously.¹ X-ray measurements show that the polymer is formed between the lamellae of the crystallites of the clay and that its segments lie flat on the surface of the lamellae.

It has been known for a long time that soils rich in montmorillonite have a protective action on the organic materials of the humus and the proteins of the soil, preventing their oxidative and microbial decay.² Some aspects of the nature of these associations and of the mechanism of the protective action were studied by Ensminger and Gieseck.^{3,4} These authors found that under certain conditions the protein can become adsorbed between the lamellae of the crystallites of the montmorillonite and thus be shielded from external attack. Quite similarly it was found here that the macromolecules synthesized through polymerization of a monolayer inserted between the lamellae of the clay seem to be shielded from external

* Presented in part at the 147th National Meeting, American Chemical Society, Philadelphia, April 1964.

† Present address: Department of Chemistry, Lowell Technological Institute, Lowell, Mass.

influences. In particular their temperature stability seems to become noticeably enhanced. In this work the results of thermal degradation of the clay-PMMA complexes under various conditions are reported, together with some preliminary results on the thermal stability of the insertion polymer.

Experimental

Complexes of montmorillonite and MMA were prepared by a technique described in part I of this series.¹ Two types of complexes were prepared, having τ_a (weight of monomer adsorbed per unit weight of dehydrated clay) equal to 0.25 and 0.35, respectively. Complexes having $\tau_a = 0.35$ were polymerized with free radical catalysts. Azobisisobutyronitrile, 1% with respect to the monomer, was predeposited on the clay from a solution in pentane. The pentane was boiled off under reduced pressure at 25°C. and the monomer-clay complex prepared, transferred into a hermetically closed glass container, and heated for 24 hr. at 95–100°C. The polymerized complex was extracted for several hours with hexane in order to eliminate the unpolymerized monomer. The powder was then passed through a 250 μ sieve and dried at 80°C. under vacuum to constant weight. The weight loss upon calcination at 1000°C. of such a complex showed a total polymer content of 19–21% (weight of polymer/weight of dehydrated clay).

Complexes having $\tau_a = 0.25$, called "retention complexes," contain a monomolecular layer of monomer covering the entire surface of the clay and almost no monomer filling the microcavities between the aggregates. These complexes were prepared directly from the dehydrated clay and polymerized with γ -ray irradiation. Irradiation doses of 6 Mrad were used. The complexes were then extracted with hexane for long periods of time and heated under vacuum to constant weight.

Samples (10 g.) of the finely powdered complexes were dispersed in a high boiling hydrocarbon and degraded at the boiling temperature, with constant vigorous stirring. Aliquots were taken at regular intervals, centrifuged, extracted with appropriate solvents, and dried at 80°C. under vacuum to constant weight. The weight losses upon calcination at 1000°C. were determined. The amount of PMMA remaining in the complex was obtained after correction for the weight loss by calcination at 1000°C. of the dehydrated montmorillonite. Correction for adsorption of very small amounts of oxidation products of the hydrocarbon were made where necessary, on the basis of blank tests performed with pure dehydrated clay suspended in the boiling hydrocarbon.

In order to test the thermal stability of the insertion polymer itself the PMMA prepared in the adsorbed monolayer was liberated and purified by a procedure previously described.⁵

Two insertion polymers were studied: one prepared from a monolayer of MMA containing 1% of ethylene glycol dimethacrylate added as crosslinking agent (polymer C), and the other prepared without addition of crosslinking agent (polymer O). Polymers O and C were compared with a

reference PMMA (polymer A) prepared at 100°C. from a 20% solution of MMA in toluene with 0.5% of benzoyl peroxide as initiator. The polymers were suspended in a large amount of dodecane in small glass containers. The containers were evacuated and filled with nitrogen several times, sealed, and maintained at 215°C. for 48 hr. The polymers were then recovered and weighed.

Results and Discussion

Figure 1 illustrates the rate of oxidative reversal to monomer of a PMMA-montmorillonite complex suspended in boiling dodecane (b.p. 215°C.). The complex was characterized by $\tau_a = 0.35$ and originally

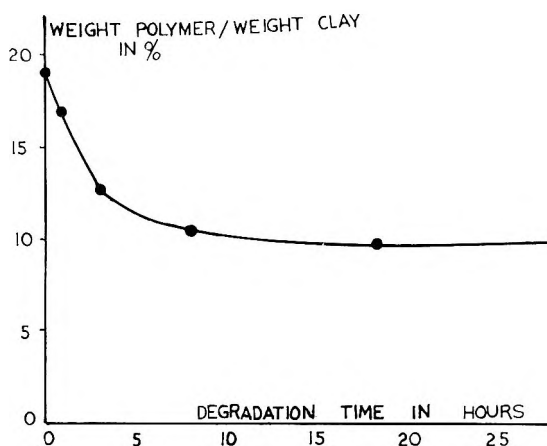


Fig. 1. Degradation at 215°C. of a complex containing inserted and external poly-(methyl methacrylate) (complex suspended in boiling dodecane in presence of air).

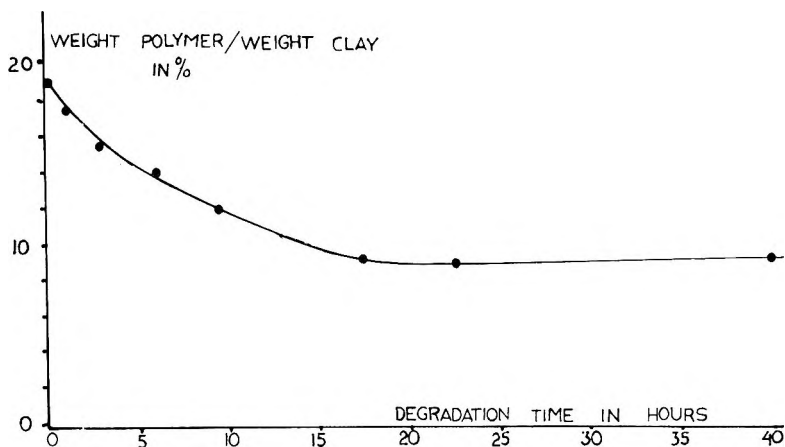


Fig. 2. Degradation at 215°C. of a complex containing inserted and external poly-(methyl methacrylate) crosslinked with 1% of ethylene glycol dimethacrylate (complex suspended in boiling dodecane in presence of air).

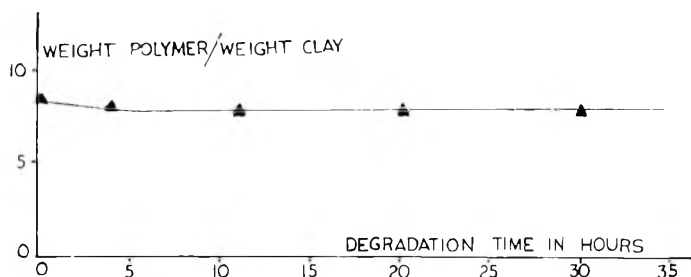


Fig. 3. Degradation at 215°C. of a retention complex containing almost no external poly(methyl methacrylate) (complex suspended in boiling dodecane in presence of air).

contained 19% total polymer. After a sharp decline, the curve levels off and no more polymer is degraded. After degradation the clay contains 9% by weight of polymer, which resists further degradation.

Figure 2 gives similar results for a complex containing 19% total polymer crosslinked with 1% of ethylene glycol dimethacrylate added originally to the monomer. Here again after a sharp decline the curve levels off at 9% of polymer, which resists further degradation.

Figure 3 shows the degradation of a retention complex containing 8.5% of inserted polymer retained by the clay and almost no "external" polymer. The leveling off occurs at 8%, and practically no degradation takes place.

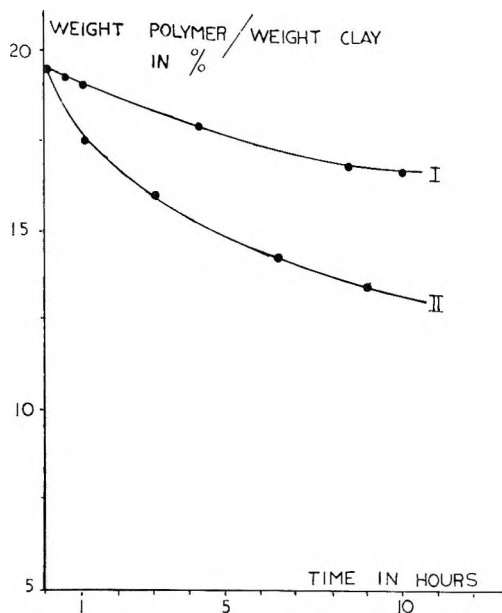


Fig. 4. Initial rates of degradation at 215°C. of complex containing inserted and external poly(methyl methacrylate) crosslinked with 1% ethylene glycol dimethacrylate: (I) under nitrogen; (II) in air.

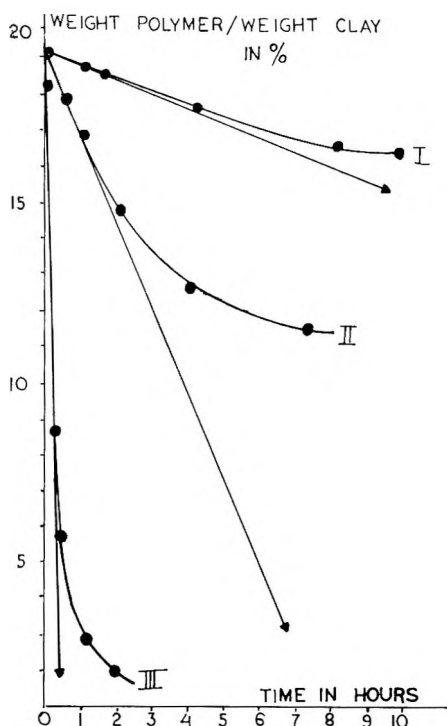


Fig. 5. Initial rates of degradation under nitrogen at different temperatures of complex containing inserted and external poly(methyl methacrylate) crosslinked with 1% of ethylene glycol dimethacrylate: (I) at 215°C. (dodecane); (II) at 252°C. (tetradecane); (III) at 320°C. (octadecane).

It is interesting to note that the 9% of polymer per weight of clay found to be undegraded at 215°C. (Fig. 1) correspond exactly to the amount of polymer retained between the lamellae after prolonged extraction with acetone of a complex characterized by yields of adsorption $\tau_a = 0.35$.¹ The same was found to be true for the other complexes. For instance, in the case of the retention complex, 8% of polymer per weight of clay is resistant to any further degradation and extraction, and this amount corresponds exactly to the amount of polymer retained between the lamellae after prolonged extraction with acetone for a retention complex¹ obtained by polymerization initiated by a dose of 6 Mrad. Figures 4 and 5 show the influence of air and of the temperature on the initial rate of degradation. These figures show that oxygen greatly accelerates the degradation process. An estimation of the overall activation energy of degradation under nitrogen from the slopes of these curves at zero time gives $E = 30$ kcal./mole. The presence of oxygen strongly reduces the overall activation energy, through formation of peroxides and subsequent decomposition to free radicals.

The results of degradation at 215°C. under air seem to indicate that, while the external polymer is completely destroyed, the inserted PMMA

retained between the lamellae of the crystallites resists degradation. This assumption is supported by the following facts: (1) all the degradation curves level off at approximately the same value of undestroyed polymer; (2) this value corresponds to the amount of polymer retained between the lamellae after extraction with acetone¹; (3) almost no degradation occurs in the case of the polymerized retention complex.

The monolayers formed by the inserted polymer are sandwiched between the lamellae of the clay and adhere strongly to their surface. The external polymer, on the other hand, is occluded in the microvoids existing between the crystallites of the clay and is thus dispersed in dodecane in a highly divided state. This allows for rapid diffusion of the monomer away from the reaction centers and favors the degradation of the polymer. The presence of oxygen and the fine division of the polymer seem to permit a complete degradation of the external PMMA at a temperature at which *in vacuo* or under nitrogen in bulk only partial degradations have been reported.⁶

The inserted polymer, on the other hand, is always degraded thermally, even when the external polymer is subjected to an oxidative degradation, since oxygen cannot penetrate between the lamellae.

Table I gives the results observed for the degradation of insertion polymers O and C and of the reference polymer A.

TABLE I
Weight Loss of Poly(methyl Methacrylates) Degraded under Nitrogen at 215°C. for 48 Hr.^a

| Polymer | $[\eta]$ (in acetone at 25°C.), ml./g. | Weight loss $\Delta P/P$ |
|---------|---|-----------------------------|
| A | 18 | 0.45 |
| O | 16 | 0.19 |
| C | 16 | 0.20 |

^a The polymers were suspended in boiling dodecane.

Figure 6 gives thermogravimetric analysis curves obtained for these polymers.

Table I shows that the insertion polymers O and C display substantially improved thermal stability at 215°C. with reference to the conventional polymer A. The thermogravimetric curves also seem to indicate a similar increase in heat stability. One should not, however, overestimate the significance of these curves in this case. With the temperature increasing at a rate of 6°C./minute, the rate of degradation may well depend on a number of factors other than the actual structure of the macromolecules (e.g., texture and morphology of the powder). The degradation at constant temperature seems a more reliable technique for this kind of investigation.

For samples of PMMA in which the chains were terminated by disproportionation, Grassie⁶ found at 215°C. an amount of degradation which was only slightly higher than the amount observed here for polymer A. This could possibly mean that polymerization in two dimensions favors recombination of radicals, thus decreasing the relative amount of macromolecules terminated by double bonds. This would not be surprising, since the confinement of the growing chains on the surface of the substrate decreases the mobility of the radical ends, and restriction of mobility is expected to favor recombination.

The insertion polymers isolated from the polymer-clay complexes and dispersed in boiling dodecane at 215°C. are more resistant to thermal degradation than the conventional PMMA. Nevertheless, the weight loss

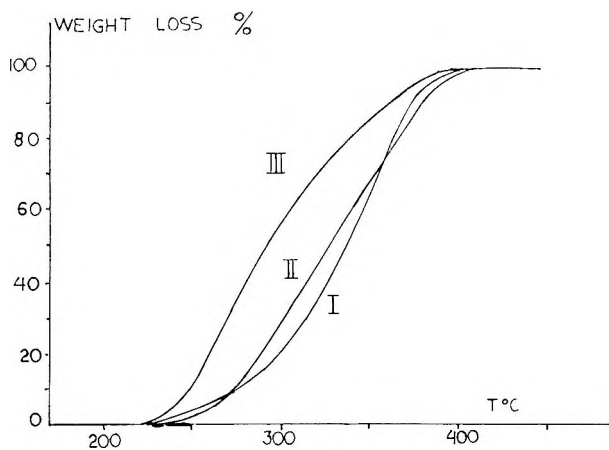


Fig. 6 Thermogravimetric analysis of PMMA: (I) polymer O; (II) polymer C; (III) polymer A. Heating rate 6°C./min.

of the insertion polymer samples was found to be 20%. Thus, the more stable structure of these polymers cannot be solely responsible for the almost complete absence of degradation of the retention complex.

On the other hand, it is also difficult to assume that the adsorption forces of polar nature, such as described by McEwan,⁷ which are small in comparison with the high energies supplied during degradation, are responsible for the increased thermal stability of the inserted polymer.

Thus it appears that the stability of the inserted polymer is due not only to its particular structure but also to steric factors restricting the thermal motion of the segments sandwiched between the two lamellae. The unzipping of the chains begins when the temperature is high enough to bring about this motion.

The author wishes to express his gratitude to Dr. F. W. Billmeyer for his interest and valuable help in this work.

The support of the National Science Foundation (Grant No. G.P. 562) is gratefully acknowledged.

References

1. Blumstein, A., *J. Polymer Sci.*, **A3**, 2653 (1965).
2. Waksman, S. A., *Humus Origin, Chemical Composition and Importance in Nature*, Williams & Wilkins, Baltimore, 1936.
3. Ensminger, L. E., and J. E. Gieseking, *Soil Sci.*, **48**, 467 (1939).
4. Ensminger, L. E., and J. E. Gieseking, *Soil Sci.*, **53**, 205 (1942).
5. Blumstein, A., *Bull. Soc. Chim. France*, **1961**, 899.
6. Grassie, N., and H. W. Melville, *Proc. Roy. Soc. (London)*, **A199**, 1, 14, 24, 39 (1949).
7. McEwan, D. M. C., *Trans. Faraday Soc.*, **44**, 349 (1948).

Résumé

Des couches monomoléculaires de méthacrylate de méthyle insérées entre les lamelles de montmorillonite ont été polymérisées. Des complexes finement divisés de polyméthacrylate de méthyle-montmorillonite ont été suspendus dans des hydrocarbures à l'ébullition et soumis à la dégradation thermique à 215°C et plus, sous air et azote, avec une agitation énergétique constante. Des aliquotes ont été prélevées en fonction du temps, centrifugées et extraites avec des solvants appropriés. Les pertes en poids par calcination à 1000°C ont été déterminées et ont permis de suivre les vitesses de reconversion en monomère. On a étudié des complexes contenant du polymère d'insertion et externe. On a trouvé que le polymère d'insertion résistait à la dégradation thermique dans les conditions pour lesquelles le polymère externe se dégrade complètement. Cet effet semble être dû aux facteurs stériques empêchant l'agitation thermique des segments de polymère intercalés entre les lamelles et les cristallites. Le polymère d'insertion, isolé à partir des complexes polymère-argile, possède une stabilité thermique plus élevée que le polyméthacrylate de méthyle produit par un système radicalaire habituel sans la présence d'argile.

Zusammenfassung

Zwischen die Lamellen von Montmorillonitton eingelagerte monomolekulare Methylmethacrylatschichten wurden polymerisiert. Feinverteilte Polymethylmethacrylat-Montmorillonitkomplexe wurden in siedenden Kohlenwasserstoffen suspendiert und bei konstanter kräftiger Rührung einem thermischen Abbau bei 215°C und darüber in Luft und in Stickstoff unterworfen. Aliquote Anteile wurden regelmässig entnommen, zentrifugiert und mit geeigneten Lösungsmitteln extrahiert. Der Gewichtsverlust bei der Kalzinierung bei 1000°C wurde bestimmt und so die Geschwindigkeit der Rückverwandlung in Monomeres erhalten. Komplexe mit eingelagerten und nicht eingelagerten Polymeren wurden untersucht. Das eingelagerte Polymere war gegen thermischen Abbau unter Bedingungen beständig, unter welchen ein vollständiger Abbau des nicht eingelagerten Polymeren auftrat. Dieser Effekt scheint durch sterische Faktoren, nämlich eine Verhinderung der thermischen Bewegung der Segmente des zwischen die Kristallitlamellen gepackten Polymeren bedingt zu sein. Das eingelagerte Polymere besass nach der Isolierung aus dem Polymer-Tonkomplex eine grössere thermische Stabilität als ein in einem normalen radikalischen System in Abwesenheit von Ton erzeugtes Polymethylmethacrylat.

Received November 20, 1964

Revised January 19, 1965

Prod. No. 4640A

Polyphenylene-*s*-Triazinyl Ethers by Interfacial Polycondensation

LEWELLYN G. PICKLESIMER and THOMAS F. SAUNDERS,*
*Nonmetallic Materials Division, Air Force Materials Laboratory, Research
and Technology Division, Wright-Patterson Air Force Base, Ohio*

Synopsis

Polyphenylene-*s*-triazinyl ethers of apparently high molecular weight have been prepared by the interfacial polycondensation of *s*-triazinyl chlorides and sodium bisphenoxides. The polymers are characterized by good thermal stability, insolubility, and infusibility. The polymers can be varied by altering the reaction conditions. A long residence time at the reactive interface leads to a polymer of low residual chlorine and thus highly crosslinked. Reduction of the contact time at the reactive interface leads to polymers containing a greater amount of chlorine and consequently some linearity.

INTRODUCTION

Several workers¹⁻⁵ have reported the formation of high molecular weight polyamides and polyesters by the interfacial polycondensation of active diacid halides, usually chlorides, with diamines or glycols. The advantages of such a system are that simple equipment is required, low temperatures are satisfactory, and the ratio of reactants may vary from stoichiometric without adversely affecting polymer yield or molecular weight. The purity of monomers is also less critical than it is with melt or solution condensations. All of these factors affect the yield and molecular weight of polymers formed by melt or solution condensation.¹

Interfacial polycondensation has been used to produce several polymers which are difficult or impossible to produce by other methods.^{4,5} This is especially true for monomers which are unstable under the conditions employed in conventional condensations or polymers which are degraded by the by-products of condensation. Another group of polymers which can be obtained by this method, which are otherwise unobtainable in high molecular weights, are those which are insoluble or infusible.¹

Polymers containing the triazine ring as part of the polymer chain are generally insoluble and infusible. However, the thermal stability of the triazine ring makes it an attractive monomer for use in high temperature polymers. Most of the work⁶ on preparing polymers containing the triazine moiety in the polymer chain has been by melt or solution condensations.

* Present address: International Business Machines Corporation, Endicott, New York.

These methods give polymers of low molecular weights which are unsuitable for fiber formation and many other uses. We have prepared poly(*s*-triazinyl ethers), of apparently high molecular weight, by the interfacial polycondensation of chloro-*s*-triazines and bisphenols. The bisphenols were reacted as the sodium salts.

EXPERIMENTAL

The chemicals used in this work were all practical or technical grade. They were used as received and no attempt was made to purify them.

Poly(*m*-phenylene-*s*-triazinyl Ether) Film

A solution of sodium resorcinate was prepared by dissolving 2.20 g. (0.02 mole) of resorcinol in 50 ml. of distilled water containing 1.60 g. (0.04 mole) of sodium hydroxide. Another solution was prepared by dissolving 3.68 g. (0.02 mole) of cyanuric chloride in 50 ml. of benzene. Slight heating was required for complete solution of the cyanuric chloride. The cyanuric chloride solution was carefully floated on the aqueous solution of sodium resorcinate. A clear, tough, coherent film formed instantly at the interface of the two solutions. The film reformed as soon as it was removed. The film continued to form until the solution approached exhaustion as indicated by a decrease in the rate at which the film was formed.

Poly(*m*-phenylene-*s*-triazinyl Ether)

A solution of sodium resorcinate, prepared by dissolving 2.20 g. (0.02 mole) of resorcinol in a solution of 1.60 g. (0.04 mole) of sodium hydroxide in 50 ml. water, was added to a 500-ml. reaction flask equipped with a mechanical stirrer. A solution containing 3.68 g. (0.02 mole) of cyanuric chloride in 50 ml. of benzene was added slowly with stirring. The mixture was stirred vigorously for 30 min. after the addition of the cyanuric chloride solution was completed.

The product when filtered was a white, powdery polymer. The product was washed four times with 50 ml. portions of benzene and then with acetone. The product was then washed with water and then dried in a desiccator over calcium chloride. The weight of polymer was 2.20 g. for a yield of 46.0%.

Poly(*p*-phenylene-*s*-triazinyl Ether)

A solution of the sodium salt of hydroquinone was prepared by dissolving 2.20 g. (0.02 mole) of hydroquinone in a solution of 1.60 g. (0.04 mole) of sodium hydroxide in 50 ml. of water. A solution containing 3.68 g. (0.02 mole) of cyanuric chloride in benzene was carefully floated on the aqueous solution of basic hydroquinone. A film formed instantly at the interface of the two solutions and by exercising moderate care could be drawn continuously from the interface as a collapsed tube.

TABLE I
Summary of Polycondensation Reaction

| Bisphenol | Triazine | Organic Solvents | Description of product |
|--|---|--|------------------------------|
| Resorcinol | Cyanuric chloride | Benzene Chloroform Chlorobenzene | Greyish-white collapsed tube |
| Hydroquinone | Cyanuric chloride | Benzene Chloroform | Tannish-white collapsed tube |
| 4,4'-Dihydroxybiphenyl | Cyanuric chloride | Benzene | Clear to white film |
| Hydroquinone | 2-Phenyl-4,6-dichloro- <i>s</i> -triazine | Dibutyl phthalate | Tan brittle film |
| 2,2-Bis(<i>p</i> -hydroxyphenyl)propane | Cyanuric chloride | Benzene Tetrachloroethylene | Opaque film |

Other bisphenols used to form polyethers were 4,4'-dihydroxybiphenyl and 2,2-bis(*p*-hydroxyphenyl)propane. The other triazine used was 2-phenyl-4,6-dichloro-*s*-triazine. Organic solvents used, in addition to benzene, were chloroform, dibutyl phthalate, chlorobenzene, phenyl ether, and tetrachloroethylene. Table I briefly summarizes the reaction.

Solubility

The polymers were all insoluble in a wide range of solvents. They were unaffected by hot and cold concentrated mineral acids as well as formic acid. They were also unaffected by alcohol, ketones, esters, nitro compounds, and chlorinated solvents. Hot concentrated sodium hydroxide and some primary and secondary amines appeared to dissolve the polymers. However, it is believed that decomposition occurred, or at least some replacement reactions, since the polymers were not precipitated by water, alcohols, or other nonsolvents.

Thermal Stability

The thermal stability of the polymers was determined on a Chevanard thermobalance in air and nitrogen. The results are given in Figures 1 and 2.

All of the polymers show a fair amount of thermal stability. The best was the polymer of 4,4'-dihydroxybiphenyl and 2-phenyl-4,6-dichloro-*s*-triazine, Figures 1 and 2. In Figure 2 melting occurs at approximately 260°C. with a 50% weight residue at 900°C.

Chlorine Content

Table II gives the chlorine content of three of the polymers as related to the condition of formation. All of the polymers were prepared at room temperature.

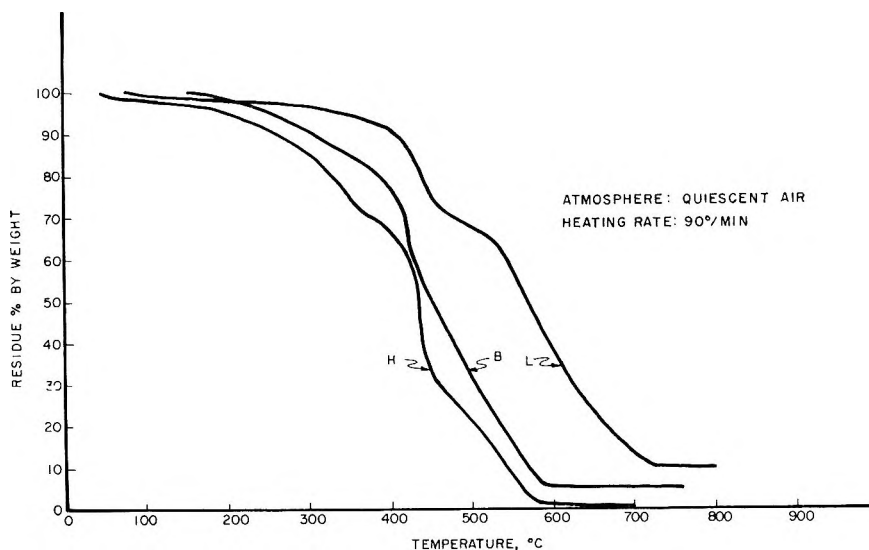


Fig. 1. Thermogravimetric curves of polymers in air: (*H*) hydroquinone-cyanuric acid polymer; (*B*) 4,4'-dihydroxybiphenyl-cyanuric chloride polymer; (*L*) 4,4'-dihydroxybiphenyl-2-phenyl-4,6-dichloro-*s*-triazine polymer.

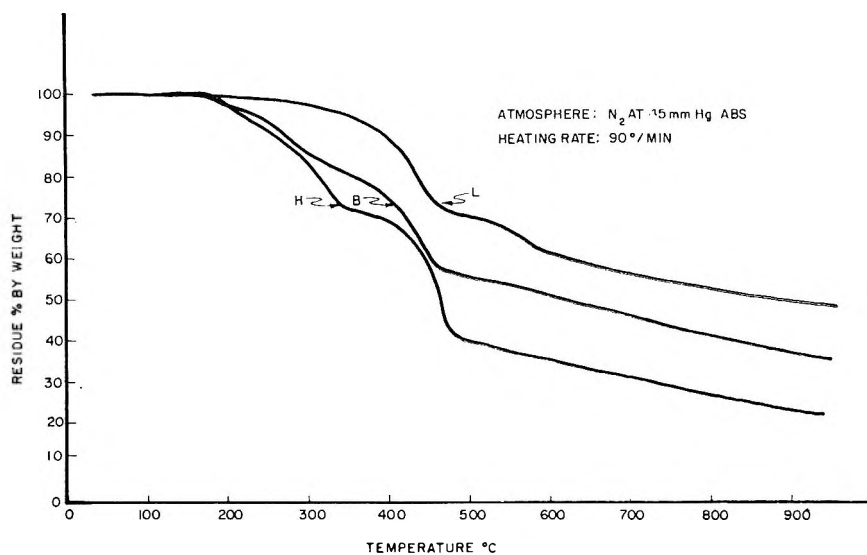


Fig. 2. Thermogravimetric curves of polymers in nitrogen: (*H*) hydroquinone-cyanuric acid polymer; (*B*) 4,4'-dihydroxybiphenyl-cyanuric chloride polymer; (*L*) 4,4'-dihydroxybiphenyl-2-phenyl-4,6-dichloro-*s*-triazine polymer.

Infrared Spectra

In order to establish the presence of the ether linkage in the polymers the infrared spectra of the polymers were obtained. Some of the spectra were obtained by the potassium bromide method and others were obtained from

TABLE II
Chlorine Content of Polymers

| Polymer | Condition of formation | Chlorine content, % | Chlorine content calculated for linear polymer, % |
|--|--|---------------------|---|
| Hydroquinone-cyanuric chloride | Stirred system | 0.65 | 15.8 |
| 4,4'-Dihydroxybiphenyl-cyanuric chloride | Film, still interface | 3.72 | 11.8 |
| 4,4'-Dihydroxybiphenyl-cyanuric chloride | Film pulled from interface as collapsed tube | 6.93 | 11.8 |

films. The spectra were recorded by the Baird Model B infrared spectrophotometer.

The spectra are presented in Figures 3-7. The spectra of all of the polymers showed a strong absorption bands at 7.3-7.4 μ and 8.3-8.5 μ , with the exception of the polymer of resorcinolcyanuric chloride, which showed a doublet at 8.6 and 8.7 μ . These absorption bands have previously⁷ been attributed to vibrations involving the aryl ether linkage. The absorption band at 7.3-7.4 μ was constant for all the polymers, but the absorption band in the region of 8.5 μ was shifted, depending upon the size and symmetry of the bisphenol monomer.

The bands in the 6-7 μ region, due to the triazine nucleus, were present in all of the spectra. The hydroxyl content appeared to be quite low, indicating that hydrolysis was not extensive.

DISCUSSION

In the formation of polyamides or polyesters by interfacial polycondensation, a highly branched and crosslinked structure results if one of the monomers is more than difunctional. In the polyamides this possibility exists when the amine is difunctional,² since the acid chloride can react at an existing amide linkage and both of the chloride atoms of the diacid chlorides are highly reactive.

With cyanuric chloride there is an important difference in the reactivity of the chlorine atoms. The replacement of chlorine on the *s*-triazine nucleus occurs in a stepwise manner and is temperature-dependent. The first chlorine is replaced by phenols, in the presence of bases, at 0-5°C., the second at 15-20°C., and the third at 30-40°C. The nature of a substituent also influences the reactivity of the remaining chlorines to subsequent replacements.⁸

The conditions of the reaction influences the replacement of chlorine and therefore the structure of the polymer. In Table II the chlorine content is presented as a function of the method of preparation. The low chlorine content of the polymer prepared in the stirred system is attributed to the long residence at the reactive interface. The comparatively high chlorine content of the film formed at the still interface is believed to be due to the

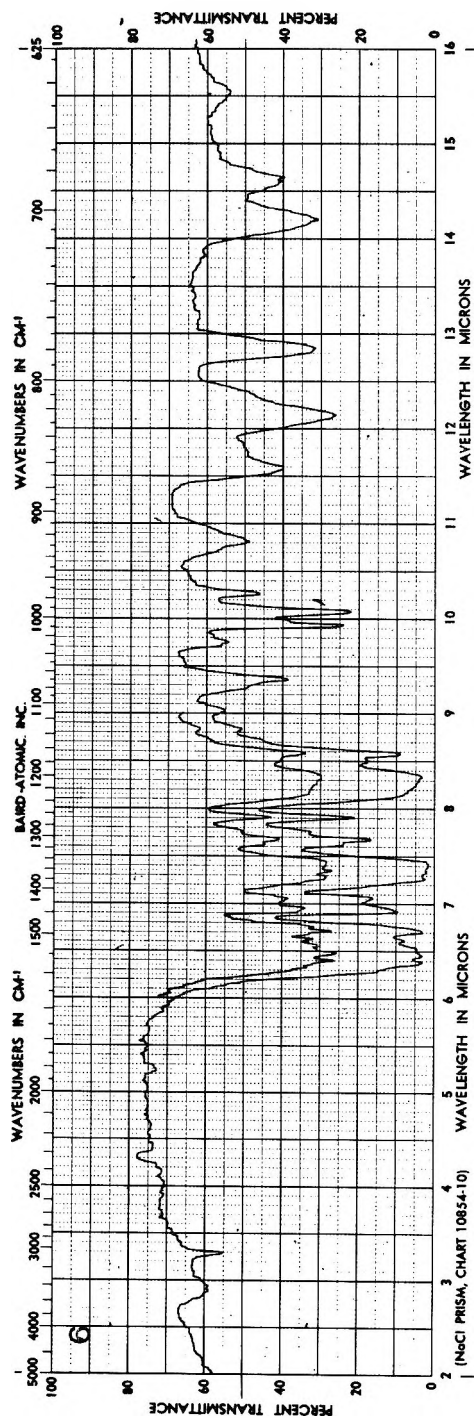


Fig. 3. Infrared spectrum of polymer from 2-phenyl-4,6-dichloro-s-triazine and 4,4'-dihydroxybiphenyl.

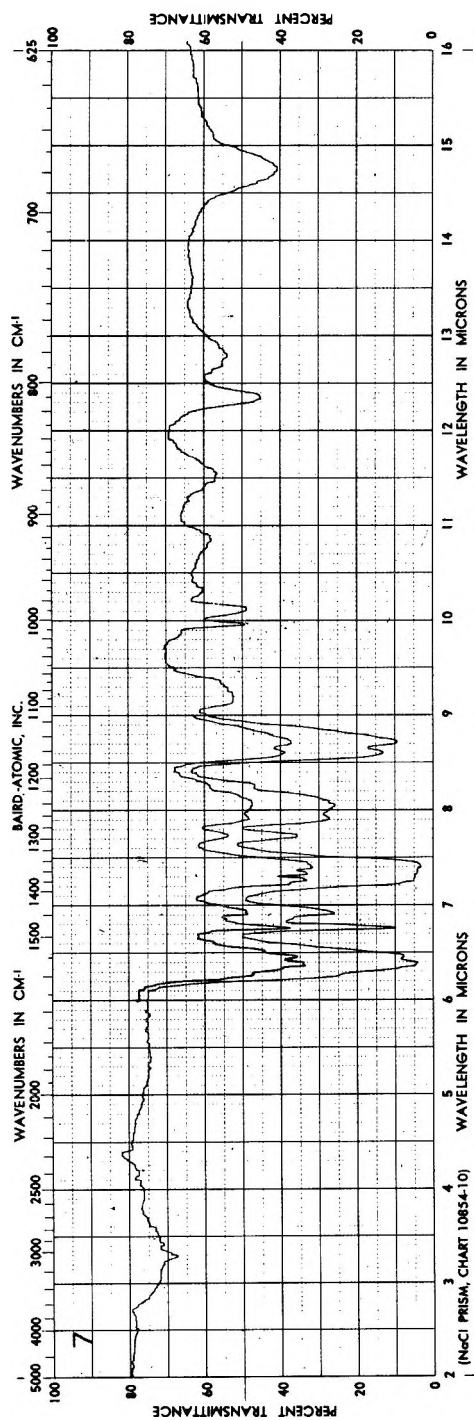


Fig. 4. Infrared spectrum of polymer from cyanuric chloride and resorcinol.

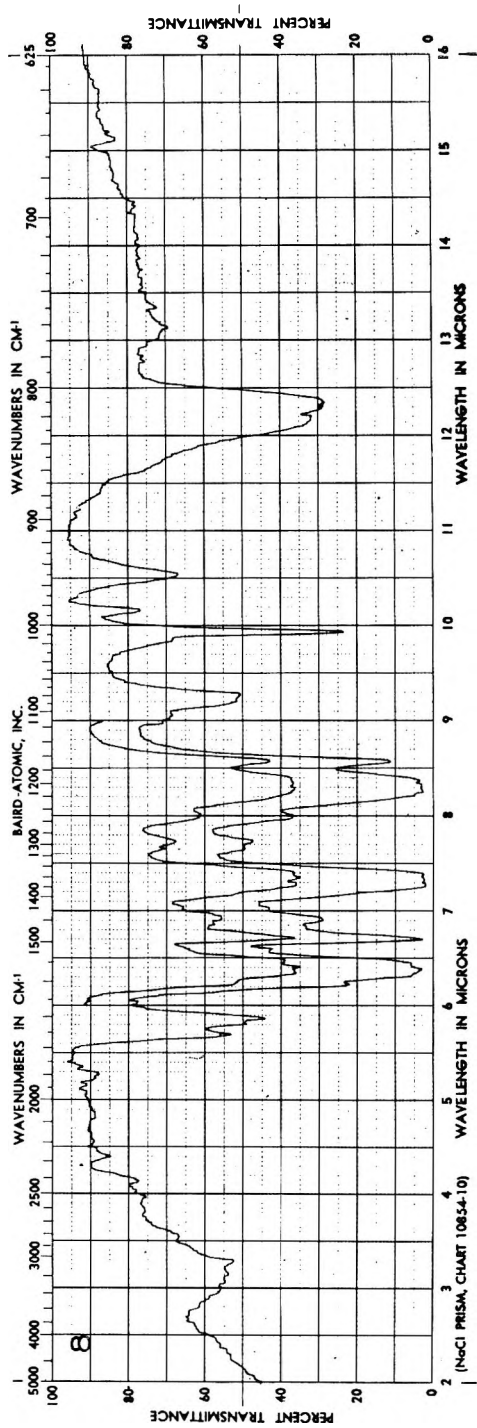


Fig. 5. Infrared spectrum of polymer from cyanuric chloride and 4,4'-dihydroxybiphenyl.

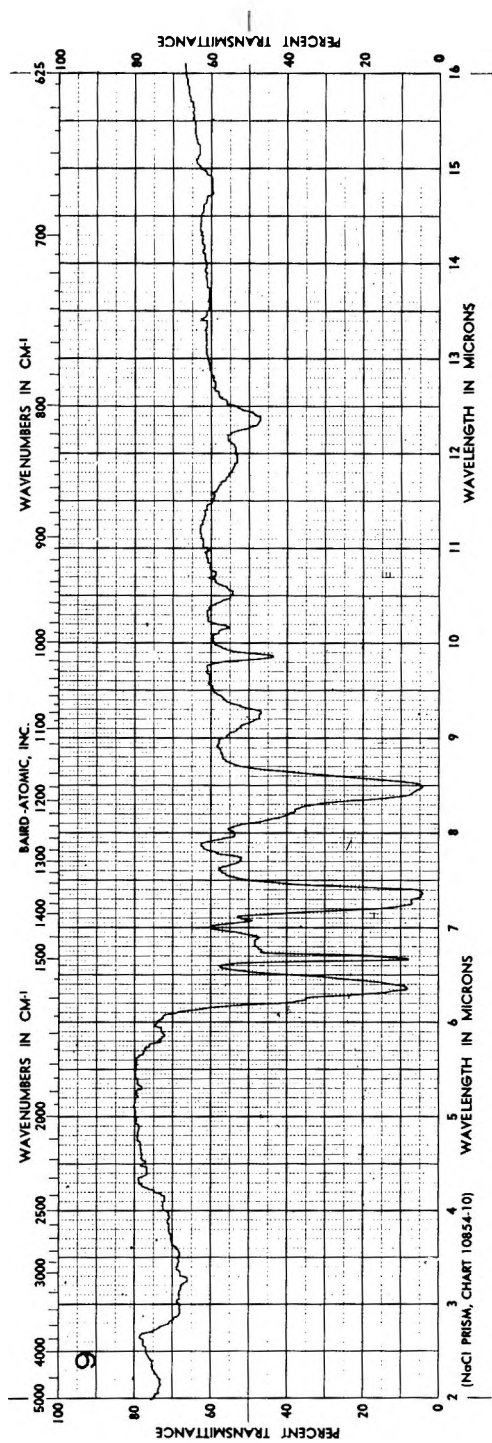


Fig. 6. Infrared spectrum of polymer from cyanuric chloride and hydroquinone.

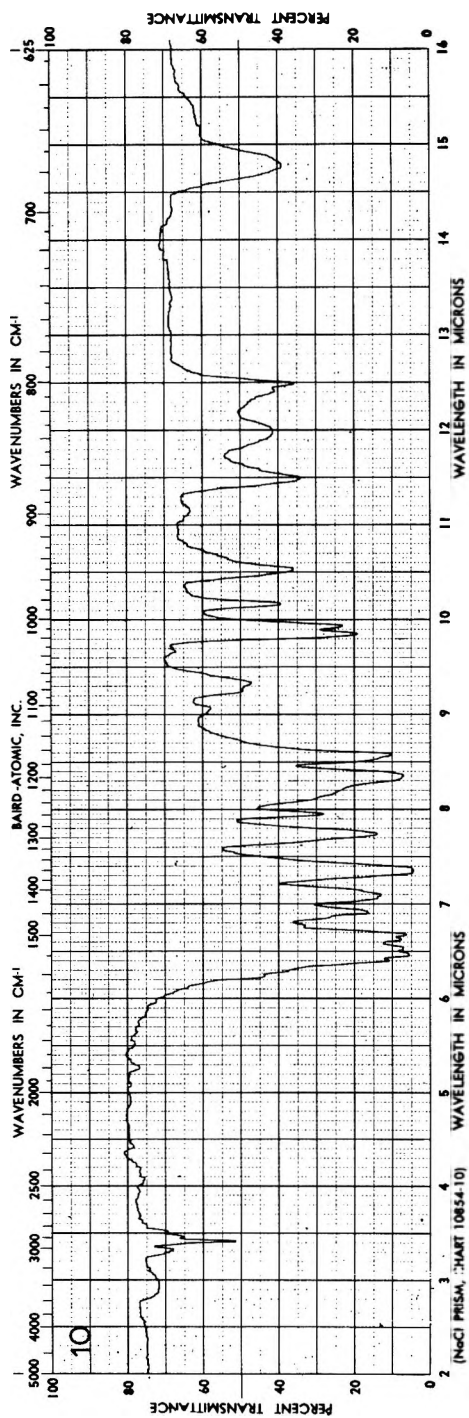


Fig. 7. Infrared spectrum of polymer from cyanuric chloride and 2,2-bis(*p*-hydroxyphenyl)propane.

formation of the film which prevented complete replacement, while the high chlorine content of the pulled polymer is due to film formation and removal from the reaction site. It is believed that a high chlorine content is indicative of a certain amount of linearity of the polymer, especially in view of the low hydroxyl content indicated by the spectra of the polymers.

The structure of the aromatic compound also influences the rate of reaction. At room temperature the rate of formation of film from hydroquinone and cyanuric chloride was fairly rapid; with resorcinol the film formed appreciably slower. A satisfactory film did not form with catechol. The films of 4,4'-dihydroxybiphenyl and 2,2-bis(*p*-hydroxyphenyl)propane formed slowly at room temperature. It seems probable that resonance and steric effects are both responsible for the observed differences in reaction rates.

The reaction conditions had a pronounced effect on polymer yield. The yields varied from 27% for the polymer drawn from the interface to 95% for polymer prepared in a stirred system. The rate of stirring was also important. If the two solutions were stirred too slowly, small globules of the added phase were encapsulated by polymer and prevented from reacting.

References

1. Whittbecker, E. L., and P. W. Morgan, *J. Polymer Sci.*, **40**, 289 (1959).
2. Morgan, P. W., and S. L. Kwolek, *J. Polymer Sci.*, **40**, 299 (1959).
3. Schaeffgen, J. R., F. H. Koontz, and R. F. Tietz, *J. Polymer Sci.*, **40**, 377 (1959).
4. Eareckson, W. M., *J. Polymer Sci.*, **40**, 399 (1959).
5. Lyman, D. J., and S. L. Jung, *J. Polymer Sci.*, **40**, 407 (1959).
6. Reimschuessel, H. K., A. M. Lovelace, and Hagerman, E. M., *J. Polymer Sci.*, **40**, 270 (1959).
7. Padgett, W. M., and W. F. Hammer, *J. Am. Chem. Soc.*, **80**, 803 (1958).
8. Modest, E. J., in *Heterocyclic Compounds*, Vol. 7, R. C. Elderfield, Ed., Wiley, New York, 1961, pp. 669-670.

Résumé

Du polyphénylène-*s*-triazinyle de poids moléculaires apparemment élevés ont été préparés par polycondensation interfaciale de chlorures de *s*-triazinyle et de bisphénoxydes de sodium. Les polymères possèdent une bonne stabilité thermique, sont insolubles, et infusibles. On peut faire varier la nature des polymères en changeant les conditions de réaction. Une longue durée de contact à l'interface réactionnelle fournit un polymère contenant un faible résidu chloré et par conséquent fortement ponté. La diminution de la durée de contact à l'interface réactionnelle fournit des polymères, contenant une plus grande quantité de chlore, et, par conséquent, linéaires.

Zusammenfassung

Offenbar hochmolekulare Polyphenylen-*s*-triazinyläther wurden durch Grenzflächenpolykondensation von *s*-Triazinylchloriden und Natriumbisphenoxyden dargestellt. Die Polymeren sind durch gute thermische Stabilität, Unlöslichkeit und Unschmelzbarkeit charakterisiert. Die Polymeren können durch Änderung der Reaktionsbedin-

gungen variiert werden. Eine lange Verweilzeit an der reaktiven Grenzfläche führt zu einem Polymeren mit niedrigem Chlorgehalt und daher hoher Vernetzung. Herabsetzung der Kontaktzeit an der reaktiven Grenzfläche führt zu Polymeren mit höherem Chlorgehalt, die daher teilweise linear sind.

Received September 3, 1964

Revised January 25, 1965

Prod. No. 4642A

Electron Spin Resonance of Heat-treated Poly(vinyl Chloride)*

ISUKE OUCHI,† *Central Research Institute, Teijin Limited,
Hino, Tokyo, Japan*

Synopsis

Poly(vinyl chloride) was heat-treated, in most cases below 400°C., either in air or in a vacuum and examined by ESR by means of a spectrometer with modified microwave circuit. The ESR signals are first observed at an early stage of degradation and increase with heating time. In the case of heat treatment in a vacuum, the ESR stops increasing when dehydrochlorination is nearly finished, while in the case of the treatment in air, the signal continues to increase after dehydrochlorination is finished. The effects of oxygen and the saturation characteristics of the ESR are quite different for the chars heat-treated below 400°C. and those heat-treated above 400°C. Below 400°C., the signal shows strong saturation in a vacuum but not in air. Oxygen easily affects the signal, shortening the spin-lattice relaxation time. For the char treated above 400°C., the signal does not saturate as strongly and is quenched by oxygen.

INTRODUCTION

Since the earlier observations of electron spin resonance (ESR) in the heat-treated products of divinylbenzene-ethylvinylbenzene copolymer¹ and poly(vinylidene chloride),² similar ESR spectra have been found in many heat-treated polymers³ including poly(vinyl chloride)^{4,5} as well as in carbon black and other carbonaceous materials.⁶ All of them are narrow singlets with g values nearly equal to that of the free electron and show common interesting behaviors. Though the nature of the spin centers has not yet been completely identified, considerable information has been accumulated about the paramagnetic properties of these substances. However, comparatively little research has been undertaken dealing with the initial stage of carbonization, probably on account of the relative weakness of the signal and the complex behavior in this region.⁷

Poly(vinyl chloride) is known to show two-step carbonization readily distinguished by its thermogram or by its abrupt change to a tarry state around 400°C.⁸ In the first stage, up to 400°C. dehydrochlorination is the chief reaction, and dehydrogenation does not occur unless by oxidation.

* Most of this paper was presented at the Symposium on Carbon, Tokyo, Japan, July 21, 1964.

† Present address: Plastics Research Laboratory, Teijin Limited, Sagami-hara, Kanagawa, Japan.

In the present study poly(vinyl chloride) was heat-treated, in most cases at below 400°C., and its ESR properties, such as the growth of spin centers and the saturation characteristics, were studied.

EXPERIMENTAL

Material

The material used was a commercial poly(vinyl chloride) free of plasticizer obtained from Nippon Carbide Co. (D.P. = 1400). This was either extracted with methanol or purified by dissolving in tetrahydrofuran and then precipitating by the addition of methanol. It was then put in a thin-walled glass tube, and heat-treated in the electric furnace either in air or in a vacuum maintained by continuous pumping.

ESR Measurement

ESR measurements were performed by a conventional X-band spectrometer with 80-cycle field modulation (JES-3, Japan Electron Optics Co.), having a modified microwave circuit as shown in Figure 1. The essential point of this modification was to supply a constant bias power to the crystal whenever the microwave power incident on the sample cavity was low. Actually the power at the cavity arm could be decreased down to 10 μ w., which was otherwise only 0.4 mw.

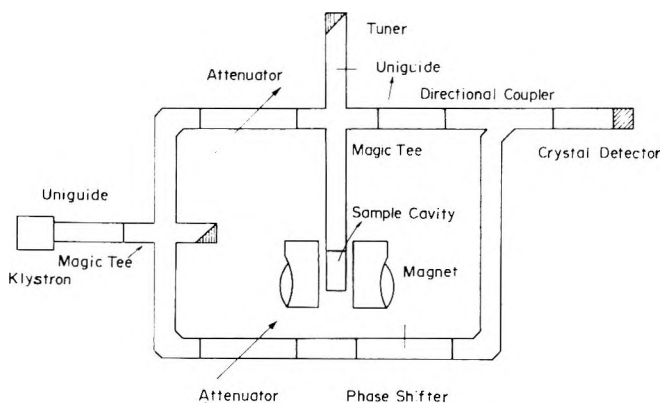


Fig. 1. Modified microwave circuit for the measurement at the low power.

Infrared and Mass Spectrometry

Infrared spectra were taken by the KBr disk method with an Infracord 337 (Perkin-Elmer) spectrometer.

Analysis of the evolved gas was carried out by mass spectrometry with a Hitachi RMU-5B instrument.

RESULTS AND DISCUSSION

Effects of Heat Treatment

When poly(vinyl chloride) is heat-treated above 180°C. in air or in a vacuum, it gradually loses weight and yields a black or dark-brown solid which shows ESR signal. The gas evolved with the weight loss was found to consist more than 95% of hydrogen chloride and less than 5% of benzene and hydrocarbons whose carbon number is less than 7 in the range 180–400°C. No hydrogen or chlorine was detected in this range. Similar results had been obtained by Stromberg et al.⁹

ESR Signals

The shape of the signal is a singlet, as for other carbonaceous materials, and is nearly Gaussian for the treatment in a vacuum or between Gaussian and Lorentzian for the treatment in air. The half width at half height is about 6 oersteds for the former and about 4.2 oersteds for the latter and almost independent of the treatment temperature in this range. The g value is 2.003 ± 0.0005 . At least in the range 120–400°K., the ESR intensity is inversely proportional to absolute temperature, obeying Curie's law.

Formation of Spin Centers

The measurement of the spin center concentration was carried out for various heat treatment temperatures both in air and in a vacuum. In Figure 2, the weight loss, which is mostly due to dehydrochlorination, is plotted with heating time and the spin center concentration is plotted with heating time both for various heat-treatment temperatures for the case of heat treatment in a vacuum. One unit on the ordinate corresponds approximately to 1×10^{17} spins/gram. It is seen that ESR signals begin to appear at an early stage of dehydrochlorination and increase until dehydrochlorination is virtually complete. But, as is seen in Figure 3, for the case of the treatment in air, ESR signals continue to increase, regardless of the weight loss curves. However, with treatment in air, the final weight loss value is nearly the same as that in a vacuum, indicating the balancing of the incorporated oxygen onto the structure and the volatilized gas. At any rate, the increase in the ESR signals continues up to 20–50 hr. of heating, which is much longer than the time required for the weight loss curves to level off. In most cases the treatment in air caused more spin centers than that in a vacuum, and the higher treatment temperature gave the greater spin concentration, though this was not always consistent on account of the heterogeneity of the reaction.

Thus it seems apparent that the formation of spin centers is related to both the dehydrochlorination and oxidation. The reason for the difference between the two kinds of curves, in air and in a vacuum, may be that the oxidation successively causes main-chain scission or volatilization,

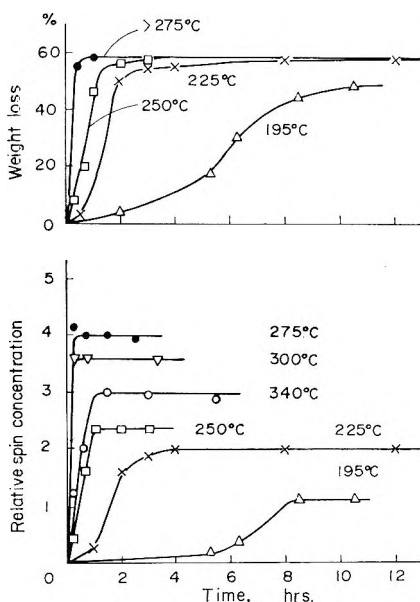


Fig. 2. Weight loss vs. time of heating (top) and relative spin concentration vs. time of heating (bottom) in a vacuum for various heat-treatment temperatures.

even after completion of the dehydrochlorination, and that such main-chain scission would contribute to the ESR absorption. Nevertheless, the ESR signals do not seem due to the scission radicals themselves, because signals from simple scission radicals would be broader and also the radicals would not be stable at such high temperatures. Rather, the main-chain scission caused by oxidation would lead to ring formation through hydrogen abstraction, and these aromatic rings would be associated with the ESR as in other chars.

On the other hand, the ESR observed in the products heat-treated in a vacuum would also be attributed to the aromatic rings. The explanation that the ESR is due to the unpaired electrons associated with long conjugated double bonds does not seem probable, because, if so, after completion of the dehydrochlorination, oxidation should shorten the length of conjugation, with broadening of the width of the ESR signal. But this is not the case. Also such radicals would not be stable at high temperatures but would disappear upon heating as shown in the γ -ray irradiation experiment of Lawton et al.¹⁰ Actually, as shown in Figure 4, the infrared spectra of poly(vinyl chloride) heat-treated at 250°C. show the presence of aromatic structures by the bands at 3030 and 1440 cm^{-1} . Furthermore, the characteristics of the ESR spectra are, as described above, quite common with other carbonaceous materials in which the most reasonable explanation ever offered for the origin of the ESR is the presence of unlocalized spin in the aromatic structure caused by the edge bond scission.¹¹ Therefore it might be safer to consider that the ESR in heat-treated poly(vinyl chlo-

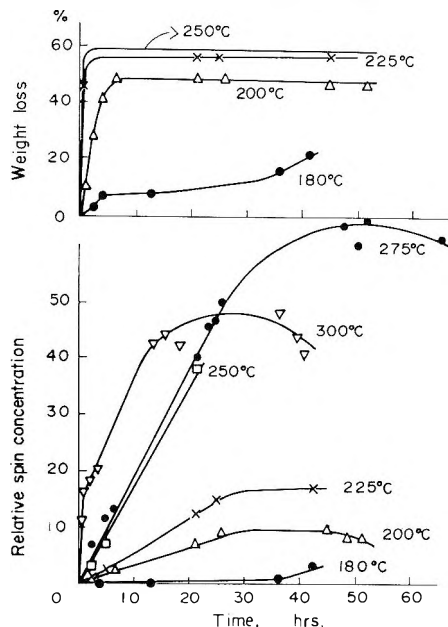


Fig. 3. Weight loss vs. time of heating (top) and relative spin concentration vs. time of heating (bottom) in air for various heat-treatment temperatures.

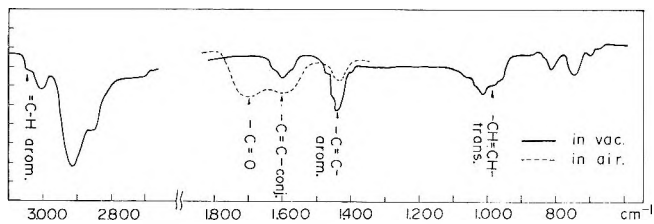


Fig. 4. Infrared spectra of poly(vinyl chloride) heat-treated at 250°C.

ride) is also associated with the unpaired spin in aromatic structures in some ways, although more detailed discussion would not be appropriate at this stage.

Oxygen Effects

The ESR signal of the poly(vinyl chloride) heat-treated below 400°C., either in air or in a vacuum, shows strong saturation when ESR is measured in a vacuum as in Figure 5. This signal is very easily affected by the presence of air. When air is admitted over the sample, the saturation is removed, so that the apparent line intensity is enhanced at the greater power. Conversely, when air is evacuated, the signal saturates again. The rate of this reversible change is quite rapid at first and becomes slow afterwards on account of oxygen diffusion. Although the apparent line intensity depends upon the oxygen pressure, there is no change in spin concentration

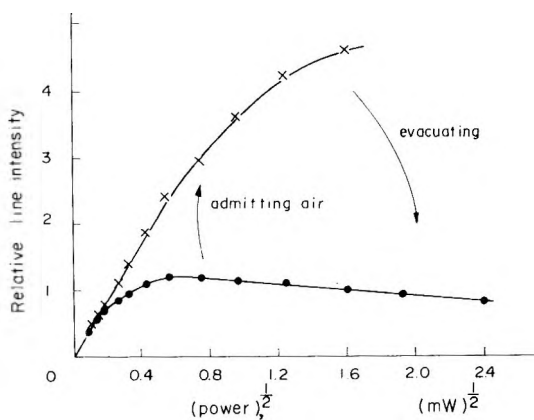


Fig. 5. Effect of oxygen on the saturation characteristics of poly(vinyl chloride) heat-treated at 250°C. in air.

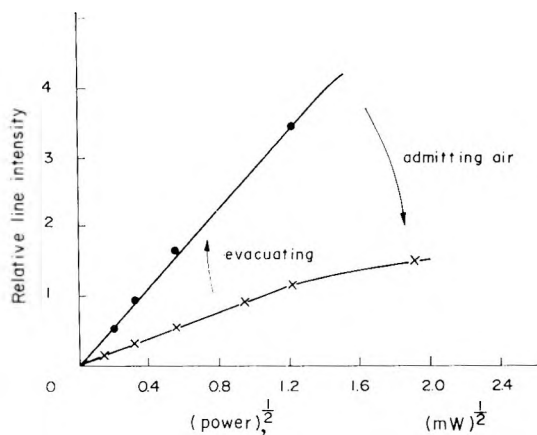


Fig. 6. Effect of oxygen on the saturation characteristics of poly(vinyl chloride) heat-treated at 460°C. in a vacuum.

on admission of air. From these facts, it is concluded that the effect of oxygen is a purely physical one, involving a decrease in the spin-lattice interaction time. The type of saturation is incomplete inhomogeneous. This suggests the width partly comes from the proton interaction.

In contrast, as shown in Figure 6, the ESR signal of the poly(vinyl chloride) heat-treated above 400°C. does not show strong saturation and reacts to oxygen in the opposite way, namely, the signal is decreased by admission of air and increased by evacuation. Here the signal changes its magnitude without changing the width, showing that the process includes the chemical reaction of spin centers. This phenomenon has been observed in other chars by many workers and interpreted as a quenching effect of oxygen due to chemisorption.⁶ The reason for the difference in ESR characteristics between the two classes of chars is not clear on the basis of

present knowledge, though it should be related to structural changes in poly(vinyl chloride) around 400°C.

SUMMARY

In summary, ESR absorption of heat-treated poly(vinyl chloride) appears at an early stage of degradation and increases with heating time. In the case of the heating in a vacuum, the ESR stops increasing when dehydrochlorination is complete, but in the case of heating in air, the ESR continues to increase even after the completion of the dehydrochlorination. Oxygen seems to serve to make more aromatic structures through chain scission.

Secondly, the ESR spectra of poly(vinyl chloride) heat-treated at less than 400°C. show strong saturation phenomena in a vacuum. The effect of oxygen is purely physical and only shortens the spin-lattice relaxation time. In the chars heat-treated above 400°C., however, oxygen is chemisorbed on the char and decreases the line intensity.

The author wishes to thank Mr. Yoshitsugu Nakamura for the mass spectrometry and also to Mr. Shigenobu Sobajima and other colleagues for aid of various sorts.

References

1. Winslow, F. H., W. O. Baker, N. R. Pape, and W. Matreyek, *J. Polymer Sci.*, **16**, 101 (1955).
2. Winslow, F. H., W. O. Baker, and W. A. Yager, *J. Am. Chem. Soc.*, **77**, 621 (1955).
3. Mrozowski, S., *Proceedings of the Fourth Carbon Conference*, University of Buffalo, Pergamon Press, London, 1961, p. 271.
4. Blayden, H. E., and D. J. Westcott, *Proceedings of the Fifth Carbon Conference*, Pennsylvania State University, Pergamon Press, London, 1963, p. 97.
5. Ootani, S., and T. Ishikawa, *Kogyo Kagaku Zasshi*, **66**, 1012 (1963).
6. Ingram, D. J. E., *Free Radicals as Studied by Electron Spin Resonance*, Butterworths, London, 1958, Section 7.7, p. 207.
7. Singer, L. S., *Proceedings of the Fifth Carbon Conference*, Pennsylvania State University, Pergamon Press, London, 1963, p. 37.
8. Gilbert, J. B., J. J. Kipling, B. McEaney, and J. N. Sherwood, *Polymer*, **3**, 1 (1962).
9. Stromberg, R. S., S. Straus, and B. G. Achhammer, *J. Polymer Sci.*, **35**, 355 (1959).
10. Lawton, E. J., and J. S. Balwit, *J. Phys. Chem.*, **65**, 815 (1961).
11. Ingram, D. J. E., *Proceedings of the Third Carbon Conference*, University of Buffalo, Pergamon Press, London, 1959, p. 93.

Résumé

Le chlorure de polyvinyle a été traité à chaud principalement en dessous de 400°C soit à l'air soit sous vide et a été examiné par ESR en utilisant le spectromètre possédant un circuit d'onde micrométrique modifié. On commence à observer les signaux ESR lors de la première étape de la dégradation et ils augmentent avec la durée du chauffage. Dans le cas du traitement thermique sous vide, les signaux ESR cessent de croître lorsque la déshydrochloration cesse, tandis que dans le cas du traitement à l'air, le signal continue à croître après la fin de la déshydrochloration. Les effets de l'oxygène et les caractéristiques de saturation des signaux ESR sont tout à fait différents entre les produits de

carbonisation traitées à chaud en-dessous de 400°C et au-dessus de 400°C. En dessous de 400°C, le signal présente une forte saturation dans le vide mais non à l'air. L'oxygène affecte facilement le signal, réduisant la durée de relaxation spin-réseau. Pour le produit de carbonisation traité audessus de 400°C, le signal n'est pas saturé aussi fortement et est réduit brutalement par l'oxygène.

Zusammenfassung

Polyvinylchlorid wurde hauptsächlich unterhalb 400°C entweder in Luft oder im Vakuum hitzebehandelt und mit ESR unter Verwendung des Spektrometers mit modifiziertem Mikrowellenkreis untersucht. Die ESR-Signale treten in einem frühen Abbau-stadium auf und nehmen mit der Erhitzungsdauer zu. Bei Hitzebehandlung im Vakuum hört die Zunahme des ESR auf, sobald der Hauptteil der Dehydrochlorierung beendet ist, während im Falle der Behandlung in Luft das Signal nach Beendigung der Dehydrochlorierung weiter wächst. Der Einfluss von Sauerstoff und die Sättigungscharakteristik von ESR sind bei den Rückständen der Hitzebehandlung unter- und oberhalb 400°C völlig verschieden. Unterhalb 400°C zeigt das Signal eine starke Sättigung im Vakuum, nicht hingegen in Luft. Sauerstoff hat einen starken Einfluss auf das Signal, indem er die Spin-Gitterrelaxationszeit verkürzt. Bei dem oberhalb 400°C erhaltenen Rückstand tritt keine starke Sättigung des Signals auf, es wird durch Sauerstoff gelöscht.

Received December 15, 1964

Prod. No. 4644A

NOTES

**Dynamic Mechanical Behavior of Polystyrene and Related
Polymers at Temperatures from 4.2°K.***

INTRODUCTION

For polystyrene a weak maximum in mechanical loss ($\tan \delta \sim 0.006-0.008$), tentatively attributed to phenyl group oscillations or wagging,¹ has been reported at 38°K. (5.6 cycle/sec.) by Sinnott¹ using a torsion pendulum and at 48°K. (6290 cycle/sec.) by Crissman and McCammon² employing a longitudinal vibration apparatus. In an attempt to gain more information concerning the nature of this low-temperature relaxation, initial tests have been carried out on two samples of an isotactic polystyrene, one being essentially noncrystalline and the other partially crystalline. In addition, the effect on the relaxation behavior of methyl substitution was investigated by study of poly(*ortho* methyl styrene), two poly(vinyl toluene) copolymers and poly(alpha methyl styrene).

APPARATUS AND MATERIALS

All measurements reported herein were obtained at resonant frequencies of 5,800-8,200 cycle/sec. with a longitudinal vibration apparatus described elsewhere.² The mechanical loss, Q^{-1} , was measured by the band-width method utilizing the half-power points of the resonance curve. All tests were carried out at very low strains and the effects observed were independent of amplitude. The elastic storage modulus was calculated from the observed resonant frequency using the values of specimen dimensions and density as given in Table I.

TABLE I
Sample Characteristics

| Polymer | Length, cm. | Diameter, cm. | Density, g./cc. | Molding temperature, °C. |
|---|----------------|------------------|--------------------|--------------------------------|
| Polystyrene (isotactic) (noncrystalline) | 15.2 | 0.635 | 1.053 (25°C.) | 235 |
| Polystyrene (partially crystalline) | 15.2 | 0.635 | 1.064 (20°C.) | 235 +175° anneal (4 hr.) |
| Poly(alpha-methyl styrene) | 17.5 | 0.762 | 1.066 (25°C.) | — |
| Poly(<i>o</i> -methyl styrene) | 14.5 | 0.623 | 1.027 (24°C.) | 145 |
| Poly(vinyl toluene (35% para-65% meta) | 15.2 | 0.613 | 1.019 (20°C.) | 145 |
| Poly(vinyl toluene (70% para-30% ortho) | 15.2 | 0.635 | 1.040 (20°C.) | 145 |

All samples were obtained from the Dow Chemical Company. The samples were supplied in pellet form, with the exception of poly(alpha methyl styrene), which was received as a compression molded plate. Specimens were prepared by compression

* Supported in part by the U. S. Atomic Energy Commission and the National Science Foundation.

molding the pellets in an evacuated mold (pressure of 1μ) at the temperatures given in Table I followed by slow cooling to room temperature. These specimens were then machined on a lathe to the dimensions noted in Table I. In order to bring about crystallization of compression molded isotactic polystyrene, this specimen was cooled from 235°C . to 175°C . and then held in the mold at 175°C . for 4 hr. followed by slow cooling to room temperature; although a maximum crystallinity of 40–50% was expected, a value of 15% was calculated for this sample from the density using the equation of Natta, Danusso, and Moraglio.³ All of the methylated polystyrenes are believed to be atactic and completely noncrystalline.

RESULTS AND DISCUSSION

Polystyrene

The mechanical loss (Q^{-1}) and dynamic elastic modulus data for the noncrystalline and the partially crystalline samples of isotactic polystyrene are given in Figure 1. The data for a commercial (atactic) sample reported earlier are included for comparison. All three samples show an internal friction peak accompanied by a modulus dispersion in the vicinity of 50°K . The partially crystalline sample, as expected, shows the highest modulus values. For the isotactic noncrystalline sample, the maximum in mechanical loss appears to occur a few degrees lower in temperature than for the partially crystalline isotactic sample (45°K . at 7075 cycle/sec vs. 48°K . at 7335 cycle/sec.); and the values of Q^{-1} appear to be slightly higher throughout the region of the relaxation peak. However, on a loss modulus [$E'' = E'(Q^{-1})$] vs. temperature plot as given in Figure 2, the two isotactic samples show almost identical behavior. It thus appears that, over the range of crystallinity studied, changes in the physical state of the specimen have little bearing on the loss modulus over the entire temperature region from 6– 150°K .

Sinnott¹ has suggested that the observed relaxation process is due either to oscillation or to wagging of the phenyl groups. This view is consistent with broad-line nuclear magnetic (NMR) studies⁴ which indicate the existence of little motion at 77°K . and only a small increase in proton mobility in the 77 – 300°K . temperature region, attributed to phenyl oscillation of increasing amplitude. The NMR studies also indicate that a second moment value corresponding to complete phenyl group rotation is not reached until temperatures rise above 400°K .

A recent study⁵ of polystyrene gave measurements of the nuclear magnetic resonance spin-lattice relaxation time (T_1) at various temperatures. The data show a minimum in T_1 at 260°K . and a plateau in the 120 – 150°K . region. Since the effective frequency

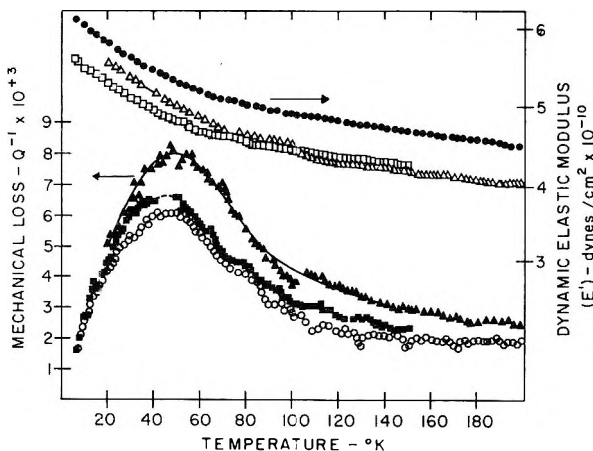


Fig. 1. Mechanical loss (Q^{-1}) and dynamic elastic modulus (E') vs. temperature: (\square, \blacksquare) polystyrene, noncrystalline isotactic; (O, \bullet) partially crystalline isotactic; (Δ, \blacktriangle) commercial, noncrystallizable.

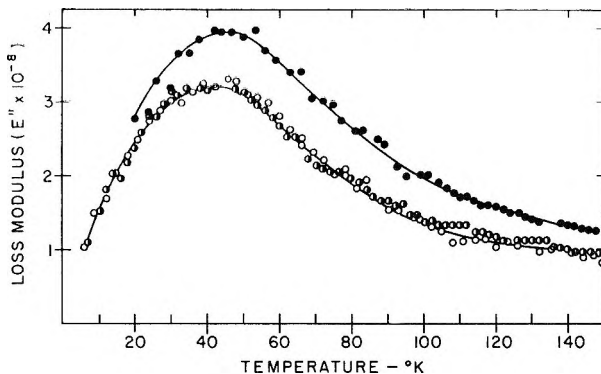


Fig. 2. Dynamic loss modulus (E'') vs. temperature: (⊙) polystyrene, noncrystalline, isotactic; (○) partially crystalline, isotactic; (●) commercial noncrystallizable.

of motion responsible for the T_1 minimum is about 3.5×10^7 cycle/sec., a similar type of motion at a measuring frequency of $\sim 10^4$ cycle/sec. would be expected to occur at lower temperatures. Therefore, one of the T_1 processes may be related to the 48°K. (6290 cycle/sec.) mechanical loss maximum. From a log frequency vs. $1/T$ plot using the loss maxima at 38°K. (5.59 cycle/sec.)¹ and at 48°K. (6290 cycle/sec.)² and the T_1 minimum at 260°K. (3.5×10^7 cycle/sec.)³ an apparent activation energy of ~ 1 kcal./mole is obtained for the observed relaxation behavior in atactic polystyrene.

Methyl-Substituted Polystyrenes

Mechanical loss and dynamic modulus data for the four methyl substituted polystyrenes are shown in Figure 3. The calculated loss modulus values are plotted vs. temperature in Figure 4 with similar data (dotted line) for the noncrystalline isotactic polystyrene sample being given for comparison purposes.

It may be seen from these two figures that the low-temperature behavior is markedly dependent upon where the methyl substitution is made. For the poly(alpha methyl styrene), $P\alpha MS$, with methyl substitution on the main chain, the mechanical loss peak is shifted to higher temperatures with the maximum occurring at about 140°K. (6731 cycle/sec.). With methyl substitution on the ring, as in poly(ortho methyl styrene), $PoMS$, the overall behavior is quite similar to that of the unsubstituted polystyrene, although the loss peak, as shown in Figure 4, is, rather surprisingly, shifted slightly to lower temperatures.

Before discussing possible interpretations of these data, it is of interest to see what type of information is available from nuclear magnetic resonance studies. For a $P\alpha MS$ sample, similar to the one used in the present study, an NMR broad line narrowing process has been reported⁶ in the 120–280°K. region. This process has been attributed to methyl group reorientation at $\geq 10^4$ cycle/sec. Although the broad mechanical loss peak measured at a comparable frequency falls in this general temperature region, it is centered about 60° below the NMR process. This would indicate that motions other than methyl reorientations are involved. In addition, an appreciable loss peak is not expected to arise purely from reorientations of an atom group with such a high degree of spherical symmetry. For example, another polymer containing alpha methyl groups viz. poly(methyl methacrylate) has also been studied in the 100–200°K. range. While broad-line NMR results⁶ indicate that a methyl group reorientation process is occurring in this temperature region, no mechanical loss maximum was found.⁷

A more likely cause of the 140°K. mechanical loss process in poly(alpha methyl styrene) is that assigned to the $\sim 50^\circ K.$ peak in polystyrene viz. oscillation or wagging of the side chain phenyl groups, possibly coupled with reorientational motions of the adjacent methyl groups. The occurrence of phenyl group motion in $P\alpha MS$ at temperatures higher than in polystyrene is a consequence of greater steric hindrance caused by the

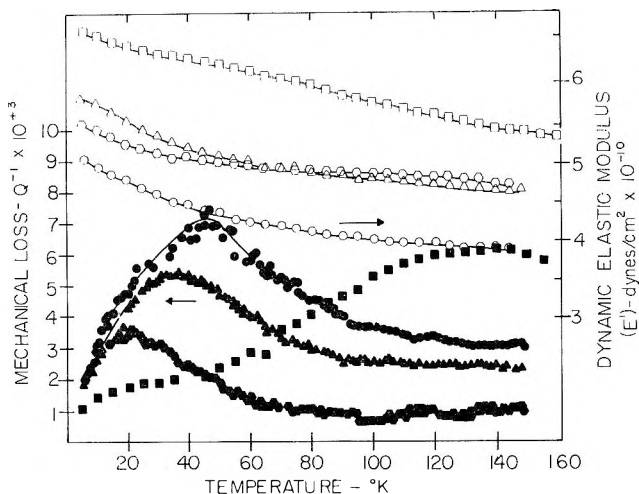


Fig. 3. Mechanical loss (Q^{-1}) and dynamic elastic modulus (E') vs. temperature: (\blacksquare, \square) poly(alpha methyl styrene); (\bullet, \circ) poly(ortho methyl styrene); ($\blacktriangle, \triangle$) poly(vinyl toluene), (70% para-30% ortho), and (\bullet, \circ) poly(vinyl toluene), (35% para-65% meta).

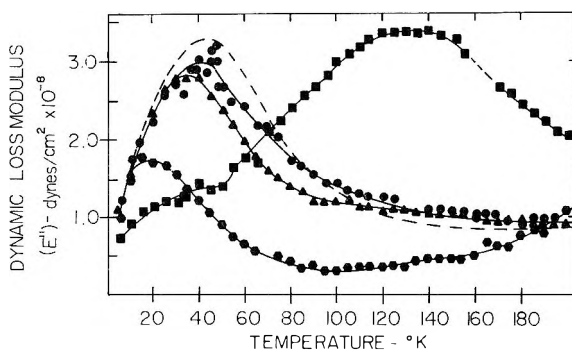


Fig. 4. Dynamic loss modulus (E'') vs. temperature for (\blacksquare) poly(alpha methyl styrene); (\bullet) poly(ortho methyl styrene); (\blacktriangle) poly(vinyl toluene), (70% para-30% ortho); (\blacklozenge) poly(vinyl toluene), (35% para-65% meta); (---) noncrystalline isotactic polystyrene.

presence of the adjacent group. It should be pointed out that the upswing in mechanical loss due to the onset of appreciable main chain mobility is known to occur⁸ about 40° higher for P α MS than for polystyrene, another apparent consequence of increased steric hindrance.

In P α MS, with methyl substitution on the ring rather than on the main chain C atom, one would expect from studies of models that the barrier to phenyl motion would be considerably reduced as compared to that in P α MS. The experimental data support this expectation as the low temperature behavior is now generally similar to that observed in the unsubstituted polystyrene. It is not clear why the loss maximum occurs at a somewhat lower temperature than for the unsubstituted polystyrene, as this would imply that the steric hindrance to phenyl motion as compared to that existing for the same motion in polystyrene has actually been somewhat decreased, rather than increased, by methyl substitution on the ring. One factor that may be involved is the amount of available free volume in the two cases. The sample densities were not measured at low

temperatures but it is known (Table I) that the density of the P α MS sample (1.027) at room temperature is less than that of the unsubstituted polymer (1.053).

The data for the two poly(vinyl toluene) copolymers also indicate that methyl substitution in ring positions has not increased the barrier to phenyl group oscillation, if this is the correct assignment for the observed relaxation behavior. For the 70% *para*-30% *ortho* methyl styrene copolymer, as Figure 4 shows, the maximum occurs at 47°K. (6703 cycle/sec.) and the data indicate that the methyl substitutions have had almost no effect on the internal friction behavior. However, for the 35% *para*-65% *meta* methyl styrene copolymer, the loss peak has been both reduced in magnitude and shifted to a lower temperature (22°K. at 7403 cycle/sec.). Here too, the amount of free volume present may be a factor as this sample had the lowest (room temperature) density of all.

Broad-line NMR studies from 77°K. have been made on ring methyl-substituted polystyrenes.⁴ These studies indicate that hindered rotation of the methyl groups at a frequency of $\geq 10^4$ cycle/sec., occurs at temperatures below 77°K. However, it is not reasonable to assign the observed mechanical loss behavior to motion of the methyl groups both because an apparently similar relaxation process occurs also in unsubstituted polystyrene and because, as noted above, the existing evidence is that methyl reorientation, by itself, does not produce a significant mechanical loss peak. Further experimental data, especially on homopolymers such as poly(*meta* methyl) styrene and poly(*para*-methyl) styrene as well as tests carried out on highly purified samples, are needed before a more definite assignment of these loss peaks can be made.

The mechanical loss vs. temperature plot for P α MS, Figure 3, shows, in addition to the large peak centered about 140°K., a broad low shoulder extending from about 10-50°K. The causes of this small secondary loss process are, at present, unknown. However, several other polymers, such as polypropylene, poly(*d,l* propylene oxide) and poly(vinyl chloride) also exhibit broad shoulders of comparable magnitude in this temperature region.⁷

We wish to express our thanks to Drs. H. W. McCormick and S. G. Turley of the Dow Chemical Company for supplying polymer samples.

References

1. Sinnott, K. M., *SPE Trans.* **2**, 65 (1962).
2. Crissman, J. M., and R. D. McCammon, *J. Acoust. Soc. Am.* **34**, 1703 (1962).
3. Natta, G., F. Danusso, and G. Moraglio, *Makromol. Chem.* **28**, 166 (1958).
4. Odajima, A., J. A. Sauer, and A. E. Woodward, *J. Polymer Sci.* **57**, 107 (1962).
5. Hunt, B. I., J. G. Powles, and A. E. Woodward, *Polymer* **5**, 323 (1964).
6. Odajima, A., A. E. Woodward, and J. A. Sauer, *J. Polymer Sci.* **55**, 181 (1961).
7. Crissman, J. M., J. A. Sauer, and A. E. Woodward, *J. Polymer Sci.*, **A2**, 5075 (1964).
8. Sauer, J. A., and D. E. Kline, *Proc. Intl. Congress Appl. Mechanics*, **5**, 368 (1957).

J. M. CRISSMAN*

Department of Physics
Pennsylvania State University
University Park, Pennsylvania

A. E. WOODWARD

Department of Chemistry
City College of the City University of New York
New York City, New York

J. A. SAUER

Department of Mechanics
Rutgers—The State University
New Brunswick, New Jersey

Received July 20, 1964

Revised October 27, 1964

* Present address: Polymer Physics Section, National Bureau of Standards.

Determination of the Copolymerization Ratio in Polyethylene Terephthalate–Isophthalate by High Resolution Nuclear Magnetic Resonance Spectroscopy

Several papers have appeared describing the determination of isophthalic acid in the presence of terephthalic acid using paper chromatography,^{2,3} ascending chromatography,⁴ gas chromatography,⁵ infrared spectroscopy,⁶ and the gravimetric method.¹

Although these methods can be used for the determination of the copolymerization ratio of polyethylene terephthalate–isophthalate (PET–I) after its hydrolysis, they might be troublesome and not very accurate. Recently, the polarographic determination of isophthalate content in nitrated PET–I polymers containing less than 30% isophthalate has been reported by L. Benisek. Nuclear Magnetic Resonance (NMR) spectroscopy has become useful for the determination of the copolymerization ratio of high polymers.⁸

This letter describes a straightforward, accurate method for isophthalate content determination in PET–I and presents NMR spectra of PET–I's and their related compounds.

Eleven samples of PET–I were obtained from isophthalic acid, terephthalic acid, and ethylene glycol by the use of the ordinary method. The amount of isophthalic acid present in the total acid was varied by 10% in each sample over the range 0–100%. The polymers obtained were dissolved in 5% trichloroacetic acid. The NMR spectra of these polymers were measured on Varian A-60 High Resolution NMR spectrometer at 80°C. (Fig. 1).

The singlet at 7.74 ppm (δ -value determined from Tetramethylsilane as a standard 0) is due to the four equivalent protons attached to the nucleus of the terephthalate unit. The complicated signals which appear at 8.21, 7.90, 7.80, 7.35, 7.22, and 7.10 ppm are due to the four protons attached to the nucleus of the isophthalate unit.

From the integrated intensities of these peaks, the content of the isophthalate unit can be calculated by the following equation:

$$\text{Isophthalate content (\%)} = \frac{\text{Iso}}{\text{Tere} + \text{Iso}} \times 100$$

where iso is the sum of the integrated intensities of the peaks due to protons in the nucleus of the isophthalate unit and tere is the integrated intensity of the peak due to protons in the nucleus of the terephthalate unit.

Isophthalate contents of the 11 copolymers which were calculated using this method

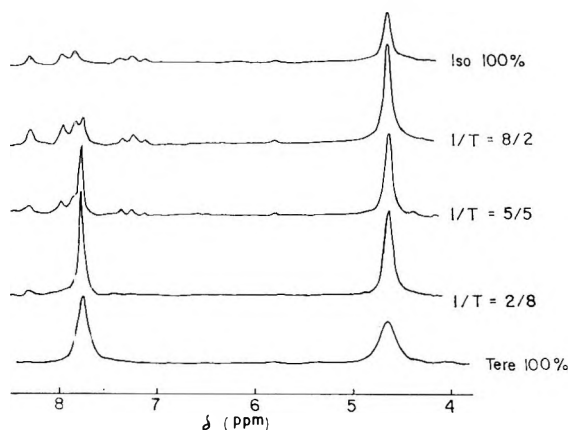


Fig. 1. NMR spectra of polyethyleneterephthalate–isophthalate copolymer.

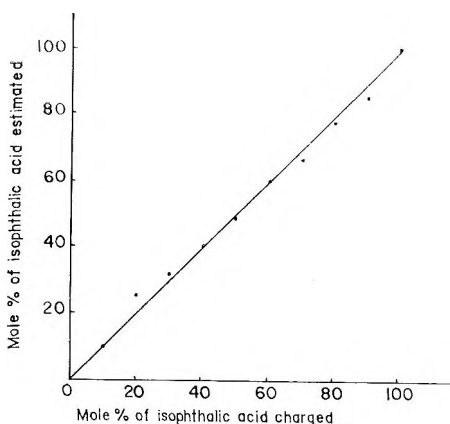


Figure 2.

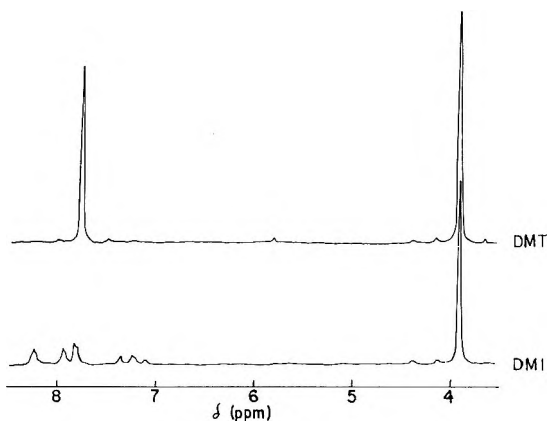

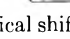


Fig. 3. NMR spectra of DMT and DMI.

are plotted against the proportions of isophthalic acid in the raw material (Fig 2). They are in fairly good agreement. When the content of isophthalate or terephthalate is low, the estimated isophthalate content deviates about 5% from the charged content because the peaks of the isophthalate or the terephthalate unit are very small. At the other points the deviations are negligible. This result is in good agreement with the data from the infrared absorption method⁹ that is based on the measurement of the intensity of the 935 cm.^{-1} band of the isophthalate unit.

Thus, by using either of these two methods (NMR or IR) the isophthalate content of PET-I can be easily determined without hydrolysis or other chemical treatments.

The proton signal of methylene groups in the glycol unit of the copolymer indicates that four kinds of CH_2 group are present: equivalent CH_2 groups in $-\text{T}-\text{CH}_2\text{CH}_2-\text{T}-$, equivalent CH_2 groups in $-\text{I}-\text{CH}_2\text{CH}_2-\text{I}-$, and two unequivalent CH_2 groups in $-\text{T}-\text{CH}_2\text{CH}_2-\text{I}-$. ($-\text{T}-$ and $-\text{I}-$ represent $-\text{O}-\text{CO}-$  $-\text{COO}-$ and $-\text{OCO}-$  $-\text{COO}-$, respectively). Any difference in chemical shifts among these CH_2 groups



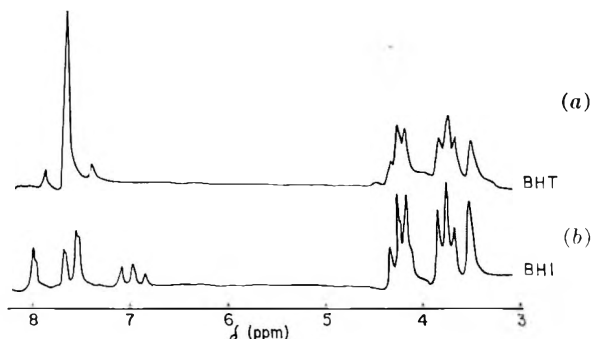



Fig. 4. NMR spectra of BHT and BHI.

has not been detected, but all of these groups are believed to have proton signals at about 4.65 ppm.

On the other hand, in the NMR spectrum of bis- β -hydroxyethyl terephthalate (BHET: $\text{HOH}_2\text{CH}_2\text{C}\cdot\text{OOC}$ —— $\text{COOCH}_2\text{CH}_2\text{OH}$), measured in the molten state at 140°C., two kinds of methylene groups show the different chemical shifts and the splittings into triplet as shown in Figure 4a. This is because the —T— is at one side and the OH at the other. A similar splitting can be seen in the spectrum of bis- β -hydroxyethyl isophthalate (BHEI) which is shown in Figure 4b. However, no detectable difference can be found between the methylene signals of BHET and BHEI. The dimethyl terephthalate (DMT) and dimethyl isophthalate (DMI) methyl signals appear at 3.87 ppm as a singlet as shown in Figure 3.

The low field signals due to protons in the nucleus of DMT and DMI as well as BHET and BHEI exhibit the same behavior as those of the polymers previously described.

References

1. Bryce-Smith, D., *Chem. and Ind.* **1953**, 244.
2. Micheel, F., and H. Schweppe, *Angew. Chem.* **66**, 137 (1954).
3. Franc, J., *Collection Czech. Chem. Commun.* **23**, 655 (1958).
4. Golosova, L. V., *Zhur. Anal. Khim.* **14**, 748 (1959).
5. Komers, R., and V. Bazant, *Dok. Akad. Nauk SSSR*, **126**, 1268 (1959).
6. Grisenthwaite, R. J., *Brit. Plastics* **32**, 428, 439 (1959).
7. Benisek, L., *Textile Res. J.*, **32**, 539 (1962).
8. Nishioka, A., Y. Kato, and H. Mitsuoka, *J. Polymer Sci.*, **62**, S10 (1962).
9. Yamadera, R., and O. Kimura, unpublished data.

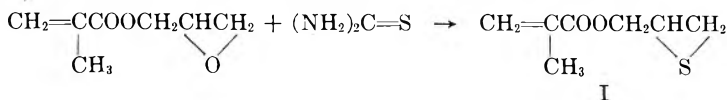
MASAO MURANO
YASUO KANEISHI
REIZO YAMADERA

Textile Research Institute
Toyo Spinning Co., Ltd.,
Katata, Shiga, Japan

Received September 21, 1964
Revised November 12, 1964

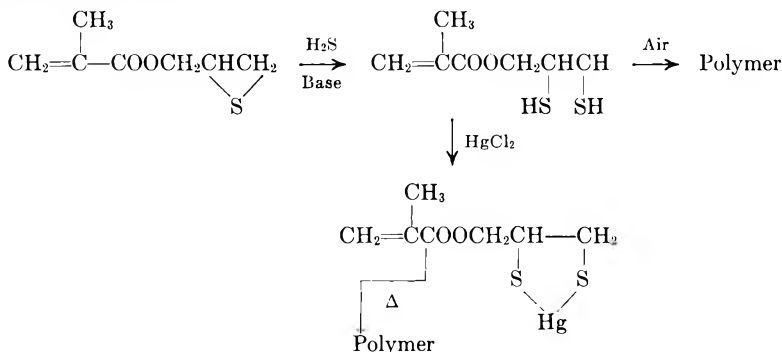
Polymerization of Monomers Containing Thiiran Rings

The reaction of epoxides and thiourea or potassium thiocyanate is a known route to episulfides.^{1,2} This reaction has been used to prepare novel vinyl monomers containing a pendant episulfide ring. Glycidyl methacrylate and vinyl cyclohexene oxide have been converted to the corresponding sulfur compounds by oxygen exchange:



The presence of the double bond and thiiran ring makes such monomers unusually reactive. The thiiran monomer can be polymerized under free radical conditions, leaving the sulfur ring intact. The copolymer of 2,3-epithiopropyl methacrylate and butyl methacrylate is soluble in common solvents but the solutions gel readily. A dioxan solution of the polymer gels at 100°C.; likewise, such solutions form gels when treated with amines, ammonia, or hydrogen sulfide and air. In the last reaction, the dithiol initially produced probably air oxidized to disulfide structure. However, the failure of a variety of reducing agents, for example sodium borohydride, to break up the gel leaves serious doubt that this is the sole reaction. Films of the dithiol derivative of the copolymer extract metal ions such as Hg^{II}, Ag^I, and Zn^{II} from their solutions.

The base catalyzed ring opening of monomer I with hydrogen sulfide yields the dithiol derivative which polymerizes on contact with air to a thick mass. When the dithiol derivative is reacted in dilute tetrahydrofuran with metal salts, organometallic products form. The Co^{II}, Zn^{II}, Fe^{II}, and Cu^{II} derivatives are not soluble in common solvents and decompose in the vicinity of 200°C. The Pb^{II} and mercuric derivatives are soluble in tetrahydrofuran and dimethyl sulfoxide and melt in the region of 100°C. Heating the mercuric compound under pressure above its melting point causes it to polymerize to a coherent gray film having a dielectric constant of 11.88, a dissipation factor of 0.012, and a density of 2.27.



Such metallo derivatives have been isolated with other vicinal dithiols and have five membered rings when divalent metals are used.^{3,4}

EXPERIMENTAL

2,3-Epithiopropylmethacrylate

The procedure of Culvenor and Davies⁵ was modified. The ratio of methanol to water in the reaction medium was chosen so that the epoxide was just soluble and the product insoluble. To glycidyl methacrylate (150 g.) in 125 ml. 60% aqueous ethanol was added 90 g. thiourea in 350 ml. 60% aqueous ethanol. The solution was allowed to stand for 3 hr. with occasional stirring. Cooling may be required at first to control the heat of reaction. After 1/2 hr. an oil began to separate. The mixture was diluted with water

and 150 ml. ether added. The organic layer was separated, washed 5 times with water, and dried over Drierite. The ether was removed and the residue distilled at reduced pressure. (Hydroquinone is added as a polymerization inhibitor and the monomer is distilled soon after preparation to minimize gelation during distillation.) The monomer is collected at b.p. 59° (1.4 mm.), yield = 34%.

$$n_D^{30} = 1.4942, D_4^{25} = 1.1005 \quad \text{Molar Refraction (Theory) 40.47} \\ \text{Molar Refraction (Found) 41.92}$$

ANAL. Calcd. for $C_7H_{10}O_2S$: C, 53.16%; H, 6.33%; S, 20.25%. Found: C, 53.37%; H, 6.57%; S, 20.16%.

Vinyl Cyclohexane Sulfide

With vinyl cyclohexene oxide, the above procedure gave the monomer in 35% yield, b.p. 56° (2 mm.), $n_D^{25} = 1.5323$.

ANAL. Calcd. for $C_8H_{12}S$: C, 68.98%; H, 7.95%; S, 23.02%. Found: C, 68.69%; H, 8.63%; S, 22.58%.

Copolymer

Butyl methacrylate (10 ml.), 2,3-epithiopropylmethacrylate (10 ml.), and azobisisobutyronitrile (0.02 g.) were heated together in benzene (40 ml.) at 60°C. under nitrogen. After heating 18 hr., the solution was cooled, and the copolymer was recovered by precipitation with methanol and vacuum dried at 57°C. Yield is 86%. Analysis found, 11.30% S (or 55% epithio monomer). The infrared spectrum shows no S-H peaks due to cleavage of the thiiran ring.

Metallo Derivatives

In a typical procedure, a solution of 5 ml. epithiopropylmethacrylate in 25 ml. THF was saturated with hydrogen sulfide at room temperature, then 3 drops of benzyl trimethyl ammonium hydroxide were added. After 45 min., the addition of H_2S was discontinued and the solution swept with nitrogen to remove unreacted H_2S . (Attempts to isolate the monomer at this point failed.) To this solution was added $HgCl_2$ (8.6 g.) in 25 ml. THF. Stirring was continued for $1/2$ hr. and the product was recovered by precipitation with methanol. The product was further purified by reprecipitation from THF. The white product starts to melt and subsequently polymerize at 90–100°C., by 120–130°C. a solid mass forms. This hard solid decomposes to a dark powder at 180–190°C. A similar procedure was used with $Cu(OAc)_2$.

Cu(II) Derivative

To cupric acetate (1.5 g.) in THF (50 ml.), methanol (50 ml.), water (60 ml.) was added 1.4 g. of 2,3-dimercaptopropyl methacrylate in THF. The blue, gray precipitate was collected and washed with water and a little cold methanol. If the product is vacuum dried at room temperature, it remains blue gray; however, when heated to 115–120°C., the color changes to light green. Both colored solids give the same IR spectra.

Continuous extraction of the blue-gray solid with methanol changes the color to light green. This solid is unaffected by aqueous ammonia but turns white with aqueous potassium cyanide [$Cu(CN)_2$ is yellow-green].

ANAL. of light green solid: Found: Cu, 19.45% S, 25.25%. Calcd. for $C_7H_{10}O_2S_2Cu$: Cu, 25.04%, S, 25.23%.

The same procedure was used to obtain metallo derivatives of Co^{II} , Fe^{II} , Pb^{II} , and Zn^{II} .

References

1. Rodd, E. H., *Chemistry of Carbon Compounds*, Vol. IVa, Elsevier, New York, 1957, p. 12.
2. Reid, E. E., *Organic Chemistry of Bivalent Sulfur*, Vol. III, Chemical Publishing Co., New York, 1960, p. 14.
3. Mathias, N., *Bols facultade filosofia cienc. letras Univ.*, **14**, 75 (1942).
4. Petrun'kin, V., *Ukr. Khim. Zh.*, **22**, 787 (1956).
5. Culvenor, C. C. J., W. Davies, N. S. Heath, *J. Chem. Soc.*, 1050 (1946).

F. E. ROGERS*

Film Dept.

E. I. du Pont Nemours and Co., Inc.
Wilmington, Delaware

Received December 3, 1964

Use of a Deeply Colored Polymer as an Indicator

It has been shown¹ that a deeply colored poly-cyclopentadiene (ref. designation¹ Polymer A) is a proton acceptor in solvent benzene and that with acids, HB, an equilibrium is set up



where P is the polymer and $\overset{+}{P}H \dots \overset{-}{B}$ is an ion pair formed by proton transfer. The ionization can be established by electrical conductance¹ and dipole moment measurements² and is in accordance with a Brønsted type relationship between the acidity of the proton donor and the equilibrium coefficient *K* of eq. (1). The electronic spectrum of the unprotonated polymer in benzene shows a peak at 350 m μ , tailing into the visible region, while the ion pair is characterized by a light absorption maximum at 610 m μ . Beer's law is valid.¹ This polymer in benzene solution can be used as an indicator, and the equilibrium coefficient, *K*, of eq. (1) can be determined by a method similar to that previously³ used for measuring indicator constants. We determined the ratio,

$$\beta = \frac{[\overset{+}{P}H \dots \overset{-}{B}]}{[P]} = \frac{d - d_o}{d_o - d} \quad (2)$$

where the expressions in square brackets are equilibrium concentrations and *d*, *d_o*, and *d_∞* are optical densities, at 610 m μ of solutions containing $\overset{+}{P}H \dots \overset{-}{B}$, P without $\overset{+}{P}H \dots \overset{-}{B}$, and $\overset{+}{P}H \dots \overset{-}{B}$ without P. The functional relationship between β and the concentration of the proton donor has been determined¹ and shows that only one acid molecule adds to one molecule of polymer. The simple stoichiometry of eq. (1) compared with the behavior of more conventional indicators in the solvent benzene⁴ is possibly due to the spreading of the positive charge over a sequence of conjugated double bonds.¹ If, on the other hand, acids in the solvent benzene react with conventional indicators or colorless bases, charge localization at the oxygen or nitrogen atom occurs and the resulting high charge density is responsible for the formation of triple ions or higher aggregates. The presence of these triple ions or higher aggregates has been demonstrated by electrical conductance measurements.⁵

In solutions containing acid, the colored polymer, and a colorless base (*B*₁), a second equilibrium is set up



* Present address: Skidmore College, Saratoga Springs, New York.

where the coefficients n and m could be larger than unity, particularly if B_1 contains more than one basic site. The observations that end points, which correspond to a 1:1 acid-base ratio, occur in electrometric or indicator titrations in benzene do not necessarily relate to the structure of partially neutralized adducts, because the coefficients n and m [eq. (3)] may vary during the course of the neutralization.

This is the background of the present investigation in which the stoichiometric simplicity of the indicator equilibrium [eq. (1)] in benzene is utilized to gain information about the mode of reaction between colorless bases and trichloroacetic acid. This particular proton donor has been selected because it had been used as a catalyst in a polymerization reaction and the influence of proton acceptors on the catalytic activity is related to some of the results of this study.

In the presence of a colorless base, B_1 , the indicator ratio $[PH \dots B]/[P]$ is given by

$$\beta_B = \frac{d_B - d'_o}{d'_\infty - d_B} \quad (4)$$

where d_B , d'_o , and d'_∞ are optical densities, also at 610 $m\mu$ of solutions containing $PH \dots B$, P and B_1 , P and B_1 without $PH \dots B$, and $PH \dots B$ and B_1 without P . The optical densities d_B and d'_o can be determined, but d'_∞ is calculated on the assumption that the molar light absorption coefficient, 610 $m\mu$, of the species $PH \dots B$ is not altered on addition of a colorless base. The assumption is supported by experiments mentioned below.

TABLE I
Interaction of Trichloroacetic Acid with Colorless Bases in Benzene,
20°C., Indicator: Cyclopentadiene Polymer A¹

| Ref. no. | Base | Concentration (mole/l.) | | | No. of tests | γ |
|----------|------------------|-------------------------|-------------------|--------------------------|--------------|---------------|
| | | Polymer $\times 10^4$ | Acid ^a | Base | | |
| 1 | Phenol | 1.40 | 0.300 | 0.0100-1.00 | 10 | 0.6 ± 0.2 |
| 2 | Maleic anhydride | 1.40 | 0.140 | 0.0200-0.300 | 9 | 0.6 ± 0.2 |
| 3 | Water | 2.12-6.58 | 0.458 | 0.100-0.500 ^b | 22 | 1.7 ± 0.4 |
| 4 | Ethyl acetate | 1.40 | 0.300 | 0.0100-0.600 | 10 | 2.0 ± 0.4 |
| 5 | Ethanol | 1.31-1.35 | 0.300 | 0.0500-1.50 | 16 | 2.2 ± 0.4 |
| 6 | Acetone | 1.04 | 0.300 | 0.100-0.600 | 8 | 2.0 ± 0.4 |
| 7 | Dioxan | 1.69 | 0.140 | 0.0100-0.300 | 15 | 2.5 ± 0.5 |

^a Stoichiometric.

^b The solubility of water in 0.3 *M* trichloroacetic acid is larger than in benzene without acid.

To demonstrate the influence of the colorless bases listed in Table I we have adopted the method of Kolthoff and Bruckenstein⁶ and calculated free acid concentrations, $[HB]_F$, from

$$[HB]_F = \beta_B/K \quad (5)$$

where β_B is obtained from eq. (4) and K is the equilibrium coefficient of eq. (1). In each set of tests at least five base concentrations, in the range given in the fifth column of Table I, were investigated; the concentrations of polymer and acid are listed in the third and fourth columns of the same Table. From the experiments the base concentration $c_{1/2}$ was estimated, by interpolation, at which the free acid concentration, $[HB]_F$, is reduced to $1/2$ of the stoichiometric acid concentration $[HB]$. Ratios γ , calculated from

$$\gamma = [HB]/c_{1/2} \quad (6)$$

are listed in the last column of Table I. If the coefficients n and m in eq. (3) were unity, γ would equal $2K_b[\text{HB}]/(K_b[\text{HB}] + 2)$ and in this case the γ values of ref. no. 1 and 2 would be compatible with $K_b[\text{HB}]$ being of the same order of magnitude as 2; the γ values ref. no. 3-7, on the other hand, require that $K_b[\text{HB}] \gg 2$. It is possible that in such adducts some acid and base molecules are held together in a 1:1 ratio by coulombic forces, while other molecules are more loosely bound, the relevant intermolecular forces being yet sufficiently strong to make the base B_1 a competitor for the indicator.

EXPERIMENTAL

The preparation and purification of cyclopentadiene polymer A, has been described.¹ A freshly prepared sample was distributed into several dozen small glass vessels, each containing 0.1-0.2 g.; the tubes were evacuated and sealed. Shortly before each experiment, one of these containers was opened and the unused polymer discarded. Solutions were stabilized by the antioxidant α -tocopherol ($\sim 10^{-5}M$); exposure to air was as short as possible. Optical densities, determined in most experiments with light of 610 $m\mu$, were back extrapolated to the time at which the polymer was dissolved. Optical path length could be varied between 0.1 and 10 cm. Measurements with light of a wave length corresponding to peak II¹ of the electronic spectrum of species $\text{PH} \dots \text{B}$ were also made and gave results similar to those obtained in tests with light of 610 $m\mu$. The reversibility of the reaction between the indicator and trichloroacetic acid has been established and it can also be shown¹ that this indicator is made, on a preparative scale, by precipitation with the bases ref. no. 3, 5, 6, and 7 of Table I. Benzene solutions containing the indicator, together with the proton acceptors ref. no. 1 or 2, gave the unchanged polymer (yield over 90%) on precipitation with ethanol or pentane. The chromophore of this polymer is not altered on prolonged treatment with alcoholic potassium hydroxide.¹ Experiments were carried out in which the sequence of mixing was varied, the base, the acid, or the indicator being the final substance added: the optical densities, d_B , showed no detectable difference. All these observations are incompatible with the assumption that there is an irreversible reaction between indicator and base.

For the calculation of free acid concentrations, $[\text{HB}]_F$, an equilibrium coefficient of $K = 10.0$ l./mol. was used throughout. This is the mean of approximately 100 determinations which were carried out during several months. It relates to a polymer more carefully protected from oxidation by air than the samples previously¹ used. A typical plot for the estimation of the concentration, $c_{1/2}$, is shown in Figure 1.

Upon addition of the base to the solution of indicator and acid, the dielectric constant, D , of the solution may increase somewhat. In view of this the molar light absorption coefficient at 610 $m\mu$, ϵ , of the species $\text{PH} \dots \text{B}$ and the equilibrium coefficient, $K = [\text{PH} \dots \text{B}]/[\text{P}][\text{HB}]$, of eq. (1) were measured⁷ in benzene, $D = 2.3$, and in mixtures of

TABLE II
Molar Light Absorption Coefficients, ϵ , and Equilibrium Coefficients, K , in Benzene and Mixtures of Benzene with Methylene Chloride, 20°C.

| Mol. fraction CH_2Cl_2 | $10^{-3}\epsilon$ (1/mol. cm.) 610 $m\mu$ | K (1/mol.) |
|--|--|------------------|
| 0 | 7.0 ± 0.3^a | 10.0 ± 1.5^a |
| 0.303 | 7.1 ± 0.4 | 16.2 ± 2 |
| 0.580 | 6.5 ± 0.4 | 28 ± 4 |
| 0.797 | 8.2 ± 0.5 | 63 ± 10 |

^a The ϵ and K values listed in ref. 1 are somewhat smaller for reasons given in the text. Other K values of ref. 1, however, determined in the presence of a base are not defined by $\beta/[\text{HB}]$ but by $\beta_B/[\text{HB}]$.

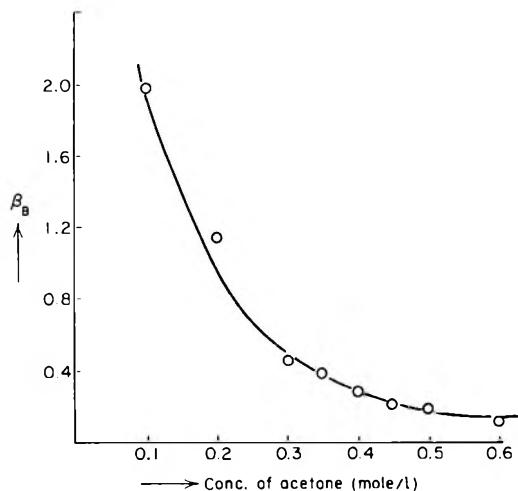


Fig. 1. Influence of acetone concentration on the ratio β_B , defined by eq. (4). Reaction mixture $1.04 \times 10^{-6}M$ with respect to the indicator and $1.00 \times 10^{-5}M$ with respect to α -tocopherol. Stoichiometric concentration of trichloroacetic acid $0.312M$. Solvent benzene, $20^\circ C$.

benzene with methylene chloride, $D = 9.1$. Representative results are shown in Table II. The figures in the second line, and similar results relating to *o*-dichlorobenzene, $D = 9.8$ (instead of methylene chloride) show that the ϵ values do not depend markedly on solvent composition. It is justified, therefore, to assume that the ϵ value of the species $\text{PH} \cdot \cdot \text{B}$ is not significantly altered upon addition of the cosolvent B_1 . The increase of the K values in the last line of Table II is not unexpected, as eq. (1) involves a charge separation. It could be suggested therefore, that the K value to be introduced into eq. (5) should be larger than the equilibrium coefficient determined without the cosolvent B_1 . In this case, however, the γ values would still be larger than those in Table I and the essential conclusions would not be altered. The influence of the cosolvent, B_1 , should be more evident in the experiments with water, ethanol, or acetone (sample no. 3, 5, and 6 of Table I), than in the tests (ref. no. 7), where neither the dielectric constant nor the concentration of the base B_1 was particularly high. No effect of this kind has actually been found.

References

1. French, P. V., L. Roubinek, and A. Wassermann, *J. Chem. Soc.*, **1961**, 1953.
2. Bauge, E., J. W. Smith, and A. Wassermann, *J. Chem. Soc.*, **1962**, 864.
3. See, e.g., Bell, R. P. and J. W. Bayles, *J. Chem. Soc.*, **1952**, 1518.
4. Hummelsted, L. E. I., and D. N. Hume, *J. Am. Chem. Soc.*, **83**, 1564 (1961).
5. Fuoss, R. M., and C. A. Kraus, *J. Am. Chem. Soc.*, **55**, 476 (1933).
6. Kolthoff, I. M., and S. Bruckenstein, *J. Am. Chem. Soc.*, **78**, 1 (1956).
7. Upadhyay, J., unpublished work.

A. A. LEVY
A. WASSERMANN

William Ramsay and Ralph Forster Laboratories
University College
London, England

Received August 20, 1964
Revised December 15, 1964

**Refractive Index–Molecular Weight Relationships for
Poly(ethylene Oxide)***

Number-average molecular weights of poly(ethylene oxide) (PEO) are generally determined from changes in solvent colligative properties, viscosity relationships, or by terminal hydroxyl analysis. It has now been established that good estimates of their molecular weights can be obtained from simple measurements of refractive index at any reasonable temperature above the softening range.

A series of PEO polymers having number-average molecular weights, M_n , from ~ 300 to $\sim 20,000$ were obtained and their refractive indices measured at $75 \pm 0.02^\circ\text{C}$. with a Valentine Improved Precision Model 450A refractometer. Values of M_n were determined from end-group hydroxyl by acetylation. The results are given in Table I. It is

TABLE I
Molecular Weights, M_n , and Refractive Indices, n_D^{75} ,
of Poly(ethylene oxides)

| Sample of poly(ethylene oxide) ^a | Density d_4^{75} | Molecular weight by acetylation ^b | Index of refraction n_D^{75c} |
|---|-----------------------|--|---------------------------------------|
| E 300 | 1.080 | 303.5 | 1.44592 |
| E 400 | 1.078 | 385.0 | 1.44776 |
| E 600 | 1.080 | 570.0 | 1.44958 |
| E 1000 | 1.082 | 991.2 | 1.45121 |
| E 1450 | 1.077 | 1523 | 1.45202 |
| E 1500 | 1.079 | 533.0 | 1.44906 |
| E 1540 | 1.080 | 1556 | 1.45227 |
| E 2000 | 1.079 | 2018 | 1.45236 |
| E 3000 | 1.079 | 3091 | 1.45311 |
| E 4000 | 1.080 | 4545 | 1.45348 |
| E 5000 | 1.080 | 5405 | 1.45354 |
| E 6000 | 1.082 | 6350 | 1.45361 |
| E 10000 | 1.082 | 9523 | 1.45374 |
| E 15000 | 1.084 | ^b | 1.45390 |
| E 20000 | 1.078 | ^b | 1.45392 |

^a Poly(ethylene oxides) obtained from Fluka AG, Buchs, Switzerland.

^b Values of 15,000 and 20,000 for molecular weight were used for E 15,000 and E 20,000. Up to molecular weights of 2000, the reproducibility is within $\pm 2\%$, and accuracy is $\sim \pm 5\%$; however, above 10,000 the experimental errors are too large to obtain significant values for molecular weights.

^c The standard deviation for a large number of refractive index measurements was ± 0.00004 .

believed that the density of these polymers at 75°C . does not vary significantly with M_n and has a value of 1.080 ± 0.002 .

Although the change in n_D^{75} with M_n is small at the higher values, the limits of error for the $n_D^{75} = M_n$ correlation do not appear to be much larger than for most end-group or colligative properties methods. Plots of n_D^{75} vs. $(M_n)^{-1}$, as shown in Figure 1, are apparent straight lines. The data at 30°C . were obtained from the literature.¹ Some early data at 60°C .² also give a linear relationship, but the slope is less than for the data at 30 and 75°C .²

* This paper represents the results of one phase of research carried out at the Jet Propulsion Laboratory, California Institute of Technology, under contract number NAS7-100, sponsored by the National Aeronautics and Space Administration.

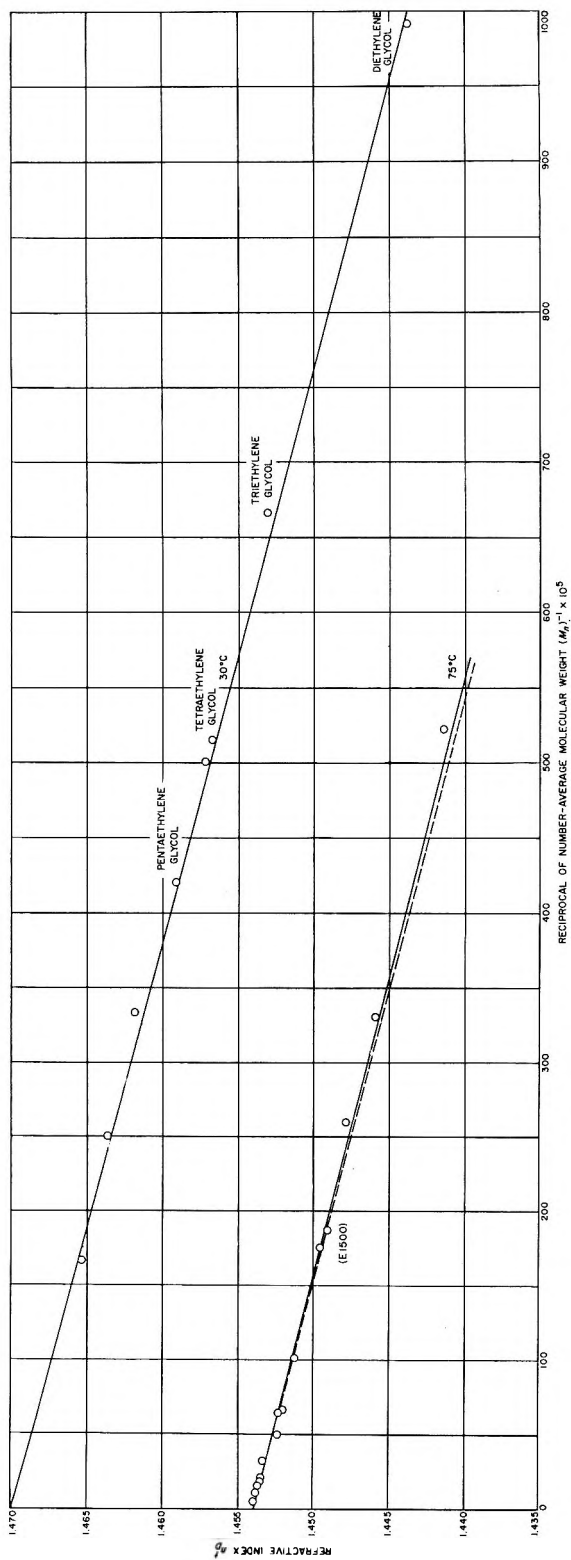


Fig. 1. The relationship of refractive index to the reciprocal of number-average molecular weight.

The one point for E 1500 (75°C. data) shows that the correlation is valid for blends of PEO of different molecular weights. This polymer is a 50:50 blend of E 1540 and E 300. The refractive index of the blend can be calculated from an equation derived on the assumption that the Gladstone-Dale specific refractions are additive:

$$\frac{100(n-1)}{d} = \frac{p_1(n_1-1)}{d_1} + \frac{(100-p_1)(n_2-1)}{d_2} \quad (1)$$

in which n is the refractive index of the blend, n_1 and n_2 are the refractive indices of the two components, d_1 and d_2 are the corresponding densities, and p_1 and p_2 are the weight percentages of components.³ The value obtained (1.44911) agrees with the measured n_D^{75} , 1.44906. Furthermore, the point for the blend (E 1500) falls reasonably close to the correlation line in Figure 1.

The dashed lines in Figure 1 represent calculated theoretical relationships at 75°C. derived from the 30°C. data as follows. The equation of Eykman was taken as the correct relationship between n and d , rather than the Lorenz-Lorentz relationship, since it has been shown to give a better representation of experimental data. This equation is:

$$C = \frac{n^2 - 1}{n + 0.4d} \quad (2)$$

or

$$n = \frac{1}{2} [Cd + (C^2d^2 + 1.6Cd + 4)^{1/2}] \quad (3)$$

in which C is a constant and n and d are the refractive index and density measured at the same temperature.⁴ C was calculated from data at 30°C. It has been shown that C is independent of temperature from 20 to 25°C. Here it has been assumed that C is constant from 30 to 75°C, but varies with molecular weight.

The equation:

$$d_4^t = 1.1422 - 0.0008t \quad (4)$$

can be used to calculate the temperature dependence of density for PEO from 30 to 70°C. with reasonable accuracy. Presumably there may be a small dependence of density on M_n but for this correlation it is negligible; thus, for each molecular weight, a value of C was calculated at 30°C. using eq. (2). Densities were then calculated for the temperature t . Using these densities and C values, n_D^t was then calculated from eq. (3) and plotted (versus M_n) as shown by the dashed lines at 75°C. on Figure 1. The agreement

TABLE II
Molecular Weights, M_n , From Refractive Indices, n_D^t

| Poly- (ethylene oxide) sample | Temp. t , °C. | Refractive index, n_D^t | Number- average molecular weight from OH | Number- average molecular weight from n_D^t |
|--|-----------------------|---------------------------------|---|--|
| E 200 | 70 | 1.44246 | 192 | 193 |
| E 300 | 50 | 1.45405 | 304 | 295 |
| E 400 | 50 | 1.45596 | 417 | 421 |
| E 600 | 50 | 1.45770 | 510 | 519 |
| E 1000 | 50 | 1.45906 | 991 | 690 |
| E 1000 | 70 | 1.45332 | 991 | 980 |
| E 1000 | 75 | 1.45121 | 991 | 935 |
| E 3000 | 75 | 1.45311 | 3091 | 3333 |

with the experimental points is remarkably good. For measurements of n_D^t at 30 or 75°C., reasonable values of the molecular weight can be obtained by reference to Figure 1 for M_n up to $\sim 10,000$.

From a measurement of n_D^t at any temperature from 30 to 75°C., M_n can be estimated by (1) calculating Cd at the temperature of n_D^t measurement from eq. (2), (2) dividing Cd by the density calculated from eq. (4) at the temperature of n_D^t to give the value of C , and (3) calculating n_D^t at 30 or 75°C. from Cd where d is the density of 30 or 75°C. and reading (M_n) from the appropriate line on Figure 1. Some typical results of molecular weight determinations from n_D^t measurements at 50 and 70°C. are shown in Table II.

Because of the apparent accumulation of errors from the density correction and refractive index measurements, for the molecular weights exceeding ~ 600 , better results are obtained if the refractive indices are measured at $\sim 75^\circ\text{C}$. and compared with a similar sample of known molecular weight.

References

1. Weissler, A., J. W. Fitzgerald, and I. Resnick, *J. Appl. Phys.*, **18**, 434 (1947).
2. Fordyce, R., E. L. Lovell, and H. Hibbert, *J. Am. Chem. Soc.*, **61**, 1905 (1939).
3. Bauer, N. and K. Fajans, in Weissberger, A., *Technique of Organic Chemistry*, Vol. 1, Part 2, Interscience, New York, 1949, p. 1150.
4. Eykman, J. F., *Rec. Trav. Chim.*, **14**, 185 (1895).
5. Dreisbach, R. R., *Ind. Eng. Chem.*, **40**, 2269 (1948).

JOHN D. INGHAM
D. DAVID LAWSON

Jet Propulsion Laboratory
California Institute of Technology
Pasadena, California

Received September 21, 1964

Crystalline Growth of Polyvinylcyclohexane

Certain x-ray parameters of crystalline polyvinylcyclohexane have been reported by Natta et al., but no literature reference has been found relating to single crystals of this polymer. We have successfully grown single crystals of PVCH in this laboratory and characterized them to some degree.

Polyvinylcyclohexane will precipitate from solution in various crystalline forms depending upon the manner of solutioning and precipitation. The polymer is soluble in trichloroethylene and chloroform and both these solvents were used to grow crystals of PVCH. However, since both solvents give equivalent results only crystals obtained from trichloroethylene solutions need be discussed here. A concentrated solution of polymer of 2.4 inherent viscosity was diluted with solvent to the desired concentrations of 0.1%, 0.05%, 0.01%, and 0.005% by weight (these concentrated solutions, approximately 18% by weight, were obtained from Dr. E. V. Kirkland of this laboratory). Ethylene chloride was then added until the cloud point was reached. The sample was then placed in the oven at a temperature which caused the polymer to redissolve. This temperature varied with each concentration. After the PVCH was redissolved the temperature was held overnight slightly below that temperature which caused redissolving (approximately 60–75°C.), and the polymer allowed to slowly precipitate. It was necessary to place the solution in the oven immediately after reaching the cloud point because the polymer had a tendency to agglomerate. These agglomerates did not redissolve.

As the concentrations of polymer were decreased, the crystalline form of the precipitate changed. The growths from the higher concentrations were dendritic. Figure 1 shows dendrites grown from a solution of 0.1% concentration. In the lower concentrations the polymers came out of solution almost entirely as single crystals—0.05% polymer



Fig. 1. Dendrites of polyvinylcyclohexane grown from a 0.1% solution in trichloroethylene.

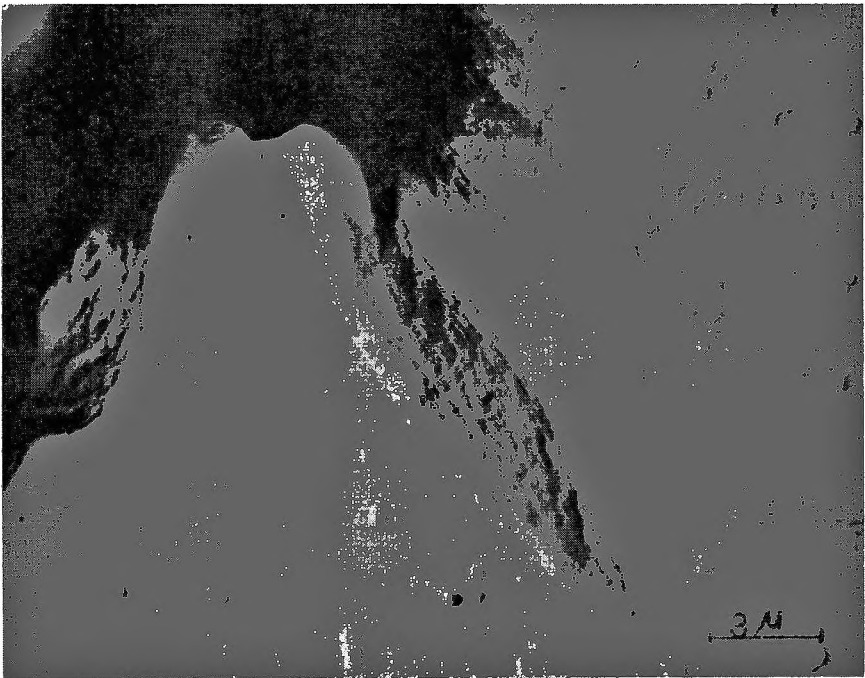


Fig. 2. Single crystals of polyvinylcyclohexane grown from a 0.05% solution in trichloroethylene.

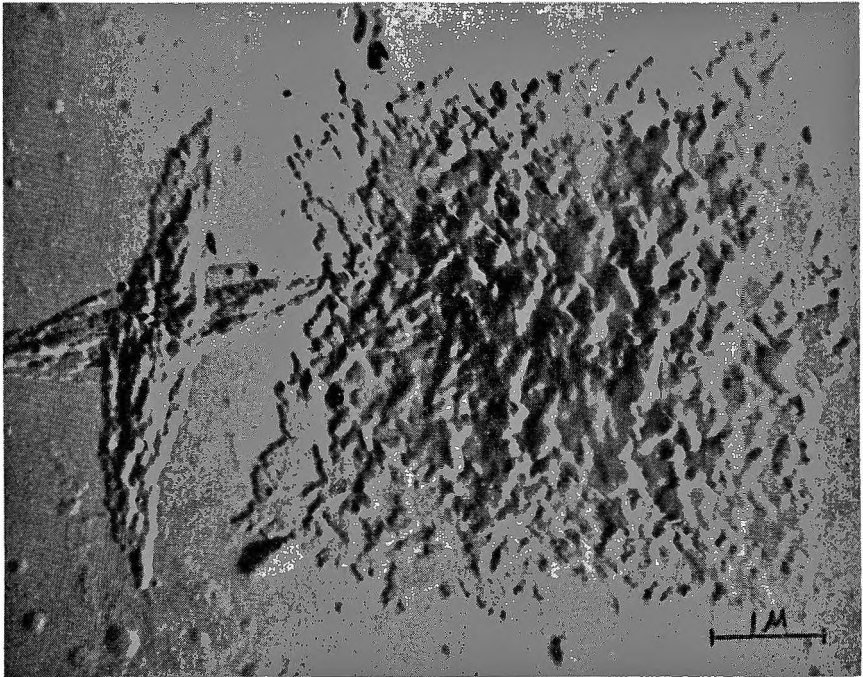


Fig. 3. Two types of crystals of polyvinylcyclohexane grown from the same solution. It is believed that the square platelet crystals formed after the polymer concentration was lowered sufficiently by the formation of the lozenge type crystals.

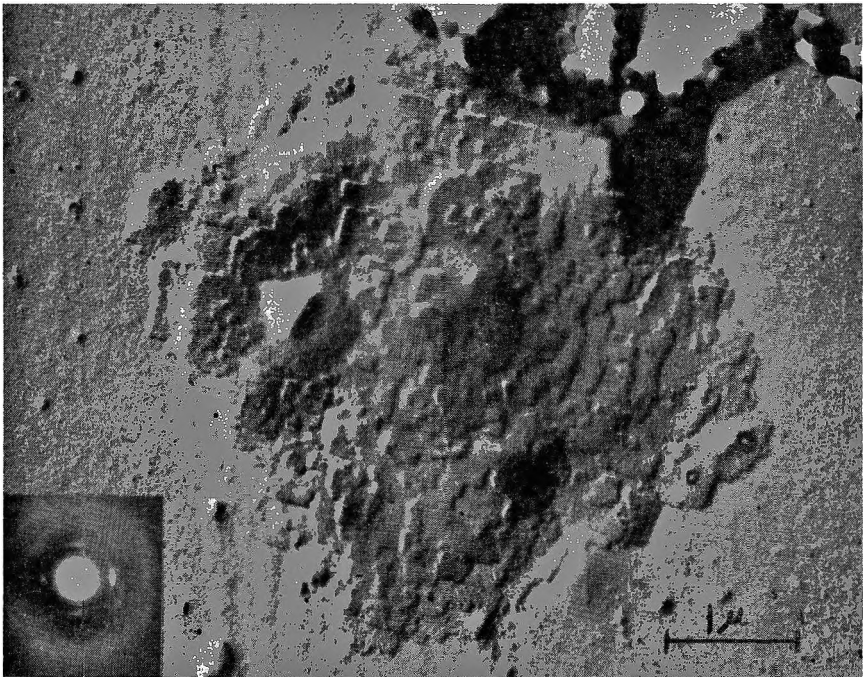


Fig. 4. Square platelets grown from a 0.005% solution in trichloroethylene. The spherical particles in the upper right hand corner are amorphous polymer.

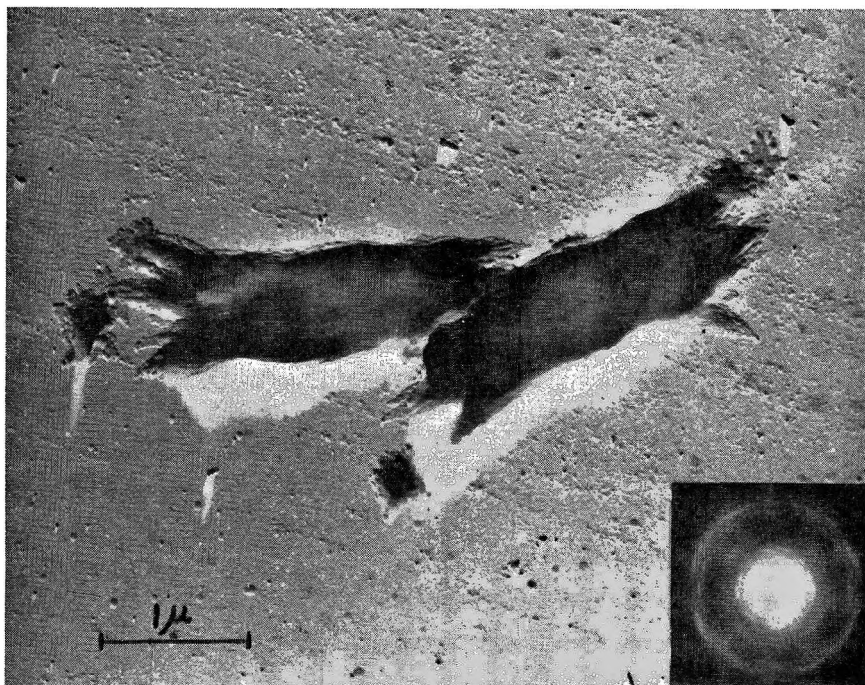


Fig. 5. Single crystals of polyvinylcyclohexane grown from a 0.005% solution in trichloroethylene. As indicated, the electron diffraction pattern is of a rolled up or folded crystal.

gave thicker lozenge type crystals as shown in Figure 2. This type of crystalline growth also formed from solutions which gave square based, platelet type, single crystals (Fig. 3). It is believed that the square based crystals formed after the polymer concentration was decreased sufficiently by the formation of the lozenge shaped crystals. In all cases some polymer precipitate appeared that had no apparent crystalline form; this can be seen in the upper right hand corner of Figure 4. In the more dilute solutions the square based crystals formed almost exclusively (this crystal appeared to be made up of stacked individual layers even though evidence showed it to be of the hollow pyramidal type). The only deviation was that in some cases these platelets seemed to roll up or fold into a bar-like shape. These are shown in Figure 5 together with the electron diffraction pattern obtained from them. This pattern is indeed one which would be expected from a rolled or folded crystal.

The height of the layers mentioned above was determined by using an internal standard (polystyrene latex particles) to calculate the magnification and shadowing angle. The electron diffraction pattern obtained from the platelet shows the direction of the molecular chain to be perpendicular to the a - b plane, and since the height of the crystal, approximately 220 Å, is much less than the length of an individual chain the crystal must be the folded chain type. The diffraction pattern confirms the unit cell proposed by Natta,¹ that is, a tetragonal unit cell. The a dimension of approximately 21.8 Å, calculated from this pattern is in close agreement with the x-ray work reported by him.

Reference

1. Natta, G., P. Corradini, J. W. Bassi, *Makromol. Chem.*, **33**, 247 (1959).

J. D. HUTCHISON

Summit Research Laboratories
 Celanese Corporation of America
 Summit, New Jersey

Received November 16, 1964

An Improved Technique for the Study of High Polymer Degradation Reactions

In a previous paper¹ a new technique for the study of polymer degradation reactions was described and tested with polymethylmethacrylate. It consists essentially of a quartz spoon gage, serving as a reaction vessel automatically recording pressure changes.

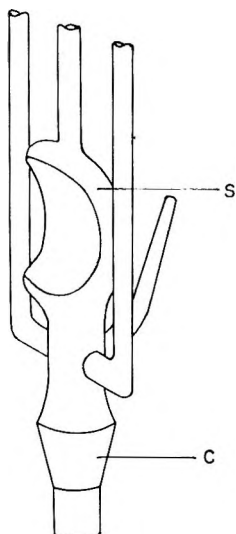


Fig. 1. Quartz spoon (S) with stainless steel pot (C).

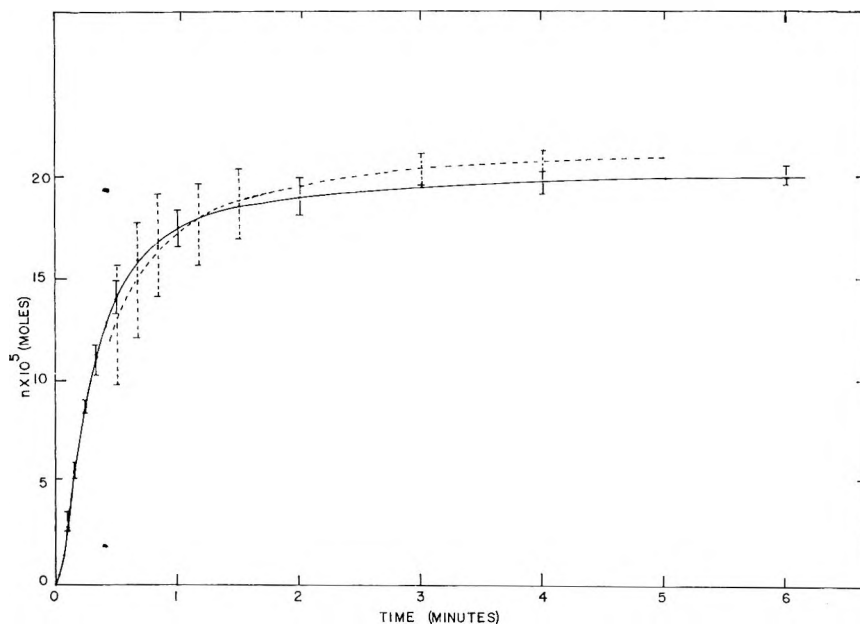


Fig. 2. Comparison of degradation of PMMA at 400°C. in quartz spoon reaction vessel (---; ref. 1, 20 mg. PMMA) with stainless steel reaction vessel (—; this paper, 19.6 mg. PMMA). Vertical lines represent standard deviations.

TABLE I
Arithmetic Mean Values of Moles n Produced and Standard Deviations at Various Times and Temperatures^a

| 375°C. | | | 400°C. | | | 425°C. | | | 450°C. | | |
|------------|--|--|---------|--|--|------------|--|--|------------|--|--|
| Time | Arith- metic mean $n \times 10^5$ | Standard deviation $\times 10^5$ | Time | Arith- metic mean $n \times 10^5$ | Standard deviation $\times 10^5$ | Time | Arith- metic mean $n \times 10^5$ | Standard deviation $\times 10^5$ | Time | Arith- metic mean $n \times 10^5$ | Standard deviation $\times 10^5$ |
| 10 sec. | 2.8 | ± 0.20 | 4 sec. | 1.4 | ± 0.76 | 2 sec. | 0.6 | ± 0.66 | 2 sec. | 3.4 | ± 0.59 |
| 20 sec. | 5.0 | 0.33 | 6 sec. | 3.1 | 0.47 | 4 sec. | 2.5 | 1.24 | 4 sec. | 7.7 | 0.78 |
| 40 sec. | 8.5 | 0.58 | 10 sec. | 5.7 | 0.41 | 7 sec. | 5.8 | 1.01 | 7 sec. | 13.3 | 0.56 |
| 1 min. | 10.8 | 0.67 | 15 sec. | 8.7 | 0.25 | 11 sec. | 10.4 | 1.07 | 11 sec. | 17.8 | 0.72 |
| 1 1/2 min. | 12.9 | 0.57 | 20 sec. | 11.0 | 0.75 | 15 sec. | 13.6 | 1.16 | 15 sec. | 19.6 | 0.57 |
| 2 min. | 14.2 | 0.67 | 30 sec. | 14.1 | 0.79 | 20 sec. | 16.1 | 0.69 | 20 sec. | 20.2 | 0.54 |
| 3 min. | 15.9 | 0.48 | 1 min. | 17.5 | 0.95 | 30 sec. | 18.5 | 0.34 | 30 sec. | 20.4 | 0.54 |
| 5 min. | 17.9 | 0.64 | 2 min. | 19.0 | 0.87 | 40 sec. | 19.4 | 0.78 | 40 sec. | 20.5 | 0.49 |
| 10 min. | 19.2 | 0.34 | 4 min. | 19.7 | 0.57 | 1 min. | 19.8 | 0.96 | 1 min. | 20.7 | 0.62 |
| 15 min. | 19.7 | 0.28 | 6 min. | 20.0 | 0.46 | 1 1/2 min. | 19.9 | 0.90 | 1 1/2 min. | 20.9 | 0.48 |
| | | | | | | 2 1/2 min. | 20.3 | 1.03 | | | |

^a 19.6 mg. films, four runs each.

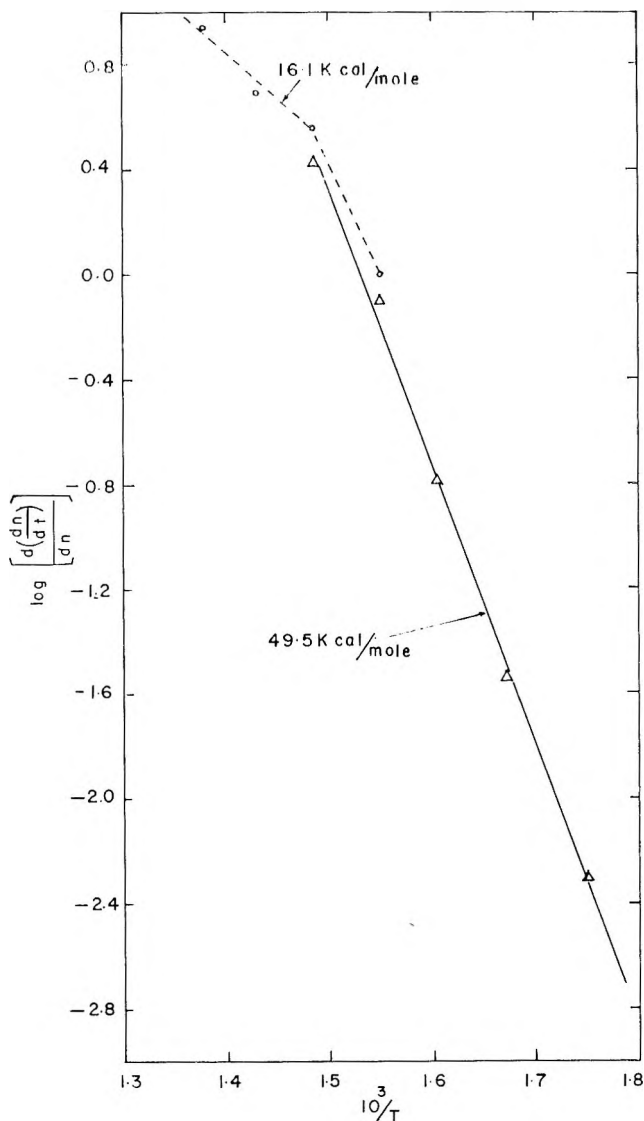


Fig. 3. $\log [d(dn/dt)/dx]$ plotted against the reciprocal absolute temperature for 60% conversion: Δ quartz vessel; O metal vessel.

The important feature of the apparatus is that it takes only 30 sec., as measured by a thermocouple, to bring the reaction vessel to the desired reaction temperature. Thus, the degradation of polymethylmethacrylate could be studied up to temperatures about 100°C . higher than was possible previously.^{1,2}

The technique has been improved by making part of the vessel of stainless steel. Thus, the time needed for heating the polymer film has been decreased considerably. In addition, the reproducibility of the results is much better than that for the quartz vessel. Measurements of the rate of degradation of polymethylmethacrylate can be obtained now another 50°C . higher than was possible before.

The apparatus was fully described previously.¹ Part of the improved apparatus is

shown in Figure 1. The reaction vessel consists now of a stainless steel pot (volume ca. 1 cm.³ excluding the ground joint, wall thickness is somewhat smaller than 1 mm.), which is connected to the quartz spoon by a ground joint lubricated with graphite, holding a vacuum of about 10⁻⁵ to 10⁻⁶ mm.Hg, even when plunged from room temperature into a bath of 600–700°C. The total capacity of the pot plus the quartz spoon is about 20–25 cm.³ The accessory apparatus was similar to that used before.¹

All solvents were analytical reagent grade. The apparatus was tested with the same sample of polymethylmethacrylate used previously¹ (benzoyl-peroxide initiated in bulk at 60°C., $M_v = 591,000$). Polymer films were deposited on the wall of the stainless steel vessel by evaporating aliquots of an 1.96% (w/v) polymer solution in acetone. The film was baked out at 70°C. in high vacuum for about 20 hr. prior to degradation. In all cases, the actual weight of the film was 19.6 mg. for each run. Figure 2 shows a comparison of an average rate curve for 400°C. obtained in the new reaction vessel with one for the same temperature obtained previously (see ref. 1, Table I). Standard deviations are indicated by vertical lines. Whereas, measurements made previously during the first 30 seconds were not usable because of the large standard deviations, reasonable measurements can now be obtained with the modified apparatus for that period. Also the standard deviations for the complete range of the degradation curves are consistently smaller for the new reaction vessel than those for the one used previously. Table I gives results for a number of temperatures.

Figure 3 shows a plot of $\log \{d(dn/dt)/dn\}$ against $10^3/T$ for 60% conversion. Here n is the number of gas moles produced during time t . The points obtained previously² in the quartz vessel are also indicated. The plots for higher percentage conversions are similar, however the energies of activation vary somewhat. All energies of activation decrease above 400°C. This change in energy of activation with increasing temperatures suggests that a different mechanism may become operative above 400°C. The increase in kinetic chain length with temperature may play a part in this change. It is also possible that the formation of monomer becomes so rapid that the reaction becomes completely diffusion controlled.

Thanks are due to the National Research Council of Canada for financial aid, which made this work possible, also to W. E. Eberhart (glassblower) and O. Brudy (machinist) for help in the construction of the apparatus. This work was carried out at the University of Windsor, Canada.

References

1. Jellinek, H. H. G., and J. E. Clark, *Can. J. Chem.*, **41**, 355 (1963).
2. Clark, J. E., and H. H. G. Jellinek, *Proc. Symp. Thermal Stability of Polymers*, Battelle Memorial Institute, Columbus, Ohio, December, 1963; *J. Polymer Sci.*, **A3**, 1171 (1965).

H. KACHI

Central Research Laboratory
Furukawa Electrical Company Ltd.
Tokyo, Japan

H. H. G. JELLINEK

Department of Chemistry
Clarkson College of Technology
Potsdam, New York

Received August 7, 1964
Revised February 5, 1965

ERRATA**Synthesis of Low Molecular Weight Polystyrene**

(article in *J. Polymer Sci.*, **A2**, 4533-4544, 1964)

By TIMOTHY ALTARES, JR., D. P. WYMAN, and V. R. ALLEN

Mellon Institute, Pittsburgh, Pennsylvania

On page 4533, Synopsis, line 9: $[\eta] = 8.4 \times 10^{-4} M^{0.5}$ should read $[\eta] = 8.5 \times 10^{-4} M^{0.5}$

Sound Velocity in Polyethylene at Ultrasonic Frequencies

(article in *J. Polymer Sci.*, **A3**, 697-701, 1965)

By A. LEVENE, W. J. PULLEN, and J. ROBERTS

*Explosives Research & Development Establishment, Ministry of Aviation, Waltham Abbey,
Essex, England*

On page 699, Equation (3) should read:

$$E = 3(1 - 2\nu)/K$$